ISSN 0021-9673

VOL. 448 NO. 1 AUGUST 31, 1988

JOURNAL OF CHROMATOGRAPHY

INTERNATIONAL JOURNAL ON CHROMATOGRAPHY, ELECTROPHORESIS AND RELATED METHODS

ELSEVIER

JOURNAL OF CHROMATOGRAPHY

Scope. The *Journal of Chromatography* publishes papers on all aspects of chromatography, electrophoresis and related methods. Contributions consist mainly of research papers dealing with chromatographic theory, instrumental development and their applications. The section *Biomedical Applications,* which is under separate editorship, deals with the following aspects: developments in and applications of chromatographic and electrophoretic techniques related to clinical diagnosis or alterations during medical treatment; screening and profiling of body fluids or tissues with special reference to metabolic disorders; results from basic medical research with direct consequences in clinical practice; drug level monitoring and pharmacokinetic studies; clinical toxicology; analytical studies in occupational medicine.

Submission of Papers. Papers in English, French and German may be submitted, in three copies. Manuscripts should be submitted to: The Editor of *Journal of Chromatography,* P.O. Box 681, 1000 AR Amsterdam, The Netherlands, or to: The Editor of *Journal of Chromatography, Biomedical Applications,* P.O. Box 681, 1000 AR Amsterdam, The Netherlands. Review articles are invited or proposed by letter to the Editors. An outline of the proposed review should first be forwarded to the Editors for preliminary discussion prior to preparation. Submission of an article is understood to imply that the article is original and unpublished and is not being considered for publication elsewhere. For copyright regulations, see below.

Subscription Orders. Subscription orders should be sent to: Elsevier Science Publishers B.V., P.O. Box 211, 1000 AE Amsterdam, The Netherlands, Tel. 5803 911, Telex 18582 ESPA NL. The *Journal of Chromatography* and the *Biomedical Applications* section can be subscribed to separately.

Publication. The *Journal of Chromatography* (incl. *Biomedical Applications* and *Cumulative Author and Subject Indexes, Vols. 401–450*) has 37 volumes in 1988. The subscription prices for 1988 are:

J. Chromatogr. (incl. *Cum. Indexes, Vols. 401–450*) + *Biomed. Appl.* (Vols. 424–460):
Dfl. 6290.00 plus Dfl. 962.00 (p.p.h.) (total *ca.* US$ 3920.00)

J. Chromatogr. (incl. *Cum. Indexes, Vols. 401–450*) only (Vols. 435–460):
Dfl. 5070.00 plus Dfl. 676.00 (p.p.h.) (total *ca.* US$ 3106.00)

Biomed. Appl. only (Vols. 424–434):
Dfl. 2145.00 plus Dfl. 286.00 (p.p.h.) (total *ca.* US$ 1314.00).

Our p.p.h. (postage, package and handling) charge includes surface delivery of all issues, except to subscribers in Argentina, Australia, Brasil, Canada, China, Hong Kong, India, Israel, Malaysia, Mexico, New Zealand, Pakistan, Singapore, South Africa, South Korea, Taiwan, Thailand and the U.S.A. who receive all issues by air delivery (S.A.L. — Surface Air Lifted) at no extra cost. For Japan, air delivery requires 50% additional charge; for all other countries airmail and S.A.L. charges are available upon request. Back volumes of the *Journal of Chromatography* (Vols. 1 through 423) are available at Dfl. 230.00 (plus postage). Claims for missing issues will be honoured, free of charge, within three months after publication of the issue. Customers in the U.S.A. and Canada wishing information on this and other Elsevier journals, please contact Journal Information Center, Elsevier Science Publishing Co. Inc., 52 Vanderbilt Avenue, New York, NY 10017. Tel. (212) 916-1250.

Abstracts/Contents Lists published in Analytical Abstracts, ASCA, Biochemical Abstracts, Biological Abstracts, Chemical Abstracts, Chemical Titles, Chromatography Abstracts, Current Contents/Physical, Chemical & Earth Sciences, Current Contents/Life Sciences, Deep-Sea Research/Part B: Oceanographic Literature Review, Excerpta Medica, Index Medicus, Mass Spectrometry Bulletin, PASCAL-CNRS, Referativnyi Zhurnal and Science Citation Index.

See inside back cover for Publication Schedule, Information for Authors and information on Advertisements.

0021-9673/88/$03.50

Printed in The Netherlands

CONTENTS

(Abstracts/Contents Lists published in Analytical Abstracts, ASCA, Biochemical Abstracts, Biological Abstracts, Chemical Abstracts, Chemical Titles, Chromatography Abstracts, Current Contents/Physical, Chemical & Earth Sciences, Current Contents/Life Sciences, Deep Sea Research/Part B: Oceanographic Literature Review, Excerpta Medica, Index Medicus, Mass Spectrometry Bulletin, PASCAL-CNRS, Referativnyi Zhurnal and Science Citation Index)

(Continued overleaf)

In articles with more than one author, the name of the author to whom correspondence should be addressed is indicated in the article heading by a 6-pointed asterisk (*)

AQUEOUS SIZE-EXCLUSION CHROMATOGRAPHY

edited by **P.L. DUBIN,** *Indiana-Purdue University*

(Journal of Chromatography Library, 40)

The rapid development of new packings for aqueous size-exclusion chromatography has revolutionized this field. High resolution non-adsorptive columns now make possible the efficient separation of proteins and the rapid and precise determination of the molecular weight distribution of synthetic polymers. This technology is also being applied to the separation of small ions, the characterization of associating systems, and the measurement of branching. At the same time, fundamental studies are elucidating the mechanisms of the various chromatographic processes.

These developments in principles and applications are assembled for the first time in this book.

- Fundamental issues are dealt with: the roles of pore structure and macromolecular dimensions, hydrophobic and electrostatic effects, and the determination and control of column efficiency.
- High-performance packings based on derivatized silica are reviewed in detail.
- Special techniques are thoroughly described, including SEC/LALLS, inverse exclusion chromatography, and frontal zone chromatography.
- Attention is focussed on special applications of size-exclusion methods, such as the characterization of micelles, separations of inorganic ions, and Hummel-Dreyer and related methods for equilibrium systems.
- Protein chromatography is dealt with in both dedicated sections and throughout the book as a whole.

This is a particularly comprehensive and authoritative work - all the contributions review broad topics of general significance and the authors are of high repute.

The material will be of special value for the characterization of synthetic water-soluble polymers, especially polyelectrolytes. Biochemists will find fundamental and practical guidance on protein separations. Researchers confronted with solutes that exhibit complex chromatographic behavior, such as humic acids, aggregating proteins, and micelles should find the contents of this volume illuminating.

Contents: Part I. Separation Mechanisms. Part II. Characterization of Stationary Phases. Part III. New Packings. Part IV. Biopolymers. Part V. Associating Systems. Subject Index.

1988 xviii + 454 pages
US$ 144.75 / Dfl. 275.00
ISBN 0-444-42957-3

ELSEVIER SCIENCE PUBLISHERS

P.O. Box 211, 1000 AE Amsterdam, The Netherlands
P.O. Box 1663, Grand Central Station, New York, NY 10163, USA

A New Training Tool

Troubleshooting HPLC Systems

A VIDEO COURSE

Developed and presented by **J.W. Dolan** and **L.R. Snyder,**
L.C. Resources Inc., San Jose, CA, USA

HPLC troubleshooting is a complex skill which is most often obtained through years of on-the-job experience. This course has condensed many years of practical experience into just under three hours of presentation, and is aimed at improving the trouble-shooting skills of chromatographers active in HPLC.

Lloyd R. Snyder's developments in the theory and application of HPLC have made practical sense out of complex theory, so that chromatographers can get better separations in less time. John Dolan is well-known for his trouble-shooting column in which he answers readers' questions.

Now these experts combine forces to bring you a powerful educational video-course, second only to hands-on experience.

Emphasis is on logical and practical steps for diagnosing why a system fails to operate properly and how to remedy the fault. The advantages and importance of preventive maintenance and record-keeping are illustrated. Exploded views, blow-ups of small parts, the handling of a delicate part like a frit, bleeding check valves, etc., are shown with clarity while John Dolan comments on what he does and why - and what to watch out for.

The course is ideally suited for self-tuition, as well as for use in a group. It may be used over and over again, at any time, at the lab or at home.

The complete course consists of three 55-minute VHS tapes, a User's Manual and an Instructor's Guide.

The tapes cover:

- **Principles of Troubleshooting**
- **Fittings, Reservoirs, Pumps and Injectors**
- **Columns, Detectors and Preventive Maintenance**

Prices:

	USA/Canada	Elsewhere
Complete course	US$1350	Dfl. 3000
Individual tapes	US$ 450	Dfl. 1000
User's manual	US$ 22	Dfl. 50
Instructor's guide	US$ 10	Dfl. 22.50

A **demonstration tape** is available at a price of US$ 25.00 or Dfl. 50.00 **(prepaid)**

All tapes are supplied in VHS format for the video system used in your country, unless otherwise requested.

Send now for a detailed brochure to:

ELSEVIER SCIENCE PUBLISHERS

Elsevier Science Publishers

Attn. Video Dept., P.O. Box 330, 1000 AH Amsterdam, The Netherlands
(telex 10704 espom nl) or
Attn. JIC Dept., P.O. Box 1663, Grand Central Station, New York, NY 10163
(tel: 212-370 5520)

7409A

JOURNAL OF CHROMATOGRAPHY

VOL. 448 (1988)

JOURNAL *of* CHROMATOGRAPHY

INTERNATIONAL JOURNAL ON CHROMATOGRAPHY, ELECTROPHORESIS AND RELATED METHODS

ELSEVIER
AMSTERDAM — OXFORD — NEW YORK — TOKYO

J. Chromatogr., Vol. 448 (1988)

0021-9673/88/$03.50

Printed in The Netherlands

Journal of Chromatography, 448 (1988) 1–9
Elsevier Science Publishers B.V., Amsterdam — Printed in The Netherlands

CHROM. 20 561

STATISTICAL OPTIMIZATION OF A REVERSED-PHASE ION-PAIR LIQUID CHROMATOGRAPHIC METHOD FOR THE ANALYSIS OF TOLMETIN SODIUM IN DOSAGE FORMS

RONA STROMBERG
U.S. Food and Drug Administration, New York Regional Laboratory, 850 Third Avenue, Brooklyn, NY 11232 (U.S.A.)
(First received December 31st, 1987; revised manuscript received March 7th, 1988)

SUMMARY

A quantitative liquid chromatographic method in which tolmetin sodium is separated from an internal standard on a C_{18} column with detection at 317 nm has been developed with the aid of two statistical optimization procedures. The effects of simultaneously varying the pH, methanol–water ratio, and the concentrations of buffer and ion-pair reagent in the mobile phase were studied. A two-level factorial design was used to investigate the interactions among the variables, and the sequential simplex procedure was used to optimize the separation. A novel quality criterion was developed for the simplex optimization. Using synthetic mixtures, the mean recovery value ± S.D. (n = 6) of tolmetin sodium was 98.7 ± 0.19% for tablets and 98.5 ± 0.12% for capsules. The assay results for commercial tablets and capsules were comparable to those obtained by the USP XXI procedure.

INTRODUCTION

Tolmetin sodium is a non-steroidal anti-inflammatory agent with analgesic and antipyretic activities. As the sodium salt dihydrate it is formulated in tablet and capsule forms, both of which are used for the treatment of rheumatoid arthritis and osteoarithritis[1].

Tolmetin has been determined in plasma samples by gas and liquid chromatographic procedures[2–7], and in solid dosage forms by spectrophotometry[8]. Its possible impurities have been quantitated by a normal-phase gradient high-performance liquid chromatography (HPLC) procedure[9]. The compendial assays for tablets and capsules entailed lengthy spectrophotometric procedures[10]. Because of the typically low recoveries of the plasma studies and the amount of time required for the spectrophotometric method, an alternate procedure suitable for the regulatory analysis of tolmetin in dosage forms was sought. This report describes the development of a rapid, accurate and selective LC method for the analysis of the drug in tablets and capsules.

The assay was developed using two mathematical statistical models–factorial

0021-9673/88/$03.50

design and simplex optimization[11–17]. These methods are used to assess the quality of a separation quantitatively. In a comparatively short time, a determination as to which variables have significant effects, and the relative importance, the degree of interaction, and the optimum levels of these variables was made.

Screening experiments were used to determine a reasonable first set of conditions, including the type of column, organic modifier, and sample concentration. These experiments also suggested the variables to be investigated. Two sets of two-level, full factorial experiments were carried out. The results were that pH, and the concentrations of buffer, ion-interaction reagent and methanol were significant and interactive. Peak shape and column retention could be closely controlled by adjusting these four variables.

The final step was to simultaneously optimize the values of the four variables using the simplex procedure. The simplex was terminated after the twelfth experiment and the best set of conditions was selected.

EXPERIMENTAL

Apparatus

A Tracor 950 chromatographic pump with 970A variable-wavelength detector and a TS-10 recorder were used (Tracor, Austin, TX, U.S.A.). Separations were performed on Zorbax ODS, 250 × 4.6 mm, 5-μm particles (DuPont, Wilmington, DE, U.S.A.), μBondapak C_{18}, 300 × 3.9 mm, 10-μm particles (Waters Assoc., Milford, MA, U.S.A.) and Ultrasphere ODS, 250 × 4.6 mm, 5-μm particles (Beckman Instruments, San Ramon, CA, U.S.A.) columns. Samples were introduced through a Rheodyne 7125 injection valve with a 20-μl sample loop (Rheodyne, Cotati, CA, U.S.A.).

Chemicals and reagents

Methanol was HPLC grade (Fisher Scientific, Fairlawn, NJ, U.S.A.). Other reagents were analytical-reagent grade. The tolmetin and zomepirac sodium dihydrates were kindly donated by McNeil Pharmaceutical (Spring House, PA, U.S.A.).

Procedure

Internal standard solution. A 420 μg/ml solution of zomepirac sodium dihydrate in methanol–water (1:1) was prepared.

Standard preparation. Approximately 22 mg of tolmetin sodium, previously dried at 105°C for 3 h was dissolved in methanol–water (1:1) in a 100-ml volumetric flask and 10.0-ml aliquots of this solution and the internal standard solution were combined and diluted to 100.0 ml with the same solvent.

Sample preparation. An amount of ground tablet or capsule powder corresponding to 200 mg of tolmetin was weighed into a 100-ml volumetric flask and diluted to volume with methanol–water (1:1). This preparation was mixed and a portion filtered through medium porosity filter paper. A 10.0-ml aliquot of the filtrate was diluted to 100 ml with methanol–water. A 10.0-ml aliquot of the resulting solution and 10.0 ml of the internal standard solution were combined in a 100-ml volumetric flask and diluted to volume with methanol–water.

Chromatographic conditions. The mobile phase was prepared by dissolving 1.36

g of monobasic potassium phosphate and 3.39 g of tetrabutylammonium phosphate in 350 ml of water, then adding 650 ml of methanol and 1 ml of acetic acid, mixing, filtering through a membrane filter (0.45 μm porosity) and degassing. The methanol–water levels may be adjusted to obtain acceptable separations. The flow-rate was set at 1.0 ml/min, the detector wavelength at 317 nm and 20 μl portions of the preparations were injected.

Calculation. The quantity (in mg) of tolmetin in the portion of powder taken is equal to (257.29/279.27) (C) (R_u/R_s), in which 257.29 and 279.27 are the molecular weights of tolmetin and anhydrous tolmetin sodium respectively, C is the concentration, in mg per ml of tolmetin sodium in the standard preparation, and R_u and R_s are the peak response ratios of the analyte to the internal standard obtained from the sample preparation and the standard preparation respectively.

RESULTS AND DISCUSSION

The decision to apply experimental design techniques to the development of the method was made after a series of screening experiments revealed that peak shape and reproducibility could not adequately be controlled by a mobile phase composed only of solvents without solute conditioning reagents such as buffers, counter ions and acids. Mobile phase additives were needed but the possible combinations of mobile phase components and the proportions of each component were numerous. In order to rationalize the decision making process, two experimental models were chosen, factorial design and simplex optimization.

TABLE I

ELUENT COMPOSITIONS, k' VALUES, AND CALCULATED EFFECTS OF FIRST SERIES OF FACTORIAL DESIGN EXPERIMENTS

Exp. No.	*Methanol–water ratio*	*Apparent pH*	*Buffer conc. (mM)*	k'	
				Tolmetin	*Zomepirac*
1	55:45	6.0	5	2.82	4.68
2	55:45	6.0	0	0.10	0.15
3	55:45	4.0	5	4.30	6.72
4	55:45	4.0	0	0.10	0.15
5	45:55	6.0	5	7.28	13.28
6	45:55	6.0	0	0.71	1.34
7	45:55	4.0	5	14.72	24.83
8	45:55	4.0	0	1.29	2.40

Variable		*Effect*	
(1)	Methanol–water ratio	−4.17	−7.54
(2)	pH	−2.38	−3.66
(3)	Buffer concentration	6.73	11.37
	Interaction 1 × 2	−2.09	−3.13
	1 × 3	−3.27	−5.82
	2 × 3	1.64	2.64

TABLE II

CONDITIONS AND RESULTS OF SECOND SERIES OF FACTORIAL DESIGN EXPERIMENTS

Exp. No.	*Methanol–water ratio*	*Apparent pH*	*Buffer conc. (mM)*	*IIR conc. (mM)*	*k'*	
					Tolmetin	*Zomepirac*
1	65:35	7.0	75	10	–	–
2	65:35	7.0	75	5	–	–
3	65:35	7.0	25	10	1.95	2.80
4	65:35	7.0	25	5	2.00	3.00
5	65:35	5.0	75	10	–	–
6	65:35	5.0	75	5	–	–
7	65:35	5.0	25	10	2.33	3.48
8	65:35	5.0	25	5	3.92	5.82
9	60:40	7.0	75	10	4.00	6.16
10	60:40	7.0	75	5	3.15	5.00
11	60:40	7.0	25	10	3.24	5.03
12	60:40	7.0	25	5	2.49	3.88
13	60:40	5.0	75	10	5.02	7.42
14	60:40	5.0	75	5	4.82	7.31
15	60:40	5.0	25	10	5.61	8.43
16	60:40	5.0	25	5	3.64	5.49

Variable		*Effect*	
(1)	Methanol–water ratio	−1.20	−1.93
(2)	pH	−1.41	−2.02
(3)	Buffer concentration	0.50	0.76
(4)	IIR concentration	0.35	0.47
	Interaction 1 × 2	0.65	0.84
	1 × 3	0.35	0.59
	1 × 4	−0.91	−1.32
	2 × 3	0.53	0.82
	2 × 4	0.17	0.24
	3 × 4	−0.01	−0.04

While it is not strictly necessary to use two design techniques, the practice has been recommended by Deming and Morgan[18]. Further, This study was originally undertaken as part of a project, the goal of which was to revise drug monographs of the *United States Pharmacopeia*[10]. In view of this goal, it was useful to combine the greater information content and ruggedness testing inherent in a factorial design with the speed of the simplex optimization.

Factorial design

A three-variable, two-level, full factorial design was chosen in order to investigate the effects of each component and their interactions. The variables were the methanol-water ratio, pH, and buffer concentration (Table I). The main effects and interactions were calculated according to Box *et al.*[19]. The effect of a variable on retention is indicated by its sign (+ or −). The capacity factor, k', was selected as a rapid means of measuring the influence of a mobile phase component on the eluting peaks. Experiments were conducted in random order.

From the table it can be seen that each of the variables had a significant effect on the retention of the compounds with the buffer exerting the most profound effect. The interaction of the methanol–water ratio with the buffer concentration was greater than the other combined effects, which indicates that the alteration in retention caused by the presence of the buffer is dependent on the methanol–water ratio.

Peak shape and reproducibility for most of the mobile phases tested were unacceptable even with those in which resolution and analysis time were adequate. An ion-interaction reagent, tetabutylammonium phosphate, which can be used for the analysis of weak organic acids, was therefore, added to the mobile phase. To explore the effect of this addition, as well as the role of other components, a second set of factorial experiments was done. Different levels of methanol–water ratio, pH, and buffer concentration were selected in order to maximize the information that could be extracted from the experimental data (Table II).

Unfortunately, precipitation of the salts occurred in the eluents when the concentrations of methanol and buffer were at their highest levels. Nevertheless, an analysis of the data could be made. Calculation of the main effects and interactions show that they had markedly decreased from those of the first set of experiments. The tolmetin and internal standard were found to be less sensitive to variations in the levels of the components of the mobile phase. The wide fluctuations in k' apparent in the first grouping were eliminated by the regulating influences of the buffer and the ion-interaction reagent and is reflected in the calculated effects. Excellent peak shape and reproducibility were also achieved.

Simplex optimization

In order to identify the optimum conditions for the analysis, a five dimensional sequential simplex optimization was undertaken. The most difficult aspect of this technique is the selection of a quantitative criterion that will permit the evaluation of a set of chromatograms. A variety of approaches have been proposed[20,21], many requiring complex measurements and calculations, and frequently, the use of a computer. An alternate criterion was sought in which the quality assessment could be based on the capacity factor, k'. The capacity factor is easily obtained. It is preferred over such other simple parameters as retention time or retention volume because it is independent of the flow rate and column volume. Previously proposed criteria include requirements for the resolution of peaks and the maximum time of analysis. The capacity factor is well-suited as a means of expressing these requirements in a usable mathematical form. Optimal k' values can be selected to locate any pair of peaks so that sufficient resolution is achieved within preselected time restrictions. For this study, optimal k' values of 2 and 4 were chosen for tolmetin and the internal standard respectively. Based on these considerations, an empirical separation factor (ESF) was developed. Excellent concordance was found between the calculated and experimental values.

$$\mathrm{ESF} = (|k'\mathrm{optA} - k'\mathrm{actA}| + |k'\mathrm{optB} - k'\mathrm{actB}|) + \left| 1 - \frac{(k'\mathrm{optB} - k'\mathrm{optA})}{(k'\mathrm{actB} - k'\mathrm{actA})} \right|$$

where k'optA,B and k'actA,B are the previously selected and experimentally determined capacity factors respectively for any pair of peaks, A and B. If the optimal

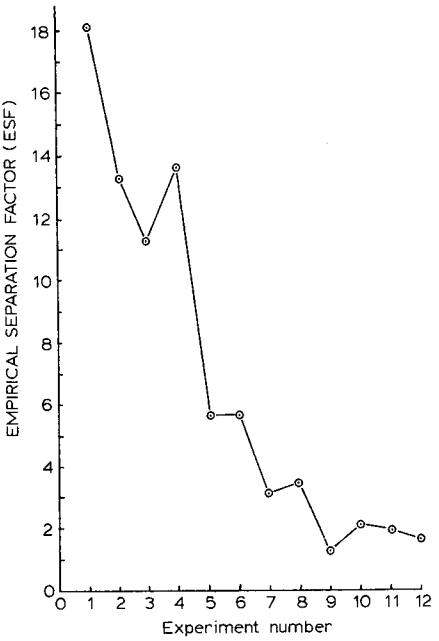

Fig. 1. Progress of the simplex.

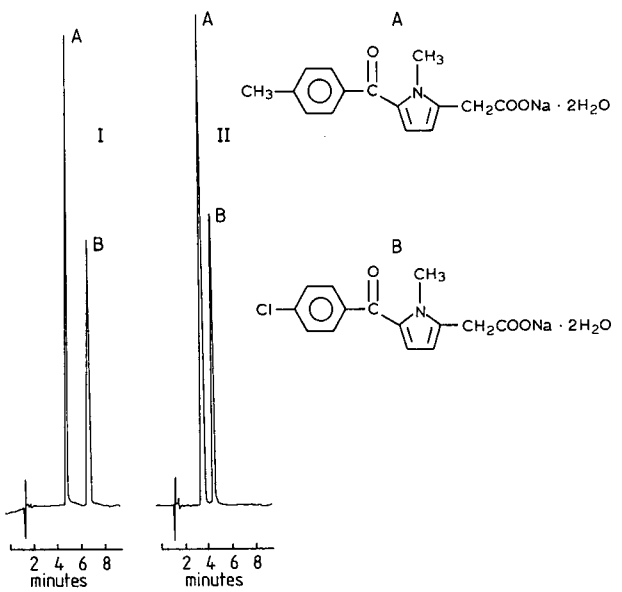

Fig. 2. HPLC separation of (A) tolmetin and (B) zomepirac, the internal standard, on two columns: I, Zorbax; II, new μBondapak.

conditions are achieved, ESF = 0. The first term of the equation sums the absolute differences between the desired and achieved capacity factors. Absolute values are needed to prevent the diminishment of the total if the differences for the two peaks are of opposite sign. Because absolute values are being used, however, the same ESF would result from a chromatogram in which resolution decreases as for one in which it increases to an equal degree. A second term was added to produce a higher less desirable ESF for the less well resolved pair. The numerator of this term is constant. The denominator decreases as resolution decreases, thus increasing the quotient and consequently the ESF. The quotient is subtracted from 1 so that the total ESF for an ideal situation is 0. The absolute value is again used in the second term to avoid the negative sum which would otherwise result when the k'act values are less than the k'opt values.

The initial conditions/step sizes for the simplex were (1) methanol–water ratio, 55:45/5%; (2) pH, 5.0/0.5; (3) buffer concentration, 10 mM/5 mM; and (4) ion-interaction reagent concentration, 10 mM/5 mM. The rapid progress of the simplex is shown in Fig. 1. The proposed method is based on the conditions of the ninth experiment. A chromatogram obtained with the optimized mobile phase is shown in Fig. 2.

Validation

The method was tested for specificity, linearity, precision, sensitivity and ruggedness according to the format proposed by Debesis *et al.*[22].

The specificity of the method was investigated by observing any interference by other compounds known to represent decomposition products and synthetic by-products of tolmetin, *i.e.*, *p*-toluic acid; 4-*p*-toluoyl-1-methylpyrrole-2-acetamide; ethyl 5-*p*-toluoyl-1-methylpyrrole-2-acetate; 1,5-dimethyl-4-(*p*-toluoyl)pyrrole-2-carboxamide; and methyl 5-*p*-toluoyl-1-methylpyrrole-2-acetate. The k' values were less than 1 for the first two compounds and greater than 3 for the others in a system in which the values for tolmetin and the internal standard were 1.5 and 2.1 respectively. Eluting sample and standard peaks were collected, and a complete ultraviolet spectrum of each peak was obtained. In all cases, sample and standard peaks were found to be identical.

The susceptibility of the method to alterations in the composition as well as in the ratio of the components of the mobile phase was evaluated using the optimization technique described earlier. The ideal method is one that will ensure that sensitive factors remain protected while those that are not (*e.g.* the methanol to water ratio) may be varied to suit column characteristics. It was verified that an increase of as much as 15% in either methanol or water, with no changes in the other components of the mobile phase, will not significantly affect the quality of the chromatograms.

Column-to-column variability was examined using three brands of octadecylsilane columns, namely Zorbax, Ultrasphere and μBondapak. For the μBondapak column, a comparison was also made between a new column and one that had been subjected to repeated use.

Zorbax columns have a high resolving power compared to most others. This method was developed using a Zorbax column with more resolution between tolmetin and the internal standard than is actually needed, on the theory that it could then be

TABLE III

ASSAY RESULTS FOR 200 mg TOLMETIN SODIUM TABLETS BY PROPOSED AND USP XXI METHODS

Composite No.	*% of declared*	
	Proposed method	*USP method*
1	100.2	100.8
2	99.2	99.9
3	99.3	100.0
4	99.7	–
5	99.7	–
6	99.4	–
7	99.6	–
8	99.7	–
9	99.7	–
10	99.4	–
Mean	99.6	100.2
S.D.	0.285	0.493
C.V. (%)	0.286	0.492

transferred to a column with less resolution and still give adequate separation. The Zorbax column had approximately three times the number of theoretical plates as the new μBondapak column, but the methods worked on both. On the old μBondapak column, the peaks were symmetrical, but not completely resolved. By decreasing the amount of methanol in the mobile phase, a good separation was achieved. Similarly, since the Zorbax column gave more separation than needed, the methanol concentration was increased to make the analysis more rapid, but with no loss in

TABLE IV

ASSAY RESULTS FOR 400 mg TOLMETIN SODIUM CAPSULES BY PROPOSED AND USP XXI METHODS

Composite No.	*% of declared*	
	Proposed method	*USP method*
1	101.2	101.8
2	101.4	101.5
3	101.2	101.1
4	101.9	–
5	101.6	–
6	101.8	–
7	101.0	–
8	101.0	–
9	101.8	–
10	101.2	–
Mean	101.3	101.5
S.D.	0.360	0.351
C.V. (%)	0.356	0.346

efficiency. The Ultrasphere column showed extreme tailing on a test mixture of methyl and ethyl parabens. This tailing was also seen in the tolmetin and internal standard peaks. These peaks were resolved, however, and the chromatogram could be used for quantitation.

Detector responses were linearly related to concentrations of tolmetin in the range 10–30 μg/ml (r = 0.99998), with a detection limit of about 1 μg/ml. The precision of the method, based on ten separate weighings of the same composites, resulted in coefficient of variation (C.V.) values of 0.286% for a tablet sample, 0.365% for a capsule sample, and 0.265% (n = 10) for reinjections of the same standard solution. The accuracy of the method was established on the basis of recoveries of the drug substance from synthetic formulations and commercial products. Recoveries (mean ± S.D. of the added amount) were: from the synthetic tablet formulation 98.7 ± 0.19% (n = 6); from the synthetic capsule formulation 98.5 ± 0.12% (n = 6); from commercial tablets 99.6 ± 0.29% (n = 3), and from commercial capsules 101.3 ± 0.36% (n = 3).

The proposed method was used to analyze commercial tablets and capsules of tolmetin sodium, and the results were compared with these obtained by the corresponding methods of USP XXI[10]. The results of these studies are presented in Tables III and IV. In general intermethod correspondence was excellent.

REFERENCES

1 *Physicians' Desk Reference*, Medical Economics, Oradell, NJ, 1987, 41st ed., pp. 1197–1198.
2 K.-T. Ng, *J. Chromatogr.*, 166 (1978) 527–535.
3 R. K. Desiraju, D. C. Sedberry, Jr. and K.-T. Ng, *J. Chromatogr.*, 232 (1982) 119–128.
4 J. Ayres, E. Sakmar, M. Hallmark and J. Wagner, *Res. Commun. Chem. Pathol. Pharmacol.*, 16 (1977) 475–483.
5 W. Cressman, B. Lopez and D. Sumner, *J. Pharm. Sci.*, 64 (1975) 1965–1967.
6 M. L. Selley, J. Thomas and E. J. Triggs, *J. Chromatogr.*, 94 (1974) 143–149.
7 J. Shimek, N. Rao, S. Khalil, *J. Liq. Chromatogr.*, 4 (1981) 1987–2013.
8 C. Janicki and K. Daly, *J. Pharm. Sci.*, 69 (1980) 147–149.
9 R. K. Gilpin and C. A. Janicki, *J. Chromatogr.*, 147 (1978) 501–506.
10 *United States Pharmacopeia*, U.S. Pharmacopeial Convention, Rockville, MD, XXI revision, 1985, pp. 1070–1071.
11 B. Sachok, R. C. Kong and S. N. Deming, *J. Chromatogr.*, 199 (1980) 317–325.
12 J. Nickel and S. Deming, *LC · GC Int., Mag. Liq. Gas Chromatogr.*, 1 (1983) 414–417.
13 F. Czech, *J. Assoc. Off. Anal. Chem.*, 56 (1973) 1489–1495.
14 R. D. Krause and J. A. Lott, *Clin. Chem.*, 20 (1974) 775–782.
15 S. Deming and M. Turoff, *Anal. Chem.*, 50 (1978) 546–548.
16 J. L. Glajch and J. J. Kirkland, *Anal. Chem.*, 55 (1983) 319A–336A.
17 W. Lindberg, E. Johansson and K. Johansson, *J. Chromatogr.*, 211 (1981), 201–212.
18 S. N. Deming and S. L. Morgan, *Anal. Chem.*, 45 (1973) 278A–283A.
19 G. E. P. Box, W. G. Hunter and J. S. Hunter, *Statistics for Experimenters*, Wiley, New York, 1978, pp. 309–324.
20 G. D'Agostino, L. Castagnetta, F. Mitchell and M. J. O'Hare, *J. Chromatogr.*, 338 (1985) 1–23.
21 M. Watson and P. Carr, *Anal. Chem.*, 51 (1979) 1835–1842.
22 E. Debesis, J. P. Boehlert, T. E. Givand and J. C. Sheridan, *Pharm. Technol.*, 6 (9) (1982) 123–137.

Journal of Chromatography, 448 (1988) 11–30
Elsevier Science Publishers B.V., Amsterdam — Printed in The Netherlands

CHROM. 20 617

THIN-LAYER CHROMATOGRAPHIC ENANTIOMERIC RESOLUTION VIA LIGAND EXCHANGE

K. GÜNTHER
Fachbereich Forschung Chemie, Degussa AG, Postfach 1345, D-6450 Hanau (F.R.G.)
(Received April 28th, 1988)

SUMMARY

A thin-layer chromatographic technique for the separation of proteinogenic and non-proteinogenic amino acids, dipeptides and α-hydroxy acids is described. Other examples are given from the field of α-methyl, N-alkyl and halogenated amino acids. The separation of the enantiomers is achieved, without derivatization, by means of ligand exchange on a reversed-phase silica gel as stationary phase, which is covered with a chiral selector (proline derivative). The resolution is so good that the respective enantiomers can be determined at trace levels ($\geq$ 0.25%). The proposed method is simple, inexpensive and needs no sophisticated instruments.

INTRODUCTION

The activity and effectiveness of chiral molecules depend largely on their configuration[1]. Often only one of the enantiomers is pharmacologically active, while the other may be at best inactive or even toxic. Only *ca.* 20% of the optically active pharmaceuticals are traded as pure enantiomers[2]. This has resulted in an increasing interest in stereoselective syntheses, and in the growing importance of optically active amino acids, which are commercially available on a large scale as a "chiral pool", as building blocks and auxiliaries for the production of biologically active peptides, in asymmetric syntheses and as pharmaceuticals.

This is the reason why efficient analytical procedures for the control of optical purity have to be developed as aids for asymmetric syntheses. Traditionally, many laboratories use polarimetry for the control of optical purity, but this method suffers from some well-known specific drawbacks. Additionally, the calculation of the enantiomeric excess (*ee*) from optical rotation may be impossible, because the specific rotation of the pure enantiomer is unknown, or calculated *ee* values may be wrong owing to impurities. Therefore direct, *e.g.* chromatographic, analytical procedures are to be preferred.

Because simple separation techniques were not available until recently, gas chromatographic[3–6] or liquid chromatographic[7–13] methods are generally used for direct determination of the enantiomeric composition. These systems need expensive instruments, are often "derivative", and, for routine application require that

0021-9673/88/$03.50

standardized stationary phases are commercially available. Therefore the application of thin-layer chromatographic (TLC) separation techniques, especially for large test series, is desirable. In addition, TLC allows easy control of a synthetic process by laboratory personnel.

With the introduction by Günther *et al.*[14] in 1983 of racemic separations by TLC based on ligand exchange, an alternative method is available that meets the requirements mentioned above and enables rapid determination of the enantiomeric distribution at trace levels. This paper describes in detail the results of this work. For the numerous and interesting papers dealing with paper chromatographic (PC) or TLC enantiomeric separations on adsorbents with chiral cavities (such as cellulose, cyclodextrin, triacetylcellulose), the reader is referred to the following literature: PC, refs. 15–34; TLC, refs. 35–46. Owing to extremely long developing times[44] these layers, with the exception of triacetylcellulose[45], today find only limited application for routine control of the optical purity of chiral compounds.

This review covers procedures for the separation of underivatized samples on chiral stationary phases. Derivatization procedures[47,48] via ligand exchange are not discussed.

TLC ENANTIOMERIC SEPARATION VIA LIGAND EXCHANGE

Mechanism of separation

Recent experimental results have confirmed the principle of chiral interaction (three-point-rule) postulated as early as 1952 by Dalgliesh[19]. Additionally the results prove that the separation models developed for ligand exchange by high-performance liquid chromatography (HPLC)[11,49,50] are also valid for TLC: the diastereomeric complexes formed with the metal ion (*e.g.* Cu^{2+}) and the chiral adsorbent have different stabilities for the different antipodes, and thus chromatographic separation is achieved.

Separation of racemates on reversed-phase layers

Because, like others, our experiments to reduce the development times on cellulose by variation of the eluent composition failed, the commercial availability of reversed-phase (RP) precoated plates offered a good opportunity to study the racemic separation of amino acids via ligand exchange on these layers.

Based on the work of Davankov *et al.*[10,49], who modified commercial HPLC columns for distribution chromatography with alkyl derivatives of L-amino acids, such as *n*-decyl-L-histidine or *n*-hexadecyl-L-proline, we used (2*S*,4*R*,2′*RS*)-N-(2′-hydroxydodecyl)-4-hydroxyproline (1)[51], which was easier to prepare, as a chiral selector.

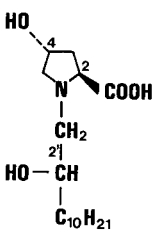

(1)

Preparation of an enantioselective layer. The following impregnation procedure proved to be most efficient. A glass plate coated with hydrophobic silica gel (RP 18 TLC) was dipped into a 0.25% copper(II) acetate solution (methanol–water, 1:9, v/v) and dried. Then the plate was immersed in a 0.8% methanolic solution of the chiral selector for 1 min. After air-drying, the plate was ready for enantiomeric separations. The first results of this work were published in 1984[52].

Further development of the plate has been made in collaboration with Macherey-Nagel (Düren, F.R.G.). The plate is now commercially available as a precoated plate under the trade name Chiralplate: preparatory dipping is no longer required.

Selection of mobile phase and influence of mobile phase composition on separation of enantiomers. The choice of eluents for the separation experiments described here was based on experience with HPLC mobile phases. In order to achieve short analysis times, ternary mixtures of a water-miscible alcohol, water and acetonitrile proved useful. Most racemate separations could be accomplished using one of two eluent systems: eluent A, methanol–water–acetonitrile (50:50:200, v/v/v), development time *ca.* 30 min; eluent B, methanol–water–acetonitrile (50:50:30, v/v/v), development time *ca.* 60 min. As expected, a decrease in the acetonitrile content significantly increased the development times.

For some substances, however, different eluent systems were more suitable: eluent C, methanol–water (10:80, v/v), development time *ca.* 90 min, for leucine; eluent D, acetone–methanol–water (10:2:2, v/v/v), development time *ca.* 50 min, for alanine and serine; eluent E, dichloromethane–methanol (45:5, v/v), development time *ca.* 20 min, for α-hydroxy acids.

Brinkman and Kamminga[53] systematically investigated the influence of binary mixtures on the enantiomeric separation of different amino acids. With TLC precoated plates (Chiralplate) of size 4 cm × 6 cm, they separated the enantiomers in 4 min in water–acetonitrile (20:80).

Chromatographic conditions. The best results on the precoated plate (Chiralplate) were obtained with the following conditions. Method: ascending, one-dimensional development in a TLC chamber with chamber saturation. Plates: TLC precoated Chiralplates (Cat. No. 811055/056, Macherey-Nagel); size, 10 cm × 20 cm; layer thickness, 0.25 mm. With eluents A, B, and C, 2 μl of a 1% solution of the racemate (methanol or methanol–water) were applied. With eluent D, 2 μl of a 0.5% solution of the racemate [0.1 *M* hydrochloric acid–methanol (1:1, v/v)] were applied. With eluent E, 2 μl of a 0.5% solution of the racemate (methanol) were applied. The migration distance was 13 cm.

Different detection methods were used, depending on the type of compound. For proteinogenic and non-proteinogenic amino acids, the dried plates were dipped for 3 s in a 0.3% ninhydrin solution in acetone (Tauchfix, Baron) and then dried in a drying cabinet for *ca.* 5 min at 110°C. Red derivatives formed on a white background. For α-hydroxycarboxylic acids, 1.82 g of vanadium pentoxide (Merck, Art. 824) were weighed into a 100-ml measuring flask, 30 ml of 1 *M* sodium carbonate were added and completely dissolved by treatment in an ultrasonic bath. After cooling, 46 ml of 2.5 *M* sulphuric acid and acetonitrile to 100 ml were added. The dried plates were briefly (set 2 s on the Tauchfix) dipped into this solution and then left to stand at room temperature for *ca.* 45 min. Blue derivatives formed on a yellow background.

SELECTED EXAMPLES OF SEPARATION

With the technique described, more than 100 racemate separations have been accomplished by our group, most of which have been published[52,54–61]. For this reason we shall not describe all the examples in this paper, but rather demonstrate the broad range of application of this method for some selected classes of compounds, such as amino acid and peptide analysis; the enantiomeric separation of α-hydroxycarboxylic acids will be discussed in detail.

Amino acids

Thus far, twelve proteinogenic amino acids have been separated without

TABLE I

TLC SEPARATION OF PROTEINOGENIC AND NON-PROTEINOGENIC AMINO ACIDS*

Racemate	R_F *value*	*(Configuration)*	*Eluent***
Alanine	0.69 (D)	0.73 (L)	D
Aspartic acid	0.50 (D)	0.55 (L)	A
Glutamic acid	0.54 (D)	0.59 (L)	A
Glutamine	0.41 (L)	0.55 (D)	A
Isoleucine	0.47 (D)	0.58 (L)	A
Leucine	0.53 (D)	0.63 (L)	C
Methionine	0.54 (D)	0.59 (L)	A
Valine	0.54 (D)	0.62 (L)	A
Phenylalanine	0.49 (D)	0.59 (L)	A
Serine	0.73 (D)	0.76 (L)	D
Tyrosine	0.58 (D)	0.66 (L)	A
Tryptophan	0.51 (D)	0.61 (L)	A
Proline	0.41 (D)	0.47 (L)	A
Cysteine (as thiazolidine-4-carboxylic acid)	0.59 (D)	0.69 (L)	A
tert.-Leucine	0.40 (D)	0.51 (L)	A
Norleucine	0.53 (D)	0.62 (L)	A
allo-Isoleucine	0.51 (D)	0.61 (L)	A
Norvaline	0.49 (D)	0.56 (L)	A
allo-4-Hydroxyproline	0.41 (L)	0.59 (D)	A
2-Phenylglycine	0.57 (D)	0.67 (L)	A
2-Cyclopentylglycine	0.43	0.50	A
Ethionine	0.52 (D)	0.59 (L)	A
(1-Naphthyl)-alanine	0.49 (D)	0.56 (L)	A
(2-Naphthyl)-alanine	0.44 (D)	0.59 (L)	A
O-Benzylserine	0.54 (D)	0.65 (L)	A
O-Benzyltyrosine	0.48 (D)	0.64 (L)	A
4-Methyltryptophan	0.50	0.58	A
4-Methoxyphenylalanine	0.52	0.64	A
5-Methoxytryptophan	0.55	0.66	A
Methioninesulphone	0.62 (D)	0.66 (L)	A
Ethioninesulphone	0.55	0.59	A
Selenomethionine	0.53 (D)	0.61 (L)	A
Dopa	0.47 (L)	0.58 (D)	B

* Migration distance 13 cm; chamber saturation.

** (A) Methanol–water–acetonitrile, 50:50:200 (v/v/v); (B) methanol–water–acetonitrile, 50:50:30 (v/v/v); (C) methanol–water, 10:80 (v/v); (D) acetone–methanol–water, 10:2:2 (v/v/v).

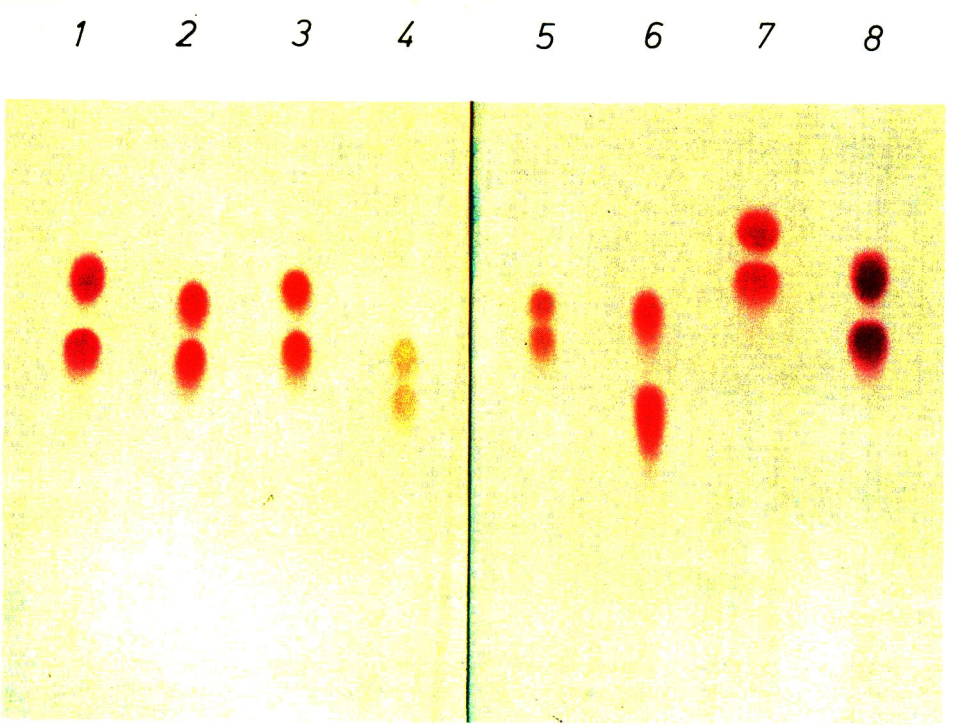

Fig. 1. Photograph of a thin-layer chromatogram of proteinogenic amino acids on Chiralplate. Spots: 1 = phenylalanine; 2 = valine; 3 = isoleucine; 4 = proline; 5 = methionine; 6 = glutamine; 7 = tyrosine; 8 = tryptophan.

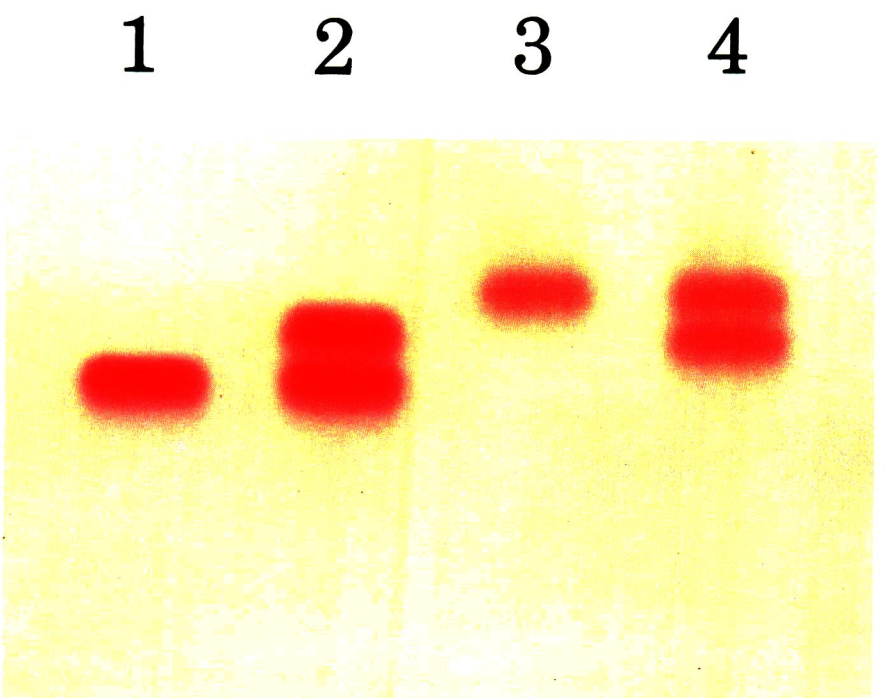

Fig. 2. Photograph of a thin-layer chromatogram of proteinogenic amino acids on Chiralplate. Spots: 1 = D-alanine; 2 = D,L-alanine; 3 = L-serine; 4 = D,L-serine. Application: 10 mm streak (Linomat IV, Fa. Camag).

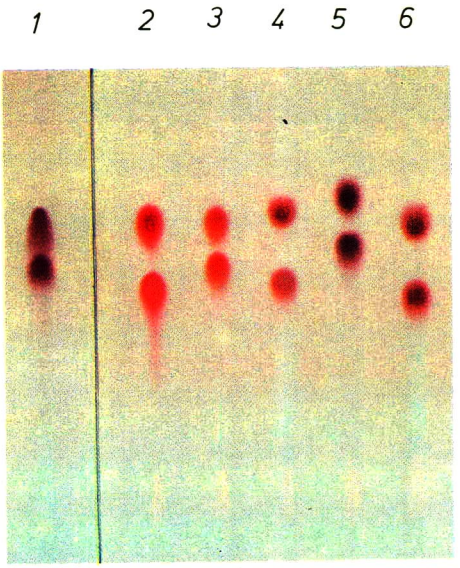

Fig. 3. Photograph of a thin-layer chromatogram of non-proteinogenic amino acids on Chiralplate. Spots: 1 = dopa; 2 = *tert.*-leucine; 3 = *allo*-isoleucine; 4 = O-benzyltyrosine; 5 = 5-methoxytryptophan; 6 = (2-naphthyl)alanine.

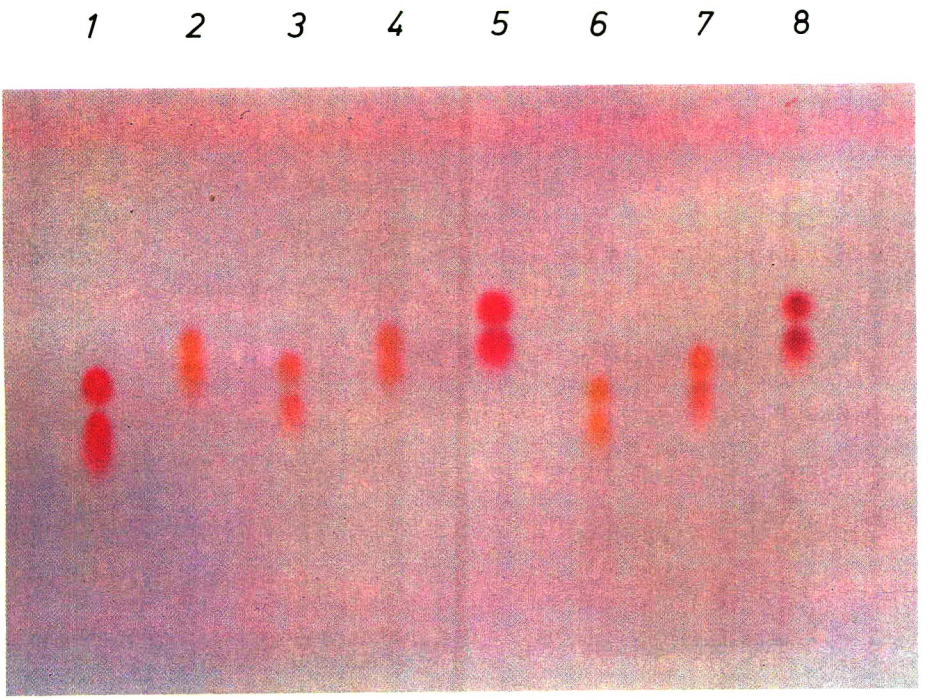

Fig. 4. Photograph of a thin-layer chromatogram of dipeptides on Chiralplate. Spots: 1 = D-Leu-L-Leu and L-Leu-D-Leu; 2 = Gly-D,L-Val; 3 = Gly-D,L-Leu; 4 = Gly-D,L-Phe; 5 = D-Ala-L-Phe and L-Ala-D-Phe; 6 = Gly-D,L-Trp; 7 = Gly-D,L-Ileu; 8 = D-Met-L-Met and L-Met-D-Met.

TABLE II

TLC ENANTIOMERIC SEPARATION OF DIPEPTIDES*

Dipeptide	R_F *value*	*(Configuration)*	*Eluent***
Gly-D,L-Phe	0.57(L)	0.63(D)	B
Gly-D,L-Leu	0.53(L)	0.60(D)	B
Gly-D,L-Ileu	0.54(L)	0.61(D)	B
Gly-D,L-Val	0.58(L)	0.62(D)	B
Gly-D,L-Trp	0.48(L)	0.55(D)	B
D-Leu-L-Leu	0.48		B
L-Leu-D-Leu	0.57		B
D-Leu-L-Leu	0.19		A
L-Leu-D-Leu	0.26		A
D-Ala-L-Phe	0.59		B
L-Ala-D-Phe	0.65		B
D-Ala-L-Phe	0.21		A
L-Ala-D-Phe	0.26		A
D-Met-L-Met	0.64		B
L-Met-D-Met	0.71		B
D-Met-L-Met	0.29		A
L-Met-D-Met	0.33		A

* Migration distance 13 cm, chamber saturation.

** (A) Methanol–water–acetonitrile, 50:50:200 (v/v/v); (B) methanol–water–acetonitrile, 50:50:30 (v/v/v).

derivatization (Table I; Figs. 1 and 2); cysteine can be determined as thiazolidine-4-carboxylic acid, which is formed from cysteine by a simple reaction with formaldehyde.

The separation of non-proteinogenic amino acids is shown in Fig. 3.

Dipeptides

For the enantiomeric separation of dipeptides (see Table II) it is remarkable that the enantiomer with the C-terminal L-configuration always has lower R_F value than the one with the C-terminal D-configuration (see Fig. 4). This method can also resolve diastereomeric dipeptides as well[57].

TABLE III

TLC SEPARATION OF ENANTIOMERIC α-METHYLAMINO ACIDS*

Racemate	R_F *value*	*(Configuration)*	*Eluent***
α-Methylmethionine	0.56(D)	0.64(D)	A
α-Methylserine	0.56(L)	0.67(D)	B
α-Methyltyrosine	0.63(D)	0.70(L)	A
α-Methylphenylalanine	0.53(L)	0.66(D)	A
α-Methyldopa	0.46(L)	0.66(D)	B

* Migration distance 13 cm; chamber saturation.

** (A) Methanol–water–acetonitrile, 50:50:200 (v/v/v); (B) methanol–water–acetonitrile, 50:50:30 (v/v/v).

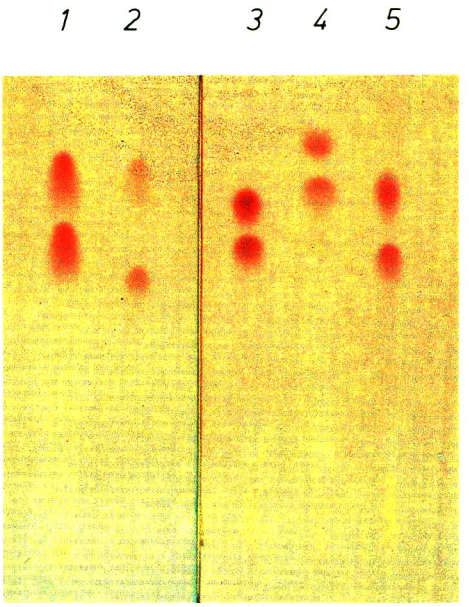

Fig. 5. Photograph of a thin-layer chromatogram of α-methylamino acids on Chiralplate. Spots: 1 = α-methylserine; 2 = α-methyldopa; 3 = α-methylmethionine; 4 = α-methyltyrosine; 5 = α-methylphenylalanine.

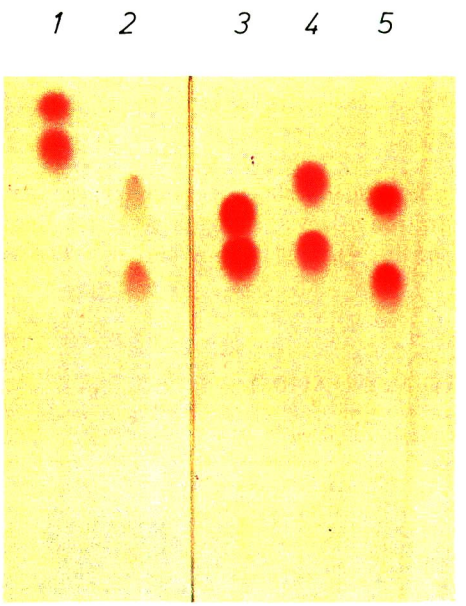

Fig. 6. Photograph of a thin-layer chromatogram of N-methyl and N-formyl amino acids on Chiralplate. Spots: 1 = N-methylvaline; 2 = N-methyl-*m*-tyrosine; 3 = N-methylleucine; 4 = N-methylphenylalanine; 5 = N-formyl-*tert.*-leucine.

TABLE IV

TLC SEPARATION OF ENANTIOMERIC N-ALKYL AND N-FORMYL AMINO ACIDS*

Racemate	R_F *value*	*(Configuration)*	*Eluent***
N-Methylleucine	0.49(L)	0.57(D)	A
N-Methylvaline	0.65(L)	0.70(D)	B
N-Methylphenylalanine	0.50(D)	0.61(L)	A
N-Methyl-*m*-tyrosine	0.36	0.52	B
N,N-Dimethylphenylalanine	0.55(D)	0.61(L)	B
N-Formyl-*tert.*-leucine	0.48 (+)	0.61 (−)	A

* Migration distance 13 cm.

** (A) Methanol–water–acetonitrile, 50:50:200 (v/v/v); (B) methanol–water–acetonitrile, 50:50:30 (v/v/v).

TABLE V

TLC SEPARATION OF HALOGENATED AMINO ACIDS*

Racemate	R_F *value*	*(Configuration)*
3-Chloroalanine	0.57	0.64
4-Bromophenylalanine	0.44	0.58
4-Chlorophenylalanine	0.46	0.59
2-Fluorophenylalanine	0.55	0.61
4-Iodophenylalanine	0.45(D)	0.61(L)
3-Fluorotyrosine	0.64	0.71
5-Bromotryptophan	0.46	0.58
Thyroxine	0.38(D)	0.49(L)

* Migration distance 13 cm; chamber saturation; eluent, methanol–water–acetonitrile, 50:50:200 (v/v/v).

TABLE VI

TLC ENANTIOMERIC SEPARATION OF OTHER CLASSES OF COMPOUNDS*

Racemate	R_F *value*	*(Configuration)*	*Eluent***
Thiazolidine-4-carboxylic acid	0.59(D)	0.69(L)	A
5,5-Dimethylthiazolidine-4-carboxylic acid hydrochloride	0.48 (D)	0.62(L)	A
3-Amino-3,5,5-trimethylbutyrolactone hydrochloride	0.50	0.59	A
Pipecolic acid	0.51	0.58	D

* Migration distance 13 cm; chamber saturation.

** (A) Methanol–water–acetonitrile, 50:50:200 (v/v/v); (D) acetone–methanol–water, 10:2:2 (v/v/v).

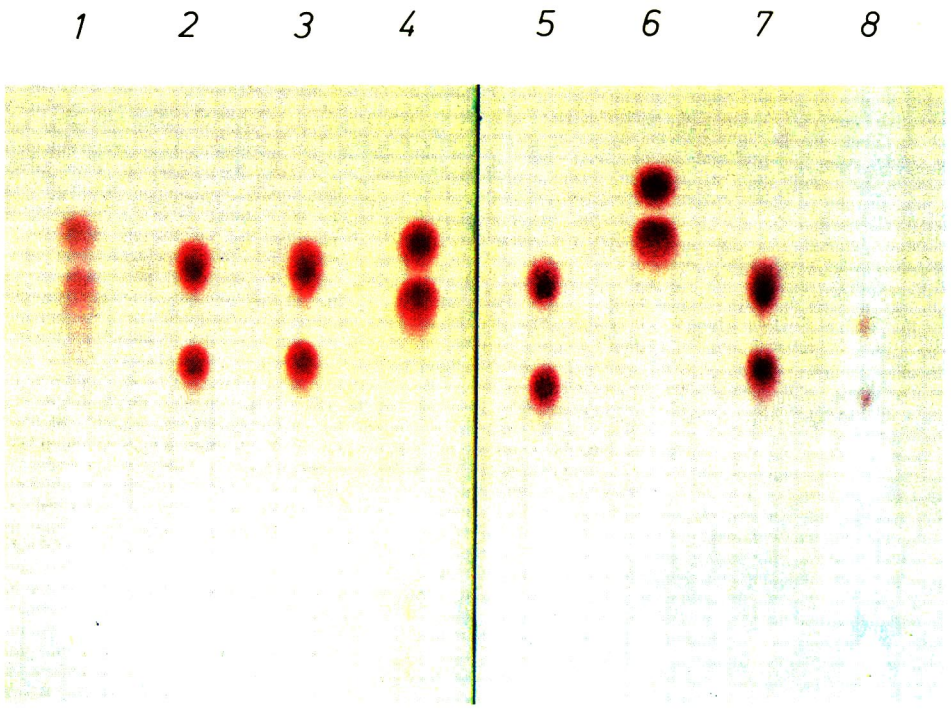

Fig. 7. Photograph of a thin-layer chromatogram of halogenated amino acids on Chiralplate. Spots: 1 = 3-chloroalanine; 2 = 4-bromophenylalanine; 3 = 4-chlorophenylalanine; 4 = 2-fluorophenylalanine; 5 = 4-iodophenylalanine; 6 = 3-fluorotyrosine; 7 = 5-bromotryptophan; 8 = thyroxine.

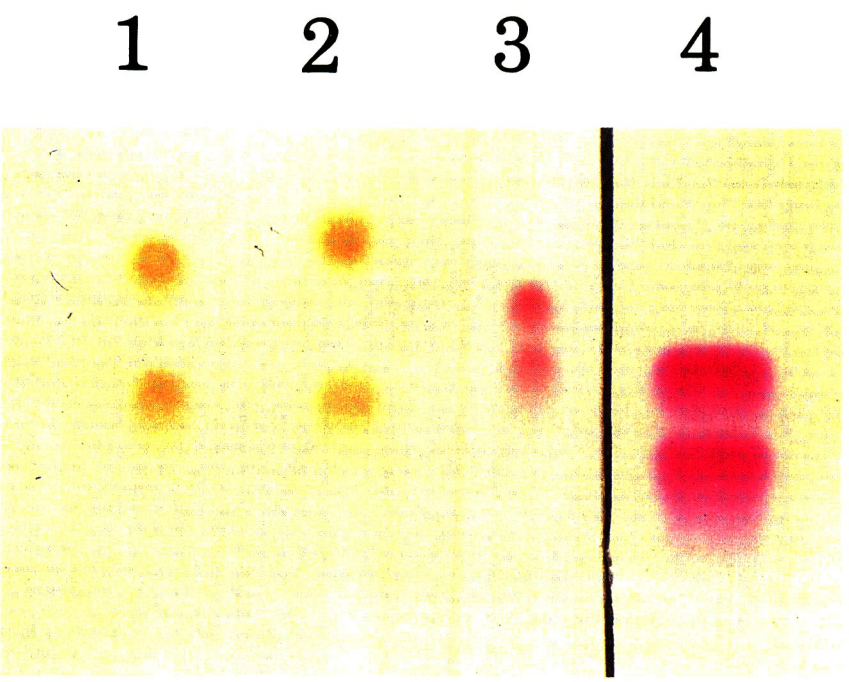

Fig. 8. Photograph of a thin-layer chromatogram of some heterocyclics on Chiralplate. Spots: 1 = thiazolidine-4-carboxylic acid; 2 = 5,5-dimethylthiazolidine-4-carboxylic acid; 3 = 3-amino-3,5,5-trimethylbutyrolactone hydrochloride; 4 = pipecolic acid.

Wang *et al.*[46] compared the migration and separation characteristics of dipeptides on Chiralplate with those on cellulose.

α-Methylamino acids

α-Methylamino acids are very important as specific enzyme inhibitors. Furthermore they can be directly inserted into numerous biologically active peptides to modify their range of activity.

Separations in this field with different eluent systems have been published independently (Fig. 5, refs. 60 and 62). As can be seen from Table III, D,L-methyldopa can also be separated without problem[59].

N-Alkylamino acids

Table IV and Fig. 6 show the separation of enantiomeric N-alkylamino acids and N-formyl-*tert.*-leucine. Further examples have been published recently[54,55]. In contrast to the examples described above, the detection of N,N-dimethylphenylalanine was achieved with iodine. The enantiomeric separation of N-carbamoyltryptophan has also been described[63].

Halogenated amino acids

Another class of compounds that show good enantiomeric resolution is the halogenated amino acids (Table V and Fig. 7). However, a differentiation between 4-chloro-, 4-bromo- and 4-iodophenylalanines is not possible[54,55].

Heterocyclic compounds

Thiazolidine-4-carboxylic acid and 5,5-dimethylthiazolidine-4-carboxylic acid are formed by formaldehyde condensation from cysteine and penicillamine, respectively. The derivatization of penicillamine has been published[58]. Table VI and Fig. 8 present an extract from these results.

α-Hydroxycarboxylic acids

During investigation of the enantioselective degradation of the biogenic

TABLE VII

TLC ENANTIOMERIC α-HYDROXYCARBOXYLIC ACIDS*

Racemate	R_F *value*	*(Configuration)*
Mandelic acid	0.46	0.53 (L)
3-Hydroxymandelic acid	0.34	0.39
4-Hydroxymandelic acid	0.32	0.36
3,4-Dihydroxymandelic acid	0.32	0.38
Vanillic acid	0.49	0.55
Hydroxyisoleucine	0.56	0.63(L)
Hydroxyleucine (sodium salt)	0.56	0.60(L)
Hydroxymethionine (sodium salt)	0.52	0.58(L)
Hydroxyphenylalanine	0.56	0.62(L)
Hydroxyvaline	0.52	0.60(L)

* Migration distance 13 cm; eluent, dichloromethane–methanol, 45:5 (v/v).

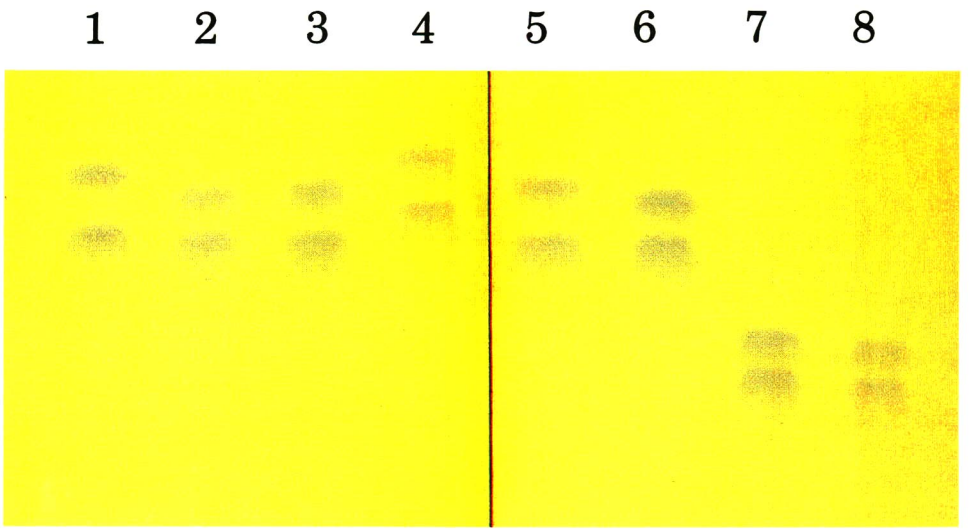

Fig. 9. Photograph of a thin-layer chromatogram of α-hydroxycarboxylic acids on Chiralplate. Spots: 1 = hydroxyisoleucine; 2 = hydroxyleucine; 3 = hydroxymethionine; 4 = hydroxyphenylalanine; 5 = hydroxyvaline; 6 = mandelic acid; 7 = 3-hydroxymandelic acid; 8 = 4-hydroxymandelic acid.

R-configurated catecholamines norepinephrine (noradrenaline) and epinephrine (adrenaline), Jork and Kany[64] for the first time succeeded in the enantiomeric separation of the resulting 3,4-dihydroxymandelic acid and vanillic acid, respectively, using the lipophilic eluent mixture dichloromethane–methanol (45:5, v/v) and post-chromatographic detection with 2,6-dichloroquinone-4-chloroimide (Merck, Art. 3037).

In preparative chemistry, mandelic acid is gaining importance as a multifunctional chiral building block and reagent for racemate separation. Table VII and Fig. 9 show the resolution of further enantiomeric α-hydroxycarboxylic acids. Vanadium pentoxide was especially useful for post-chromatographic derivatization[65].

QUANTITATIVE EVALUATION OF TLC-SEPARATED ENANTIOMERS

General

Phenylalanine (2), *tert.*-leucine (3), 5,5-dimethylthiazolidine-4-carboxylic acid (4) and hydroxyphenylalanine (5) have been chosen as models for the direct quantitative evaluation of thin-layer chromatograms.

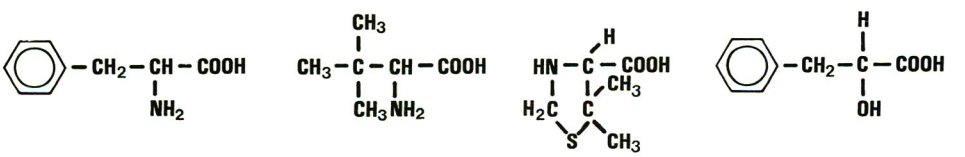

2 3 4 5

Emphasis has been placed on the evaluation of detection limits for the TLC-separated enantiomers, because exact determination of trace levels of a D- or L-enantiomer in an excess of the other is increasingly important[61,66,67].

In order to enhance specificity and sensitivity, post-chromatographic derivatization with ninhydrin or vanadium pentoxide was used. Dipping the plates into the reagent solution proved most useful because it can be automated[68]. Quantification of the minor enantiomer was achieved by *in situ* remission measurement with the CS-930 double beam scanner (Shimadzu) or the densitometer CD 60 (Desaga), and comparison with external standard solutions. Additionally, possible proportional systematic deviations were excluded by the standard addition method[69].

For every substance investigated the absorption maximum was determined independently prior to the quantification experiments.

Preparation of test solutions and standard solutions

Successful separation of amino acids on the TLC plate inherently depends on the concentration and often on the hydrochloric acid content of the applied solution. Addition of hydrochloric acid generally improves the solubility of the amino acids and often considerably enhances the enantiomeric resolution.

Phenylalanine test solution (U_{Ph}). Weigh 200 mg of D-phenylalanine into a 10-ml measuring flask and fill to the mark with 50% methanolic hydrochloric acid solution (10 g of acid per litre of solution).

Phenylalanine standard solution (V_{Ph}). Weigh 100 mg of L-phenylalanine into a 100-ml measuring flask and fill to the mark with methanol–0.1 *M* hydrochloric acid (1:1).From this stock solution the standard solutions are prepared for the working range required. Dilute 200 µl, 400 µl, 600 µl, etc. of the stock solution to 10 ml with hydrochloric acid (10 g of acid per litre of solution)–methanol (1:1). Thus 0.1–0.3% solutions of the L-enantiomer relative to the 200 mg of D-phenylalanine are obtained.

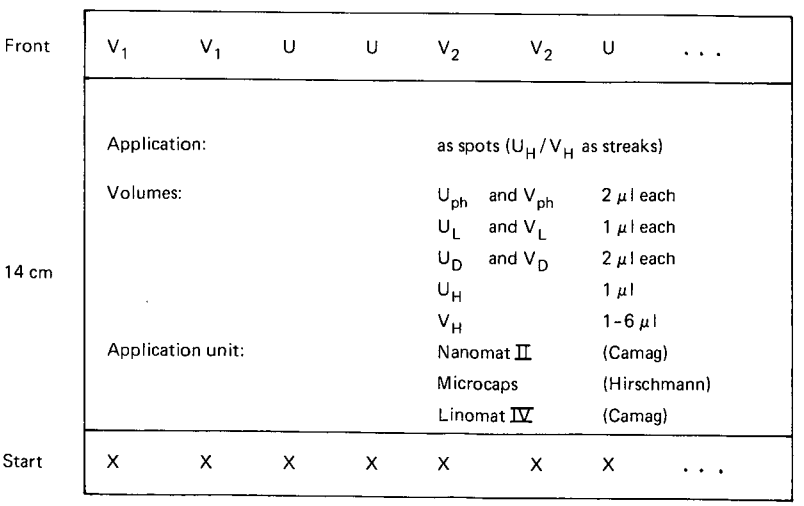

Fig. 10. The application pattern for direct quantification of the enantiomers of phenylalanine (Ph). *tert.*-leucine (L), 5,5-dimethylthiazolidine-4-carboxylic acid (D) and hydroxyphenylalanine (H).

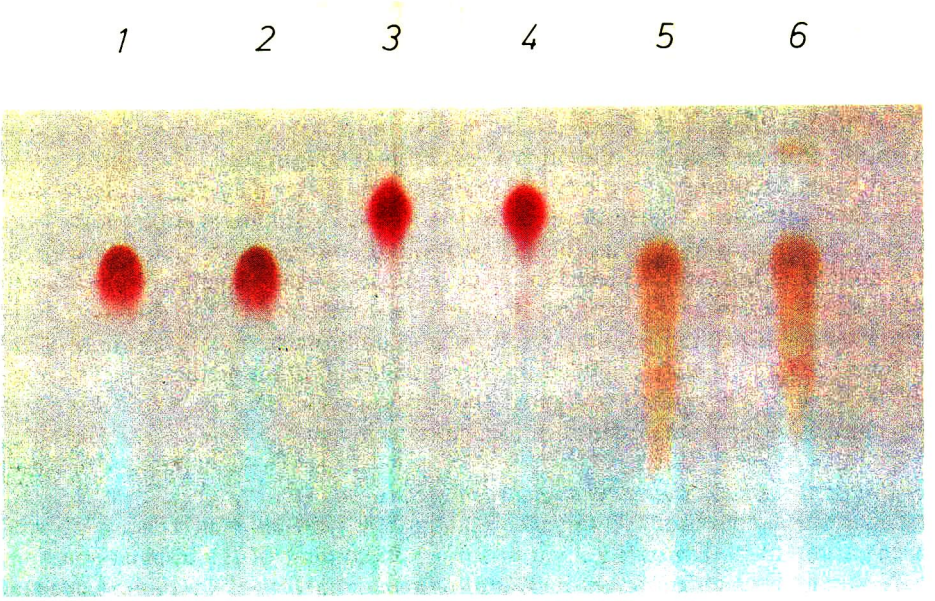

Fig. 11. Photograph of a thin-layer chromatogram on Chiralplate with eluent A. Spots: 1 = D-phenylalanine; 2 = 1% L-Phe in D-Phe; 3 = L-*tert.*-leucine; 4 = 1% D-*tert.*-leucine in L-*tert.*-leucine; 5 = D-5,5-dimethylthiazolidine-4-carboxylic acid; 6 = 3% L-5,5-dimethylthiazolidine-4-carboxylic acid in D-5,5-dimethylthiazolidine-4-carboxylic acid.

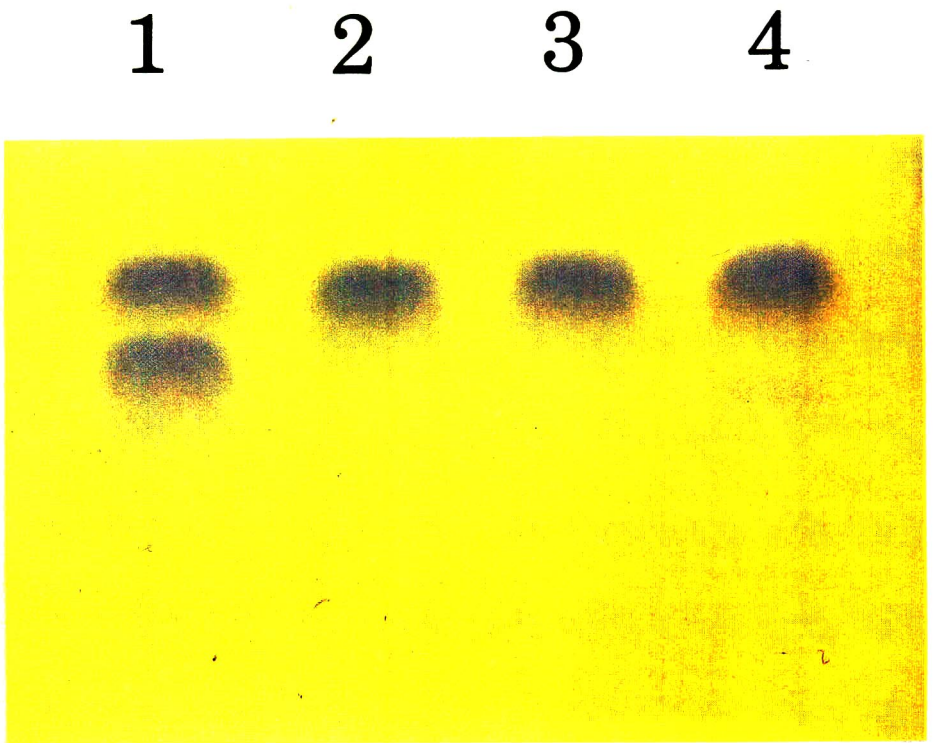

Fig. 12. Photograph of a thin-layer chromatogram on Chiralplate with eluent E. Spots: 1 = D,L-hydroxyphenylalanine; 2 = L-hydroxyphenylalanine; 3 = 3% D-hydroxyphenylalanine in L-hydroxyphenylalanine; 4 = 10% D-hydroxyphenylalanine in L-hydroxyphenylalanine.

tert.-Leucine test solution (U_L). Dissolve 200 mg of L-*tert.*-leucine in 10.0 ml of 50% methanol.

tert.-Leucine standard solution (V_L). Dissolve 100 mg of *tert.*-leucine in 100 ml of 50% methanol. Dilute 200 µl, 400 µl, 600 µl, etc. of this stock solution to 10 ml with 50% methanol to obtain 0.1–0.3% D-enantiomer relative to 200 mg of L-*tert.*-leucine.

5,5-Dimethylthiazolidine-4-carboxylic acid test solution (U_D). Add 500 µl of concentrated hydrochloric acid to 500 mg of D-5,5-dimethylthiazolidine-4-carboxylic acid and make up to 10 ml with isopropanol.

5,5-Dimethylthiazolidine-4-carboxylic acid standard solution (V_D). Add 500 µl of concentrated hydrochloric acid to 100 mg of L-5,5-dimethylthiazolidine-4-carboxylic acid and make up to 100 ml with isopropanol. Add 500 µl of concentrated hydrochloric acid to 500 µl, 1000 µl, 1500 µl, etc. of this stock solution, and make up to 10 ml with isopropanol. These solutions correspond to 0.1–0.3% of the L-enantiomer relative to 500 mg of D-5,5-dimethylthiazolidine-4-carboxylic acid.

Hydroxyphenylalanine test solution (U_H). Weigh 300 mg of L-hydroxyphenylalanine into a 10-ml measuring flask and fill to the mark with methanol.

Hydroxyphenylalanine standard solution (V_H). Dissolve 30 mg of D-hydroxyphenylalanine in 100 ml of methanol, and 1 µl, 2 µl, 3 µl, etc. of this stock solution correspond to 1–3%of the D-enantiomer relative to 300 mg of L-hydroxyphenylalanine.

Application pattern and sample volumes

For direct quantification of the enantiomers of phenylalanine, *tert.*-leucine, 5,5-dimethylthiazolidine-4-carboxylic acid and hydroxyphenylalanine the pattern of application shown in Fig. 10 has been used.

Chromatographic conditions

In general, the separation conditions for quantitative evaluation were similar to those for qualitative enantiomer separations by TLC. Any differences will be explained below. The plates were TLC precoated Chiralplates (Cat. No. 811 58, Macherey-Nagel); sizes, 20 cm × 20 cm; layer thickness, 0.25 mm. They were activated for 15 min at 110°C in a drying cabinet prior to use. The details of the eluents and detection procedures were as given above for the qualitative separation.

Spectrophotometric conditions

Instrument, double-beam TLC scanner CS 930 (Shimadzu, Japan); measuring set-up, monochromator —sample (remission); light source, tungsten lamp; wavelength, see under remission-location curves in figures; measuring area, 1.2 mm × 3 mm; feed, 0.05 mm.

Instrument, densitometer CD 60 (Desaga, F.R.G.); measuring set-up, monochromator —sample (remission); light source, tungsten lamp; wavelength, see under remission-location curves in figures; measuring area, 6.0 mm × 0.4 mm; feed, 0.1 mm.

For the evaluation, the absorption curve is measured in the chromatographic direction. The measured peak areas resp. peak heights, plotted against the amount of sample per spot, give the calibration lines.

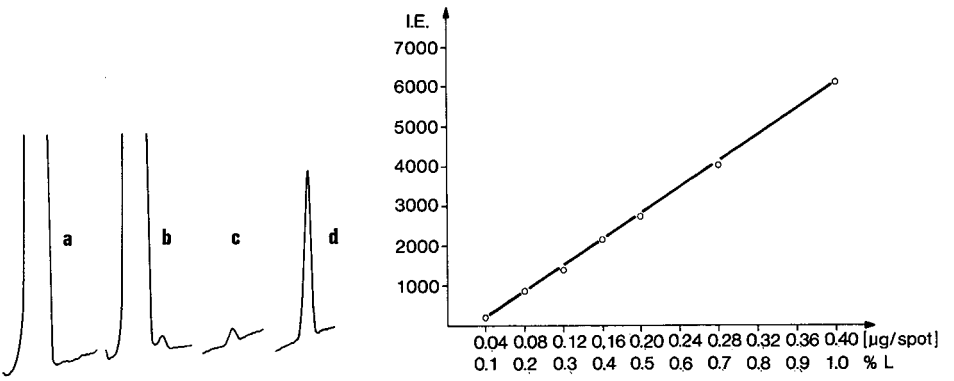

Fig. 13. Remission-location curves; (a) D-phenylalanine (Phe); (b) D-Phe spiked with 0.1% L-Phe; (c) 0.1% L-Phe; (d) 1% L-Phe. Conditions: eluent A; λ = 540 nm.

Fig. 14. Calibration line for L-phenylalanine (V). I.E. = integration units; $y = -463 + 16349\,x$; $r = 0.9992$; $S_{x_0} = 0.0038$ µg/spot (69); λ = 540 nm.

RESULTS

For better visualization of zones in Figs. 11 and 12, samples were spiked with more of the D-enantiomer than cited for the remission-location curves.

Phenylalanine

Fig. 13 shows, among others, the remission-location curve for two standard solutions with widely different L-phenylalanine concentrations. The calibration line in Fig. 14 shows that quantitative determinations of L-phenylalanine in D-phenylalanine is possible in a working range of 0.04–0.4 µg/spot without any problem.

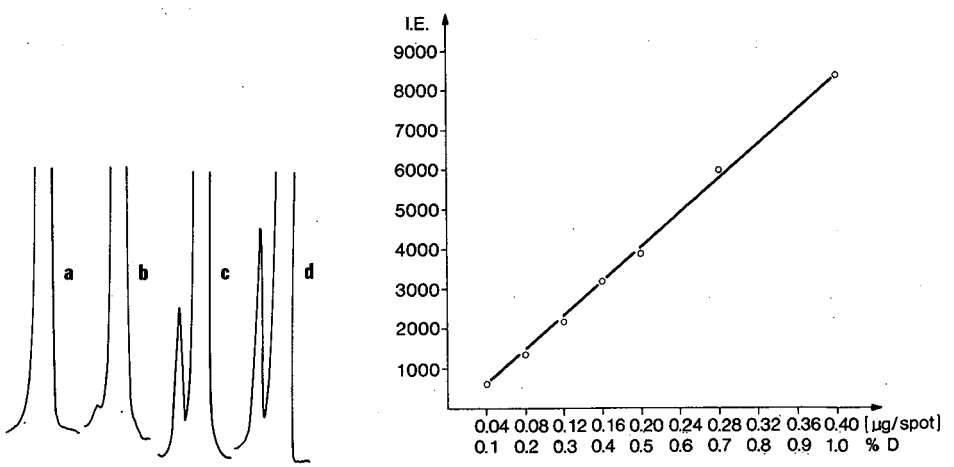

Fig. 15. Remission-location curves: (a) L-*tert.*-leucine (Degussa); (b) L-*tert.*-Leu + 0.1% D-*tert.*-Leu; (c) L-*tert.*-Leu + 1% D-*tert.*-Leu; (d) external reference sample. Conditions: eluent C; λ = 520 nm.

Fig. 16. Calibration line for D-*tert.*-leucine. I.E. = integration units; $y = -375 + 21984x$; $S_{x_0} = 0.0060$ µg/spot; $r = 0.9980$; λ = 520 nm.

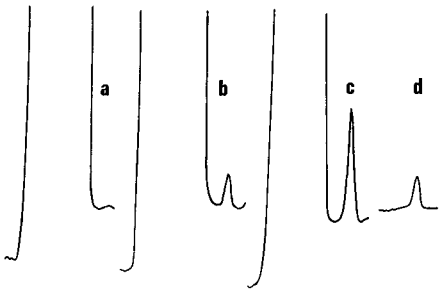

Fig. 17. Remission-location curves; (a) D-5,5-dimethylthiazolidine-4-carboxyiic acid; (b) and (c) D-5,5-dimethylthiazolidine-4-carboxylic acid + 0.1% and 0.5%, respectively, of the L-enantiomer; (d) 0.1% L-5,5-dimethylthiazolidine-4-carboxylic acid. Conditions: eluent A; λ = 370 nm.

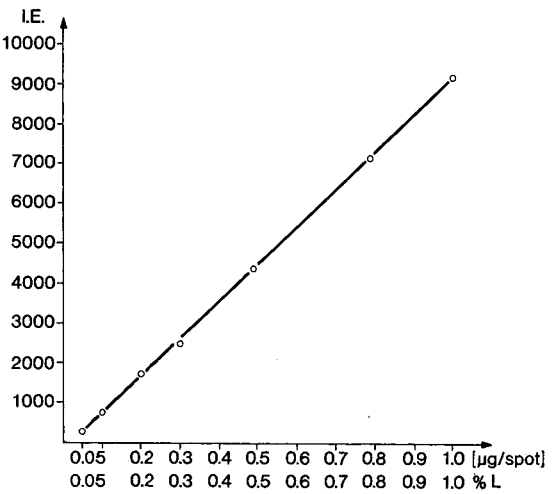

Fig. 18. Calibration line for L-5,5-dimethylthiazolidine-4-carboxylic acid. I.E. = integration units; $y = -192 + 9224x$; S_{x_0} = 0.015 µg/spot; r = 0.9985; λ = 370 nm.

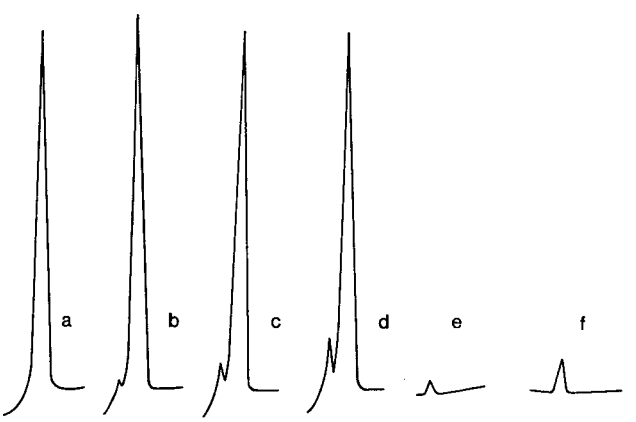

Fig. 19. Remission-location curves: (a) L-hydroxyphenylalanine; (b) 1% D-hydroxyphenylalanine in the L-enantiomer; (c) 3% D-hydroxyphenylalanine in the L-enantiomer; (d) 5% D-hydroxyphenylalanine in the L-enantiomer; (e) 1% D-hydroxyphenylalanine; (f) 3% D-hydroxyphenylalanine.

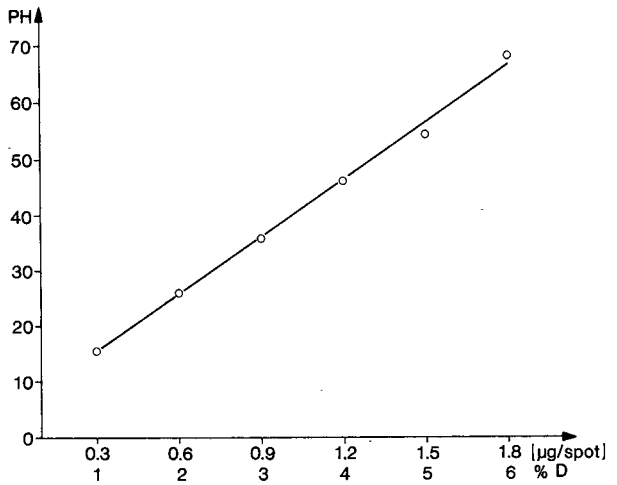

Fig. 20. Calibration line for D-hydroxyphenylalanine (V). PH = peak height; $y = 4.91 + 34.2x$; $r = 0.9981$; $S_{x_0} = 0.038$ µg/spot; $\lambda = 590$ nm.

tert.-Leucine

The remission-location curve (Fig. 15) and the calibration line (Fig.16) of *tert.*-leucine show clearly that the D-enantiomer can also be determined with high sensitivity in the L-amino acid.

5,5-Dimethylthiazolidine-4-carboxylic acid

The remission-location curve (Fig. 17) and the calibration line (Fig. 18) show that even 0.1–1% of the L-enantiomer can easily be quantitated.

α-Hydroxyphenylalanine

The remission-location curve (Fig. 19) and the calibration curve (Fig. 20) show good evaluation of the amount of D-enantiomer in the working range 1–6%.

CONCLUSION

The experimental results justify the use of a densitometer for quantitation of antipodes at trace levels. Contrary to the "classical" methods GC and HPLC, TLC is very well suited for simultaneous separation of several samples and can therefore be used for economical routine analyses. Further optimization of separation conditions may even improve the actual detection limits of $\geqslant 0.1\%$ of the minor enantiomer. Racemic separations of other classes of compounds —be they derivative or nonderivative— will be studied in our laboratory.

REFERENCES

1 J. Knabe, *Dtsch. Apoth.-Ztg.*, 124 (1984) 685.
2 K. Drauz, A. Kleeman and J. Martens, *Angew. Chem.*, 94 (1982) 590; *Angew. Chem. Int. Ed. Engl.*, 21 (1982) 584.
3 H. Frank, G. J. Nicholson and E. Bayer, *Angew. Chem.*, 90 (1978) 396.

4 R. H. Liu and W. W. Ku, *J. Chromatogr.*, 271 (1983) 309–323.
5 V. Schurig, *Angew. Chem.*, 96 (1984) 733–752.
6 W. A. König, E. Steinbach and K. Ernst, *J. Chromatogr.*, 301 (1984) 129–135.
7 R. Audebert, *J. Liq. Chromatogr.*, 2 (1979) 1063–1095.
8 W. H. Pirkle, D. W. House and J. M. Finn, *J. Chromatogr.*, 192 (1980) 143–158.
9 G. Blaschke, *Angew. Chem.*, 92 (1980) 14–25.
10 V. A. Davankov, A. S. Bochkov and Yu. P. Belov, *J. Chromatogr.*, 218 (1981) 547–557.
11 W. Lindner, *Chimia*, 35 (1981) 294–307.
12 S. Weinstein, M. H. Engel and P. E. Hare, *Anal. Biochem.*, 121 (1982) 370–377.
13 G. Gübitz, *GIT*, Suppl. 4 (1985) 6–11.
14 K. Günther, J. Martens and M. Schickedanz, *EP-PS 143147*, Degussa AG, Hanau.
15 M. Kotake, T. Sakan, N. Nakamura and S. Senoh, *J. Am. Chem. Soc.*, 73 (1951) 2973.
16 G. B. Bonino and V. Carassiti, *Nature (London)*, 167 (1951) 569.
17 J. Fujisawa and J. Osaka, *City Med. Center*, 1 (1951) 7–13.
18 M. Mason and C. P. Berg, *J. Biol. Chem.*, 195 (1952) 515.
19 C. E. Dalgliesh, *J. Chem. Soc.*, (1952) 3940.
20 K. Closs and C. M. Haug, *Chem. Ind.*, (1953) 103.
21 E. A. H. Roberts and D. J. Wood, *Biochem. J.*, 53 (1953) 332.
22 J. P. Lambooy, *J. Am. Chem. Soc.*, 76 (1954) 133.
23 R. Weichert, *Acta Chem. Scand.*, 8 (1954) 1542.
24 L. E. Rhuland, E. Work, R. F. Denman and D. S. Hoare, *J. Am. Chem. Soc.*, 77 (1955) 4844.
25 R. Weichert, *Acta Chem. Scand.*, 9 (1955) 547.
26 H. Blaschke and D. B. Hope, *Biochem. J.*, 63 (1956) 7P.
27 V. Klingmüller and L. Maier-Sihle, *Hoppe-Seyler's Z. Physiol. Chem.*, 308 (1957) 49.
28 G. Losse and H. Jeschkeit, *Pharmazie*, 15 (1960) 164.
29 J. Kikkawa, *J. Pharm. Soc., Jpn (Yakugaku Zasshi)*, 81 (1961) 732; *C.A.*, 55 (1961) 26005.
30 B. Franck and G. Schlingloff, *Justus Liebigs Ann. Chem.*, 659 (1962) 123.
31 C. L. De Ligny, H. Nieboer, J. J. M. De Vijlder and J. Willigen, *Recueil*, 82 (1963) 213.
32 S. F. Contractor and J. Wragg, *Nature (London)*, 208 (1965) 71.
33 B. Franck and G. Blaschke, *Justus Liebigs Ann. Chem.*, 695 (1966) 144.
34 R. Weichert, *Ark. Kemi*, 31 (1970) 517–532.
35 R. R. Paris, M. Sarsunova and M. Semonsky, *Ann. Pharm. Franç.*, 25 (1967) 177.
36 R. Kido, T. Noguchi, T. Tsuji, M. Kawamoto and J. Matsumura, *Wakayama Med. Rep.*, 11 (1967) 129.
37 A. Chimiak and T. Polonski, *J. Chromatogr.*, 115 (1975) 635.
38 R. L. Munier, A. M. Drapier, C. Gervais and J. Tréfouel, *C.R. Acad. Sci. Ser. D*, 282 (1976) 1761.
39 K. Bach and H. J. Haas, *J. Chromatogr.*, 136 (1977) 186.
40 S. Yuasa, A. Shimada, K. Kameyama, M. Yasui and K. Adzuma, *J. Chromatogr. Sci.*, 18 (1980) 311–314.
41 S. Yuasa and A. Shimada, *Sci. Rep. Osaka U.*, 31 (1982) 13–22.
42 S. Yuasa, M. Itoh and A. Shimada, *J. Chromatogr. Sci.*, 22 (1984) 288–292.
43 D. W. Armstrong, *36th Pittsburgh Conference on Analytical Chemistry and Applied Spectroscopy, New Orleans, February 1985*, paper no. 1138; published as A. Alak and D. W. Armstrong, *Anal. Chem.*, 58 (1986) 582–584.
44 S. Yuasa, A. Shimada, M. Isoyama, T. Fukuhara and M. Itoh, *Chromatographia*, 21 (1986) 79–82.
45 M. Faupel, *4th International Symposium on Instrumental TLC, Selvino/Bergamo, Italy, 1987.*
46 K. T. Wang, S. T. Chen and L. C. Lo, *Z. Anal. Chem.*, 324 (1986) 339–340.
47 S. Weinstein, *Tetrahedron Lett.*, 25 (1984) 985–986.
48 N. Grinberg and S. Weinstein, *J. Chromatogr.*, 303 (1984) 251–255.
49 V. A. Davankov, A. S. Bochkov and A. A. Kurganov, *Chromatographia*, 13 (1980) 677.
50 A. A. Kurganov, T. M. Ponomaryova and V. A. Davankov, *Inorg. Chim. Acta*, 86 (1984) 145–149.
51 J. Martens, H. Weigel, E. Busker and R. Steigerwald, *DE-PS 31 43 726*, Degussa AG, Hanau.
52 K. Günther, J. Martens and M. Schickedanz, *Angew. Chem.*, 96 (1984) 514; *Angew. Chem. Int. Ed. Engl.*, 23 (1984) 506.
53 U. A. Th. Brinkman and D. Kamminga, *J. Chromatogr.*, 330 (1985) 375–378.
54 K. Günther, J. Martens and M. Schickedanz, *Naturwissenschaften*, 72 (1985) 149.
55 K. Günther and R. Rausch, *Proceedings of the 3rd International Symposium on Instrumental HPTLC, Würzburg, 1985*, Institute for Chromatography, Bad Dürkheim, 1985, pp. 469–474.
56 K. Günther, J. Martens and M. Schickedanz, *Z. Anal. Chem.*, 322 (1985) 513.

57 K. Günther, J. Martens and M. Schickedanz, *Angew. Chem.*, 98 (1986) 284; *Angew. Chem. Int. Ed. Engl.*, 25 (1986) 278.
58 K. Günther, J. Martens and M. Schickedanz, *Arch. Pharm. (Weinheim Ger.)*, 319 (1986) 461.
59 K. Günther, J. Martens and M. Schickedanz, *Arch. Pharm. (Weinheim Ger.)*, 319 (1986) 572.
60 K. Günther, M. Schickedanz, K. Drauz and J. Martens, *Z. Anal. Chem.*, (1986) 325.
61 K. Günther, *GIT*, Suppl. 3 (1986) 6–12.
62 H. Brückner, I. Bosch, T. Graser and P. Fürst, *J. Chromatogr.*, 395 (1987) 569–590.
63 L. K. Gont and S. K. Neuendorf, *J. Chromatogr.*, 391 (1987) 343–345.
64 H. Jork and E. Kany, *GDCh-Fortbildungskurs*, No. 301, Saarbrücken, 1986.
65 R. Klaus and W. Fischer, *Chromatographia*, 23 (1987) 137–140.
66 K. Günther and M. Schickedanz, *GIT*, Suppl. 3 (1987) 27–32.
67 K. Günther and R. Rausch, *4th International Symposium on Instrumental TLC, Selvino/Bergamo, Italy, 1987.*
68 W. Funk and M. Heiligenthal, *GIT*, Suppl. 4 (5) (1984) 49–51.
69 W. Funk, V. Dammann, C. Vonderheid and G. Oehlmann, *Stat. Methoden in der Wasseranalytik*, VCH Weinheim,1985.

Journal of Chromatography, 448 (1988) 31–39
Elsevier Science Publishers B.V., Amsterdam — Printed in The Netherlands

CHROM. 20 597

SAMPLE SOLVENT EFFECTS IN AN APPARENT CHIRAL HIGH-PERFORMANCE LIQUID CHROMATOGRAPHIC SEPARATION ON β-CYCLODEXTRIN

TERRY D. WILSON
Pharmaceutical Sciences Department, Sterling-Winthrop Research Institute, Rensselaer, NY 12144 (U.S.A.)
(Received April 25th, 1988)

SUMMARY

The effect of sample solvent on chromatographic peak shape using a β-cyclodextrin column has been investigated. Sample solvents ranging in polarity from hexane to mobile phase (water–methanol–0.5 *M* pH 4.5 borate buffer, 600:400:1) were used with assessments of column efficiency made by calculating theoretical plates as $N_{5\sigma}$, $N_{4\sigma}$ and N_{SYS}. Best agreement with observed peak shape resulted from use of $N_{5\sigma}$ especially in the narrow polarity span from 40 to 100% methanol. No chiral separation was obtained on the cyclodextrin column for the aminoalkylindole compounds investigated, although one possessed a naphthaldehyde substituent which should have promoted such separation.

INTRODUCTION

The use of chiral stationary phases (CSPs) in high-performance liquid chromatographic (HPLC) separations of enantiomers has grown rapidly with recent developments along several lines of column technology. These have been reviewed recently with indications of future applicability[1–5]. Commercially available, the Pirkle stationary phases have provided separation of amines, alcohols, amino alcohols, amino esters and amino amides. Another commercially available CSP is the bonded cyclodextrin column which has been applied to separate enantiomers of mandelic acid derivatives[6], aromatic carboxylic acids[7,8], naphthylamide, dansyl and benzoyl amino acids, barbiturates and dioxalanes[9,10]. β-Cyclodextrin (β-CD) bonded to a polyether polymer has also been used in separating isomers of indole alkaloids[11]. Derivatization of enantiomers is generally necessary prior to chiral separation on either Pirkle or β-CD columns to give dansyl, naphthyl, benzoyl, dinitrobenzoyl or similar functionalities.

The effect of sample solvent on chromatographic peak shape can be major or minor and is often perplexing to the practicing chromatographer. It can be the source of differences in results calculated by peak height *versus* peak area measurements by lab automation systems and should be accounted for in all quantitations requiring precision and accuracy. Use of mobile phase as sample solvent is often sufficient to

0021-9673/88/$03.50

overcome these potential problems while it may not necessarily be the optimal solvent as far as concentration–peak response is concerned. Occasionally because of sample solubility considerations it is not possible to use mobile phase as a sample solvent and a more or less polar solvent is substituted which can affect peak shape.

The effect of sample solvent on chiral separations using a β-CD column has not been reported although the source of normal-phase chromatographic peak broadening and splitting has been ascribed to sample solvent polarity differences with the mobile phase, sample solvent volume injected and flow-rate[12–14]. A dynamic adsorption–desorption model was used in one of these studies[13] to account for observed peak splitting based on competition between the sample solvent and mobile phase for adsorption sites.

Sample solvent polarity differences from the mobile phase have also been implicated in reversed-phase peak broadening and splitting[15,16]. While in an ion-pairing reversed-phase system, peak splitting was said to be due to competition between two different retention mechanisms, ion pairing and dynamic ion exchange[17], peak broadening for cyclosporine was shown in another study to result from various conformational isomers[18]. The effect of amine modifiers on peak symmetry in the reversed-phase retention of amine solutes was shown to result from characteristics associated with hydrogen bonding to silanol sites on the silica gel support[19].

In order to measure column efficiency as related to peak broadening and splitting effects the expression for number of theoretical plates calculating peak width at 4.4% peak height (5σ), eqn. 1 can be used[20,21].

$$N_{5\sigma} = 25\,(t_R/w_{4.4})^2 \tag{1}$$

Here t_R is the retention time and $w_{4.4}$ is the peak width at 4.4% of its height. Values calculated from this expression can be contrasted to the number of theoretical plates calculated from the usual eqn. 2 or its equivalent, eqn. 3.

$$N_{4\sigma} = 5.54\,(t_R/w_{0.5})^2 \tag{2}$$

$$N_{4\sigma} = 16\,(t_R/w)^2 \tag{3}$$

where $w_{0.5}$ is the peak width at one-half the maximum height and w is the peak width at its base.

Another measure of column efficiency is N_{SYS} proposed by Foley and Dorsey[22] which is calculated as

$$N_{SYS} = \frac{41.7\,(t_R/w_{0.1})^2}{b/a + 1.25} \tag{4}$$

where $w_{0.1}$ is the peak width at one-tenth of the maximum peak height, and a and b are distances measured at the same 10% peak height from the leading edge to the perpendicular dropped from the peak maximum and the distance from this perpendicular to the tailing edge of the peak respectively.

In addition peak asymmetry can be calculated using eqn. 5 (ref. 23), for peak symmetry, or eqn. 6 (ref. 24) for tailing factor

$$S = \frac{b}{a} \tag{5}$$

$$T = \frac{a + b}{2a} \tag{6}$$

where a and b have the same meanings as above except that in eqn. 6 they are measured at 5% maximum peak height.

The present study is an investigation of the sources of an observed peak splitting phenomenon on a β-CD bonded phase originally thought to be a chiral separation. Compounds included in this study are {1-[1-methyl-2-(4-morpholinyl)ethyl]-1*H*-indol-3-yl}-(1-naphthalinyl)methanone, I, and its parent compound 1-[1-methyl-2-(4-morpholinyl)-ethyl]-1*H*-indole, II. The former should have been a good candidate for separation on a β-CD column according to published accounts although the indole group alone substituted on a chiral carbon could have given a separation of enantiomers on this column.

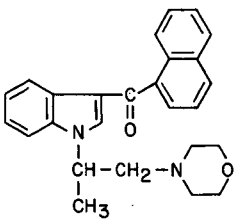

(I)

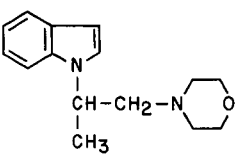

(II)

EXPERIMENTAL

Apparatus

A modular HPLC system was used consisting of a Waters 6000A pump, a Waters 440 UV absorbance detector operated at 254 nm, a Rheodyne 7125 injection valve with a 20-μl sample loop and a Fisher Recordall 5000 strip-chart recorder. The columns used were a β-CD (Cyclobond I), 25 cm × 4.6 mm I.D. (Astec, Whippany, NJ, U.S.A.), a Partisil PXS ODS-3, 25 cm × 4.6 mm I.D. (Whatman, Clifton, NJ, U.S.A.) and a Pirkle 1A ionic D-phenylglycine column, 25 cm × 4.6 mm I.D. (Regis Chemical, Morton Grove, IL, U.S.A.).

Chemicals and reagents

(+/−) I and (+/−) II were from Sterling-Winthrop Research Institute. The following chemicals were reagent grade: boric acid and copper(II) sulfate from Mallinckrodt, L-phenylalanine from Chemical Dynamics and D-camphorsulfonic acid from Eastman-Kodak. HPLC grade solvents from J. T. Baker were used including methanol, methylene chloride, acetonitrile, hexane, 2-propanol and chloroform while butyl chloride was HPLC grade from Burdick and Jackson. Water was Nanopure from a Sybron/Barnstead Nanopure II system.

Mobile phases

The mobile phase used with the β-CD and the ODS-3 columns consisted of water–methanol–0.5 *M* pH 4.5 borate buffer (600:400:1). Hexane–2-propanol, 95:5, 90:10 and 85:15 mobile phases were used with the Pirkle 1A column. Reversed-phase chiral mobile phases consisted of methylene chloride–acetonitrile–D-camphorsulfonic acid (60:40:0.005 *M* overall) to (20:80:0.05 *M* overall) and L-phenylalanine–Cu^{2+} (0.005 *M*:0.0025 *M* overall) and (0.010 *M*:0.005 *M* overall) in water. A flow-rate of 1.0 ml per min was used in all studies except in the reversed-phase ODS-3 study where 0.7 ml per min was used.

Sample preparation

Samples were prepared in mobile phase, hexane, butyl chloride, 2-propanol, chloroform, methanol, 90%, 80%, 70% and 60% (v/v) methanol in water at about 0.04 mg/ml each.

RESULTS AND DISCUSSION

The attempted chiral separation of (+/−) I began with use of a Pirkle 1A ionic chiral column with the racemate dissolved in hexane. Mobile phase variation from 95:5 to 85:15 (hexane–2-propanol) gave no separation of isomers for either the naphthyl ketone derivative I, or the parent II. Similarly use of the chiral mobile phase containing D-camphorsulfonic acid in methylene chloride–acetonitrile on a reversed-phase column was unsuccessful in separating racemic I or racemic II. This method had previously been used for a methylphenidate chiral resolution by diastereometic ion-pair formation in the mobile phase[25]. Another reversed-phase chiral separation method involving charge transfer complex formation in the mobile phase containing copper(II) ions and phenylalanine did not give separation of enantiomers of II. This method has proven useful for resolution of optical isomers of a guanine derivative[26].

The apparent separation of enantiomers of I on the β-CD column using the water–methanol–borate buffer mobile phase is shown in Fig. 1A. This was obtained when the sample was dissolved in methanol as recommended by previous reports. The fact that a single peak resulted when the sample was prepared in mobile phase, as shown in Fig. 1B, and that chromatograms identical to Fig. 1A were obtained when methanolic solutions of the separate (+) and (−) isomers of I were run alone, revealed that the separation in Fig. 1A was an artifact. This could have resulted from a mixed retention mechanism involving both reversed-phase partitioning and chiral retention by the cyclodextrin bonded phase or from kinetic factors which were accentuated by sample solvent conditions.

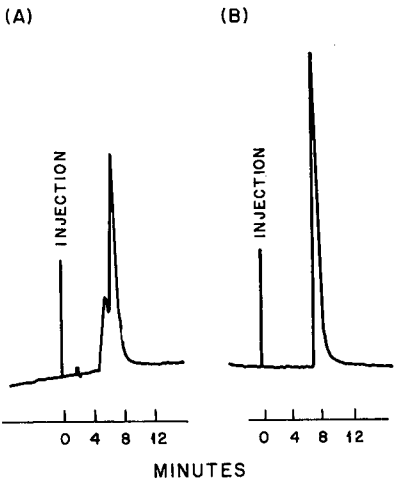

Fig. 1. Chromatograms of I at 0.04 mg/ml using a β-cyclodextrin column with the sample solvents (A) methanol and (B) mobile phase.

To indicate that the observed peak splitting did not result from a degree of reversed-phase partitioning inherent in the β-CD column, retention on an ODS-3 column with the same water–methanol–borate buffer mobile phase was studied. This possibility was investigated since separations on a β-CD column can be modified in much the same way as a reversed-phase column according to the manufacturer. Variation in methanol–water content of the mixed mobile phase can be used to give appropriate retention times for chromatographic peaks. Fig. 2A and B are chromatograms of solutions of (+/−) I in methanol and mobile phase respectively on the ODS-3 column where no splitting or shifts in retention time were seen. This indicated that the observed peak splitting on β-CD was due to a kinetic relationship between the sample in its solvent and the unique structure of the bonded phase which gives the enantio-separating power to the column.

The effect of sample solvent polarity was studied by dissolving the naphthyl ketone derivative, I, in solvents ranging from mobile phase to hexane. Results in terms of column efficiency calculated as $N_{5\sigma}$, $N_{4\sigma}$ and N_{SYS} are shown in Table I. While extremely low theoretical plate values were obtained from all three equations, it is clear that no simple relationship is followed between sample solvent polarity and column efficiency at least over this wide range of polarities. Best agreement between column efficiency and qualitatively observed peak shape was obtained by use of $N_{5\sigma}$ where the much improved peak shape using mobile phase rather than methanol as sample solvent corresponded to a near tripling of theoretical plates. Conversely, using either $N_{4\sigma}$ or N_{SYS}, a higher plate count was found for samples injected from methanol in contrast to direct observation of peak shapes.

This points out the artificially high plate count resulting from the assumption of Gaussian peak shape in eqn. 2 as well as the low order of correspondence between peak width measured at half-height and overall peak shape. This agrees with previous work by Vivilecchia *et al.*[20] on gel permeation peaks where $N_{5\sigma}$ was shown to be more closely related to peak shape than $N_{4\sigma}$. In the same way the use of eqn. 4 to

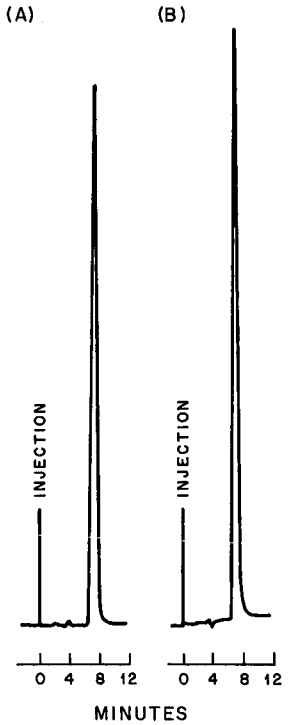

Fig. 2. Chromatograms of I at 0.04 mg/ml using an ODS-3 column with the sample solvents (A) methanol and (B) mobile phase.

calculate N_{SYS} is based on the assumption of exponentially modified gaussian (EMG) peak shape[22]. The values of N_{SYS} related well to results calculated for skewed peaks in that study and it gives a higher order of correspondence with the observed peak shape in the present study than does $N_{4\sigma}$. The inversion of plate counts for methanol *versus* mobile phase found here using eqn. 4, however, as compared to actual peak shapes most likely derives from the increased emphasis of the b term in this equation

TABLE I

COLUMN EFFICIENCY/SAMPLE SOLVENT POLARITY DATA

Sample solvent	*Polarity index**	$N_{5\sigma}$	$N_{4\sigma}$	N_{SYS}
Mobile phase	8.2**	268	407	108
Methanol	5.1	91	410	122
Chloroform	4.1	193	328	218
2-Propanol	3.9	56	107	85
Butyl chloride	1.0	29	152	9
Hexane	0.1	178	254	132

* Ref. 31.

** $P_i \approx \varphi_1 P_1 + \varphi_2 P_2$, where φ_1 and φ_2 are volume fractions and P_1 and P_2 are polarity indices for water and methanol in the mobile phase respectively.

TABLE II

PEAK ASYMMETRY/SAMPLE SOLVENT POLARITY DATA

Sample solvent	*Polarity index**	*Symmetry factor (S) (eqn. 5)*	*Tailing factor (T) (eqn. 6)*	*Qualitative peak description***
Mobile phase (40% methanol)	8.2	2.25	1.62	a
60% Methanol	7.1	3.27	2.14	a
70% Methanol	6.6	1.58	1.29	a
80% Methanol	6.1	1.36	1.18	b
90% Methanol	5.6	1.06	1.03	b
100% Methanol	5.1	0.70	0.85	c
Chloroform	4.1	1.11	1.06	c
2-Propanol	3.9	0.51	0.75	b
Butyl chloride	1.0	4.09	2.54	d
Hexane	0.1	3.0	2.0	a

* Ref. 31.

** a, Single peak with tailing; b, single peak with fronting; c, split peak on fronting edge; d, split peak on tailing edge.

appearing as an inverse cubic power. The higher b value in the tailing peak (Fig. 1B) than in the split peak (Fig. 1A), gave the lower value of N_{SYS} for mobile phase as sample solvent than for methanol. The lack of relation between column efficiency calculated using either eqn. 1, 2 or 4 and sample solvent polarity over this broad range of solvents must be concluded, however.

Results found for peak symmetry and tailing factors calculated for the various sample solvents including the narrower range of polarity differences from 100% to 40% methanol (mobile phase) are shown in Table II. Approximate agreement is found between each of these measures for each sample solvent with values > 1.0 for tailing peaks and values < 1.0 for fronting peaks. A somewhat wider variation was found for the symmetry factor than for the tailing factor. While these calculations do not give a direct indication of peak splitting, they incorrectly show that the sample solvent closest to ideal is 90% methanol. This results from the fronting portion of the peak of approximately the same length as the tailing portion.

When $N_{5\sigma}$ calculations were made for various percentages of methanol in the sample solvent, results shown in Fig. 3 were obtained. The smooth transition from

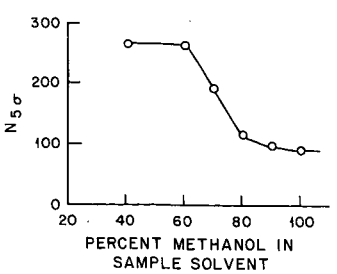

Fig. 3. Relationship between column efficiency (number of theoretical plates calculated as 5σ) and percent methanol in sample solvent for I on a β-cyclodextrin column.

split peak to a single peak is indicated as the sample solvent methanol content approached that of the mobile phase. This behavior is what could result from a kinetically controlled interaction in which a single rate of mass transfer between stationary phase and mobile phase is attained. Using methanol as sample solvent, a portion of I bound to the β-CD is solubilized and carried forth as an additional peak on the front edge of the main peak. This could result from a disruption of hydrogen bonds between I and hydroxyl groups at the mouths of the β-CD cavities when methanol is the sample solvent. It was not seen when methanol was sample solvent on the ODS-3 column because of a lower rate constant for mass transfer from stationary to mobile phase.

The question remains as to why no actual separation of enantiomers of I or II occurred on the β-CD stationary phase. According to the Dalgliesh three point theory, three bonds must be formed between the enantiomer and substrate to distinguish between (+) and (−) isomers[27]. In the case of the β-CD stationary phase whose retention mechanism was investigated by Hinze *et al.*[10], enantioselectivity results from the inclusion complexation plus two interactions with hydroxyl groups on the cyclodextrin cavity's rim. Little more is known as to exact molecular requirements for separation on a β-CD column although inclusion complexation by β-CD has previously been discussed[28–30]. From a literature review of the successful separations on this column, it is apparent that each enantiomer contains a naphthyl, indole or phenyl ring system at a distance of 1–3 atoms from the chiral center. In the present investigation the chiral carbon of the naphthyl ketone derivative (I) is five atoms away from the chiral center whereas the indole moiety of both I and II, although 1 atom away from the chiral carbon, does not fulfill the requirements for a chiral separation. It can be concluded that enantiomers must possess the correct functional groups which fulfill appropriate geometrical requirements for enantiomeric separation on- β-CD to occur. In addition, the proper choice of sample solvent must be made to avoid pseudochiral separations. The chromatographer should be aware of this possible obstacle to developing chiral separations.

ACKNOWLEDGEMENT

The author wishes to thank Ms. N. L. Valcik for manuscript typing assistance.

REFERENCES

1 D. Armstrong, *J. Liq. Chromatogr.*, 7 (1984) 353.
2 I. Wainer and T. Doyle, *LC, Liq. Chromatogr. HPLC Mag.*, 2 (1984) 88.
3 W. Pirkle, M. Hyun, A. Tsipouras, B. Hamper and B. Banks, *J. Pharm. Biomed. Anal.*, 2 (1984) 173.
4 W. H. Pirkle, M. H. Hyun and B. Bank, *J. Chromatogr.*, 316 (1984) 585.
5 I. Wainer, T. Doyle and C. Breder, *J. Liq. Chromatogr.*, 7 (1984) 731.
6 J. Debowski, J. Jurczak and D. Sybilska, *J. Chromatogr.*, 282 (1983) 83.
7 K. Feitsma, B. Drenth and R. de Zeeuw, *J. High Resolut. Chromatogr. Chromatogr. Commun.*, 7 (1984) 147.
8 K. G. Feitsma, J. Bosman, B. F. H. Drenth and R. A. de Zeeuw, *J. Chromatogr.*, 333 (1985) 59.
9 D. Armstrong and W. De Mond, *J. Chromatogr. Sci.*, 22 (1984) 411.
10 W. Hinze, T. Riehl, D. Armstrong, W. De Mond, A. Alak and T. Ward, *Anal. Chem.*, 57 (1985) 237.
11 B. Zsadon, L. Décsei, M. Szilasi, F. Tüdós and J. Szejtli, *J. Chromatogr.*, 270 (1983) 127.
12 P. Guinebault and M. Broquaire, *J. Chromatogr.*, 217 (1981) 509.

13 J. Mertens, *J. Liq. Chromatogr.*, 5 (1982) 1467.
14 D. Saunders, *J. Chromatogr. Sci.*, 15 (1977) 372.
15 K. J. Williams, A. Li Wan Po and W. J. Irwin, *J. Chromatogr.*, 194 (1980) 217.
16 P. Tseng and L. Rogers, *J. Chromatogr. Sci.*, 16 (1978) 436.
17 G. K. C. Low, P. R. Haddad and A. M. Duffield, *J. Chromatogr.*, 336 (1984) 15.
18 L. D. Bowers and S. E. Mathews, *J. Chromatogr.*, 333 (1985) 231.
19 J. S. Kiel, S. L. Morgan and R. U. Abramson, *J. Chromatogr.*, 320 (1985) 313.
20 R. Vivilecchia, B. Lightbody, N. Thimot and H. Quinn, *J. Chromatogr. Sci.*, 15 (1977) 424.
21 L. Snyder and J. Kirkland, *Introduction to Modern Liquid Chromatography*, Wiley, New York, 1979, p. 223.
22 J. Foley and J. Doresy, *Anal. Chem.*, 55 (1983) 730.
23 L. Snyder and J. Kirkland, *Introduction to Modern Liquid Chromatography*, Wiley, New York, 1979, p. 222.
24 *The U.S. Pharmacopeia*, USP Convention, Rockville, MD, 21st ed., 1985, p. 1230.
25 H. K. Lim, M. Sardessai, J. W. Hubbard and K. K. Midha, *J. Chromatogr.*, 328 (1985) 378.
26 U. Forsman, *J. Chromatogr.*, 303 (1984) 217.
27 C. Dalgliesh, *J. Chem. Soc.*, (1952) 3940.
28 J. Szejtli, *Cyclodextrins and their Inclusion complexes*, Akademiai Kiado, Budapest, 1982, p. 95.
29 M. Mikolajczyk and J. Drabowicz, *J. Am. Chem. Soc.*, 100 (1978) 2510.
30 S. Jones, D. Grant, J. Hadgraft and G. Parr, *Acta Pharm. Technol.*, 30 (1984) 213.
31 L. Snyder and J. Kirkland, *Introduction to Modern Liquid chromatography*, Wiley, New York, 1979, p. 248.

Journal of Chromatography, 448 (1988) 41–53
Elsevier Science Publishers B.V., Amsterdam — Printed in The Netherlands

CHROM. 20 553

USE OF COMPLEXING AGENTS FOR SELECTIVE SEPARATION IN HIGH-PERFORMANCE CAPILLARY ELECTROPHORESIS

CHIRAL RESOLUTION VIA CYCLODEXTRINS INCORPORATED WITHIN POLYACRYLAMIDE GEL COLUMNS

A. GUTTMAN, A. PAULUS, A. S. COHEN, N. GRINBERG* and B. L. KARGER*
Barnett Institute and Department of Chemistry, Northeastern University, 360 Huntington Avenue, Boston, MA 02115 (U.S.A.)
(First received April 18th, 1988; revised manuscript received May 24th, 1988)

SUMMARY

The incorporation of a complexing agent within a polyacrylamide gel column provides a general means of manipulating the selectivity of a capillary electrophoresis separation. As an example of this approach, chiral resolution of dansylated amino acids by high-performance capillary electrophoresis has been achieved by adding β-cyclodextrin within the gel matrix. A retention model has been developed which can be used for selectivity optimization. Various parameters, such as concentration of cyclodextrin, addition of methanol to the buffer, and temperature, have been examined in terms of their influence on retention and selectivity. From this study high-performance separations have been developed. Efficiencies as high as 100 000 plates in 15 cm have been achieved.

INTRODUCTION

High-performance capillary electrophoresis (HPCE) is a method undergoing rapid development at the present time[1–7]. With on-column detection, the method has analogy to high-performance liquid chromatography (HPLC) in terms of its instrumental approach and potential for automation. HPCE is characterized as a rapid, highly efficient separation tool. This arises in part from the ability to operate the columns at high electric field for fast migration through the capillary and, when axial diffusion controls band broadening, for high efficiency. Significant Joule heat is produced at high power levels, and this heat must be removed to take full advantage of the high fields. Capillaries are advantageous in this regard since for a given power level the temperature gradient between the column center and the walls is proportional to the square of the tube radius[8].

As in HPLC, the versatility of HPCE can be extended via the incorporation of

* Present address: Merck, Sharp & Dohme, Rahway, NJ, U.S.A.

chemical selectivity into the migration process. The need for new approaches to manipulate retention in HPCE has been noted by others[9]. Micelles have been used in open tubes for separation of neutral species[10] and differential metal chelate complexation on the surface of the micelles for selective ligand exchange[11]. In addition, selective interaction with the buffering components or other additives has been employed in the open tube for hydrophobic[12] and chiral separations[13].

As a further example of selectivity manipulation, we have explored the use of cyclodextrins (CDs) as selective complexing agents in HPCE. CDs have been shown in HPLC to separate closely related species, including chiral species, via the formation of inclusion complexes[14]. Amino acids, barbiturates, prostaglandins and other drugs have been successfully resolved using CDs, either bound to the stationary phase or as an additive to the mobile phase[15]. Interestingly, positional isomers were resolved using a modified charged form of the CDs via micellar CE[16]. Also penicillins have recently been separated by capillary isotachophoresis with the addition of CD to the buffer[17].

CDs are non-ionic cyclic polysaccharides of glucose with a shape of a toroid or hollow truncated cone. The particular name of a CD depends on the number of glucose units; α-, β-, and γ-CD corresponds to six, seven and eight glucose units, respectively. The cavity is relatively hydrophobic while the external faces are hydrophilic, with the edge of the torus of the larger circumference containing chiral secondary hydroxyl groups[18].

Fig. 1 shows a possible complex of a dansylated amino acid (Dns-AA) with β-CD[19], as well as the dimensions of this CD. Note that the non-polar dansyl portion of the molecule is found inside the cavity and that the amino group forms hydrogen bonds with the hydroxyl groups at the rim of the toroid. Selectivity or differential complexation of individual Dns-AA results from the size of the hydrophobic group with respect to the ability of the solute to penetrate the cavity. In addition, chiral selectivity can arise from hydrogen bonding at the entrance of the cavity with the chiral glucose moiety.

We first tested CDs as additives to the buffer in open tube HPCE with

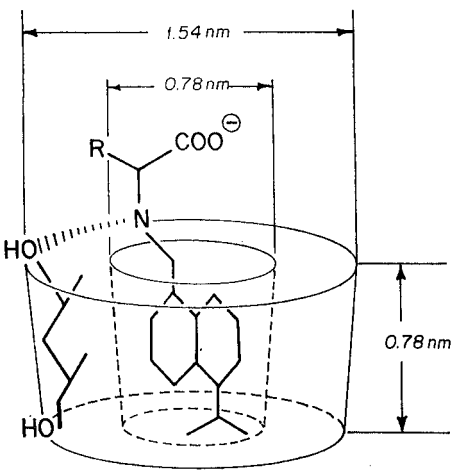

Fig. 1. Schematic diagram of the β-cyclodextrin–Dns-amino acid complex.

electroosmotic flow but found no influence on retention or separation of dansylated amino acids. Previously, we have reported on the successful use of HPCE polyacrylamide gel columns for the sodium dodecyl sulfate electrophoresis of peptide and proteins[20]. When we incorported CDs into polyacrylamide gel capillary columns, chiral separation was obtained. The addition of biorecognition agents into polyacrylamide gel slabs has also been used in affinity electrophoresis[21].

This paper reports the HPCE results with polyacrylamide gel columns on the chiral resolution of dansylated amino acids using CDs. In this work, plate counts of 50 000–100 000 in columns of 15 cm effective length have been obtained using fields up to 1000 V/cm. The principles of retention and selectivity optimization are developed. The general requirements for high-performance rapid separation in capillary electrophoresis using selective complexing agents within polyacrylamide gels are presented. This approach can readily be used with a wide variety of complexing agents for selective separations in HPCE, thus extending the scope of the methodology.

THEORY

Retention and selectivity

The retention model for separation with incorporated complexing agents follows that used in affinity electrophoresis[21,22]. In general, when a complexating agent C is present in a capillary electrophoretic system, a fraction of the solute A will occur as uncomplexed or free in solution (R) and the remainder will exist as a complex ($1 - R$). The net mobility of the solute μ will then be the weighted sum of the mobility of the free solute μ^f and the complexed solute μ^c

$$\mu = R\mu^f + (1 - R)\mu^c \tag{1}$$

The fraction R is equal to c^f/c^t where c^f = concentration of uncomplexed A and c^t = total concentration of A. R can be related to the formation constant for complexation K by

$$A + C \rightleftharpoons AC \tag{2}$$

$$K = \frac{[AC]}{[A]\,[C]} \tag{3}$$

and

$$R = \frac{c^f}{c^t} = \frac{1}{1 + K[C]} \tag{4}$$

$$1 - R = \frac{K[C]}{1 + K[C]} \tag{5}$$

The formation constant is an apparent value since concentrations are used instead of activities. Substitution of eqns. 4 and 5 into 1 yields the general mobility expression

$$\mu = \frac{\mu^f}{1 + K[C]} + \frac{K[C]\mu^c}{1 + K[C]} \tag{6}$$

The retention of a solute in electrophoresis t_R can be written as

$$t_R = \frac{l}{\mu E} = \frac{lL}{\mu V} \tag{7}$$

where l = effective length of the capillary tubing (from injection to detection point), E = electric field, V = applied voltage and L = overall length of the capillary between the two reservoirs. The relative retention α can be expressed as

$$\alpha = \frac{t_{R2}}{t_{R1}} = \frac{\mu_1}{\mu_2} \tag{8}$$

where subscripts 1 and 2 refer to the earlier and later migrating species, respectively (*e.g.*, L and D). Note that in comparison to chromatography, with gel capillary columns there is no bulk flow and therefore subtraction of the unretained solute time t_0 from t_R does not result. If open tubes with electroosmotic flow were employed, subtraction of t_0 would be required[2].

Combination of eqns. 6 and 8 yields the general expression for relative retention with complexing agents

$$\alpha = \frac{\mu_1^f}{\mu_2^f} \underbrace{\left\{\frac{1 + K_1[C]\,(\mu_1^c/\mu_1^f)}{1 + K_2[C]\,(\mu_2^c/\mu_2^f)}\right.}_{\text{I}} \cdot \underbrace{\left.\frac{1 + K_2[C]}{1 + K_1[C]}\right\}}_{\text{II}} \tag{9}$$

Three cases can be envisioned from eqn. 9. First, if the mobility of the uncomplexed solute is much greater than that of the complex AC, *i.e.*, $\mu^f \gg \mu^c$, then term I on the right hand side will be approximately unity and

$$\alpha = \frac{\mu_1^f}{\mu_2^f}\left(\frac{1 + K_2[C]}{1 + K_1[C]}\right) \tag{10}$$

As will be noted later, eqn. 10 is the relevant expression when CDs are incorporated within the gel matrix. When $K[C] \gg 1$ and for chiral pairs, eqn. 10 simplifies to

$$\alpha = \frac{K_2}{K_1} \tag{11}$$

where μ_2^f is assumed equal to μ_1^f (L and D isomers of uncomplexed species). Eqn. 11 represents the maximum value of α in the chiral system.

Secondly, the complex may move much faster than the free solute, *i.e.*, $\mu^f \ll \mu^c$ and term I in eqn. 9 will now override term II. Note that in this case the elution order will reverse relative to that in eqn. 10. Finally, if AC moves at the same rate as A,

α approaches unity, and no separation is possible. It can be concluded that separation is best achieved when one of the extreme cases exists, *i.e.*, $\mu^c/\mu^f \gg 1$ or $\ll 1$.

Resolution

The resolution R_s of a chiral pair of solutes can be written as

$$R_s = \frac{\Delta t_R}{4\sigma_t} \tag{12}$$

where Δt_R = retention time difference of the D,L pair and σ_t = time based standard deviation of the band. Since

$$N = \left(\frac{t_R}{\sigma_t}\right)^2 \tag{13}$$

combination of eqns. 7 and 13 with 12 yields

$$R_s = \frac{1}{4}\left(\frac{\alpha - 1}{\alpha}\right) N^{1/2} \frac{\mu E}{l} \tag{14}$$

or

$$R_s = \frac{1}{4}\left(\frac{\alpha - 1}{\alpha}\right) \frac{\mu E}{H^{1/2} l^{1/2}} \tag{15}$$

The resolution is seen to be proportional to the field, if H (height equivalent to a theoretical plate) is independent of E. Also, as in chromatography, the value of $\alpha - 1$ can dramatically affect resolution when α is close to one[23].

EXPERIMENTAL

Apparatus

A regulated high voltage power supply, 0–30 kV and 0–1 mA, Model PS/EG 30P1-RV-II (Glassman High Voltage, Whitehouse Station, NJ, U.S.A.) was used. Electrophoresis was performed in 30 cm × 75 μm I.D. fused-silica capillary tubing (Scientific Glass Engineering, Austin, TX, U.S.A.). At 15 cm approximately 1 cm of polyimide coating was carefully burned off to expose the fused silica for on-column detection which was accomplished with a microbore UV system (ISCO, Lincoln, NE, U.S.A.). Care was exercised to position the fused silica in the light path of the source. The temperature of the fused-silica capillary was controlled by a specially designed water cooling system. Each end of the capillary was connected to a separate 3-ml vial (Wheaton Science, Mellville, NJ, U.S.A.) filled with buffer. Platinum wire electrodes were inserted into the two vials for connection to the electrical circuit. The electropherogram signals were acquired and stored on an IBM PC/XT computer via a Model 762 SB A/D interface (Nelson Analytical, Cupertino, CA, U.S.A.). Sample injection was accomplished by placing one of the capillaries in the sample vial and applying a field for a fixed length of time.

Materials

The dansylated D,L-amino acids (Dns-DL-AA) were purchased from Sigma (St. Louis, MO, U.S.A.) and used as received. The water was deionized and triply distilled. Before use, all buffer and sample solutions were filtered through a Nylon 66 filter unit of 0.2 μm pore size (Schleicher & Schuell, Keene, NH, U.S.A.) and then degassed. The polyacrylamide columns were made with appropriate amounts of a CD dissolved in the gel buffer solution prior to polymerization. The formation of the polyacrylamide gel columns thus incorporated the CD into the porous network.

RESULTS AND DISCUSSION

Retention and separation

Our initial efforts in achieving chiral selectivity involved the addition of β-CD, a complexing agent known to resolve Dns-DL-AAs[19], to the buffer of open tube capillaries. With a variety of conditions, no change in retention or separation was observed. This could mean no complexation took place. However, assuming complexation occurred, the change in mobility upon complexation may have been small. Eqn. 9 shows that no separation would take place, if $\mu_1^c = \mu_1^f$ and $\mu_2^c = \mu_2^f$. As clearly seen in this equation, the formed complex has to differ significantly in mobility from that of the free amino acid. One could consider manipulating the mass or charge of the cyclodextrin to create a difference in mobility of the complex and free species as employed in micelle CE[16] as well as more generally in affinophoresis[24]; however, we decided on an alternative approach.

We reasoned that incorporating the CD into a polyacrylamide gel matrix would substantially slow down or immobilize the Dns-AA–CD complex. First, by virtue of the neutrality of CDs, these agents by themselves would not move in a gel matrix under the influence of an electric field. Secondly, as seen in Fig. 1, the distance across the wide edge of the toroid for β-CD is *ca.* 1.6 nm which is relatively wide for a non-polymeric species. Both from charge and size considerations, the Dns-AA–CD complex would be expected to migrate slowly, if at all, through the porous network. In this manner, there is direct analogy to chromatography when a CD is attached to a stationary chromatographic phase[14].

While it is possible to attach the CD covalently to polyacrylamide gels[21], we further reasoned that the simplest and most reproducible approach would be to incorporate the complexing agent directly into the porous matrix without bonding during the polymerization step. This was accomplished by simply adding the CD to the solution prior to free radical polymerization.

Fig. 2A shows the separation of Dns-Glu, Dns-Ser and Dns-Leu in a gel without any CD present. The retention order is in the expected direction of decreasing electrophoretic mobility with the doubly charged Dns-Glu migrating fastest and the singly charged bulky Dns-Leu migrating slowest. As expected, no chiral resolution is observed since a chiral complexing agent is not present. Fig. 2B shows the same sample injected on a gel column now polymerized from a solution containing 75 m*M* α-CD. Separation is similar to Fig. 2A, and no chiral resolution is found. It is known that the cavity size of α-CD is too small for effective penetration of dansylated amino acids, and no chiral resolution is expected[14].

Fig. 2C shows the baseline separation of the D,L pairs of each of the three

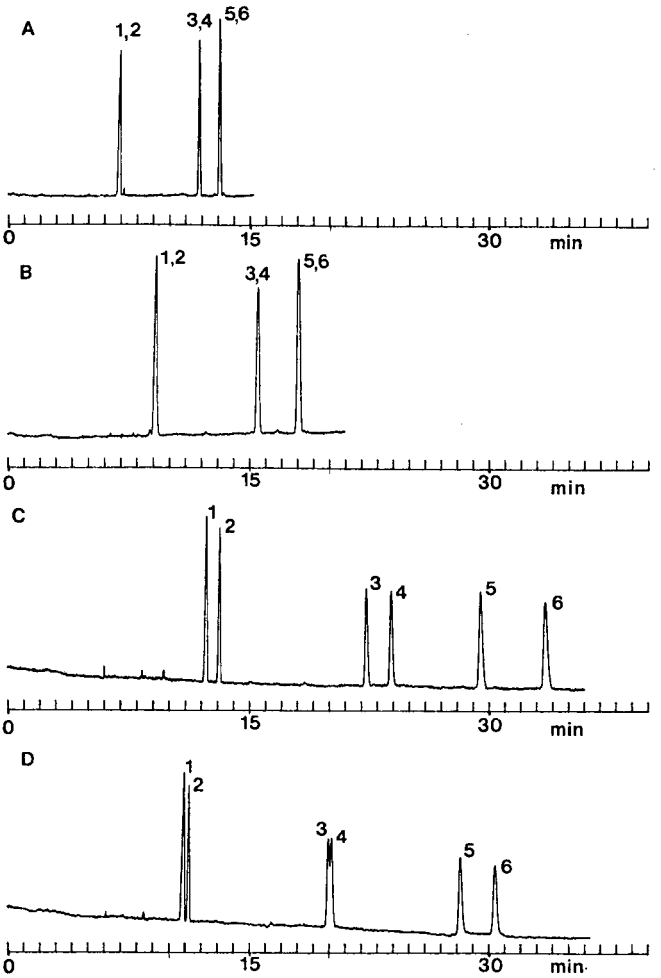

Fig. 2. Separation of Dns-DL-AAs. 1 = Dns-L-Glu; 2 = Dns-D-Glu; 3 = Dns-L-Ser; 4 = Dns-D-Ser; 5 = Dns-L-Leu; 6 = Dns-D-Leu. (A) Buffer: 0.1 *M* Tris–0.25 *M* boric acid (pH 8.3), 7 *M* urea, Gel: T = 5%, C = 3.3%, 0.1 *M* Tris–0.2 *M* boric acid (pH 8.3), 7 *M* urea. Capillary: 150 mm × 0.075 mm I.D., 400 V/cm, 8 μA. Electroinjection: 250 V/cm, 5 μA, 30 s, detection wavelength, 254 nm. (B) Addition of 75 m*M* α-CD to the buffer and the gel mixture. (C) Addition of 75 m*M* β-CD to the buffer and the gel mixture. (D) Addition of 75 m*M* γ-CD to the buffer and the gel mixture.

Dns-AAs in a gel column containing 75 m*M* β-CD. This complexing agent is known to be ideal for these substances[15]. In addition, the retention order is found to be L migrating faster than D. This order agrees with the literature where it is known that the Dns-L-AA forms the weaker complex with β-CD[14]. It can also be seen that for any Dns-AA, retention is longer in the case of β-CD than α-CD, no doubt primarily due to the retardation caused by complexation with β-CD. It is to be noted that 7 *M* urea has been included in the buffer in all cases of Fig. 2. It was found that the urea increased relative retention, thus providing improved separation. It is known that additives to the mobile phase in LC affect selective binding to CDs[14,15].

TABLE I

CHIRAL SELECTIVITY (α) FOR Dns-DL-AMINO ACIDS WITH β-CYCLODEXTRIN IN A POLYACRYLAMIDE GEL COLUMN

Column, 100 m*M* β-CD in a 5%T, 3%C gel, 7 *M* urea; buffer, 0.1 *M* Tris–0.25 *M* boric acid (pH 8.3), T = 25°C.

Dns-DL-AA	α	
	Buffer (400 V/cm, 8 μA)	*Buffer + 10% methanol (700 V/cm, 10 μA)*
Dns-DL-Leu	1.18	1.12
Dns-DL-Ser	1.12	1.09
Dns-DL-Val	1.09	1.12
Dns-DL-Glu	1.09	1.06
Dns-DL-Asp	1.08	1.09
Dns-DL-Met	1.09	1.11
Dns-DL-Thr	1.09	1.12
Dns-DL-Norleu	1.11	1.13
Dns-DL-NorVal	1.07	1.09
Dns-DL-α-amino-*n*-butyric acid	1.06	1.08
Dns-DL-Phe	1.04	1.08
Dns-DL-Trp	1.025	1.05

Finally, Fig. 2D shows a similar separation with 75 m*M* γ-CD. Chiral resolution is in general poorer with this CD, relative to β-CD. This result is again expected, since it is known that if the cavity is too wide, poor selectivity results[14]. As noted above, the optimum fit for the inclusion complex with Dns-AAs occurs with β-CD.

Further data with β-CD can be found in Table I which presents α values for twelve Dns-AAs both in the aqueous buffer and a buffer containing 10% (v/v) methanol. It can be seen that, as expected[14,15], relative retention varies with addition of methanol. In some cases, *e.g.*, Dns-DL-Leu, α is lower with added methanol; however, for the aromatic amino acids there is a substantial increase in α. As already noted, eqns. 14 and 15 show that improvement in α, when the relative retention is close to unity, can greatly increase resolution. This can be clearly seen in Fig. 3 where Dns-DL-Phe and Dns-DL-Trp are separated with and without the addition of methanol. The improvement in separation in the case of added methanol is self-evident. As in chromatography, organic modifier in the buffer can be used to manipulate selectivity when CDs are in the system. Finally, it can be noted in Table I and Fig. 3 that a much higher field with added methanol produces approximately the same current as a lower field with the aqueous buffer. This result is a consequence of the decreased dielectric constant in the solution of 10% (v/v) methanol.

Factors influencing chiral resolution

Eqn. 10 is an expression similar to that found in HPLC when secondary chemical equilibria are present[25]. As already noted, α will be greatest when $K[C]\mu^f \gg 1$. Below this limit, the concentration of β-CD in the gel matrix should influence α. Fig. 4 shows plots of α *versus* concentration of β-CD in the polymerizing solution, with the α value tending to a plateau at a high concentration of β-CD. The greatest curvature, as

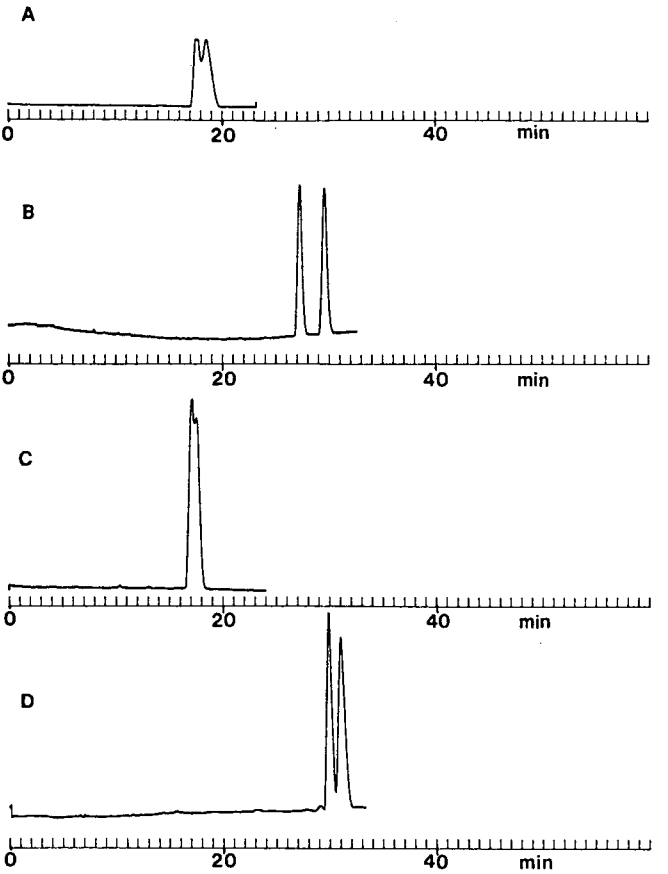

Fig. 3. Effect of methanol on chiral selectivity, conditions as in Fig. 2C, except as noted. (A) Dns-DL-Phe, E = 400 V/cm. (B) Dns-DL-Phe, E = 700 V/cm, buffer contains 10% (v/v) methanol. (C) Dns-DL-Trp, E = 400 V/cm. (D) Dns-DL-Trp, E = 700 V/cm, buffer contains 10% (v/v) methanol.

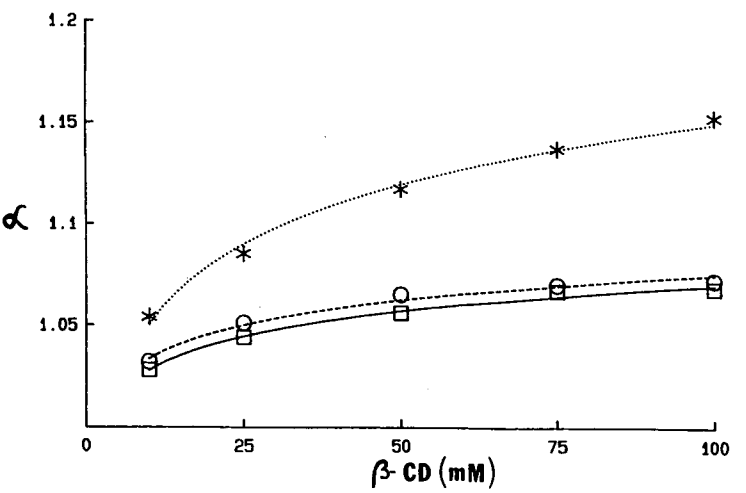

Fig. 4. Dependence of chiral selectivity, α, on β-CD concentration in the gel. Test mixture: * = Dns-DL-Leu; ○ = Dns-DL-Ser; □ = Dns-DL-Glu. All other conditions are given in Fig. 2C.

TABLE II

Dns AMINO ACID–β-CYCLODEXTRIN ASSOCIATION CONSTANTS (K) IN A POLYACRYLAMIDE GEL COLUMN

Temperature, 25°C; buffer, 0.1 M Tris–0.25 M boric acid (pH 8.3); no methanol added.

Dns-DL-AA	K (M^{-1})
Dns-L-Glu	6.4
Dns-D-Glu	7.6
Dns-L-Ser	7.3
Dns-D-Ser	8.6
Dns-L-Leu	13.3
Dns-D-Leu	17.6

expected, occurs with Dns-DL-Leu which has the highest binding constant of the amino acids in this figure (see Table II). The concentration of β-CD has not yet reached a sufficient level to yield the maximum value of α, *i.e.*, the plateau has not yet been reached.

As further evidence of the model, Fig. 5 shows plots of retention time of dansylated D-amino acids *versus* β-CD concentration. The linear behavior can be seen by combination of eqns. 6 and 7 and noting that $\mu^c \ll \mu^f$.

$$t_R = \frac{l(1 + K[C])}{\mu^f E} \tag{16}$$

Eqn. 16 suggests that the greatest slope of the plot of t_R *versus* E would be expected for Dns-D-Leu which has the strongest binding (see Fig. 5). In addition, μ^f for Dns-D-Leu

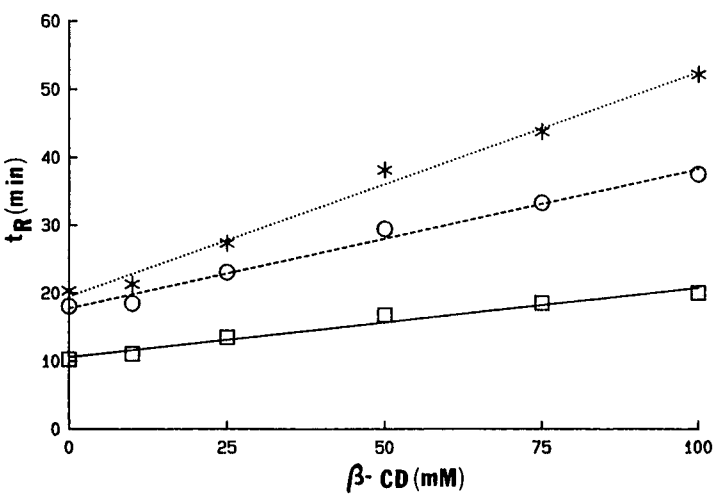

Fig. 5. Dependence of solute retention time, t_R, on β-CD concentration in the gel. Test mixture: * = Dns-D-Leu; ○ = Dns-D-Ser; □ = Dns-D-Glu. All other conditions are given in Fig. 2C.

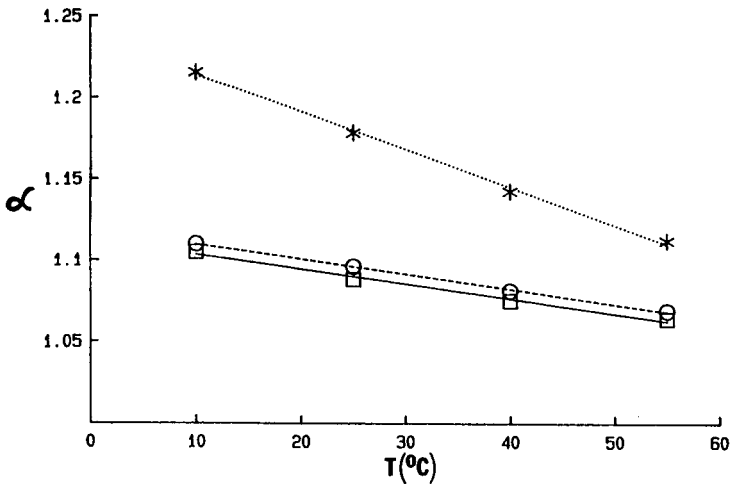

Fig. 6. Dependence of chiral selectivity, α, on column temperature, T. Test mixture is same as in Fig. 4. The buffer and the gel contained 10% (v/v) methanol. All other conditions are given in Fig. 2C.

is the lowest of the three Dns-AAs and therefore this substance would be expected to have the largest intercept value, as also observed in Fig. 5. Eqn. 16 and Fig. 5 can be used to calculate the apparent formation constants from the slope of the plots. Results for these constants in buffer are shown in Table II.

We next explored the influence of column temperature on separation. In this study, the column temperature was varied between 10°C and 55°C. Retention decreased with increasing temperature, as K is known to become smaller at elevated temperatures[26] and μ^f is larger at higher temperatures (see eqn. 16). The α value was also found to decrease with temperature, as shown in Fig. 6. Interestingly, the rate of change of α with temperature was greatest for the strongest binding amino acid, Dns-Leu. With the largest K values for the Dns-DL-Leu pair, the $\Delta(\Delta H)$ (difference in heats of complexation for the enantiomeric pair) is found to be the greatest. Fig. 6 shows that, as in chromatography, temperature can be used for manipulation of selectivity.

Columns of high efficiency are possible with complexing agents incorporated into the gel matrix. Fig. 7A shows the separation of the three enantiomeric pairs in which the bands of the Dns-Ser pair each achieve roughly 100 000 theoretical plates in the column of 15 cm effective length and a buffer of 10% (v/v) methanol. For Dns-DL-Ser, the resolution is 6.4, in spite of the fact that α is only 1.12. More typically, *ca.* 50 000–80 000 plates are obtained, as found for the Dns-DL-Leu pair. The high efficiency arises in part from the high field of 700 V/cm. Attention was paid to minimize the extra column effects of injection (*ca.* 5 nl) and the detector (*ca.* 2nl). With further reduction in extra column band broadening, increases in efficiency will probably be possible. As a further example, Fig. 6B shows an identical separation to Fig. 6A except that the field was increased to 1000 V/cm with the 10% methanol buffer. The separation is now achieved in roughly half the time, or 10 min.

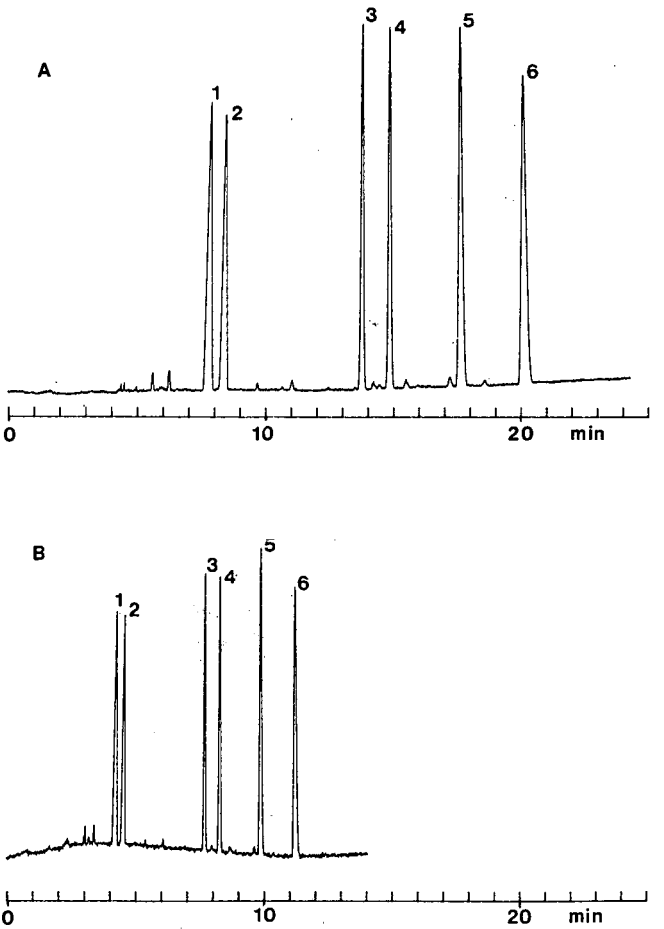

Fig. 7. High efficiency separation of Dns-DL-AAs. The test mixture is the same as in Fig. 2. All the other conditions are given in Fig. 6. (A) E = 700 V/cm; (B) E = 1000 V/cm.

CONCLUSIONS

High-performance capillary gel electrophoresis in which a complexing agent is incorporated into the gel matrix expands the potential of HPCE. We have found that high-performance, rapid separation and controlled selectivity are possible with these columns. High-performance chiral separation of Dns-DL-AAs has been achieved using β-CD. A model of the separation equilibria has been developed, from which it is emphasized that the mobility of the free species and the complex must differ significantly from one another in order to utilize the complexation equilibria to the fullest. Undoubtedly, the neutral character of the CDs themselves as well as the width of the toroid play a role in creating a low mobility of the solute–CD complex. In addition, the rates of association and dissociation must be rapid to take advantage of the high efficiency possible with the electrophoresis system. It is straightforward to

visualize tailor-made columns for high-performance separation of microamounts of specific samples. Separated fractions can be conveniently collected for further characterization, as recently shown by us[27] and others[28].

ACKNOWLEDGEMENTS

B. L. Karger gratefully acknowledges support of the National Science Foundation, the Dow Chemical Company and the James L. Waters Chair in Analytical Chemistry. A. Paulus acknowledges the NATO Science Council and the DAAD, Bonn F.R.G., for fellowship support. This is Contribution No. 342 from the Barnett Institute.

REFERENCES

1 F. E. P. Mikkers, F. M. Everaerts and Th. P. E. M. Verheggen, *J. Chromatogr.*, 19 (1979) 1.
2 J. W. Jorgenson and K. D. Lukacs, *Science (Washington, D.C.)*, 222 (1983) 266.
3 S. Hjertén, *J. Chromatogr.*, 270 (1983) 6.
4 H. H. Lauer and D. McManigill, *Anal. Chem.*, 58 (1986) 166.
5 R. A. Wallingford and A. G. Ewing, *Anal. Chem.*, 60 (1988) 258.
6 R. D. Smith and H. R. Udseth, *Nature (London)*, 331 (1988) 639.
7 A. S. Cohen, A. Paulus and B. L. Karger, *Chromatographia*, 24 (1987) 15.
8 R. J. Wieme, in E. Heftmann (Editor), *Chromatography: A Laboratory Handbook of Chromatography and Electrophoretic Methods*, Van Nortland, New York, 3rd ed., 1975, Ch. 10.
9 H. H. Lauer and D. McManigill, *Trends Anal. Chem.*, 5 (1986) 11.
10 S. Terabe, K. Otsuka and T. Ando, *Anal. Chem.*, 57 (1985) 834.
11 A. S. Cohen, S. Terabe, J. A. Smith and B. L. Karger, *Anal. Chem.*, 59 (1987) 1021.
12 Y. Walbroehl and J. W. Jorgenson, *Anal. Chem.*, 58 (1986) 479.
13 P. Gozel, E. Gassmann, H. Michelsen and R. N. Zare, *Anal. Chem.*, 59 (1987) 44.
14 D. W. Armstrong and W. DeMond, *J. Chromatogr. Sci.*, 22 (1984) 411.
15 W. L. Hinze, *Sep. Purif. Methods*, 10 (1981) 159.
16 S. Terabe, H. Ozaki, K. Otsuka and T. Ando, *J. Chromatogr.*, 332 (1985) 211.
17 I. Jelínek, J. Snopek and E. Smolková-Keulemansová, *J. Chromatogr.*, 405 (1987) 379.
18 J. Szejtli, *Cyclodextrins and their Inclusion Complexes*, Academic Press, Budapest, 1982.
19 D. W. Armstrong, T. J. Wart, R. D. Armstrong and T. E. Beesley, *Science (Washington, D.C.)*, 232 (1986) 113.
20 A. S. Cohen and B. L. Karger, *J. Chromatogr.*, 397 (1987) 409.
21 V. Hořejši and M. Tichá, *J. Chromatogr.*, 376 (1986) 49.
22 V. Hořejši and M. Tichá, *J. Chromatogr.*, 216 (1981) 43.
23 B. L. Karger, *Anal. Chem.*, 39 (1967) 24A.
24 K. Shimura and K. Kasai, *Anal. Biochem.*, 161 (1987) 200.
25 B. L. Karger, J. N. LePage and N. Tanaka in Cs. Horvath (Editor), *High Performance Liquid Chromatography; Advances and Prospectives*, Vol. 1, Academic Press, New York, 1978.
26 S. M. Han and N. Purdie, *Anal. Chem.*, 56 (1984) 2825.
27 A. S. Cohen, D. R. Najarian, A. Paulus, A. Guttman, J. A. Smith and B. L. Karger, submitted for publication.
28 D. J. Rose and J. W. Jorgenson, *J. Chromatogr.*, 438 (1988) 23.

Journal of Chromatography, 448 (1988) 55–72
Elsevier Science Publishers B.V., Amsterdam — Printed in The Netherlands

CHROM. 20 613

OPTIMIZATION OF THE DIRECT CHIRAL SEPARATION OF POTENTIAL CYTOTOXIC α-METHYLENE-γ-BUTYROLACTONES AND α-METHYLENE-γ-BUTYROLACTAMS BY LIQUID CHROMATOGRAPHY

M. LIENNE*, M. CAUDE and R. ROSSET
Laboratoire de Chimie Analytique de l'Ecole Supérieure de Physique et Chimie de Paris, 10 rue Vauquelin, 75231 Paris Cedex 05 (France)
and
A. TAMBUTE
Direction des Recherches et Etudes Techniques, Centre d'Etudes du Bouchet, BP 3, Le Bouchet, 91710 Vert-le-Petit (France)
(First received November 27th, 1987; revised manuscript received May 2nd, 1988)

SUMMARY

The direct enantiomeric resolution of a series of racemic α-methylene-γ-butyrolactones and α-methylene-γ-butyrolactams was carried out on various commercially available chiral stationary phases (CSPs). Particular interest was paid to compounds which exhibit physiological activity as cytotoxic agents. On a Pirkle-type column packed with (*R*)-N-(3,5-dinitrobenzoyl)phenylglycine (DNBPG) covalently bonded to γ-aminopropylsilanized silica gel, only α-methylene-γ-lactams containing two aromatic groups were resolved; a chiral recognition mechanism is proposed. (+)-Poly-(triphenylmethyl methacrylate) (PTrMA) coated on silica gel [Chiralpak OT(+)] with methanol as eluent afforded fairly good selectivities (up to 1.8) especially for α-methylene γ-lactones. Temperature had a great influence on the resolution. Cellulose tribenzoate and triphenylcarbamate (Chiralcel OB and OC, respectively) coated on macroporous silica gel displayed selectivities from 1.1 to 1.3, but, because of the very poor efficiency of these CSPs, no baseline resolution was achieved. Investigations on two protein CSPs are reported, α_1-acid glycoprotein (α_1-AGP) and bovine serum albumin (BSA) immobilized on microparticulate silica gel (Enantiopac and Resolvosil-BSA, respectively). The separations were performed using an aqueous sodium phosphate buffer as eluent and 2-propanol as organic modifier to regulate retention and selectivity. Both CSPs exhibited a good chiral recognition ability, especially towards cytotoxic solutes with resolution factors between 1 and 2.

INTRODUCTION

The synthesis of various α-methylene γ-butyrolactams has been carried out by Alami *et al.*[1,2] in order to develop a new series of therapeutic agents for the treatment of cancer. This study was performed[2,3] by comparison with α-methylene-γ-

0021-9673/88/$03.50

TABLE I

STRUCTURES OF THE α-METHYLENE-γ-BUTYROLACTONES AND α-METHYLENE-γ-BUTYROLACTAMS STUDIED

α-Methylene γ-lactones:

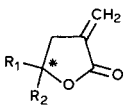

Substituent	*1*	*2*	*3*	*4*
R_1		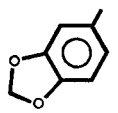	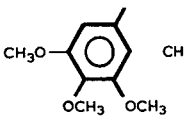	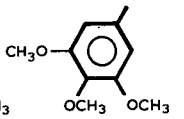
R_2	H	H	H	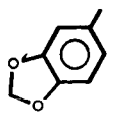

α-Methylene γ-lactams:

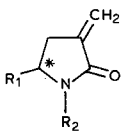

Substituent	*5*	*6*	*7*	*8*	*9*	*10*
R_1					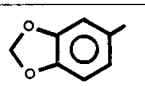	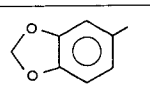
R_2		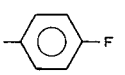	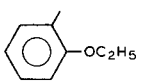	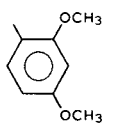	-CH₃	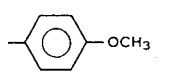

	11	*12*	*13*	*14*	*15*
R_1	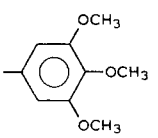	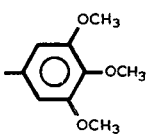	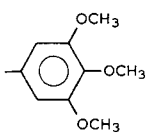	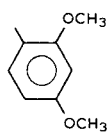	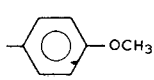
R_2	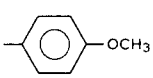	-CH₃			

butyrolactones[4], already known as cytotoxic agents but which often display toxic effects. The major direct factor responsible for the cytotoxicity of these compounds is the introduction of the $O=\overset{|}{C}-\overset{|}{C}=CH_2$ group. However, Alami[2] observed that some other specific structural parameters were required for biological activity, *e.g.*, the presence of an alkyl group on the nitrogen atom was necessary and lipophilic aryl groups R_1 (methoxyphenyl, 3,4-methylenedioxyphenyl) greatly enhanced the cytotoxicity (Table I, cytotoxic compounds in bold type). All these compounds bear an asymmetric carbon.

It has been extensively reported[5] that the two enantiomers of a chiral drug often provide different biological responses. Improvement of the therapeutic activity of a chiral drug molecule needs pharmacological investigations on the relative activities (toxicity/cytotoxicity for the case of our solutes) of its enantiomers. Thus, the development of rapid and accurate methods, such as liquid chromatography on chiral stationary phases (CSPs), for the determination of the enantiomeric purity of chiral solutes constitutes a necessary tool for biologists. This paper deals with the direct separation, without prior derivatization, of the aforementioned lactones and lactams on various commercially available CSPs. We intended to test easily accessible CSPs with very different structures and operating with various mobile phases in order to optimize the separations and make them suitable for further optical purity controls.

THEORETICAL

According to the solute structures, three types of CSPs were chosen after examination of literature data. Our classification of the CSPs studied was based on their chemical structures and on the possible chiral recognition mechanisms that were supposed to be involved. Type I CSPs are obtained by covalently bonding a chiral moiety on an achiral support via an achiral spacer; we used a Pirkle-type column derived from (*R*)-N-(3,5-dinitrobenzoyl)phenylglycine (DNBPG) grafted on microparticulate silica gel. The resolution of some lactones[6,7], phthalides[6,7] and β-, γ- and δ-lactams[6,8] have been previously described on such a CSP. However, the chiral recognition mechanism proposed by the authors (on an ionic CSP) for 3-aryl-γ-lactams predicted that substitution of the hydrogen on the nitrogen atom led to a decrease in selectivity[9].

Type II CSPs consists of synthetic or derivatized natural polymers coated (in thin layers) on macroporous silica gel. These polymers possess many centres of asymmetry and/or asymmetric environments called chiral cavities. We report investigations on optically active (+)-poly(triphenylmethyl methacrylate) [(+)-PTrMA]-derived CSP [Chiralpak OT(+)]. Okamoto and Hatada[10] suggested that this CSP is able to resolve various compounds lacking functionalities but bearing aryl groups (suitable for hydrophobic interactions) in the vicinity of the asymmetric centre, and/or having a rigid structure similar to our compounds. The resolution of lactones[11,12] and lactams[12] on cellulose derivative CSPs such as cellulose tribenzoate (Chiralcel OB) and triphenylcarbamate (Chiralcel OC) has been reported. Here also the geometric structure of the solute seems to play an important role in chiral recognition.

Finally, Type III CSPs include two protein CSPs which have been developed

recently and which appear to be very useful for the resolution of chiral pharmaceuticals[13,14]. Enantiopac and Resolvosil BSA columns were synthetized by immobilization of α_1-acid glycoprotein[13] (α_1-AGP) and bovin serum albumin (BSA)[14], respectively, on wide-pore microparticulate silica gel. These proteins have interesting binding properties in biological media which could make them very attractive for the resolution of our potential cytotoxic compounds.

EXPERIMENTAL

Apparatus

Analytical chromatography was performed with a Model 1084B liquid chromatograph (Hewlett-Packard, Waldbronn, F.R.G.) equipped with an automatic sampling system (79842 A) and a variable-wavelength detector (190–540 nm) (79875 A), or with a Model 8100 liquid chromatograph (Spectra-Physics, Santa Clara, CA, U.S.A.) equipped with a variable-wavelength detector (190–600 nm) (SP-8440) and a dual-channel computing integrator (SP 4200).

Experiments on the Chiralpak OT(+) column were performed with a modular liquid chromatograph (Gilson, Villiers-le-Bel, France) equipped with a Model 303 pump, a Model 802C manometric modula, a Gilson 811 (1.5-ml) dynamic mixer and a Holochrome HMD (analytical cell, 11 μl) spectrophotometer. All results were recorded with a Shimadzu CR3A integrator (Touzart et Matignon, Vitry-sur-Seine, France). For the control of the column and solvent temperature we used a Haake Model D8-V circulator bath (0–150°C) (Roucaire, Vélizy-Villacoublay, France) and a water-cooling jacket (purchased with the column). All tubing connections were heat-insulated.

UV detection was carried out at 254 nm with organic mobile phases and at 230 nm with aqueous buffer eluents.

Materials

n-Hexane, ethanol, 2-propanol, methanol and acetonitrile were of LiChrosolv grade, purchased from Merck (Darmstadt, F.R.G.). Chloroform stabilized with 0.6% (w/w) of ethanol was of analytical-reagent grade, purchased from Prolabo (Paris, France). Aqueous buffer solutions used with protein CSPs were prepared either directly[15] from mixtures of 0.2 *M* solutions of sodium dihydrogenphosphate dihydrate ($NaH_2PO_4 \cdot 2H_2O$) and sodium hydrogenphosphate dihydrate ($Na_2HPO_4 \cdot 2H_2O$), extra-pure grade, purchased from Merck, or from a commercially available sodium phosphate buffer (25 mmol, pH 6.88).

Deionized water was doubly distilled on a Büchi-Fontavapor 285 apparatus (Roucaire). The pH of the aqueous buffer eluents was controlled with a Model Minisis 8000 pH/millivoltmeter (Tacussel, Villeurbanne, France), Tacussel glass TB/HS and Tacussel C8 calomel reference electrodes.

Aqueous solvents were filtered through 0.65-μm Type DAWP Millipore membrane filters (Touzart et Matignon) before being degassed in an ultrasonic bath, whereas organic mobile phases were filtered through a 0.5-μm Type FHLP Millipore membrane filter and then degassed with helium (with the Spectra-Physics chromatograph) or *in vacuo* (with the Hewlett-Packard chromatograph).

Sodium chloride was of analytical-reagent grade, purchased from Merck.

LiChrosorb-NH_2 γ-aminopropylsilica gel (irregular particles; diameter, d_p = 5 μm) was purchased from Merck.

Pirkle-type column preparation

The chiral moiety, (*R*)-N-(3,5-dinitrobenzoyl)phenylglycine (DNBPG), was prepared as described[16]. Covalent grafting of the (*R*)-N-3,5-DNBPG was carried out as previously described[17]. Starting from 100 g of γ-aminopropylsilica gel and 27.6 g of chiral moiety (0.8 mmol g^{-1}) we obtained 114 g of CSP with the following elemental analysis: C 18.7, H 2.5, N 2.2, Si 21.9%, corresponding to 0.43 mmol of chiral sites per gram of support. The CSP was then packed into 250 × 4.6 mm I.D. stainless-steel columns by the usual slurry technique at 400 bar with ethanol as pumping solvent.

Commercially available CSPs

Chiralpak OT(+), Chiralcel OB and Chiralcel OC packings consisted of optically active (+)-PTrMA, cellulose tribenzoate and cellulose triphenylcarbamate, respectively, coated on macroporous silica gel (particle diameter, d_p = 10 μm; mean pore diameter 1000 Å). Packed in 250 × 4.6 mm I.D. stainless-steel columns, they are available from Daicel Chemical Industries (J. T. Baker, Sochibo, Velizy-Villacoublay, France).

The 100 × 4.0 mm I.D. Enantiopac column was purchased from LKB (Les Ulis, France): the plasma protein α_1-AGP is immobilized on a 10 μm diethylaminoethylsilica gel by ionic bonding followed by cross-linking.

BSA-silica of 7 μm particle size was purchased as Resolvosil-BSA-7 from Macherey-Nagel (Düren, F.R.G.) (150 × 4.0 mm I.D. stainless-steel column).

Solutes

Samples of α-methylene-γ-butyrolactones and α-methylene-γ-butyrolactams were given to us by Professor J. Villieras, Laboratory of Selective Organic Synthesis, University of Nantes, France. The syntheses have been described previously by Alami[2]. The solvents used for solubilizing the solutes were chosen as follows: hexane–2-propanol (50:50, v/v) with the Pirkle-type and Chiralcel OB and OC columns, methanol with the Chiralpak OT(+) column and phosphate bufferr (7.5 m*M*, pH 7)–2-propanol (50:50, v/v) with the protein columns. On the protein columns the solubility of the solute was improved by addition of 2-propanol; the peak shape was then improved (less broad and more symmetric). We often noticed that the efficiency and as a consequence, the resolution could be greatly affected by the choice of solubilizing solvents.

RESULTS AND DISCUSSION

Type I CSP: Pirkle-type phase

Enantiomers of the α-methylene-γ-butyrolactones in Table I were not resolved on the Pirkle-type CSP. Only γ-butyrolactams bearing an aryl substituent on the nitrogen atom (*i.e.*, R_2, Table I) were resolved (Table II). These results suggest the mechanism for chiral recognition depicted in Fig. 1. This model involves the formation of a charge-transfer complex between the π-electron acceptor 3,5-dinitroben-

TABLE II

RESOLUTION OF α-METHYLENE γ-LACTAMS ON A PIRKLE-TYPE CSP

Solute	*2-Propanol in mobile phase* (%, v/v)*	k'_2**	α***	R_s§
5	5	4.4	1.16	1.3
6	5	3.7	1.12	0.9
7	12	4.5	1.55	3.5
8	12	11.2	1.58	4.4
10	12	10.1	1.21	3.0
11	12	16.0	–	–

* Mobile phase: *n*-hexane–2-propanol.

** k'_2 is the capacity factor of the second eluted enantiomer, $k'_2 = (t_{r_2}/t_0) - 1$, where t_{r2} is the retention time of the second eluted enantiomer and t_0 the retention time of a non-retained solute.

*** The selectivity between two enantiomers is the ratio of their respective capacity factors (k'_2/k'_1).

§ R_s (resolution factor) = 2(distance of the two enantiomer peak positions/sum of the band width of the two peaks at their bases): $R_s = 2(t_{r_2} - t_{r_1})/(w_2 + w_1)$.

zoyl group of the CSP and the π-electron donor aryl substituent R_2 of the lactam, and hydrogen bonding of the 3,5-dinitrobenzamide hydrogen of the CSP and the carboxy oxygen of the lactam. The difference in size between the hydrogen atom and the phenyl group R_1 on the chiral carbon of the solute induces a steric discrimination of the *R* and *S* configurations. In the case of the *R* configuration our model shows that the bulky phenyl group (R_1) would be inserted between the CSP and the lactam ring, which may hinder both π–π interaction and hydrogen bonding, thus leading to a less stable diastereomeric complex. In Fig. 1 the conformation of the lactam 8 was

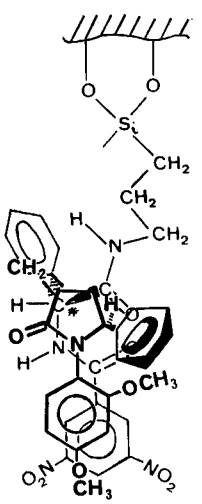

(S)-enantiomer

Fig. 1. Proposed mechanism for chiral recognition of racemate 8 on a Pirkle-type CSP.

chosen according to the examination of the CPK* molecular models in order to give the preferred one (where the mean plane of the lactam ring and the aromatic nucleus R_2 are coplanar). It also illustrates more obviously the chiral discrimination. The (*R*)-N-(3,5 DNB) phenylglycine CSP was drawn according to the conformation proposed by Lipkowitz *et al.*[18] from the conformational analysis computed with the Allinger MM_2 force field method. The observed α values are in good agreement with our model, which shows the importance of the π–π interaction between the nitrogen substituent R_2 and the CSP: α increases regularly with the π-electron donor character of the aryl group R_2 (Table II); compound 10 was resolved but compound 11 was not. From this we can argue that the stronger π-electron donor trimethoxyphenyl group (R_1) competes with the less strong methoxyphenyl group (R_2) for the π-acceptor site of the CSP, leading to a lack of selectivity. In addition, we failed to resolve the lactam containing the phenyl group at R_1 and a hydrogen atom as R_2. This is in accordance with our model of discrimination: a π–π interaction between R_1 and the 3,5-DNB group of the CSP and simultaneous hydrogen bonding or a dipolar interaction between the amide group of the lactam and the 3,5-DNB amide group of the CSP cannot occur because of the rigid quasi-planar conformation of the lactam ring. This quasi-planar system provides an additional steric restraint. The magnitude of the resolution factor R_s shows that this CSP is suitable for chiral preparative chromatography of compounds 7, 8 and 10.

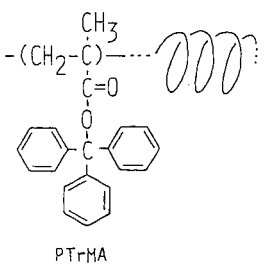

Scheme 1. Structure of the PTrMA polymer chains.

Type II CSPs

(+)-PTrMA coated silica gel [Chiralpak OT(+) column]. As we failed to resolve the cytotoxic lactones and some lactams on the DNBPG column, we investigated the chiral recognition ability of optically active PTrMA coated on silica gel. The polymer possesses a rigid helical conformation which arises from the asymmetric polymerization of triphenylmethyl methacrylate (Scheme 1). With methanol as the eluent most of the compounds were resolved. Data obtained at 5 and 25°C are presented in Table III (compounds that have been omitted were not separated). It was puzzling that compounds 13 and 14 were not resolved whatever the temperature, whereas enantiomers of lactams 12 and 15 were separated with selectivity values of *ca.* 1.2 at 5°C ($R_s > 1.1$).

For all compounds, methanol appeared to be the most suitable eluent; ex-

* CPK precision molecular models are improved versions of the Corey–Pauling models designed at the California Institute of Technology in the late 1940s, with new connectors by Dr. W. Koltun.

TABLE III

INFLUENCE OF TEMPERATURE ON THE RESOLUTION OF SOME α-METHYLENE-γ-BUTYROLACTONES AND -γ-BUTYROLACTAMS

Stationary phase, (+)-PTrMA coated on silica gel [Chiralpak OT(+) column]; mobile phase, methanol; flow-rate, 0.5 ml min^{-1}; column, 250 × 4.6 mm I.D.

Compounds	*Solute*	*5°C*			*25°C*		
		k'_2	α	R_s	k'_2	α	R_s
α-Methylene-γ-butyrolactones	1	0.76	1.40	1.8	0.54	1.30	1.2
	2	0.61	1.13	0.6	0.46	1.07	0.5
	3	0.61	1.24	1.1	0.44	1.15	0.7
	4	2.00	1.32	1.5	1.49	1.45	2.7
α-Methylene-γ-butyrolactams	5	1.09	1.09	0.5	0.81	–	–
	6	0.59	1.05	0.4	0.46	–	–
	7	1.32	1.43	0.85	1.16	1.32	1.05
	8	1.17	1.30	1.2	0.99	1.31	1.25
	10	1.56	1.29	1.2	1.11	1.13	0.8
	11	1.30	–	–	1.05	1.19	0.9
	12	1.07	1.19	1.1	0.68	1.13	0.8
	15	0.65	1.23	1.15	0.49	1.23	0.95

periments carried out with hexane–ethanol or hexane–2-propanol mixtures did not result in chiral recognition. This suggests a contribution of hydrophobic interactions between the numerous non-polar sites of our compounds (R_1 and R_2 are often aryl substituents) and the triphenylmethyl groups of the polymer chains; these hydrophobic interactions occur in polar media such as methanol and are thus disfavoured with apolar hexane–alcohol mobile phases, leading to a decrease in enantioselectivity. The chiral recognition mechanism may thus result from a combination of these hydrophobic interactions and an inclusion phenomenon of the solute in the intrinsically chiral (+)-PTrMA.

The importance of temperature on the resolution of the racemates is evident from the data at 25 and 5°C given in Table III. However, this dependence on tem-

TABLE IV

EFFECT OF TEMPERATURE ON THE EFFICIENCY OF THE (+)-PTrMA COLUMN FOR RACEMATE 4

T (°C)	k'_2	N_2*	h_2**
5	2.00	780	32
10	1.81	940	27
15	1.73	1240	20
20	1.61	1420	18
25	1.49	1870	13

* The efficiency N was calculated according to the equation given by Foley and Dorsey[20] for non-Gaussian peaks.

** $h = L/(Nd_p)$, where L is the column length and d_p the mean diameter of silical gel particles. Other operating conditions as in Table III.

perature varied greatly according to the compound and we sometimes observed opposite behaviours. For all compounds the efficiency of the column increased with increasing temperature (higher solute diffusion coefficients in the mobile phase). The theoretical plate number, N, and the reduced plate height, h, for the best resolved compound, the lactam 4, are listed in Table IV. N more than doubled when the temperature increased from 5 to 25°C.

A parallel study of the dependence of the selectivity, α, on temperature revealed unusual trends such as an increase in α with increasing temperature for compounds 4 and 11 (Fig. 2). This abnormal behaviour has already been observed by Okamoto *et al.*[19] on (+)-PTrMA columns. They also studied the chiral discrimination ability of (+)-PTrMA as a function of the density of polymer coated on the silica gel. They suggested that heavily (+)-PTrMA-coated silica gel could show an ordered structure of associated chains leading to the formation of chiral spaces between the chains responsible for the chiral recognition process. With lightly coated silica gel, the polymer chains remained isolated from each other and could act as independent chiral

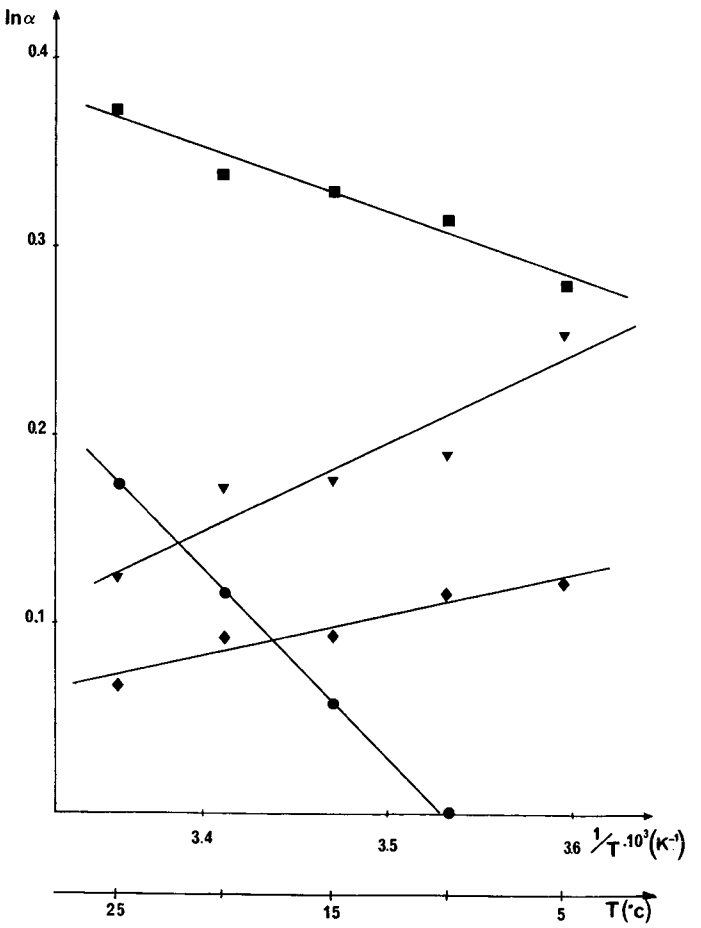

Fig. 2. Dependence of ln α for compounds (◆) 2, (■) 4, (▼) 10 and (●) 11 on temperature. Operating conditions as in Table III.

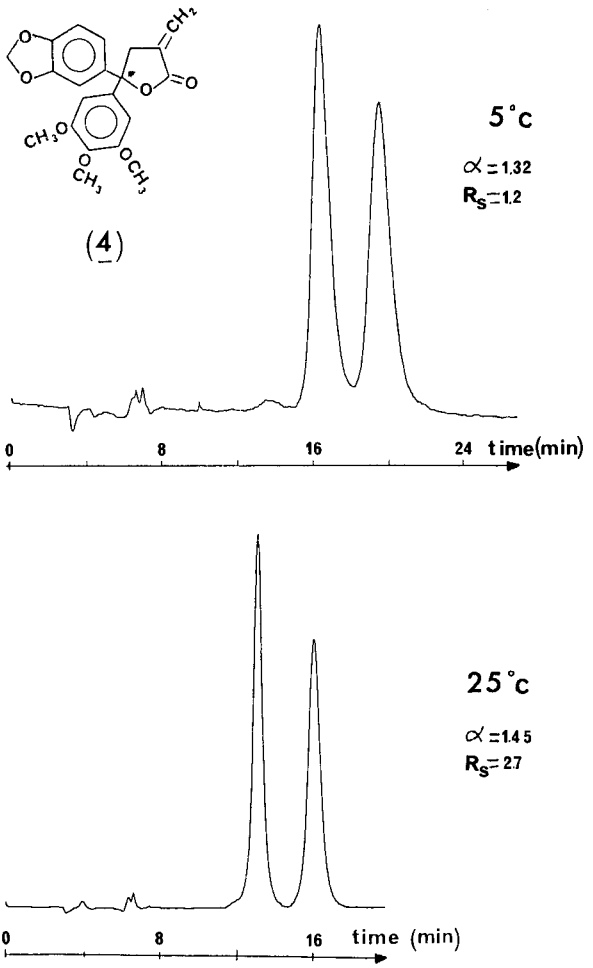

Fig. 3. Optimization of the resolution of solute 4 on the (+)-PTrMA column by increasing the temperature. Operating conditions as in Table III; UV detection at 254 nm.

sites. For a given compound one of these two chiral recognition mechanisms may be more suitable.

However, we do not know the (+)-PTrMA to silica gel weight ratio of the commercially available columns we used. We can assume that even small variations in temperature may alter the conformation of the polymer chains, modifying either the helical structure or the shape of the chiral spaces. This may then entail changes in the chiral recognition mechanism whether the chains act isolatedly or cooperatively; for some solutes an increase in temperature may thus happen to be more suitable for chiral discrimination. Also, a change in temperature may induce an alteration of the conformation of the solute itself that may be either favourable or unfavourable with respect to stereoselectivity. These comments emphasize the role of inclusion with such polymers; the solute has to fit to the chiral macromolecular structure.

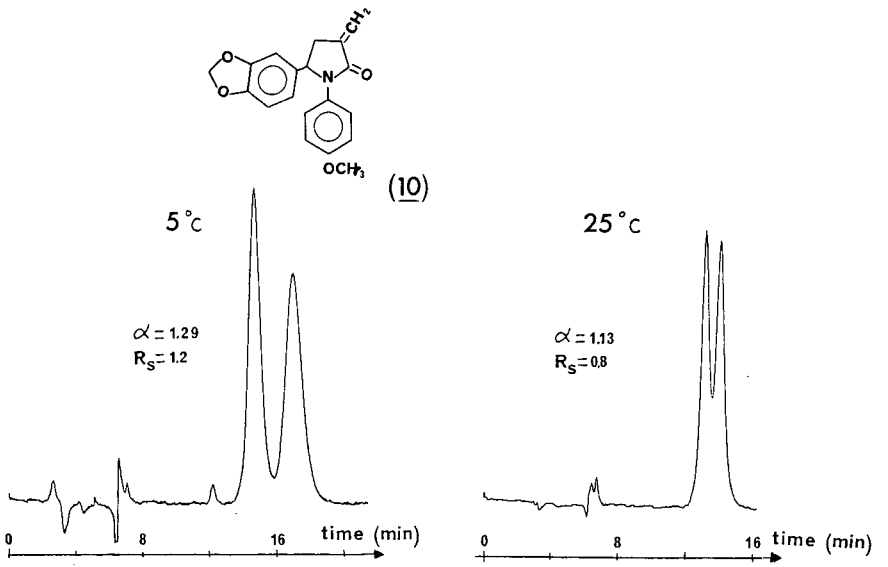

Fig. 4. Optimization of the resolution of solute 10 on the (+)-PTrMA column by decreasing the temperature. Operating conditions as in Table III; UV detection at 254 nm.

In Fig. 3 the chromatograms obtained at 5 and 25°C for the lactone 4 show that both the efficiency and selectivity increase with increasing temperature. However, for lactam 10 the resolution was improved at low temperatures (Fig. 4) because the selectivity gain, with a decrease in temperature from 25 to 5°C, was important enough to compensate for the small decrease in efficiency.

In conclusion, we can say that 10–15°C is a suitable temperature range for the use of a (+)-PTrMA column, noting that Okamoto *et al.*[19] have shown that the solvolysis of the triphenylmethyl ester groups of the polymer was reduced below 15°C. With regard to the magnitude of the resolution factor, R_s, optical purity determinations can be carried out on a (+)-PTrMA column for compounds 1, 4, 8 and 10.

Cellulose derivative CSPs. The structures of the two commercially available cellulose derivative CSPs that we used are depicted in Scheme 2. Mobile phases consisting of hexane–ethanol, hexane–2-propanol and hexane–2-propanol–acetonitrile were studied. OB- and OC-CSPs display good ability for chiral recognition towards our compounds (Tables V and VI). The selectivity values varied from 1.1 to 1.3; OC-CSP was more efficient than OB-CSP for the separation of γ-lactams. However, because of the low efficiency of the columns (a reduced plate height of 40–50, *i.e.*,

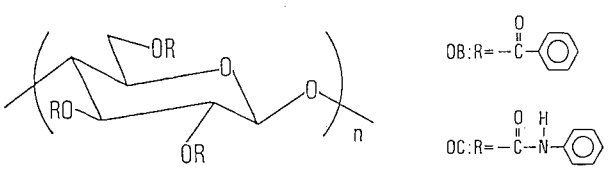

Scheme 2. Structures of the cellulose derivative CSP Chiralcel OB and Chiralcel OC.

TABLE V

RESOLUTION OF SOME α-METHYLENE-γ-LACTONES AND -γ-LACTAMS ON A CELLULOSE TRIPHENYLBENZOATE DERIVATIVE COATED ON SILICA GEL (CHIRALCEL OB COLUMN)

Mobile phase, *n*-hexane–polar solvent mixture; flow-rate, 1 ml min^{-1}, temperature, 26°C; column, 250 × 4.6 mm I.D.

Solute	*Polar solvent in mobile phase (%, v/v)*	k'_2	α	R_s
1	Ethanol (8)	6.9	1.27	1.2
2	Acetonitrile–2-propanol (75:25, v/v) (8)	5.4	1.22	1.0
6	2-Propanol (15)	4.8	1.24	0.6
13	2-Propanol (15)	7.9	1.70	0.8
15	Acetonitrile–2-propanol (75:25, v/v) (1)	9.5	1.64	1.0

600 theoretical plates for the first peak of 1 on the OB-CSP), baseline resolution was not achieved.

Figs. 5 and 6 show the chromatograms of the lactone 1 on OB-CSP and of the lactams 9 and 13 on OC-CSP. These two CSPs are sensitive to the geometric structure of the solutes. For example, we noticed that the compounds containing the 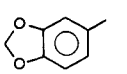 unit on the asymmetric carbon were partly resolved on OC-CSP (compounds 2, 4, 9 and 10). Unfortunately, our investigations on γ-lactams and γ-lactones did not allow us to formulate simple rules concerning chiral recognition on such CSPs. Nevertheless, some general assumptions have been proposed previously by other workers[21] which can suit our experiments: the chiral recognition process may involve the formation of π–π interactions, occurring between the phenyl group of the CSPs and the aryl groups of the solutes; hydrogen bonding between the carboxy group of

TABLE VI

RESOLUTION OF SOME α-METHYLENE-γ-LACTONES AND -γ-LACTAMS ON A CELLULOSE TRIPHENYLCARBAMATE DERIVATIVE COATED ON SILICA GEL (CHIRACEL OC COLUMN)

Mobile phase, *n*-hexane–ethanol; flow-rate, 1 ml min^{-1}; temperature, 26°C; column, 250 × 4.6 mm I.D.

Solute	*Polar solvent in mobile phase (%, v/v)*	k'_2	α	R_s
2	15	9.2	1.14	0.7
4	25	10.8	1.08	0.6
8	15	10.8	1.29	1.1
9	15	8.9	1.17	0.9
10	20	15.4	1.22	1.0
12	20	10.7	1.08	0.7
13	15	7.6	1.28	1.0
15	10*	5.3	1.10	0.6

* Mobile phase, *n*-hexane–2-propanol.

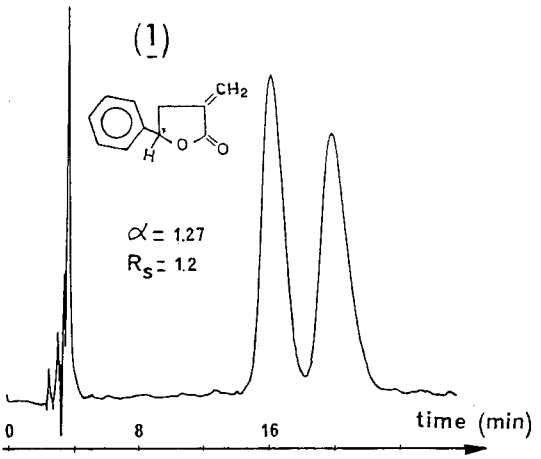

Fig. 5. Separation of the enantiomers of the lactone 1 on the Chiralcel OB column. Column, 250 × 4.6 mm I.D.; mobile phase, *n*-hexane–ethanol (92:8, v/v); flow-rate, 1 ml min^{-1}; temperature, 26°C; UV detection at 254 nm.

the lactones and lactams, and the carbamate hydrogen for the case of OC-CSP, may also contribute to the chiral recognition. A steric chiral discrimination based on the inclusion of the solute in the chiral cavities of the CSPs is probably essential and involves the structure and "flexibility" of the molecule.

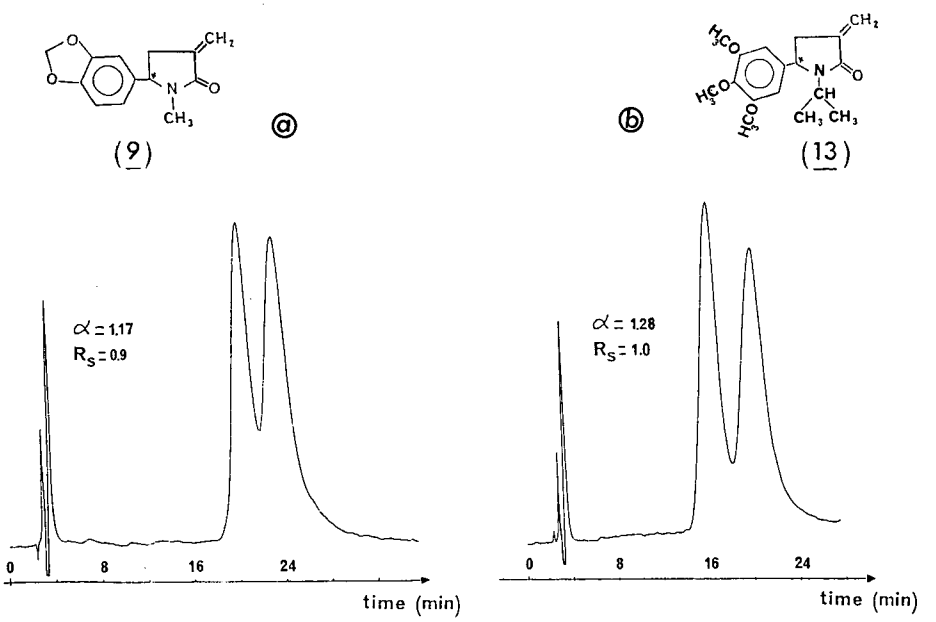

Fig. 6. Separation of the enantiomers of the lactams 9 and 13 on the Chiralcel OC column. (a) Racemate 9; (b) racemate 13. Column, 250 × 4.6 mm I.D.; mobile phase, *n*-hexane–ethanol (85:15, v/v); flow-rate, 1 ml min^{-1}; temperature, 26°C; UV detection at 254 nm.

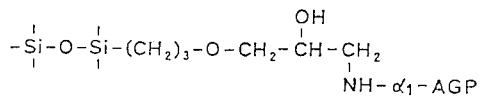

Scheme 3. Structure of the α_1-AGP CSP.

Type III CSPs: protein CSPs

Investigations carried out on the BSA-CSP (Resolvosil-BSA) led to surprising results: most of the compounds were not (or poorly) resolved ($R_s \approx 0.5$–0.6), except for lactone 2, for which baseline resolution was achieved (selectivity $\alpha = 2.1$) within a short analysis time (*ca.* 15 min). On the other hand, the α_1-AGP-CSP (Enantiopac; see Scheme 3) exhibited a noticeable chiral recognition ability towards our compounds, and especially towards cytotoxic ones, with selectivity values varying from 1.3 to 4.7. Table VII gives the selectivities and resolution factors for compounds 1–15 on the α_1-AGP-CSP. Because of the very low efficiency of the α_1-AGP columns a selectivity higher than 1.5 is generally required to achieve a baseline resolution. Furthermore, the columns are sensitive to an increase in pressure; a bed compression was then observed together with a decrease in efficiency which affected the resolution.

The 2-propanol content in the mobile phase was responsible for the regulation of the retention and selectivity factors and was adjusted for each solute. From Table VII, α-methylene-γ-butyrolactams, 5–8, are eluted with similar magnitudes of α, R_s and k', indicating that the phenyl group R_1 may play an important part in the chiral recognition (through hydrophobic and steric interactions). Compounds 14 and 15,

TABLE VII

RESOLUTION OF α-METHYLENE-γ-BUTYROLACTONES AND -γ-BUTYROLACTAMS ON α_1-AGP IMMOBILIIZED ON SILICA GEL (ENANTIOPAC COLUMN)

Mobile phase, 8 m*M* sodium phosphate buffer (pH 7)–0.1 *M* NaCl–2-propanol; flow-rate, 0.3 ml min^{-1}; temperature, 25°C; column, 100 × 4 mm I.D.

Solute	*2-Propanol in mobile phase (%, v/v)*	k'_2	α	R_s
1	2	7.7	2.02	3.0
2	2	5.5	1.23	0.9
3	2	5.8	1.74	1.2
4	2	34	1.29	1.2
5	6	9.0	1.09	<0.5
6	6	10.3	1.17	0.6–0.7
7	6	10.8	1.17	0.5–0.6
8	6	10.0	1.15	0.5–0.6
9	2	4.5	1.50	1.2
10	6	8.4	1.26	0.8
11	2	17.0	1.10	0.5
12	4	4.1	4.7	1.7
13	2	9.0	1.8	1.0
14	6	5.5	1.34	0.9
15	4	6.6	1.39	1.0

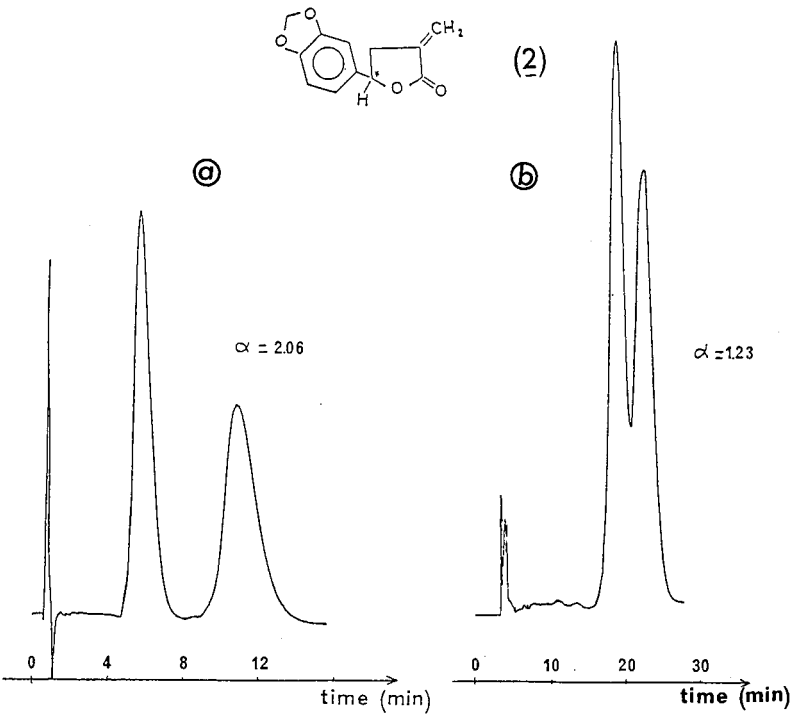

Fig. 7. Comparison of the resolution of racemate 2 on two protein-derived CSPs. (a) BSA immobilized on silica gel (Resolvosil-BSA-7 column), d_p = 7 μm. Column, 150 × 4.6 mm I.D.; mobile phase, 7.5 m*M* phosphate buffer (pH 6.9)–1.5% (v/v) 2-propanol; D = 2 ml min^{-1}. (b) α_1-AGP immobilized on silica gel (Enantiopac column), d_p = 10 μm. Column, 100 × 4 mm I.D.; mobile phase, 8 m*M* sodium phosphate buffer (pH 7)–0.1 *M* NaCl–2% (v/v) 2-propanol, D = 0.3 ml min^{-1}. Temperature, 25°C; UV detection at 230 nm.

which have similar structures, also exhibit similar chromatographic behaviour. The presence of an alkyl substituent R_2 on the nitrogen atom favours contribution to the chiral discrimination, as shown by comparing compounds 9 and 10 or 11 and 12. The chiral recognition process associated with these macromolecular proteins (BSA and α_1-AGP) is complex. Hydrogen bonding and hydrophobic interactions are the largest contributors. However, these proteins consists of hundreds of amino acids all possessing asymmetric carbon atoms available for chiral discrimination. Also, the secondary structure of the proteins takes part in the chiral recognition mechanism by means of helical parts of the protein, which are similar to the helical polymer chains of (+)-PTrMA.

Figs. 7–9 are typical chromatograms obtained on the BSA and α_1-AGP columns for the present series of lactams and lactones.

CONCLUSION

Each racemic α-methylene-γ-butyrolactone and -γ-butyrolactam was resolved on at least one of the CSPs studied in this work. The control of the optical purity for

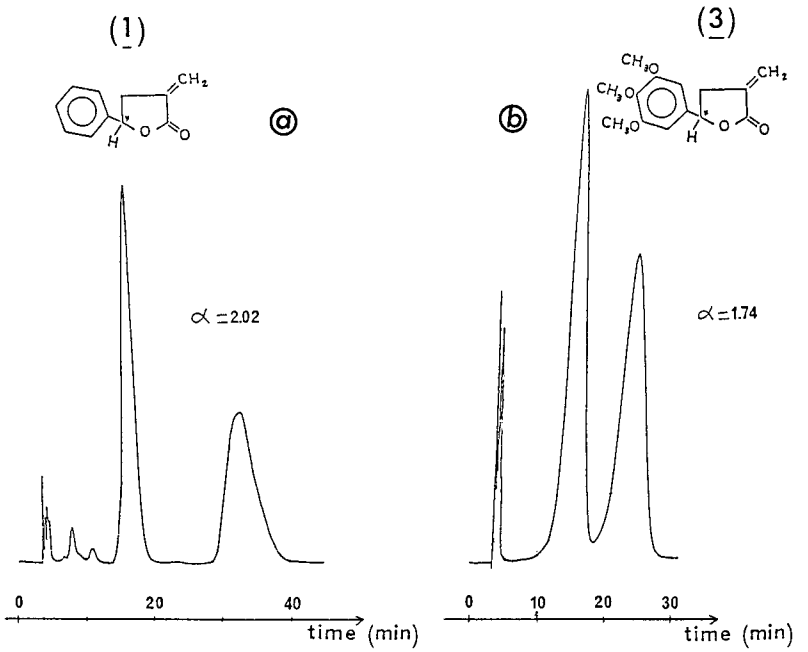

Fig. 8. Resolution of cytotoxic γ-methylene-γ-lactones 1 and 3 on the Enantiopac column. (a) Racemate 1; (b) racemate 3. Mobile phase, 8 m*M* sodium phosphate buffer (pH 7)–0.1 *M* NaCl–2% (v/v) 2-propanol; other operating conditions as for racemate 2 in Fig. 7.

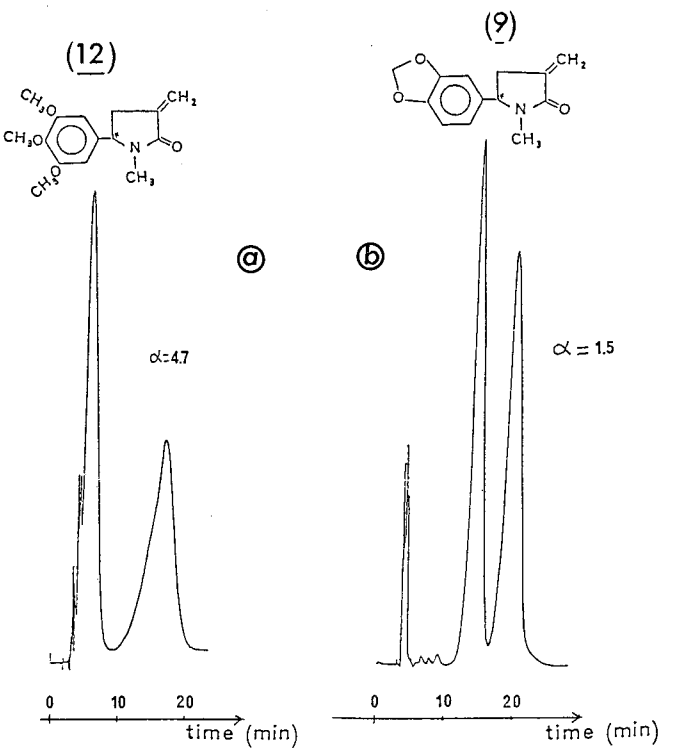

Fig. 9. Resolution of cytotoxic γ-methylene-γ-lactams 9 and 12 on the Enantiopac column. (a) Racemate 12; (b) racemate 9. Mobile phase, 8 m*M* sodium phosphate buffer (pH 7)–0.1 *M* NaCl–2-propanol [2 and 4% (v/v), respectively, for 9 and 12]; other operating conditions as for racemate 2 in Fig. 7.

TABLE VIII

CHOICE OF THE CSP FOR THE RESOLUTION OF CYTOTOXIC α-METHYLENE-γ-LACTONES AND -γ-LACTAMS

The most suitable CSPs are given in bold type.

Solute	*CSP*
1	**Enantiopac (α_1-AGP)**
	Chiralpak OT(+)
	Chiralcel OB
2	**Resolvosil-BSA-7**
	Enantiopac (α_1-AGP)
	Chiralcel OB and OC
3	**Enantiopac (α_1-AGP)**
	Chiralpak OT(+)
4	**Chiralpak OT(+)**
9	**Enantiopac (α_1-AGP)**
	Chiralcel OC
12	**Enantiopac (α_1-AGP)**
	Chiralpak OT(+)

such compounds, in particular for the cytotoxic agents, can be easily carried out. However, it should be noted that none of these CSPs was able to resolve the complete series of lactones and lactams (with R_s values higher than 0.8). There is an antagonism for one given CSP to exhibit both high enantioselectivities and a large scope of application. In Table VIII are reported the different CSPs suitable for the resolution of α-methylene-γ-lactones and -γ-lactams of our series which can act as cytotoxic agents; for each compound the CSP which gives the best resolution is in bold type, (+)-PTrMA [Chiralpak OT(+)] and α_1-AGP (Enantiopac) display the widest applicability. The chiral recognition ability of these polymers is related to the presence of numerous chiral sites of interaction different in nature and available for various types of interactions (asymmetric centres, chiral spaces arising from helical structures, etc.). However, the kinetics of the chromatographic process are slow, probably owing to the polymer structure of the CSPs, which results in low efficiencies of the columns. Baseline resolution often requires a selectivity higher than 1.5. It should also be mentioned that these CSPs are fragile and there can be problems concerning reproducibility.

ACKNOWLEDGEMENTS

The authors are grateful to Professor J. Villieras and Drs. N. E. Alami and C. Belaud for gifts of the α-methylene-γ-butyrolactones and -γ-butyrolactams.

REFERENCES

1 N. E. Alami, C. Belaud and J. Villieras, *Tetrahedron Lett.*, 28 (1987) 59.
2 N. E. Alami, *Doctor's Thesis*, University of Nantes, 1987.
3 C. Belaud, C. Roussakis, Y. Letourneux, N. E. Alami and J. Villieras, *Synth. Commun.*, 15 (1985) 1233.

4 P. A. Grieco, *Synthesis*, (1975) 69.
5 K. Williams and E. Lee, *Drugs*, 30 (1985) 333.
6 W. H. Pirkle, J. M. Finn, B. C. Hampers, J. Schreiner and J. R. Pribish, in E. L. Eliel and S. Otsuka (Editors), *Asymmetric Reactions and Processes in Chemistry*, ACS Symposium Series, American Chemical Society, Washington, DC, 1982, p. 245.
7 W. H. Pirkle and T. J. Sowin, *J. Chromatogr.*, 387 (1987) 313.
8 W. H. Pirkle, A. Tsipouras, M. H. Hyun, D. J. Hart and C.-S. Lee, *J. Chromatogr.*, 358 (1986) 377.
9 J. M. Finn, *Ph.D. Thesis*, University of Illinois, Urbana-Champaign, 1982, pp. 30–37; *C.A.*, 97 (1982) 197518g.
10 Y. Okamoto and K. Hatada, *J. Liq. Chromatogr.*, 9 (1986) 369.
11 E. Francotte, R. M. Wolff, D. Lohmann and R. Mueller, *J. Chromatogr.*, 347 (1985) 25.
12 T. Shibata, I. Okamoto and K. Ishii, *J. Liq. Chromatogr.*, 9 (1986) 313.
13 R. Bishop, I. Hermansson, B. Jäderlund, G. Lindgren and P. Pernow, *Int. Lab.*, Jan./Feb. (1986) 46.
14 S. Allenmark, *LC, Liq. Chromatogr. HPLC Mag.*, 3 (1985) 348.
15 D. D. Perrin and B. Dempsey, *Buffers for pH and Metal Ion Control*, Chapman and Hall, London, 1979, p. 138.
16 W. H. Pirkle and M. H. Hyun, *J. Org. Chem.*, 49 (1984) 3043.
17 A. Tambuté, P. Gareil, M. Caude and R. Rosset, *J. Chromatogr.*, 363 (1986) 81.
18 K. B. Lipkowitz, D. J. Malik and T. Darden, *Tetrahedron Lett.*, 27 (1986) 1759.
19 Y. Okamoto, S. Honda, K. Hatada and H. Yuki, *J. Chromatogr.*, 350 (1985) 127.
20 J. P. Foley and J. G. Dorsey, *Anal. Chem.*, 55 (1983) 730.
21 I. W. Wainer and M. C. Alembik, *J. Chromatogr.*, 358 (1986) 85.

Journal of Chromatography, 448 (1988) 73–86
Elsevier Science Publishers B.V., Amsterdam — Printed in The Netherlands

CHROM. 20 600

SEPARATION OF PROTEINS BY MICROCOLUMN LIQUID CHROMATOGRAPHY BASED ON THE REVERSED-PHASE AND SIZE-EXCLUSION PRINCIPLES

CHERYL L. FLURER, CLAUDIO BORRA, FRANCA ANDREOLINI and MILOS NOVOTNY*
Department of Chemistry, Indiana University, Bloomington, IN 47405 (U.S.A.)
(First received December 29th, 1987; revised manuscript received April 12th, 1988)

SUMMARY

Slurry-packed fused-silica microcolumns of 250 μm I.D., are characterized for use in high-performance liquid chromatographic studies of proteins. The present work utilizes the reversed-phase and size-exclusion chromatographic modes for the separation of standard protein mixtures. A 5-μm, 300-Å octyl material is utilized for the reversed-phase studies, and the size-exclusion studies are accomplished with 5-μm diol material of 60-, 100- and 300-Å pore sizes. Column efficiency and packing reproducibility, as well as sample capacity in a micropreparative mode, are discussed. In addition, the inherent mass sensitivity of a microcolumn liquid chromatography system as applied to protein detection is demonstrated.

INTRODUCTION

Modern liquid chromatography (LC), using rigid particle materials, has been firmly established as a vital method for rapid and effective separation of proteins. Various retention mechanisms (size exclusion, reversed phase, hydrophobic interaction, ion exchange, bioaffinity, etc.) have been under extensive development to satisfy the needs of modern biochemical research and biotechnology. Particle technologies leading to the preparation of reversed-phase and size-exclusion columns appear less involved than those of the remaining systems.

An overwhelming majority of modern analytical protein separations involves 4.6 mm I.D., columns which permit microgram to milligram amounts of injected samples, leading to concentrations of the recovered protein solutes on the order of μg/ml. These methods are generally compatible with subsequent amino acid determination and sequencing methods. However, proteins in some biological samples are present only in nanogram quantities.

Several studies[1–5] have demonstrated the trace enrichment and micropreparative capabilities of smaller diameter columns (either 2.1 mm or 1 mm I.D.). These column types were chosen to minimize analysis time and contact time between the stationary phase and a protein, thereby decreasing bandbroadening and increasing protein recovery. Due to the strict dependence of protein capacity factors on the

0021-9673/88/$03.50

organic modifier concentration[6,7], submicrogram amounts of peptide or protein, present in a large sample volume, can be concentrated onto the reversed-phase support at less-than-critical organic modifier concentrations. Trace enrichment has been demonstrated by Nice *et al.*[1], who concentrated protein contained in 2 ml of sample down to an eluent volume as small as 25 μl. The recovered concentrations are on the order of mg/ml, which allows the use of fractions in gas-phase sequencers without further manipulations and sample loss. Nice *et al.*[1] also demonstrated low nanogram levels of detectability of epidermal growth factor (EGF_{α_1}) by using a 7.5 × 0.21 cm column.

Short columns have also been shown to be advantageous in similar directions[1,3,4,8]. Since column length does not appear to significantly affect resolution of protein peaks[9], other inherent advantages of shorter columns can be exploited. There are indications of improved recovery and fewer problems with underloading while using such columns[10]. Although the maximum loading capacity is only a few milligrams of protein, this is usually adequate for isolation and purification in a micropreparative mode.

During the last several years, microcolumn LC has been increasingly utilized for the separation of biologically important molecules[1–5,8,11]. Slurry-packed, fused-silica capillary columns[12–24] impart analytical advantages to relatively small biological solutes, such as high column efficiencies, increased mass sensitivity of concentration-sensitive detectors, and the ability to work with very small specimens. Our laboratory has recently become interested in extending certain of these capabilities to biopolymers.

The isolation of small quantities of proteins appears to be among the most desirable features of microcolumn (capillary) LC. Encouraged by the successful scale-down results with 2.1 and 1.0 mm I.D., columns[1–5], this direction is further justified by the recent developments in ultrahigh-sensitivity determinations of protein degradation products[2,4,8,25] for the sake of structural characterization.

We feel that fused-silica, slurry-packed microcolumns have the following major advantages to offer to the field of protein chromatography: (a) significantly less adsorptive behavior, due to the column materials inherently associated with this column technology, as well as the drastically reduced quantities of the sorption materials contacting the protein molecules; (b) enhanced mass sensitivity of the concentration-sensitive detectors (based on UV-absorption or native fluorescence) that are typically employed in protein detection; and (c) compatibility with small-scale sample manipulations. We have already demonstrated in a previous report[26] that subpicomolar amounts of model proteins can be detected and isolated using these microcolumns. The purpose of the investigations described here has been to characterize several different types of microcolumns with respect to the separation of common protein mixtures. The current scope of such studies has been limited to the reversed-phase and size-exclusion systems. Basic parameters of the protein analytical separations addressed here include column efficiency, sample capacity, and relative retention. Finally, the findings of these studies are correlated with various literature data obtained on larger-diameter columns.

TABLE I

PROTEINS USED IN THIS STUDY

Protein	*Abbreviation*	*Source*	*Molecular weight in kilodalton*
Thyroglobulin	Thy	Porcine	165
Transferrin	Trans	Bovine	77
Albumin	BA	Bovine	66
Ovalbumin	Ova	Chicken egg	45
β-Lactoglobulin A	LA	Bovine milk	35
Carbonic Anhydrase	CA	Bovine erythrocytes	29
α-Lactalbumin	Lalb	Bovine milk	14.2
Ribonuclease A	Rnase	Bovine pancreas	13.5
Cytochrome *c*	Cyt	Horse heart	11.7
Insulin	Ins	Bovine pancreas	11.5

MATERIALS AND METHODS

Reagents

Chromegabond MC-8 (ES Industries, Marlton, NJ, U.S.A.), and SynChropak GPC 60, 100, and 300 (SynChrom, Lafayette, IN, U.S.A.), having nominal particle sizes of 5 μm, were chosen as the stationary phases. HPLC grade acetonitrile and 85% phosphoric acid, and sodium phosphate dibasic were obtained from Fisher Scientific (Fair Lawn, NJ, U.S.A.). ChromAR HPLC grade methanol and sodium phosphate monobasic were purchased from Mallinckrodt (Paris, KY, U.S.A.). Distilled and deionized water was prepared in our laboratory. Mobile phase solutions were filtered with either 0.45-μm Millex-HV units (Millipore, Bedford, MA, U.S.A.), or a 0.5-μm in-line filter unit (Upchurch Scientific, Oak Harbor, WA, U.S.A.).

The protein standards, listed in Table I, were purchased from Sigma (St. Louis, MO, U.S.A.). Blue dextran (BD) and L-serine (Ser) (Sigma), as well as tetraglycine [$(Gly)_4$], a gift from Dr. Frank R. N. Gurd (Indiana University), were also utilized in this study. Samples were dissolved in 0.1 *M* phosphate buffer solutions of pH 2 (for reversed phase) or pH 7 (for size exclusion), and were filtered with Millex-HV units.

Column packing

After a porous frit was fixed at the column end[27], fused-silica capillaries (Polymicro Technologies, Phoenix, AZ, U.S.A.) (50 cm × 250 μm I.D.) were slurry-packed using a Model LC-5A pump (Shimadzu, Kyoto, Japan). The volume of the slurry reservoir, 1.6 mm I.D., varied according to the packing material.

Chromegabond (reversed-phase) MC-8 material required a fast packing technique[28]. An amount of 55 mg of the material was slurried with 200 μl of 1.5% Nonidet P-40 (Sigma) in acetonitrile, and the column was packed using acetonitrile as the solvent.

With the size-exclusion packings, the best results were obtained when methanol was used as the solvent. A slurry ratio of 40 mg packing to 120 μl methanol, and a slow packing technique[28] produced columns with the best efficiencies. The column

was slurry-packed at 5 μl/min constant flow-rate until the pressure reached 210 kg/cm^2. The pump was turned off, and the pressure allowed to decrease to zero. The column was then equilibrated with the mobile phase used for column evaluation.

Chromatographic systems

Reversed-phase chromatography (RPC). Separations were carried out on columns of 30-, 20-, and 10-cm in length. Analyses were done using a Model μLC-500 syringe pump (ISCO, Lincoln, NE, U.S.A.) operated in the constant-flow mode, and a μLC-10 UV–VIS detector (ISCO) fitted with a 1-mm pathlength (30 nl volume) flow cell. Proteins were detected at 215 nm. Injections were made using a four-port internal loop (air-actuated) injection valve (Model ACI4W, Valco Instruments, Houston, TX, U.S.A.) with a 0.2-μl rotor, and the moving-injection method[29]. Proteins were eluted using a stepwise gradient[19] from 20% to 55% acetonitrile in 0.1 *M* H_3PO_4–NaH_2PO_4 buffer at pH 2.

The step gradient utilizes PTFE reservoir tubes between 3 and 15 μl in volume. The tubes are filled and stacked from weakest eluent to next weakest, etc. The syringe pump is filled with the strongest eluent, in this case, the highest acetonitrile concentration. As the chromatographic run begins, eluent is displaced from segment to segment, through the column, thereby generating the step gradient.

Size-exclusion chromatography (SEC). Separations were carried out on columns between 40 and 50 cm in length. Analyses were done using the ISCO syringe pump in the constant-pressure mode, and a UVIDEC-100-V detector (Jasco, Tokyo, Japan) fitted with an in-house modified 150-nl cell, at 215 nm. Sample injections were made with an electrically-activated Valco valve, Model ECI4W, fitted with a 0.2-μl rotor. The samples were eluted isocratically using a 0.1 *M* NaH_2PO_4–Na_2HPO_4 buffer at pH 7, with 10% methanol added to the mobile phase for the GPC 100 and 300 materials.

The injection time and, consequently, the injected sample amount were controlled by an IBM personal computer, connected to the electrical actuator. The same computer, employing programs developed in this lab, acquired and calculated the peak moment data. Column efficiency data were compared using the totally included species, which were Ser for GPC 60, and $(Gly)_4$ for GPC 100 and 300. The mobile phase linear velocity was calculated using the totally excluded species, BA for GPC 60 and BD for GPC 100 and 300.

RESULTS AND DISCUSSION

The RPC and SEC principles for protein separation have been useful in different directions. RP-HPLC systems are very adaptable due to the wide variety of stationary phase–mobile phase combinations. Examples of their utilization include the study of hormonal polypeptides and proteins[30,31], histones[32], immunoglobulins[33], and pancreatic proteins[34], purification of hydrophobic virus membrane proteins[35], as well as highly efficient separations of cyanogen bromide[36,37] and tryptic[38,39] fragments of proteins. SEC has also been utilized extensively due to the ease with which separation of proteins based on size, or hydrodynamic volume, can be accomplished. Different size-exclusion materials allow the preliminary characterization of unknown mixtures as for their molecular weight ranges. The wide variety of

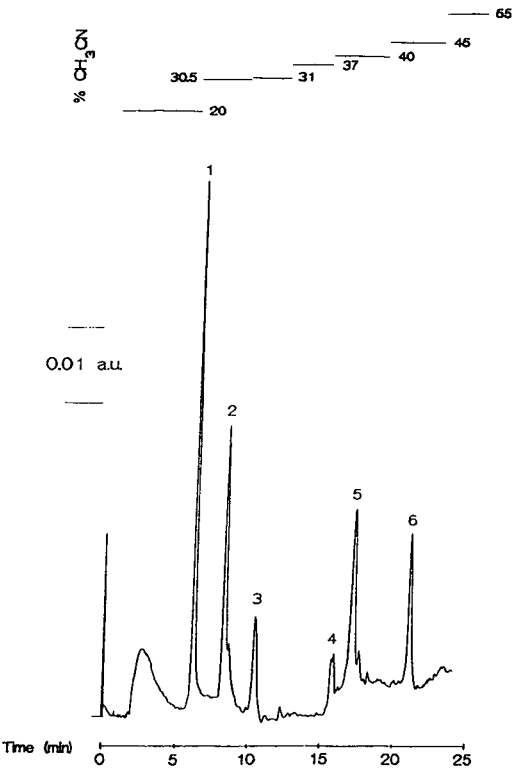

Fig. 1. Chromatographic separation of standard proteins on 10 cm × 250 μm I.D., octyl column. Proteins in order of elution: 1 = 3 ng Rnase, 2 = 3 ng Ins, 3 = 2 ng Cyt, 4 = 3 ng BA, 5 = 2 ng Lalb, 6 = 2 ng LA. Acetonitrile gradient in 0.1 *M* sodium phosphate buffer, pH 2, as shown above the chromatogram. Flow-rate = 2.1 μl/min.

buffers and mobile phase additives often makes the retention of native structure and activity possible, although, if desirable, denaturants[40,41] or surfactants[42,43] can also be added. The general utility of RP-HPLC and SEC have prompted our initial efforts toward column miniaturization in these areas.

Since the earlier investigations[9,37,44–47] had shown the superiority of large-pore materials in RP-HPLC, an octyl substituted, 300-Å pore size material was chosen in our studies. Among various alternatives available for efficient SEC, we chose silica-based materials derivatized with a glycerylpropylsilane to form a diol surface moiety[48,49]. Packing procedures for these materials were based on our experience[28] with somewhat similar packings for the separations of smaller molecules.

The first example of protein separation, shown in Fig. 1, was obtained on a 10-cm microcolumn packed with a 300-Å octyl material, with the gradient profile and sample amounts indicated. The advantages of high mass sensitivity with the miniaturized UV detector are indicated. Clearly, subpicomolar amounts of the model proteins form well-shaped peaks. As shown in a recent communication[26] concerned with the micro-isolation capabilities of such microcolumns, there are only very small losses of proteins involved; a small peak of insulin was still detectable at the 58-pg

TABLE II

PROTEIN CAPACITY FACTORS AS A FUNCTION OF COLUMN LENGTH FOR THE 300-Å OCTYL PACKING

Proteins	*Capacity factors**		
	10 cm	*20 cm*	*30 cm*
Rnase	2.4	1.3	0.8
Ins	4.4	2.1	1.3
Cyt	5.6	2.4	1.4
BA	7.9	3.8	2.2
Lalb	8.5	4.3	2.6
LA	10.0	5.1	3.2

* t_0 measured by dead volume peak that occurred due to slight differences in buffer concentrations of solute and mobile phase.

level. For the proteins with native fluorescence, even smaller quantities could be detectable.

Table II lists capacity factors for the model proteins on the C_8 microcolumns of different lengths. When continuous gradients in conventional systems are utilized, the values are not expected to vary with length. We attribute the changes observed in Table II to the difficulty in decreasing the volumes of the gradient segments proportionally to the column length. These volume differences effectively change the gradient slope, which has been shown to affect both peak shape and recovery in protein separations[33,50,51]. Despite the differences in values indicated by the table, we observed that the proteins do elute at the same acetonitrile concentration on different columns, indicating that the column length does not influence the relative retention of proteins[9].

Perhaps it is pertinent to address the problems associated with the use of microcolumns at this point. As with any column, clogs may develop due to sample precipitation or the presence of "foreign matter". Because fused silica is easy to cut, this problem can be addressed by simply removing the first few millimeters of column, without seriously affecting retention times or separation efficiency.

A more serious drawback of the microcolumn technique is the utilization of a step gradient. The step gradient itself is reproducible, because one has control over the volumes and concentrations of the eluents used. However, it would be prohibitively difficult for use in the analysis of complex protein samples, due to the large number of segments that would be required. The use of a continuous gradient, either linear or exponential, would aid in the ease and speed of analysis, particularly by decreasing the amount of time devoted to choosing proper gradient concentrations and volumes for optimum component separation. However, we are severely limited by the mixing volumes allowable. Total gradient volumes are typically on the order of 40–50 μl for a 30-cm column, and even less for shorter columns. Unfortunately, these volumes are much lower than the mixing-delay volumes available in most commercial and homemade gradient devices[52–55]. Until other options are made available, we appear to be limited to the utilization of the step gradient for microcolumn LC.

As can be seen in Fig. 2, the resolution for the Ins/Cyt pair decreases as the

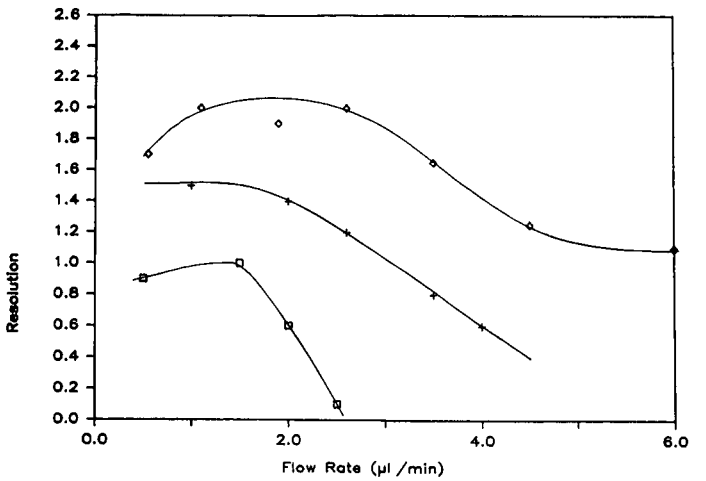

Fig. 2. Ins/Cyt resolution as a function of flow-rate for (□) 30-cm, (+) 20-cm, and (◇) 10-cm columns. Gradient conditions similar to those of Fig. 1. Resolution is $2(t_{R_B} - t_{R_A})/(W_A + W_B)$.

flow-rate increases for all column lengths tested, as has been observed in other systems[2,56]. As indicated by Schlabach and Wilson[2] and Jones *et al.*[56], lower flow-rates are better for protein resolution in gradient elution. Similar results were obtained for the BA/Lalb pair. Fig. 2 also seems to indicate that resolution increases as column length decreases, as was noted by Blanquet *et al.*[50]. Obviously, similar behavior is

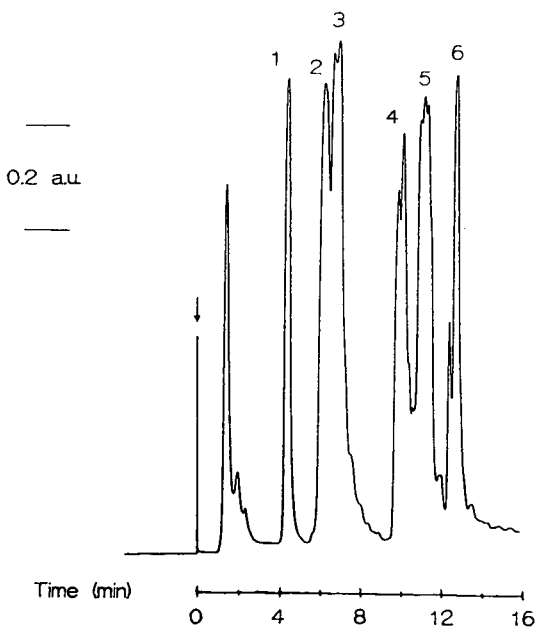

Fig. 3. Loadability of a 10 cm × 250 µm I.D., octyl column. Proteins in order of elution: 1 = 1.6 µg Rnase, 2 = 1.7 µg Ins, 3 = 1.8 µg Cyt, 4 = 1.5 µg BA, 5 = 1.7 µg Lalb, 6 = 1.8 µg LA. Gradient conditions as in Fig. 1. Flow-rate = 2.5 µl/min.

noticed here with our microcolumns. In terms of both relative retention and component resolution, microcolumns prepared successively from the same sorption material were found to be reproducible.

Column loading capacity is an important consideration if one wishes to take full advantage of the micropreparative capabilities of a microcolumn system with samples containing varying amounts of proteins. As demonstrated in Fig. 3, adequate component resolution can be achieved at microgram quantities. A blank gradient then was initiated to estimate the extent of "ghosting", that is, the appearance of solute peaks in subsequent runs. At the maximum loading capacity of the column, a peak corresponding to bovine albumin reappeared, with a peak area of approximately 2% of that from the previous solute run. No peaks corresponding to the other proteins were seen, and another blank run failed to produce another bovine albumin "ghost" peak. This phenomenon is not a product of the use of a step gradient, but a problem that exists in protein chromatography when the solubility limits of hydrophobic proteins, in particular, are exceeded. In fact, the use of microcolumns seems to reduce the number of subsequent blank gradients needed to clean the column, even at maximum loading. Our microcolumns thus exhibit an adequate "dynamic range" for the protein samples, from the microgram quantities down to the minimum detectable amounts, as demonstrated in a related publication[26], in the high picogram range.

In the area of SEC, we have evaluated three packing materials that are applicable to different molecular weight ranges. The plate height values as a function of the mobile phase velocity were determined, as demonstrated in Fig. 4. The results for the GPC 60 and 100 materials reflect a general increase in the slope of the linear portion as the molecular weight increases; this trend is seen more clearly in the data obtained on the GPC 300 column. It has been observed[48] that proteins eluting immediately after the dead volume tend to have broader peaks than the others. This is due to limited diffusion as the molecular dimensions approach those of the pore, and could account for the non-linearity observed in the thyroglobulin data. It is also possible that thyroglobulin aggregation or denaturation could be occurring; at this point, only speculations are possible.

Similar to the observations of Yamamoto *et al.*[57] with the HW55F gel, the height equivalent to a theoretical plate (HETP) value extrapolated to $u=0$ for the GPC 300 material did not change appreciably with the molecular weight. The GPC materials also demonstrate that HETP depends very little on flow-rate for Ser and $(Gly)_4$, because their movement is not limited by their diffusion coefficients[58]. Table III summarizes the efficiencies in plates per meter and the reduced plate height values, averaged from three consecutively prepared microcolumns for each packing material. The results obtained for efficiencies are comparable to those obtained by Rokushika *et al.*[58] with the TSK-GEL 2000 and 3000 SW columns, and appear to be better than those obtained by SynChrom[59] on conventional columns.

Protein standards were separated on the GPC 60 and 100 columns as shown in Figs. 5 and 6, respectively, with good resolution. It is apparent that the mass detection sensitivity inherent to microcolumn LC makes the detection of nanogram amounts of proteins routine.

The GPC 300 material was studied in more detail, because of the larger molecular weight range. Fig. 7 demonstrates the typical sigmoidal calibration curve

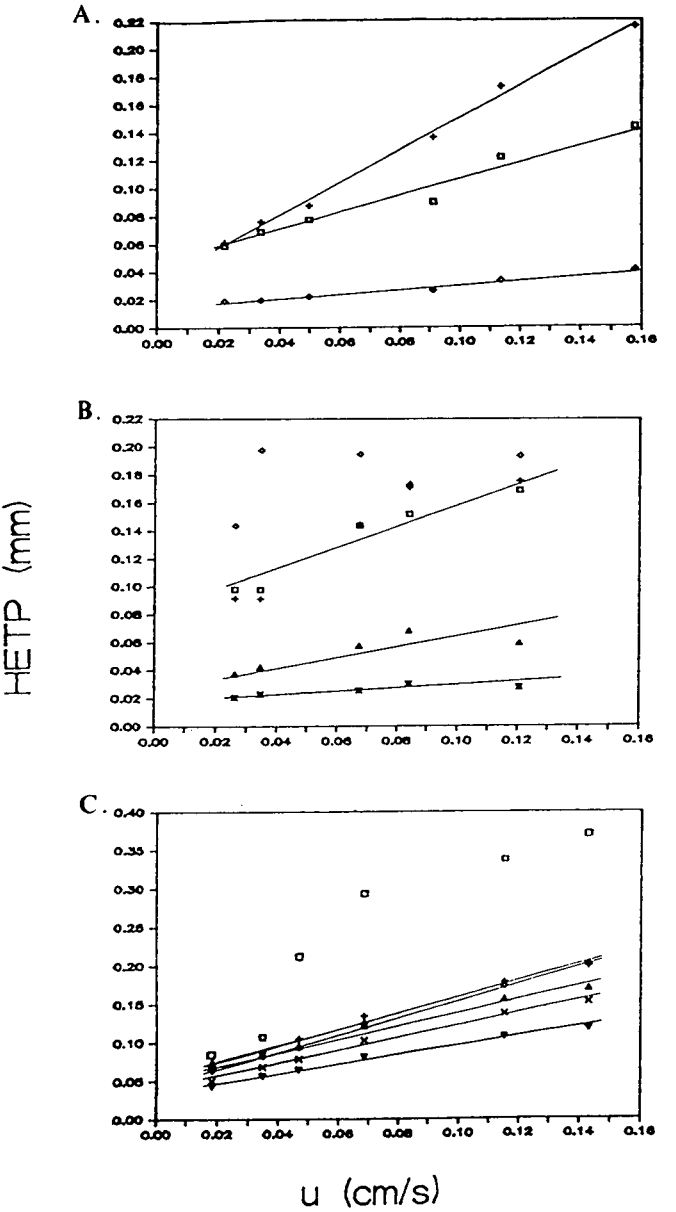

Fig. 4. HETP as a function of mobile phase linear velocity (u) for (A) GPC 60, (B) GPC 100, and (C) GPC 300. Mobile phases: (A) 0.1 *M* sodium phosphate buffer, pH 7; (B) and (C) 10% methanol in 0.1 *M* sodium phosphate buffer, pH 7. Key: A, (□) BA; (+) Rnase; (◇) Serine; B, (□) Thy; (+) Trans; (◇) LA; (△) Lalb; (×) $(Gly)_4$; C, (□) Thy; (+) Trans; (◇) BA; (△) LA; (×) CA; (▽) Rnase.

TABLE III

AVERAGE COLUMN PERFORMANCE FOR SYNCHROPAK GPC MATERIALS

Mobile phase flow-rate was 0.4 μl/min for all determinations.

	N/m	*h*
GPC 60		
BA	11300	19
Rnase	10200	20
Ser	42000	4.9
GPC 100		
Thy	9700	20
Trans	11000	19
LA	6000	34
Lalb	22000	9.2
$(Gly)_4$	43700	4.6
GPC 300		
Thy	9000	22
Trans	11300	18
BA	12300	16
LA	10000	21
CA	15400	13
Rnase	17300	12
$(Gly)_4$	42100	4.8

obtained with the model proteins, plus the excluded and included solutes. All the proteins behaved linearly, with a correlation coefficient of 0.98.

Fig. 8 demonstrates the separation of a standard mixture of proteins and $(Gly)_4$. Problems were encountered with the coelution of Trans and BA, and, as the

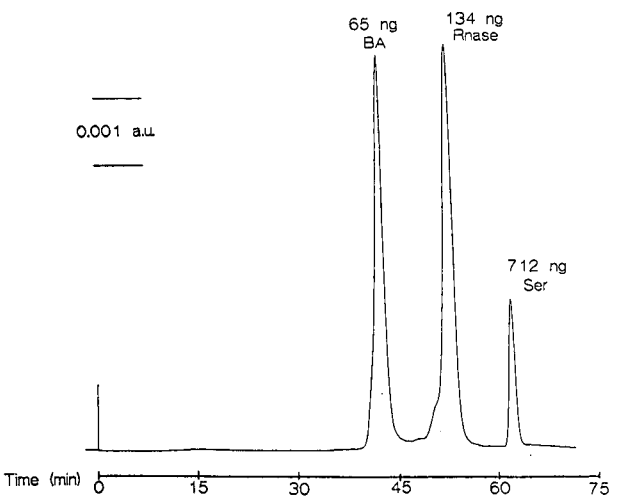

Fig. 5. Chromatography of standard proteins on a 53 cm × 250 μm I.D., GPC 60 column. Mobile phase: 0.1 *M* sodium phosphate buffer, pH 7, at a flow-rate of 0.27 μl/min.

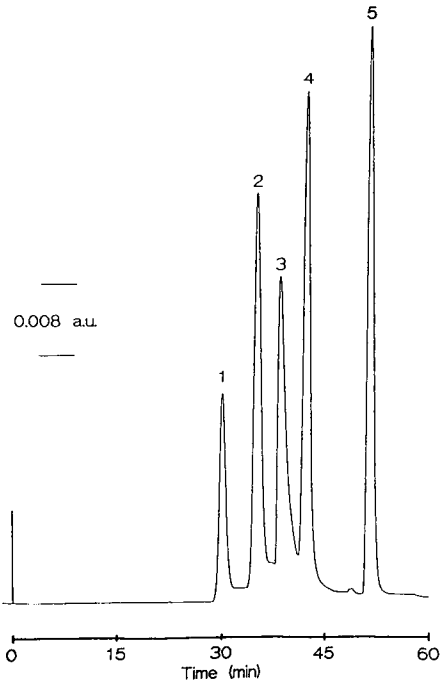

Fig. 6. Chromatography of standard proteins on a 51 cm × 250 μm I.D., GPC 100 column. Proteins in elution order: 1 = 86 ng Thy, 2 = 124 ng Trans, 3 = 94 ng LA, 4 = 124 ng Lalb, 5 = 166 ng $(Gly)_4$. Mobile phase: 10% methanol in 0.1 *M* sodium phosphate buffer, pH 7, at a flow-rate of 0.33 μl/min.

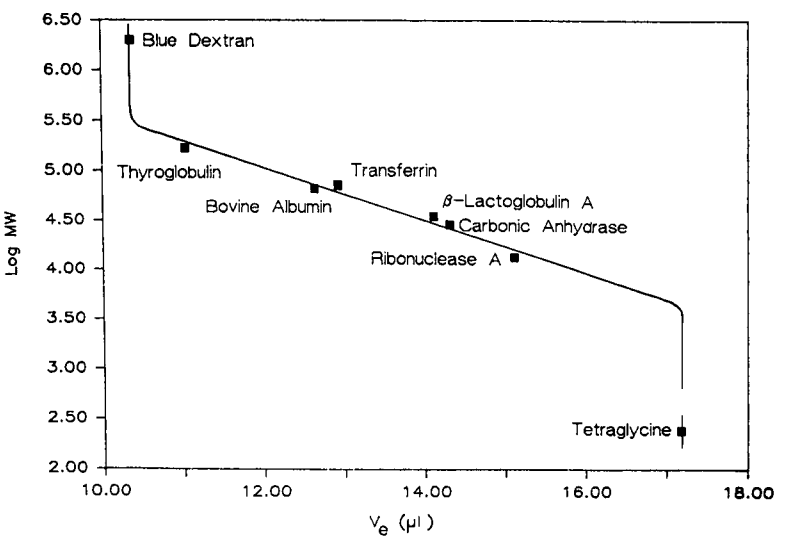

Fig. 7. Relationship of log MW to elution volume on a 48 cm × 250 μm I.D., GPC 300 column. Mobile phase: 10% methanol in 0.1 *M* sodium phosphate buffer, pH 7.

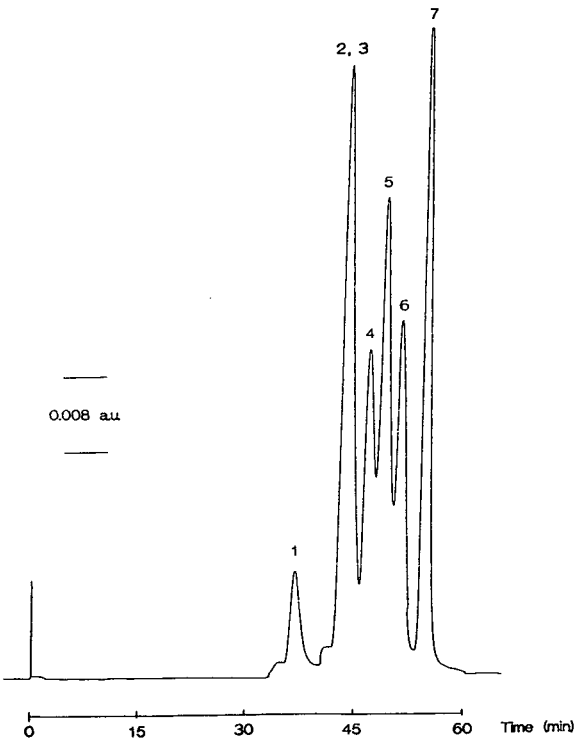

Fig. 8. Chromatography of standard proteins on a GPC 300 column. Proteins in order of elution: 1 = 90 ng Thy, 2 = 101 ng Trans, 3 = 89 ng BA, 4 = 86 ng LA, 5 = 95 ng CA, 6 = 92 ng Rnase, 7 = 178 ng $(Gly)_4$. Other conditions same as in Fig. 7, at a flow-rate of 0.33 μl/min.

sample was diluted further, LA and CA also coeluted. It has been observed that there must be a two-fold difference in molecular weight before two solutes may be resolved, even with a good SEC column[48]. This fact seems to be supported by the observed coelution problem. Although Rokushika *et al.*[58] demonstrated the separation of low nanogram amounts of protein at 205 nm on a TSK-GEL 3000 SW column, our results reported elsewhere[26] demonstrate separation and detection of subpicomolar amounts.

As shown in this communication, microcolumn LC technologies have considerable potential in the investigations of very small protein samples. The initial work shown with the reversed-phase and size-exclusion systems must now be expanded to the other separation modes that include ion-exchange, hydrophobic interaction and affinity principles for the retention of biological activity. Microcolumns can be used to isolate proteins in quantities that are compatible with structure elucidation procedures that are currently available. However, we have also demonstrated the ability to isolate low nanogram quantities of proteins, which are clearly too low for use with gas-phase sequencers. Consequently, highly sensitive protein characterization techniques must be developed to match the protein microisolation capabilities. Work is underway in this laboratory to achieve these goals, and preliminary

results on the ultrahigh-sensitivity determination of amino acids[26] through laser-based fluorescence detection have already been reported.

ACKNOWLEDGEMENT

This work was supported by Grant Number RO1 GM24349 from the National Institute of General Medical Sciences, U.S. Department of Health and Human Services.

REFERENCES

1 E. C. Nice, C. J. Lloyd and A. W. Burgess, *J. Chromatogr.*, 296 (1984) 153.
2 T. D. Schlabach and K. J. Wilson, *J. Chromatogr.*, 385 (1987) 65.
3 B. Grego, E. C. Nice and R. J. Simpson, *J. Chromatogr.*, 352 (1986) 359.
4 B. Grego, I. R. van Driel, P. A. Stearne, J. W. Goding, E. C. Nice and R. J. Simpson, *Eur. J. Biochem.*, 148 (1985) 485.
5 R. C. Simpson and P. R. Brown, *J. Chromatogr.*, 385 (1987) 41.
6 B. Grego and M. T. W. Hearn, *Chromatographia*, 14 (1981) 589.
7 D. W. Armstrong and R. E. Boehm, *J. Chromatogr. Sci.*, 22 (1984) 378.
8 E. C. Nice, B. Grego and R. J. Simpson, *Biochem. Intl.*, 11 (1985) 187.
9 J. D. Pearson, N. T. Lin and F. E. Regnier, *Anal. Biochem.*, 124 (1982) 217.
10 J. D. Pearson, *Anal. Biochem.*, 152 (1986) 189.
11 R. B. Taylor, K. E. Kendle, R. G. Reid and C. T. Hung, *J. Chromatogr.*, 385 (1987) 383.
12 R. P. W. Scott and P. Kucera, *J. Chromatogr.*, 125 (1976) 251.
13 R. P. W. Scott, *Analyst (London)*, 103 (1978) 37.
14 R. P. W. Scott and P. Kucera, *J. Chromatogr.*, 169 (1979) 51.
15 R. P. W. Scott and M. Munroe, *J. Chromatogr.*, 186 (1979) 475.
16 T. Tsuda and M. Novotny, *Anal. Chem.*, 50 (1978) 271.
17 T. Tsuda and M. Novotny, *Anal. Chem.*, 50 (1978) 632.
18 Y. Hirata, M. Novotny, T. Tsuda and D. Ishii, *Anal. Chem.*, 51 (1979) 1807.
19 Y. Hirata and M. Novotný, *J. Chromatogr.*, 186 (1979) 521.
20 M. Novotny, *Anal. Chem.*, 53 (1981) 1294A.
21 D. Ishii, K. Asai, K. Hibi, T. Jonokuchi and M. Nagaya, *J. Chromatogr.*, 144 (1977) 157.
22 D. Ishii, K. Hibi, K. Asai and M. Nagaya, *J. Chromatogr.*, 152 (1978) 341.
23 T. Tsuda, K. Hibi, T. Nakanishi, T. Takeuchi and D. Ishii, *J. Chromatogr.*, 158 (1978) 227.
24 D. Ishii, T. Tsuda and T. Takeuchi, *J. Chromatogr.*, 185 (1979) 73.
25 K. L. Stone and K. R. Williams, *J. Chromatogr.*, 359 (1986) 203.
26 C. Flurer, C. Borra, S. Beale and M. Novotny, *Anal. Chem.*, in press.
27 D. C. Shelly, J. C. Gluckman and M. V. Novotny, *Anal. Chem.*, 56 (1984) 2990.
28 F. Andreolini, C. Borra and M. V. Novotny, *Anal. Chem.*, 59 (1987) 2428.
29 M. C. Harvey and S. D. Stearns, *J. Chromatogr. Sci.*, 21 (1983) 473.
30 M. J. O'Hare and E. C. Nice, *J. Chromatogr.*, 171 (1979) 209.
31 B. Grego and M. T. W. Hearn, *J. Chromatogr.*, 336 (1984) 25.
32 H. Lindner, W. Helliger and B. Puschendorf, *J. Chromatogr.*, 357 (1986) 301.
33 M. J. O'Hare, M. W. Capp, E. C. Nice, N. H. C. Cooke and B. G. Archer, *Anal. Biochem.*, 126 (1982) 17.
34 P. J. Padfield, M. Griffin and R. M. Case, *J. Chromatogr.*, 369 (1986) 133.
35 R. van der Zee, T. Hoekzema, S. Welling-Wester and G. W. Welling, *J. Chromatogr.*, 368 (1986) 283.
36 W. Kopaciewicz and F. E. Regnier, *J. Chromatogr.*, 358 (1986) 119.
37 J. D. Pearson, W. C. Mahoney, M. A. Hermodson and F. E. Regnier, *J. Chromatogr.*, 207 (1981) 325.
38 A. J. Banes, G. W. Link and L. R. Snyder, *J. Chromatogr.*, 326 (1985) 419.
39 P. A. Hartman, J. D. Stodola, G. C. Harbour and J. G. Hoogerheide, *J. Chromatogr.*, 360 (1986) 385.
40 N. Ui, *Anal. Biochem.*, 97 (1979) 65.
41 B. S. Welinder, *J. Liq. Chromatogr.*, 3 (1980) 1399.
42 T. Imamura, K. Konishi, M. Yokoyama and K. Konishi, *J. Biochem.*, 86 (1979) 639.

43 Y. Kato, K. Komiya, H. Sasaki and T. Hashimoto, *J. Chromatogr.*, 193 (1980) 29.
44 R. V. Lewis, A. Fallon, S. Stein, K. D. Gibson and S. Udenfriend, *Anal. Biochem.*, 104 (1980) 153.
45 E. C. Nice, M. W. Capp, N. Cooke and M. J. O'Hare, *J. Chromatogr.*, 218 (1981) 569.
46 K. J. Wilson, E. van Wieringen, S. Klauser, M. W. Berchtold and G. J. Hughes, *J. Chromatogr.*, 237 (1982) 407.
47 K. A. Cohen, K. Schellenberg, K. Benedek, B. L. Karger, B. Grego and M. T. W. Hearn, *Anal. Biochem.*, 140 (1984) 223.
48 F. E. Regnier, *Methods Enzymol.*, 91 (1983) 137.
49 F. E. Regnier and K. M. Gooding, *Anal. Biochem.*, 103 (1980) 1.
50 R. S. Blanquet, K. H. Bui and D. W. Armstrong, *J. Liq. Chromatogr.*, 9 (1986) 1933.
51 N. H. C. Cooke, B. G. Archer, M. J. O'Hare, E. C. Nice and M. Capp, *J. Chromatogr.*, 255 (1983) 115.
52 V. Berry, D. Ishii and T. Takeuchi, *J. Liq. Chromatogr.*, 9 (1986) 1529.
53 K. Slais and V. Preussler, *J. High Resolut. Chromatogr. Chromatogr. Commun.*, 10 (1987) 82.
54 V. Berry, *LC, Liq. Chromatogr. HPLC Mag.*, 2 (1985) 110.
55 H. E. Schwartz, B. L. Karger and P. Kucera, *Anal. Chem.*, 55 (1983) 1752.
56 B. N. Jones, R. V. Lewis, S. Pääbo, K. Kohima, S. Kimura and S. Stein, *J. Liq. Chromatogr.*, 3 (1980) 1373.
57 S. Yamamoto, M. Nomura and Y. Sano, *J. Chromatogr.*, 394 (1987) 363.
58 S. Rokushika, T. Ohkawa and H. Hatano, *J. Chromatogr.*, 176 (1979) 456.
59 *GPC Product Bulletin*, SynChropak.

Journal of Chromatography, 448 (1988) 87–93
Elsevier Science Publishers B.V., Amsterdam — Printed in The Netherlands

CHROM. 20 562

EFFECT OF THE PORE STRUCTURE OF SILICA GEL ON RETENTION BEHAVIOUR IN PRESSURE PROGRAMMING SUPERCRITICAL FLUID CHROMATOGRAPHY

AKIRA NOMURA*, JOSEPH YAMADA and KIN-ICHI TSUNODA
Division of Analytical Chemistry, National Chemical Laboratory for Industry, Tsukuba, Ibaraki 305 (Japan)
(First receved January 15th, 1988; revised manuscript received March 15th, 1988)

SUMMARY

The retention behaviour of polar and non-polar compounds on packed ODS-silica gel columns of various pore structures was investigated using pressure programming supercritical fluid chromatography (SFC) with carbon dioxide as a mobile phase. The pressure programming was useful in packed SFC as well as in capillary SFC, and polystyrene oligomers were separated efficiently according to their polymerization degree. The retention behaviour of polar compounds such as pyridine was affected by both the pore structure and the carbon content of the ODS-silica gel.

INTRODUCTION

In recent years, supercritical fluid chromatography (SFC) has been recognized as a powerful technique for the separation of non-volatile and thermally labile compounds such as oligomers and polyaromatic hydrocarbons not amenable to gas chromatography (GC)[1–4]. The retention of a solute in SFC is controlled by the composition and the density of the mobile phase, the nature of the stationary phase and the temperature. Pressure–density programming is advantageous for retention control in SFC, somewhat analogous to temperature programming in GC and gradient elution in high-performance liquid chromatography (HPLC). Although pressure programming is common in capillary SFC using a small capillary tube as a flow restrictor at the outlet, it is not so common in packed column SFC because the use of a regulation valve or back-pressure valve is popular to maintain the entire eluent system at high pressure, and therefore it is necessary to adjust the valve automatically for the pressure control[5–14].

In packed column SFC, the addition of polar modifiers to supercritical fluids has been reported by several investigators to improve the retention behaviour, because alkyl-bonded silica columns, typically ODS-silica gel for HPLC, give some problems due to the residual silanol groups which interact with polar compounds and cause undesirable tailing and irreversible adsorption on the columns; great efforts have been made to solve this problem[15–21].

In this work the chromatographic behaviour of ODS-silica gels having various

0021-9673/88/$03.50

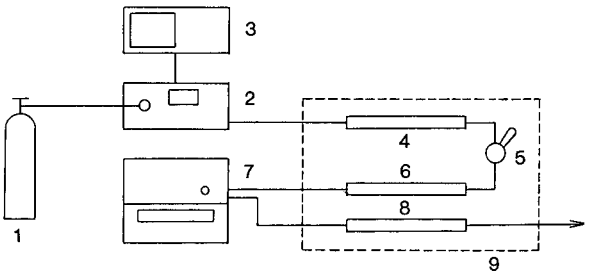

Fig. 1. Schematic flow diagram of the SFC apparatus. 1 = Carbon dioxide cylinder; 2 = pump; 3 = pump controller; 4 = precolumn; 5 = sample injector; 6 = separation column; 7 = UV detector; 8 = restrictor; 9 = oven.

pore structures was investigated by pressure programming SFC using carbon dioxide as the mobile phase without a modifier, to obtain basic knowledge for the development of completely inert SFC columns based on silica gel.

EXPERIMENTAL

Apparatus

The SFC system used is shown in Fig. 1. It consisted of a Shimadzu LC-6A pump the head of which was cooled, a Shimadzu LC-6A system controller for the pressure programming, a sample injector Model 7125 from Rheodyne with a 20-μl sample loop, an UBILOG-60 UV detector from Oyo-Bunko Kiki, a capillary restrictor (20 cm × 50 μm I.D.) protected by a copper tube and a column oven from a Shimadzu LC-1 system.

Materials

The silica gels used for the preparation of ODS-silica gels were Super Micro Beads for HPLC (particle size 10 μm, spherical) from Fuji-Davison Chemical and

TABLE I

PORE STRUCTURES AND ALKYL CONTENTS OF ODS-SILICA GELS

FD = Super Micro Bead from Fuji-Davison Chemical.

	Specific surface area (m^2/g)	*Pore volume (ml/g)*	*Pore diameter (Å)*	*ODS-silica gel*					
				ODS-L		*ODS-M*		*ODS-H*	
				%C	*n**	*%C*	*n**	*%C*	*n**
FD-70	485	0.85	70	–	–	–	–	17.82	0.92
FD-100	390	0.96	98	4.46	0.29	14.58	0.94	17.20	1.10
FD-150	197	1.20	164	3.60	0.46	9.90	1.26	11.41	1.45
FD-300	90	1.22	327	2.37	0.66	5.31	1.48	6.34	1.76
FD-500	72	1.15	505	2.59	0.90	4.01	1.39	4.64	1.61
FD-800	52	1.11	787	1.98	0.95	2.77	1.33	3.12	1.50
FD-1000	32	1.00	1078	1.96	1.53	2.21	1.73	2.49	1.95

* Number of alkyl chains per 100 Å^2.

their properties are summarized in Table I along with the carbon contents and the number of alkyl chains per unit surface area (100 A^2). Silica particles of 10 μm in diameter were chosen instead of those of 5 μm because of the ease of column packing. Dimethyloctadecylchlorosilane was obtained from Shin-etsu Silicone Chemicals. Toluene from Wako Pure Chemical Industries was dried over calcium chloride before use as a solvent in the preparation of the ODS-silica gels. Polystyrene oligomers with average molecular weights of 300 (A-300) and 500 (A-500) used as samples were from Toyo Soda Manufacturing, and dissolved in hexane. As samples, pyridine from Kokusan Chemical Works and phenol from Nakarai Chemicals were dissolved in chloroform and methanol, respectively. Other reagents were of reagent grade and used without purification.

Preparation of ODS-silica gel packings

Silica gels summarized in Table I were modified with 2 mmol/g of dimethyloctadecylchlorosilane in toluene under reflux for 3 h with stirring. Three types of ODS-silica, that is low-carbon content (ODS-L), medium-carbon content (ODS-M) and high-carbon content (ODS-H), were prepared under different conditions such as with or without a catalyst. After cooling to room temperature, the ODS-silica gel was separated from the solvent by vacuum filtration using a sintered glass funnel, washed three times with benzene then, three times with dichloromethane and dried under vacuum at 110°C overnight. It was then subjected to elemental analysis (C, H, N) using a CHN Corder Type MT-3 from Yanagimoto. The ODS-silica gels were packed into a 250 mm × 4 mm I.D. stainless-steel column with a slurry method using 2-propanol as a slurry solvent, and washed with methanol before attaching to the SFC apparatus.

RESULTS AND DISCUSSION

The solvating power of a supercritical fluid depends on the density and can be controlled as a function of pressure. Fig. 2 shows the effect of pressure programming (A) on the retention behaviour of a polystyrene oligomer compared with a constant-pressure mode of 230 kg/cm^2 (B) on a FD-300, ODS-H column. The pressure programming SFC was carried out by holding the pressure at 150 kg/cm^2 for 5 min after sample injection, followed by a linear pressure gradient up to 350 kg/cm^2 for 25 min and holding the pressure at 350 kg/cm^2 until all the sample had eluted. Styrene monomer was eluted first and other oligomers were eluted sequentially according to their polymerization degree. In the constant-pressure mode, the chromatographic peaks were broader and the sample retention increased as the polymerization degree of the oligomer increased. In the case of pressure programming, on the other hand, the peak shapes and the retention balance of the chromatogram were improved.

Three types of chromatogram of polystyrene oligomer obtained by the same pressure programming conditions as in Fig. 2A are shown in Fig. 3. The chromatograms were obtained on the high-carbon content ODS (ODS-H) silica gel columns prepared from FD-100, -300 and -1000. The separaton profiles were better on the ODS-silica gels of smaller pore size and the samples were eluted more rapidly on the larger pore size columns. The poor shape of the later peaks was due to the presence of isomers in the peaks. Furthermore, the effect of the pore size of ODS-H silica gels

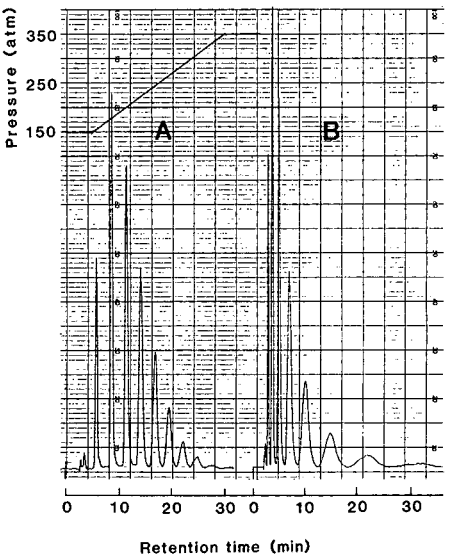

Fig. 2. Effect of pressure programming. Column: FD-300, ODS-H, 250 mm × 4 mm I.D.; temperature; 50°C. Sample: polystyrene oligomer. (A) Pressure programming; (B) constant pressure, 230 kg/cm².

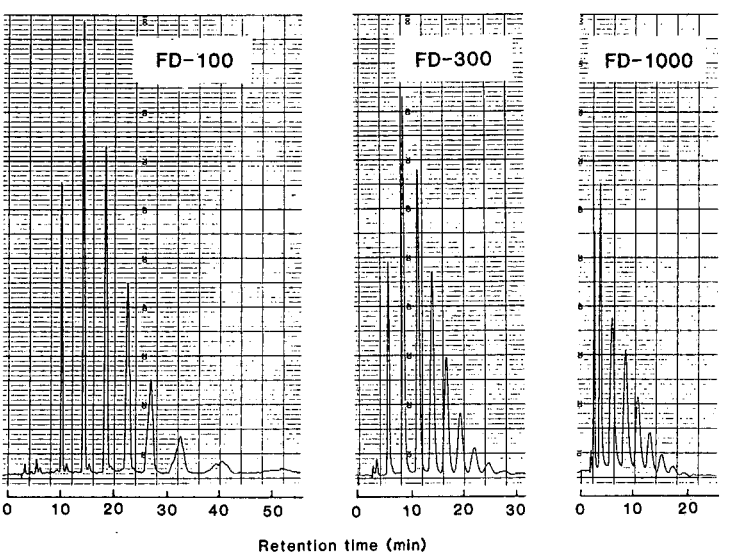

Fig. 3. Chromatograms of polystyrene oligomer on various ODS-silica gel columns. Column: ODS-H, 250 mm × 4 mm I.D. Other conditions as in Fig. 2A.

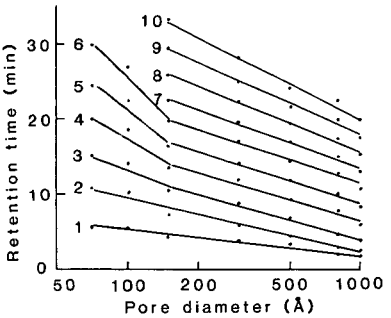

Fig. 4. Retention time of styrene oligomer *vs.* logarithm of pore diameter of ODS-silica gel. Conditions as in Fig. 3.

(logarithmic scale) on the retention behaviour of polystyrene oligomer under the same pressure programming conditions is shown in Fig. 4. The retention time of the sample increased as the polymerization degree increased, and decreased linearly as the pore diameter of the packings increased above the diameter of 150 Å. The retention behaviour of the styrene trimer ($n=3$) and heptamer ($n=7$), for instance, on the columns of different carbon contents of ODS-silica gel (ODS-L,M,H) is also shown in Fig. 5. The retention time of both samples decreased as the pore diameter of ODS-silica gel increased, and almost no dependence on the carbon content was observed. Therefore, the retention behaviour of non-polar compounds such as polystyrene oligomers, is suggested to be influenced by the pore structure much more

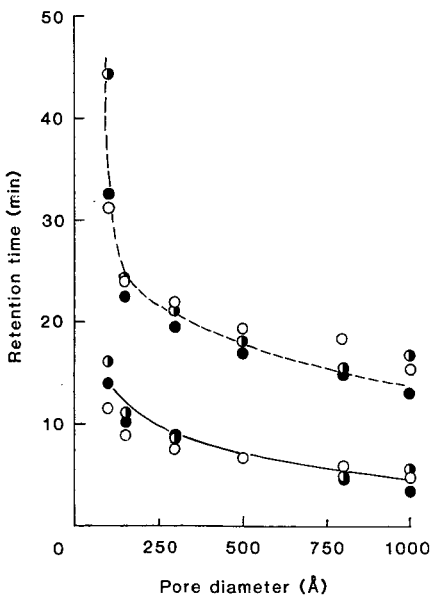

Fig. 5. Effect of the carbon content of ODS-silica gel on retention behaviour of polystyrene oligomer. ○, ODS-L; ◑, ODS-M; ●, ODS-H. ———, Styrene trimer ($n=3$); – – –, styrene heptamer ($n=7$). Other conditions as in Fig. 2A.

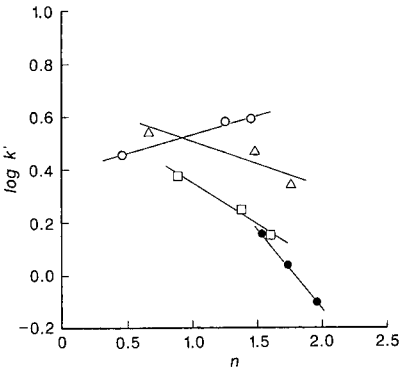

Fig. 6. Dependence of log k' for styrene pentamer ($n=5$) on the number of alkyl chains per 100 Å^2 in various pore sizes of ODS-silica gel columns. ○, FD-150; △, FD-300; □, FD-500; ●, FD-1000. Conditions: column, 250 mm × 4 mm I.D.; column temperature, 50°C; pressure, 230 kg/cm^2.

than the hydrophobicity or the remaining silanol groups on the ODS-silica gel packings. The dependence of log k' for styrene pentamer ($n=5$) on the number of alkyl chains per 100 Å^2 in various pore sizes of ODS-silica gel under constant pressure is shown in Fig. 6. The results provide evidence in support of the suggestion above and are inconsistent with those of reversed-phase liquid chromatography.

The residual silanol groups on chemically bonded silica gel tend to interact with polar compounds and give some problems such as irreversible adsorption or non-Gaussian peak shapes. The retention behaviour of polar compounds, for example pyridine and phenol on different carbon contents of ODS-silica gel was investigated in terms of the pore structure of the silica gel using a constant pressure of 230 kg/cm^2 at 50°C as shown in Figs. 7 and 8, respectively. The retention behaviour

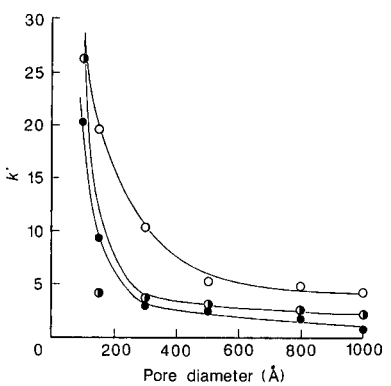

Fig. 7. Retention behaviour of pyridine on various ODS-silica gel columns: ○, ODS-L; ◑, ODS-M; ●, ODS-H. Other conditions as in Fig. 6.

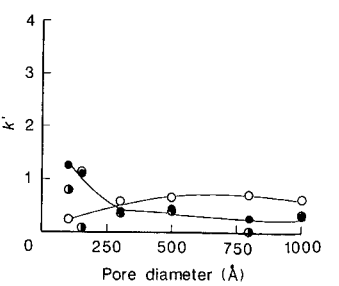

Fig. 8. Retention behaviour of phenol on various ODS-silica gel columns: ○, ODS-L: ◑, ODS-M; ●, ODS-H. Other conditions as in Fig. 7.

of pyridine was affected by both the pore structure and carbon content of the ODS-silica gel. This is presumably because more silanol groups remain on the ODS-silica gel packings having smaller pore sizes, that is larger specific surface areas, and also on those containing less bonded octadecyl. On the contrary, the retention behaviour of phenol was not affected by the pore structure or the carbon content of ODS-silica gel packings, presumably because phenol and silanol groups are both acidic and their interaction is much less than that of pyridine and silanol groups.

REFERENCES

1 J. C. Giddings, M. N. Myers and J. W. King, *J. Chromatogr. Sci.*, 7 (1969) 276.
2 E. Klesper, *Angew. Chem., Int. Ed. Engl.*, 17 (1978) 738.
3 M. Novotny, S. R. Springston, P. A. Peaden, J. C. Fjeldsted and M. L. Lee, *Anal. Chem.*, 53 (1981) 407A.
4 Y. Hirata and F. Nakata, *J. Chromatogr.*, 295 (1984) 315.
5 U. van Wasen and G. M. Schneider, *Angew. Chem., Int. Ed. Engl.*, 19 (1980) 575.
6 P. A. Peaden, J. C. Fjeldsted, M. L. Lee, S. R. Springston and M. Novotny, *Anal. Chem.*, 54 (1982) 1090.
7 J. C. Fjeldsted and M. L. Lee, *Anal. Chem.*, 56 (1984) 619A.
8 A. L. Blilie and T. Greibrokk, *J. Chromatogr.*, 349 (1985) 317.
9 R. D. Smith, E. G. Chapman and B. W. Wright, *Anal. Chem.*, 57 (1985) 2829.
10 Y. Hirata, F. Nakata and M. Nawasaki, *J. High Resolut. Chromatogr. Chromatogr. Commun.*, 9 (1986) 633.
11 P. J. Schoenmakers and F. C. C. J. G. Verhoeven, *J. Chromatogr.*, 352 (1986) 315.
12 K. H. Linneman, A. Wilsch and G. M. Schneider, *J. Chromatogr.*, 369 (1986) 39.
13 R. D. Smith, J. L. Fulton, R. C. Petersen, A. J. Kopriva and B. W. Wright, *Anal. Chem.*, 58 (1986) 2057.
14 K. R. Jahn and B. W. Werclawiak, *Anal. Chem.*, 59 (1987) 382.
15 J. A. Nieman and L. B. Rogers, *Sep. Sci.*, 10 (1975) 517.
16 J. E. Conaway, J. A. Graham and L. B. Rogers, *J. Chromatogr. Sci.*, 16 (1978) 102.
17 D. R. Gere, R. Board and D. McManigill, *Anal. Chem.*, 54 (1982) 736.
18 Y. Hirata, *J. Chromatogr.*, 315 (1984) 31.
19 Y. Hirata, *J. Chromatogr.*, 315 (1984) 39.
20 P. Mourier, P. Sassiat, M. Caude and R. Rosset, *J. Chromatogr.*, 353 (1986) 61.
21 Ph. Morin, M. Caude and R. Rosset, *J. Chromatogr.*, 407 (1987) 87.

Journal of Chromatography, 448 (1988) 95–108
Elsevier Science Publishers B.V., Amsterdam — Printed in The Netherlands

CHROM. 20 608

INTERNAL STRUCTURES OF WIDE-PORE PACKING MATERIALS FOR HIGH-PERFORMANCE LIQUID CHROMATOGRAPHY STUDIED BY TRANSMISSION ELECTRON MICROSCOPY*

NOBUO TANAKA*, KATSUSHI HASHIDZUME and MIKIO ARAKI
Kyoto Institute of Technology, Faculty of Textile Science, Matsugasaki, Sakyo-ku, Kyoto 606 (Japan)
HAJIME TSUCHIYA and AKITOSHI OKUNO
Nitto Technical Information Centre, Ibaraki, Osaka 567 (Japan)
KAZUFUSA IWAGUCHI and SEIICHIRO OHNISHI
Nakarai Chemical Co., Kuze, Minami-ku, Kyoto 601 (Japan)
and
NOBUHARU TAKAI
Institute of Industrial Science, University of Tokyo, Roppongi, Minato-ku, Tokyo 106 (Japan)
(First received March 2nd, 1988; revised manuscript received March 27th, 1988)

SUMMARY

Internal structures of high-performance liquid chromatographic column packing materials, including porous glass particles, silica gels and polymer gels, were studied by transmission electron microscopy. Clear micrographs of the internal structures were obtained for macroporous particles by using ultrathin sections, with staining in the case of polymer gels. Corpuscular structures were seen with silica gels with relatively small pores, while porous glass particles showed a typical spongy structure. Spherical silica particles with large pores in the range 50–500 nm from different sources possess common spongy structures with a difference in the presence of a shell at the outer surface. Several silica packing materials of 30–400 nm nominal pore size were found to be mixtures of two or more kinds of silica particles of different pore sizes, which accounted for the broad, in some instances bimodal, pore size distribution found in nitrogen adsorption measurements and in inverse size-exclusion chromatography. A bimodal pore size distribution was also seen for unmixed macroporous polymer gel particles, with one of the maxima in a small pore size range, presumably due to the presence of micropores formed by the network structures in microgels.

INTRODUCTION

The characterization of porous particles for high-performance liquid chromatography (HPLC) is important in understanding the chromatographic properties of

* Part of this work was presented at the *36th Annual Meeting of the Japan Society for Analytical Chemistry, Kumamoto, October 1987.*

0021-9673/88/$03.50

different column packing materials and in the development of new ones. Porous packing materials have customarily been subjected to characterization procedures such as measurement of surface area and pore size by nitrogen adsorption, mercury intrusion and size-exclusion chromatography (SEC). These methods provide data for the overall porosity and pore size distribution of porous materials, but do not give information on the shape of the pores, or how the pores penetrate the bulk particle structure.

A variety of structures have been described as the internal structures of porous particles[1,2]. The determination of physical parameters such as pore size and pore size distribution depends on the shape of the pores[2,3]. In studies of the preparation and characterization of reversed-phase materials, geometric factors of silica pores are related to the chromatographic properties of the resulting stationary phase[4,5]. Therefore, it is desirable to include a pore structure study in the characterization of porous packing materials.

With respect to the size and shape of the pores in HPLC column packings, transmission electron microscopy (TEM) seems to give the most straightforward information and to be best suited for such a pore structure study. There have been a few reports on electron microscopic studies of column packing materials[6–15]. A difficulty has been encountered with the thickness of the sample, which hinders the close observation of the internal structures of silica particles with nominal 6–10 nm pores most commonly used in HPLC. Scanning electron microscopy (SEM) may not afford information on internal structures, because some silica particles are covered with a surface layer, or a shell at the outer surface. Tracz and Barna[14] recently reported the preparation of ultrathin samples of porous materials for TEM by ion milling.

It is of great interest to examine directly the actual internal structures of silica and polymer particles from various manufacturers to see the shape of pores, and any possible differences in internal structures produced by the difference in the method of preparation. We report here the TEM observation of ultrathin sections of various packing materials, including silica gel of 30–400 nm nominal pore sizes, porous glass particles and macroporous polymer gels. Clear internal structures obtained by both TEM and SEM will show whether the packing materials actually possess the stated pore size and uniformity. This will help researchers attempting studies on the effect of pore geometry on the physical and chromatographic properties of packing materials.

EXPERIMENTAL

Materials

The following silica particles were purchased: LiChrospher Si 500, Si 1000 and Si 4000 (particle size 10 μm) (Merck, Darmstadt, F.R.G.), Nucleosil 100, 300, 1000 and 4000 (5 μm) (Machery, Nagel & Co., Düren, F.R.G.), Spherisorb 300 (5 μm) (Phase Separations, Norwalk, CT, U.S.A.), Hypersil 300 (5 μm) (Shandon, Runcorn, Cheshire, U.K.) and Vydac TP (10 μm) (Separations Group, Hesperia, CA, U.S.A.). Porous glass particles were prepared at the Institute of Industrial Science of the University of Tokyo. TSK G4000PW and G4000H polymer gels were obtained from Tosoh (Tokyo, Japan). The particles are listed in Table I.

Samples for TEM were prepared as follows: porous particles were embedded in Spurr epoxy resin (Polysciences, Warrington, PA, U.S.A.), then hardened at 70°C for 8

TABLE I

MACROPOROUS COLUMN PACKING MATERIALS EMPLOYED FOR TEM STUDY

Packing material	*Surface area** (m^2/g)	*Pore size** (*nm*)	*Pore volume** (*ml/g*)	*Particle size** (*μm*)
LiChrospher 500	50 (69**)	50	0.8 (0.90**)	10
1000	20	100	0.8	10
4000	6	400	0.8	10
Nucleosil 300	100 (109**)	30	0.8 (0.81**)	5
1000	25	100	0.8	5
4000	10	400	0.7	5
Hypersil 300	60	30	0.6	5
Spherisorb 300	190	30	1.5	5
Vydac TP	80	30	0.6	10
Porous glass	(386**)	(55***)	(0.72**, 0.49***)	10
TSK G4000H§	(333**)	–	1.29 (1.19**)	12
TSK G4000PW§§	(64**)	–	(0.64**)	10

* Manufacturer's specification.
** Determined by nitrogen adsorption.
*** Determined by mercury intrusion.
§ Polystyrene–divinylbenzene gel.
§§ Acrylate or methacrylate gel.

h. G4000PW gel was stained with ruthenium tetraoxide vapour[16] prior to epoxy resin impregnation. Samples for SEM were coated with platinum–palladium by ion sputtering. Polystyrene standards were obtained from Pressure Chemicals (Pittsburg, PA, U.S.A.).

Instruments

An H 800 electron microscope (Hitachi, Tokyo, Japan) was operated at 200 kV. A Sorvall MT-6000 ultramicrotome (DuPont, Wilmington, DE, U.S.A.) was used to prepare ultrathin sections of about 80 nm thickness from the embedded porous particles. Electron microscopy was carried out at the Nitto Technical Information Centre. The HPLC system consisted of an 800 PU pump and 875 UV detector (Jasco, Tokyo, Japan), a 98.00 refractive index detector (Knauer, Berlin, F.R.G.) and a 7000A data processer (System Instruments, Tokyo, Japan).

Measurements

HPLC measurements were carried out at 30°C. The inverse SEC method of Knox and co-workers[17,18] was employed to calculate pore size distributions. Nitrogen adsorption measurements were carried out at the Shiseido Toxicological and Analytical Research Centre (Yokohama, Japan).

RESULTS AND DISCUSSION

Clear electron micrographs of pore structures were obtained by employing ultrathin sections of about 80 nm thickness for silica gels, porous glass and polymer gels. As shown below, most of the pores were filled with the epoxy resin. In the

transmission electron micrographs, the light area represents the epoxy resin in the pores and in the interparticle space, and the dark area the skeleton, or ruthenium in the case of G4000PW gel. Channels in particles not perpendicular to the cross-section are shadowed owing to the partial electron adsorption by the skeleton.

Fig.1 shows a comparison of internal structures between porous glass particles and LiChrospher Si 500 silica particles. The pores in the glass particles were round and relatively uniform in size, whereas those in LiChrospher Si 500 were irregularly shaped, and possessed a broad size distribution. In other words, the glass particles possess the features of a spongy system, consisting of channels in solids, whereas the silica particles possess those of a corpuscular system, consisting of aggregates of microstructures[1,2]. In agreement with the microscopic observations, a relatively

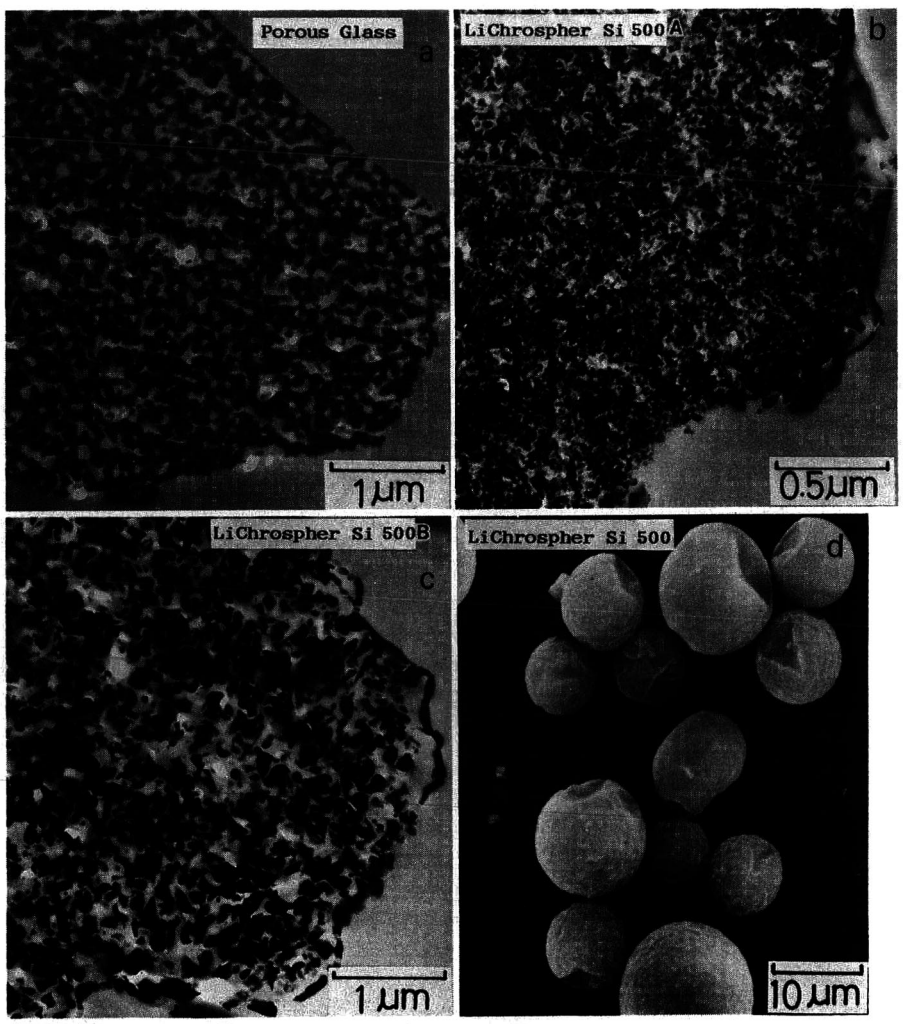

Fig.1. TEM photographs of (a) porous glass particles and (b and c) LiChrospher Si 500 and (d) an SEM photograph of LiChrospher Si 500.

narrow pore size distribution was found with the porous glass particles compared with the silicas except in the micropore region, in nitrogen adsorption measurements and in mercury intrusion, as shown in Fig. 2. Differences in pore sizes determined by different methods can be seen in Fig. 2, where the nitrogen adsorption method gave smaller pores sizes for both silica and glass particles.

Fig. 1b and c were obtained from a single batch of LiChrospher Si 500. The internal structures of the silica particles are evidently different, indicating that the packing material is actually a mixture of two types silica particles, (the two types of particles cannot be made in the same preparation, because no particles in between were found in the batch; the same is true for the mixed particles shown below). One type of particle possesses a pore diameter of less than 30 nm and the other up to 300 nm. The difference cannot be observed by SEM, however, owing to the existence of a shell at the outer surface of this silica (Fig. 1d). Fig. 1b and c show a dark area at the periphery of the spheres in spite of the highly porous structure of the particles. The thickness of the shell is slightly less than 100 nm.

Fig. 3 shows the micrographs of LiChrospher Si 1000. This silica was also found to be a mixture of two types of particles, one with 50–100-nm pores and the other with pores up to 200 nm. The surface structures of LiChrospher Si 1000 and Si 4000 are similar to those of Si 500. The surface shell seems to have been made by heat treatment after the formation of spheres, as shown by the appearance of the sintered structure in Fig. 4c. The particles with higher porosity possess the thicker surface shell. The surface shell developed on highly porous LiChrospher Si 4000 seems to be relatively fragile, because a considerable portion was broken by ultrasonication in about 10 min (Fig. 4b and e), as pointed out by Unger and Gimpel[19]. Therefore, prolonged ultrasonication prior to column packing should be avoided.

Fig. 4d and e shows that LiChrospher Si 4000 consists of two types of silicas, one of which is similar to that in LiChrospher Si 1000. The pore structures in Figs. 3 and 4 have some similarities to those of a spongy system. As mentioned by Unger[2], silica particles can have a spongy structure depending on the method of preparation. Another feature of LiChrospher Si 4000 is the development of some crystallinity of the silica skeleton of particle B, as shown by the moire pattern in Fig. 4e. The crystallinity was lost during the TEM observation. Whether the crystallinity has any effect on chromatographic properties is yet to be studied.

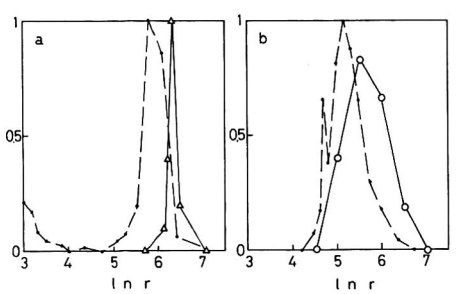

Fig. 2.(a) Pore size distribution of porous glass: solid line, mercury intrusion method; dashed line, nitrogen adsorption method. (b) Pore size distribution of LiChrospher Si 500: dashed line, nitrogen adsorption; solid line, inverse SEC. The vertical axis corresponds to fraction of pore volume, normalized in the case of inverse SEC.

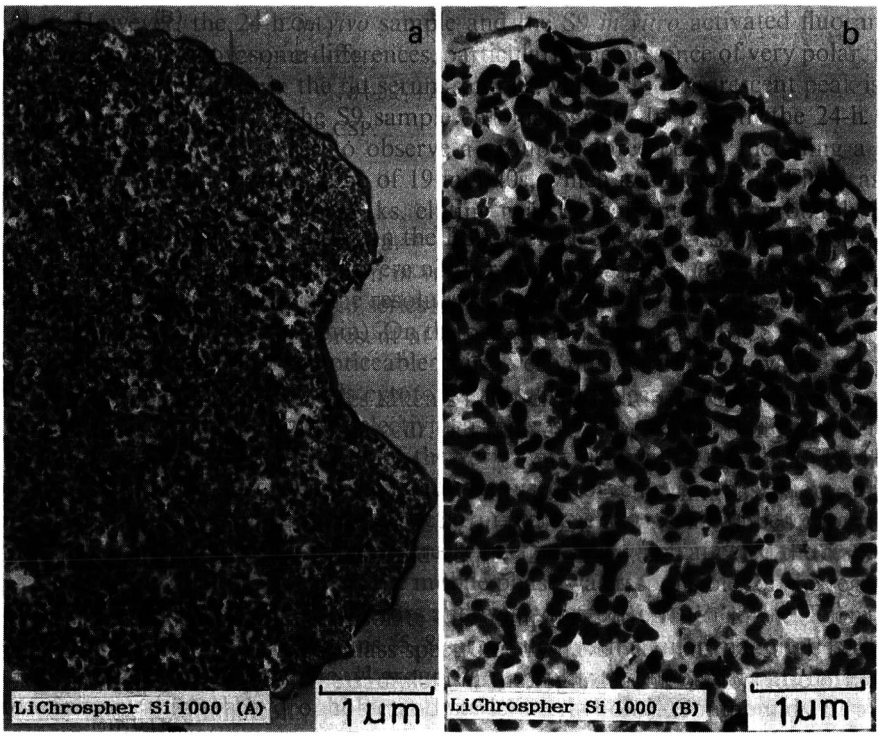

Fig. 3. TEM photographs of LiChrospher Si 1000.

With LiChrospher particles, the presence of the surface shell made it difficult to determine the particle composition, although more than one type of internal structure can be observed with many ultrathin sections prepared from this silica. On the other hand, the internal structures of Nucleosil particles can be examined from the appearance. Fig. 5 shows micrographs of Nucleosil 300. The micrographs showed that at least three kinds of particles having different surface roughness constitute the packing material. About 10% of the particles (C in Fig. 5a) possess a rough surface with a pore size of 50–100 nm, as shown in the insets in Fig. 5b. The other two types of particles in Fig. 5b possess much more compact structures, their pore sizes being smaller than 30 nm. Whereas a corpuscular structure was seen with particles A and B, a spongy structure was seen with particle C, as with the macroporous LiChrospher.

Nitrogen adsorption measurements on Nucleosil 300 showed a bimodal distribution of pore size, one maximum agreeing with that of Nucleosil 100 and the other greater than 50 nm, as shown in Fig. 6a. The SEC calibration graph obtained with standard polystyrenes in tetrahydrofuran for this silica indicates an extremely broad range for permeation of the standards with molecular weight from 500 to 10^6 or above, as shown in Fig. 6c. The pore size distribution curves in Fig. 6b were calculated by the method of Knox and co-workers[17,18]. The calculated pore size distribution of Nucleosil 300 is considerably broader than the others. In Fig. 6b, part of the pore size range of Nucleosil 300 overlaps with those of Nucleosil 100, 1000 and 4000. Smaller

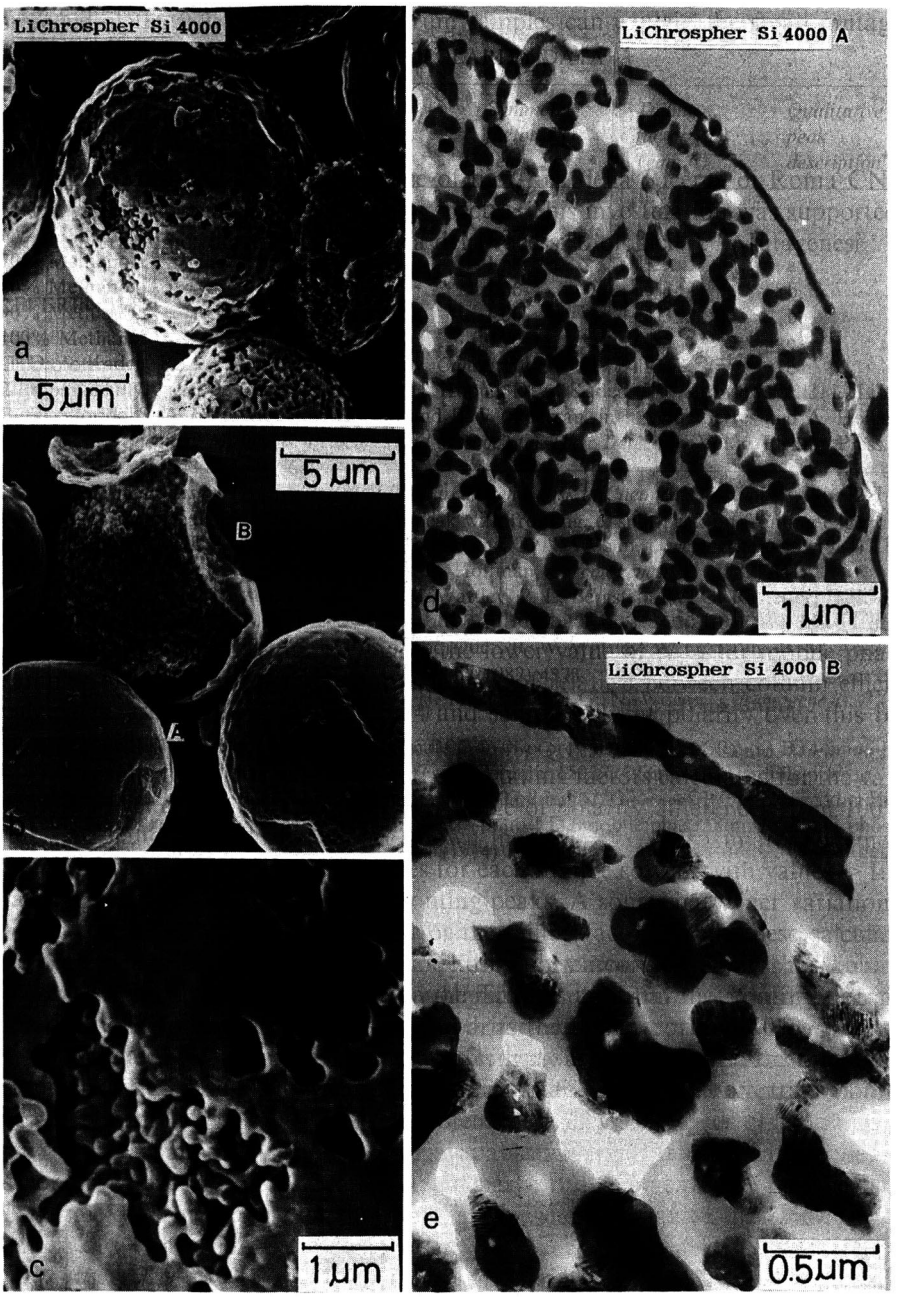

Fig. 4. (a–c) SEM photographs and (d and e) TEM photographs of LiChrospher Si 4000.

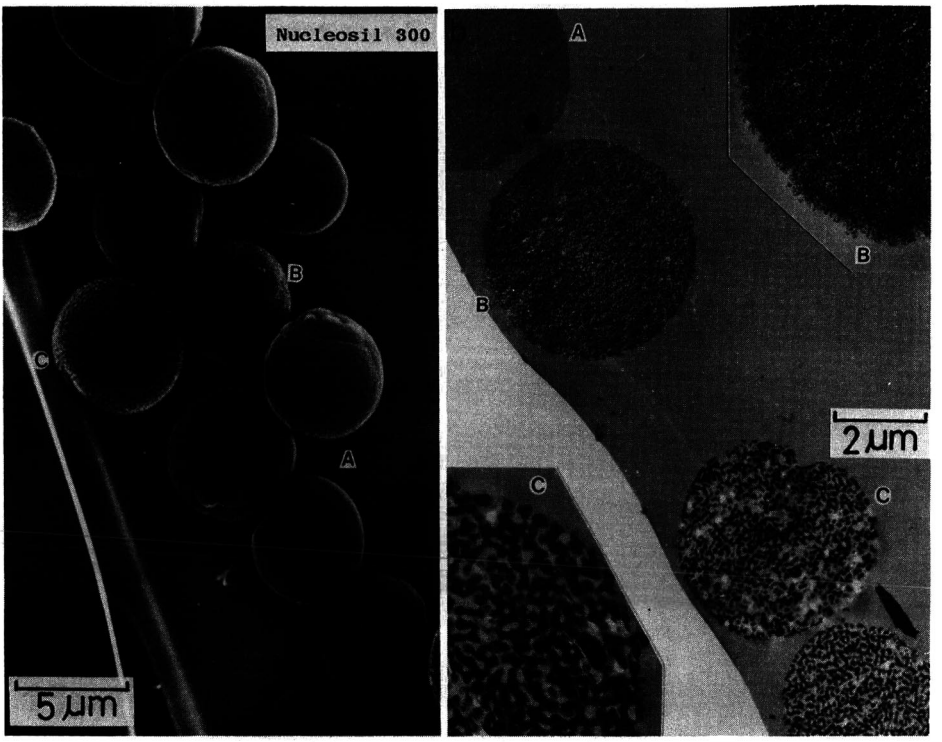

Fig. 5. (a) SEM photograph and (b) TEM photograph of Nucleosil 300. Particles B and C are enlarged 2.5 times in the insets.

pore sizes were obtained from the SEC data by using the method by Halasz and Martin[20,21] but with a similarly broad range of pore size distribution for Nucleosil 300. This silica thus provides a wide linear portion in the molecular weight–elution volume curve. This is a desirable feature in a packing material for SEC, and suitable for the size separation of solutes with a wide molecular weight range. The intention of the manufacturers who offer mixed particles is supposed to be a linear molecular weight–elution volume curve over a wide range for SEC, and the adjustment of the surface area and the pore size distribution within a specification for each batch of commercial products.

Nucleosil 1000 and 4000 were also found to be mixtures of two or three types of silicas, as shown in Figs. 7 and 8. Nucleosil 1000 contained one type of particles (A) that were much more compact than the other (B), which possess a pore size of 200–300 nm. Nucleosil 4000 contained at least three major constituents in comparable amounts, as seen in Fig. 8a. Two (A and B) are similar to those in Nucleosil 300 and 1000. Particle C, with pores up to 500 nm, shows the development of a surface shell to some extent, and some crystallinity of the silica skeleton (Fig. 8c), similarly to LiChrospher Si 4000 in Fig. 4e. Very small amounts of smooth particles (D) are contained in Nucleosil 4000. This type of particle, however, may not be mixed intentionally, because only a few of them were observed.

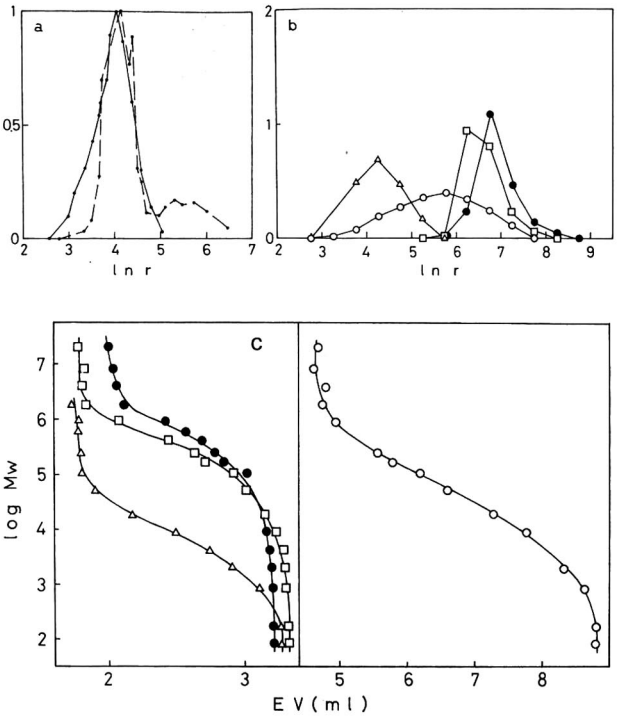

Fig. 6. (a) Pore size distribution of Nucleosil 100 (solid line) and 300 (dashed line) measured by nitrogen adsorption; (b) pore size distribution of Nucleosil 100 (△), 300 (○), 1000(□) and 4000 (●) measured by inverse SEC; (c) molecular weight–elution volume curves obtained on Nucleosil 100, 300, 1000 and 4000. Columns of 25 cm × 4.6 mm I.D. were used for Nucleosil 100, 1000 and 4000, and 25 cm × 8 mm I.D. for Nucleosil 300. The vertical axis in (a) and (b) is as in Fig. 2.

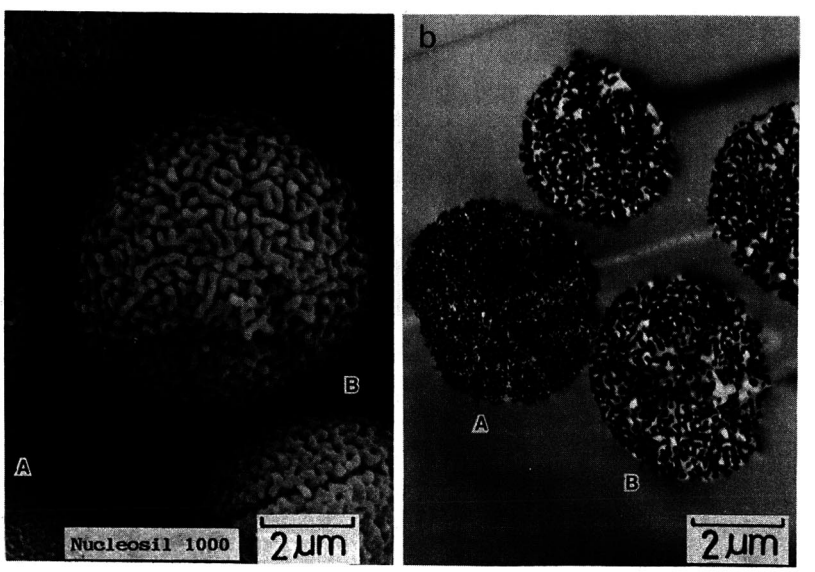

Fig. 7. (a) SEM and (b) TEM photographs of Nucleosil 1000.

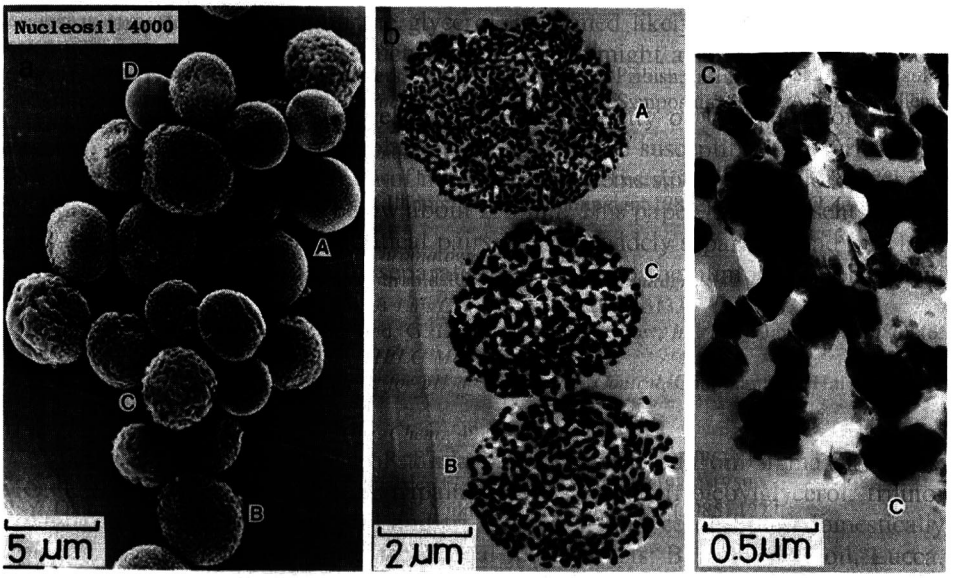

Fig. 8. (a) SEM and (b and c) TEM photographs of Nucleosil 4000.

Not all the commercially available silica particles with a pore size of about 30 nm are mixtures. Hypersil 300, Spherisorb 300 and Vydac TP seemed to consist of one type of silica particles. Among these, Hypersil and Spherisorb showed a typical corpuscular structure, whereas Vydac showed an irregular internal structure, or the presence of a large void, as might be expected from the rough surface structure shown by SEM[22].The porosity of Spherisorb 300 particles is much higher than those of the other materials, as shown in Fig. 9b and indicated in the pore volume (1.5 ml/g), which may account for the extremely large surface area per unit mass of this packing material.

The transmission electron micrograph of TSK G4000H, a polystyrene–divinylbenzene gel, can be obtained directly without appreciable structural changes of the particle, whereas ruthenium tetraoxide staining was needed for TSK G4000PW, an acrylate or methacrylate gel. Without staining, the TSK G4000PW gel rapidly softened under the electron beam, and disintegration of the particle structure resulted. TSK G4000H particles are aggregates of microspheres, a typical corpuscular system, whereas TSK G4000PW particles possess the features of a spongy system.

The pore structures shown in the micrographs in Figs. 10 and 11 cannot account for the bimodal distribution of pore size seen in the inverse SEC and nitrogen adsorption measurements for these particles (Fig. 12). The pore sizes determined by nitrogen adsorption were smaller than those obtained by inverse SEC, as with silica particles. The large pores found in SEC, nitrogen adsorption and TEM correspond to the nominal pore sizes of these particles. The smaller pores seen only in SEC and nitrogen adsorption measurements are common to most polymer gels[23], and have been used in gel chromatography in the separation of small molecules[24,25]. Such micropores have not been seen with ordinary silica particles for HPLC. The size of these micropores, about 1 nm radius or smaller, suggests that they are formed by the network of cross-linked polymer chains. The results of SEC and nitrogen adsorption imply a biporous

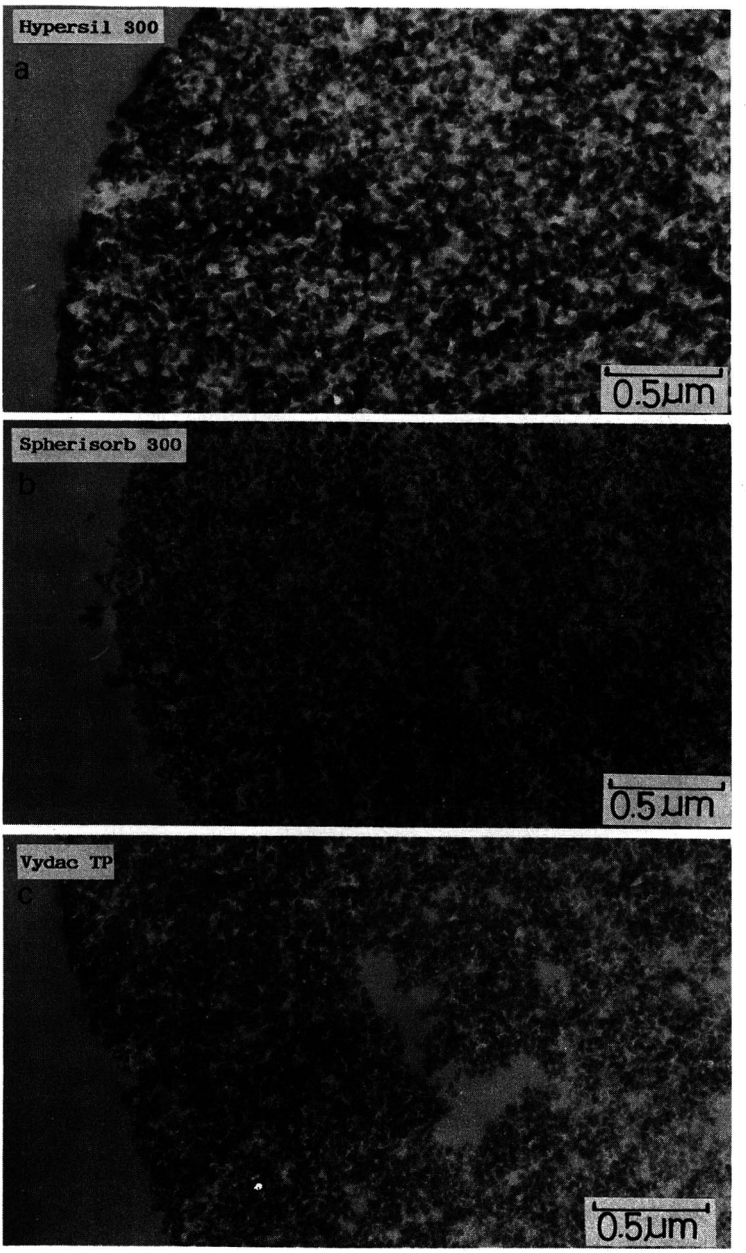

Fig. 9. TEM photographs of (a) Hypersil 300, (b) Spherisorb 300 and (c) Vydac TP.

structure of polymer gels[23], beads composed of aggregates of microporous microgranules. The micropores seem to play an important role in determining both the performance and the shape selectivity, namely selective binding of rigid molecules of a certain size, found in the reversed-phase (RP) HPLC of various hydrocarbons[26,27]. Polymer-based stationary phases showed large differences in performance and in

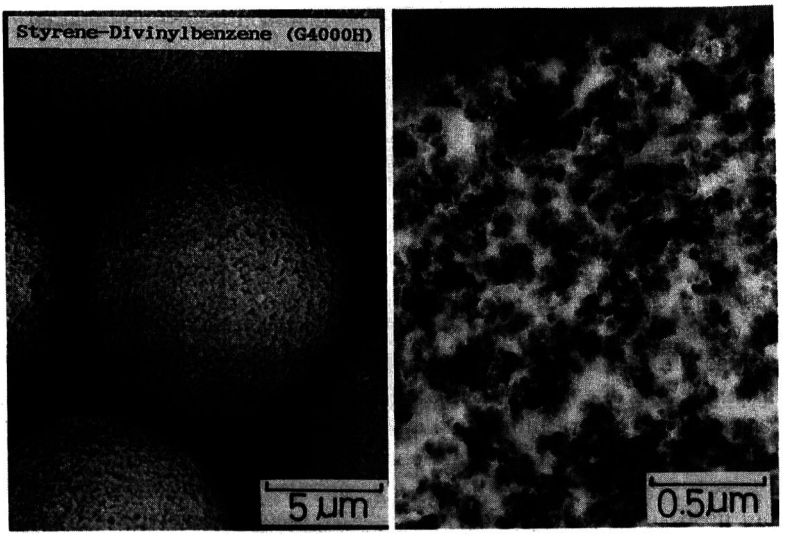

Fig. 10. (a) SEM and (b) TEM photographs of TSK G4000H.

selectivity compared to silica-based phases in RP-HPLC based on solute structures. The relationship between these properties and the pore structures is currently under investigation. These macroporous polymer-based phases are often employed in the separation of large molecules, although they sometimes show poor performance for small molecules depending on the elution conditions[28].

As some packing materials were found to be mixtures, one should be aware whether the packing material in use is a mixture or not when examining the effect of pore size on chromatographic and other properties[29] and when studying the agreement of experimental with theoretical results based on pore models.

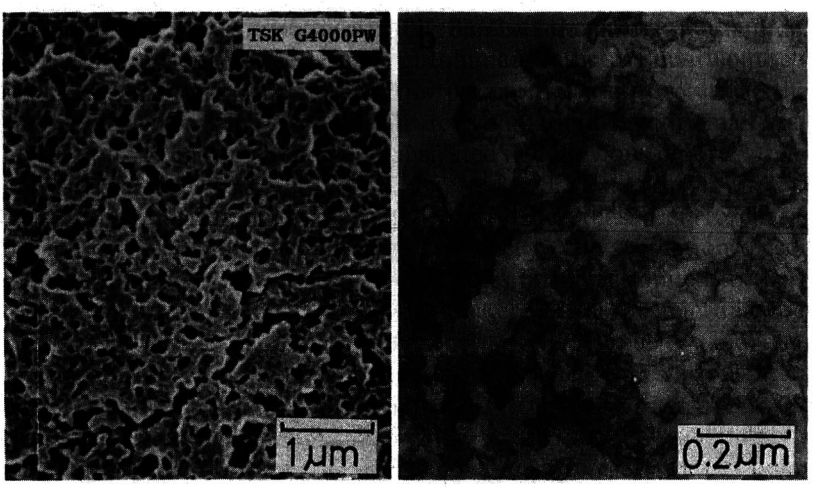

Fig. 11. (a) SEM and (b) TEM photographs of TSK G4000PW.

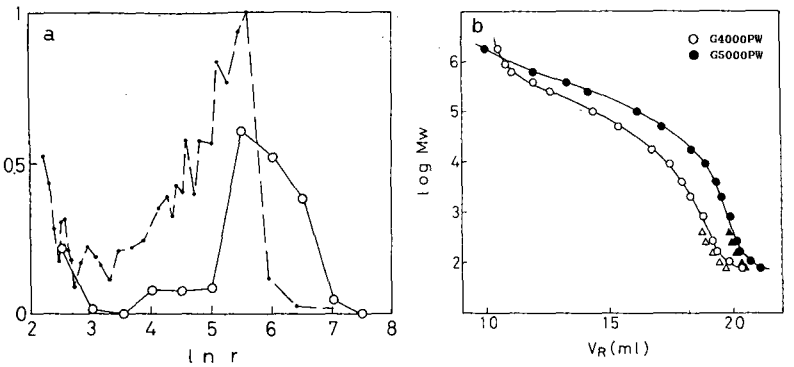

Fig. 12. (a) Pore size distribution of TSK G4000PW measured by nitrogen adsorption (dashed line) and by inverse SEC (solid line), the latter based on the molecular weight–elution volume curve shown in (b). Column, 60 cm × 7.5 mm I.D. Vertical axis as in Fig. 2.

It would be of great interest to examine the effect of the surface shell found with some silica particles on the chromatographic properties and on the determination of pore size and pore size distribution by nitrogen adsorption or mercury intrusion. Direct characterization of porous materials might be possible if the pores are sufficiently large and clear micrographs are obtainable.

CONCLUSION

TEM of ultrathin sections was shown to be a reliable and straightforward method for examining the internal structure of macroporous particles, including silica, glass and polymer gel particles. Some silica particles were covered with a shell due to sintering, which can be broken by excessive ultrasonication in the case of particles with high porosity. Several silica packing materials of 30–400 nm nominal pore size were found to be mixtures of several different types of particles. These packing materials usually give a broad, sometimes bimodal, pore size distribution on measurement by nitrogen adsorption and inverse SEC.

ACKNOWLEDGEMENTS

We thank Prof. K. K. Unger of Johannes Gutenberg University and Prof. S. Hirayama of Kyoto Institute of Technology for helpful suggestions, Dr. Y. Kato of Tosoh for gifts of the polymer particles and Dr. Y. Ohtsu of Shiseido for nitrogen adsorption measurements. This work was supported in part by the grants No. 61470038 and No. 62303007 from the Ministry of Education.

REFERENCES

1 A. P. Karnaukhov, in S. Modry (Editor), *Proceedings of Rilem/IUPAC International Symposium on Pore Structure and Properties of Materials*, Vol. I, Academia, Prague, 1974, p. A-3.
2 K. K. Unger, *Porous Silica*, Elsevier, Amsterdam, 1978, Ch. 2.
3 S. D. Christian and E. E. Tucker, *Int. Lab.*, Nov./Dec. (1981) 48; Jan./Feb. (1982) 40.
4 D. Farin and D. Avnir, *J. Chromatogr.*, 406 (1987) 317.

5 D. Avnir, *J. Am. Chem. Soc.*, 109 (1987) 2931.
6 E. Grimaud, J. C. LeCoq, E. Boschetti and M. Corgier, *J. Chromatogr.*, 166 (1978) 37.
7 R. Rüchel, R. L. Steere and E. F. Erbe, *J. Chromatogr.*, 166 (1978) 563.
8 J. Hradil, D. Horák, Z. Pelzbauer, E. Votavová, F. Švec and J. Kálal, *J. Chromatogr.*, 259 (1983) 269.
9 D. Horak, Z. Pelzbauer, F. Svec, J. Labsky and M. Bleha, *Angew. Makromol. Chem.*, 117 (1983) 117.
10 J. Hradil and F. Svec, *Angew. Makromol. Chem.*, 130 (1985) 81.
11 E. Tracz, J. Skubiszewska and R. Leboda, *J. Chromatogr.*, 287 (1984) 136.
12 E. Tracz and R. Leboda, *J. Chromatogr.*, 346 (1985) 346.
13 E. Tracz, R. Leboda and E. Mizera, *J. Chromatogr.*, 355 (1986) 412.
14 E. Tracz and A. Barna, *J. Chromatogr.*, 355 (1986) 421.
15 H. Colin and G. Guiochon, *J. Chromatogr.*, 126 (1976) 43.
16 J. S. Trent, J. I. Scheinbeim and P. R. Couchman, *Macromolecules*, 16 (1983) 589.
17 J. H. Knox and H. P. Scott, *J. Chromatogr.*, 316 (1984) 311.
18 J. H. Knox and H. J. Ritchie, *J. Chromatogr.*, 387 (1987) 65.
19 K. K. Unger and M. G. Gimpel, *J. Chromatogr.*, 180 (1979) 93.
20 I. Halasz and K. Martin, *Angew. Chem., Int. Ed. Engl.*, 17 (1978) 901.
21 F. V. Warren, Jr. and B.A. Bidlingmeyer, *Anal. Chem.*, 56 (1984) 950.
22 J. Köhler and J. J. Kirkland, *J. Chromatogr.*, 385 (1987) 125.
23 F. Nevejans and M. Verzele, *Chromatographia*, 20 (1985) 173.
24 R. V. Vivilecchia, B. G. Lightbody, N. Z. Thimot and H. M. Quinn, *J. Chromatogr. Sci.*, 15 (1977) 424.
25 E. Ozaki, K. Saitoh and N. Suzuki, *J. Chromatogr.*, 177 (1979) 122.
26 N. Tanaka, K. Hashizume and M. Araki, *J. Chromatogr.*, 400 (1987) 33.
27 T. Ebata, K. Hashizume, N. Tanaka and M. Araki, *31st Annual Meeting of the LC Research Society, Kyoto, January 1988*, Abstracts, p. 25.
28 L. D. Bowers and S. Pedigo, *J. Chromatogr.*, 371 (1986) 243.
29 E. Wellner, D. Rojanski, M. Ottolenghi, D. Huppert and D.Avnir, *J. Am. Chem. Soc.*, 109 (1987) 575.

Journal of Chromatography, 448 (1988) 109–116
Elsevier Science Publishers B.V., Amsterdam — Printed in The Netherlands

CHROM. 20 572

MODIFIED GENERAL AFFINITY ADSORBENT FOR LARGE-SCALE PURIFICATION OF PENICILLINASES

LÁSZLÓ KISS
Department of Biochemistry, L. Kossuth University, Debrecen H-4010 (Hungary)
and
ANDREA TAR, SUSANNE GÁL, BELA L. TOTH-MARTINEZ* and FERENC J. HERNÁDI
Chemotherapy Section, Department of Pharmacology, University Medical School of Debrecen, H-4012 Debrecen (Hungary)
(Received April 19th, 1988)

SUMMARY

N-Acetyl-D-(−)-penicillamine as a stable second-generation biospecific affinity ligand has previously been suggested for purification of *Bacillus cereus* 569/H β-lactamase I. A complex spacer arm is coupled with the matrix by using epichlorohydrin and phloroglucinol doubly activated with divinyl sulphone in the *meta* position. Coupling of D-(−)-penicillamine ligand resulted in an active affigel. However, we found that two affinity ligands in close proximity prevents simultaneous binding of two penicillinase molecules, therefore one ligand is superfluous. Our results show that: (1) shortening the spacer arm by direct activation of the matrix with divinyl sulphone is satisfactory to produce the affinity material with N-acetyl-D-(−)-penicillamine; (2) incorporation of 15 μmol of N-acetyl-D-(−)-penicillamine per ml of wet Sepharose 4B satisfies the maximum binding capacity requirements of the affigel (about half of the originally incorporated amount of ligand); (3) our simplified affinity adsorbent is generally applicable for large-scale purification of penicillinases to homogeneity from various bacterial sources by the convenient batch method without prior concentration of these enzymes; (4) reacetylation for four/five times can regenerate the original binding capacity of the affigel.

INTRODUCTION

In view of the worldwide and considerable β-lactamase resistance of Gram-positive and Gram-negative bacteria, much attention has been paid to the purification of these enzymes, mainly by classical column chromatographic methods but several affinity chromatography procedures have also been reported[1–9]. The inherent instability of the early first generation ligands (specific β-lactams) rendered the absorbents unsuitable for repeated use[2–7].

The present report describes the application of N-acetyl-D-(−)-penicillamine in a simplified manner[8,9] for the biospecific affinity purification of penicillinases to homogeneity from various bacterial strains. This stable affinity ligand was originally

0021-9673/88/$03.50

introduced into laboratory practice by Clarke *et al.*[1]. Quantitation of the optimization of the penicillinase binding capacity of N-acetyl-D-(−)-penicillamine–Sepharose 4B, however, convinced us that there is no need to attach approximately 24.5 μmol of D-(−)-penicillamine per ml of matrix because less than 1% of the coupled ligand can bind penicillinases on a mol per mol basis. On the other hand, only the N-acetylated ligand is an active binder, therefore special care must be taken to regenerate the affigel from time to time to maintain its performance.

EXPERIMENTAL

Materials

Divinyl sulphone (DVS) was obtained from Aldrich (Aldrich Europe, c/o Jansen Pharmaceuticals, Belgium). D-(−)-Penicillamine (DPA) was a product of Biogal (Debrecen, Hungary). Sepharose 4B was obtained from Pharmacia (Uppsala, Sweden). 5,5′-Dithiobis(2-nitrobenzoic acid) (DTNB) was from Sigma (Dorset, U.K.).

Bacterial strains

Bacillus cereus 569/H and *B. cereus* 569/H/9 (a hyper magno mutant) constitutive β-lactamase producing (β-lactamase I as exopenicillinase and β-lactamase II as exocephalosporinase) and *B. licheniformis* 749 C strains were kindly provided by Dr. S. Fleming, Department of Molecular Biology, University of Edinburgh, U.K. *Staphylococcus aureus* NCTC 9789 samples were supplied by Dr. R. H. Pain, Department of Biochemistry, University of Newcastle upon Tyne, U.K. or by Dr. I. N. Simpson and Dr. G. W. Ross, Chemotherapy Department, Microbiology Division, Glaxo Group Research, Greenford, U.K. and also by Dr. R. P. Ambler, Department of Molecular Biology, King's Building, University of Edinburgh, U.K. *S. aureus* PC 1 1711 E was a gift from Dr. I. N. Simpson, or from Dr. G. W. Ross and from Dr. R. P. Ambler (*S. aureus* PC 1 11195 NCIB). In order to control the penicillinase specificity of our affigel we used caphalosporinases of different origins: *Escherichia coli* J5-3 R46$^+$ (OXA-2) and *E. coli* J6-2 RTEM-1$^+$ strains from Dr. J. T. Smith, Microbiology Section, School of Pharmacy, University of London, U.K.; *Pseudomonas aeruginosa* MAR, a TEM-1-like β-lactamase producing strain from Dr. A. M. Philippon, Service de Biologie, C. H. U. Cochin, Paris, France; *E. cloacae* 53 strain from Dr. J. T. Smith.

Enzyme assay, protein determination

β-Lactamase activity was assayed by measuring the absorbance of nitrocefin at 486 nm in a cell of pathlength 1 cm as described by O'Callaghan *et al.*[10]. One unit is that amount of enzyme which is able to hydrolyze 1 μmol of nitrocefin in 1 min at 37°C.

The protein content of the enzymes was estimated by measuring their absorbances at 280 nm or as described by Lowry *et al.*[11].

In vitro susceptibility studies

Minimum inhibitory concentration (MIC) values were measured by the broth dilution method with two-fold serial dilutions. Inocula of 10^8 c.f.u. (colony forming unit) ml^{-1} were used for induction in preparative scale studies. All MIC values were determined in Brain-Heart Infusion (BHI) medium (Code CM 225; Oxoid, Basingstoke, U.K.).

Monitoring of exopenicillinase induction

BHI was used for excess enzyme production by induction. Overnight inocula of the *S. aureus* strains were diluted in the same broth (200 ml in 500-ml conical flasks) containing inducers and grown at 37°C with shaking at 120 rpm. In order to reduce the lag phase, we selected an initial c.f.u. value of 10^8 for preparative exopenicillinase production. Changes of about two orders of magnitude in c.f.u. were monitored in 10 h with *S. aureus* NCTC 9789 strains. An activity of 0.78 U ml^{-1} enzyme was found in the non-induced control culture, 6 U ml^{-1} in the culture induced by 1 $\mu g\ ml^{-1}$ Methicillin (MET) (MIC/3). *S. aureus* PC 1 1911 E produced maximum enzyme level of 30 U ml^{-1} in 8 h without induction, however induction with 0.1 $\mu g\ ml^{-1}$ MET (MIC/30) in 12 h resulted in 479.5 U ml^{-1} enzyme or with 1 $\mu g\ ml^{-1}$ MET (MIC/3), 1800 U ml^{-1} exopenicillinase were found in 12 h. *S. aureus* PC 1 11195 NCIB showed a basic enzyme level of 223.1 U ml^{-1} without induction in 8 h, while the use of 0.39 $\mu g\ ml^{-1}$ of Cefotaxim (MIC/4) gave 377.6 U ml^{-1} enzyme in 8 h and 0.19 $\mu g\ ml^{-1}$ Cefoxitine (MIC/4) produced a 353.6 U ml^{-1} increase by induction in 8 h.

Preparation of affinity absorbent

N-Acetyl-D-(−)-penicillamine–Sepharose 4B was prepared either according to Clarke *et al.*[1] or by simplification and modification of the original method as follows.

A 10-ml volume of Sepharose 4B was suspended in 10 ml of 1 *M* sodium hydroxide–sodium bicarbonate buffer, pH 11.0, and directly treated with 1.5 ml of DVS at 40°C, keeping the pH constant. The time dependence of the DVS activation was investigated: 4-ml samples were removed from the reaction mixture at 20-, 30-, 40- and 60-min intervals. The gel samples were then filtered in small sintered glass funnels and washed extensively with distilled water to neutrality. The wet activated gel samples were treated separately and uniformly with 40 mg of DPA in 2 ml of 0.05 *M* phosphate buffer, pH 7.0, with shaking for 18 h at room temperature to achieve maximum incorporation of the ligand.

Coupling of DPA to the activated gel was assessed by monitoring the absorbance at 412 nm, $A^{1\ cm}_{412\ nm}$, produced upon treatment of a suitable aliquot of the reaction mixture with DTNB[12]. Quantitation of the results revealed 7 μmol of DPA bound in the 20-min, 15 μmol in the 30-min, 25 μmol in the 40-min and 30 μmol in the 60-min DVS-activated gel samples per ml. The excess of DPA was then removed by filtration in sintered glas funnels and the gel samples were resuspended in 2 ml of distilled water and treated with 1 ml of acetic anhydride continuously added over a

TABLE I

TIME DEPENDENCE OF DIRECT DVS ACTIVATION OF SEPHAROSE 4B AS MEASURED BY CHANGES IN THE BINDING CAPACITY OF *B. CEREUS* 569/H β-LACTAMASE I

DVS activation time (min)	*Ligand bound (μmol)**	*Binding capacity (mg enzyme)**
20	7	0.09
30	15	0.58
40	25	0.6
60	30	0.61

* Per ml affigel.

TABLE II

TIME DEPENDENCE OF N-ACETYL-DPA LIGAND INCORPORATION AS MEASURED BY CHANGES IN THE BINDING CAPACITY OF *S. AUREUS* PC 1 1711 E EXOPENICILLINASE

DPA incorporation time (h)	*Ligand bound (μmol)**	*Binding capacity (mg enzyme)**
4	7.5	0.06
8	15	0.38
13	25	0.4
18	30	0.4

* Per mg affigel.

period of 80 min at pH 8.0. The mixtures were then tested separately for maximum *B. cereus* 569/H β-lactamase I binding capacity in proportionally reduced volumes of a crude extract as described below. The results are shown in Table I.

Unfortunately, direct assessment of the extent of DVS activation is not possible, therefore, based on the above findings, we activated 10 ml of Sepharose 4B with 1.5 ml of DVS for 60 min and investigated the time dependence of the incorporation of DPA into this activated matrix to determine the stoichiometry of the N-acetyl-DPA for penicillinase binding on a mol per mol basis. Simple calculation shows that in principle much less than 1% of the ligand incorporated by Clarke *et al.*[1] is sufficient to achieve maximum enzyme binding capacity to their affigel.

Under the above experimental conditions, the wet DVS-activated gel was treated with 100 mg of DPA in 10 ml of 0.05 *M* phosphate buffer, pH 7.0, and 4-ml samples were withdrawn at 4-, 8-, 13- and 18-h intervals. Assessment of DPA with the DTNB method[12] revealed about 25% ligand incorporation (7.5 μmol per ml gel) in 4 h, 50% (15 μmol per ml gel) in 8 h, 83% (25 μmol per ml) in 13 h and 100% (30 μmol per ml) in 18 h. Incorporation of greater than 30 μmol of DPA cannot occur under these experimental conditions. Acetylation was performed as described above. The binding capacity with *S. aureus* PC 1 1711 E exopenicillinase is shown in Table II.

As by 8 h of incorporation the maximum enzyme binding capacity was achieved for *B. cereus* 569/H or *B. cereus* 569/H/9 β-lactamase I (0.6 mg pure enzyme per ml affigel), we concluded that the incorporation of 15 μmol of DPA per ml gel is sufficient. An 100-ml volume of Sepharose 4B was converted into N-acetyl-D-(−)-penicillamine–Sepharose 4B affinity material using the above reaction conditions. Further proportional increases in the amounts of Sepharose 4B and the reactants are possible.

The chemical reactions involved in the preparation of the affigel are illustrated in Scheme 1.

Preparation of crude enzymes

In the case of Gram-positive bacteria, the cell-free BHI media of induced cultures were considered as crude enzyme preparation only; however, Gram-negative bacteria were grown overnight without induction in Nutrient Broth media, followed by centrifugation of the cells. The sediments were treated by sonication in 0.05 *M* phos-

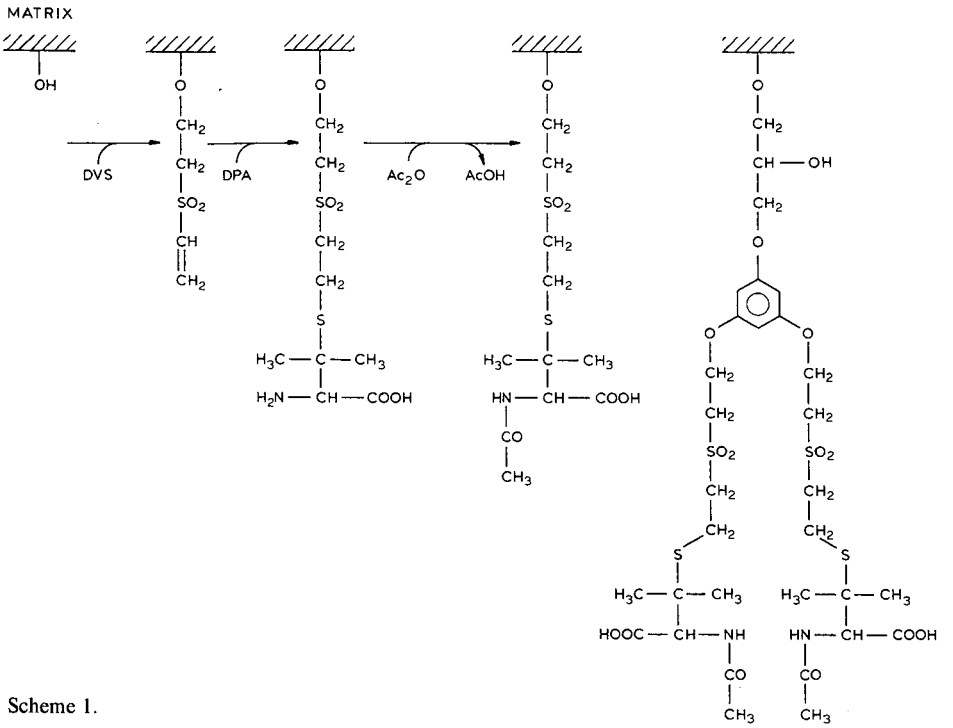

Scheme 1.

phate buffer, pH 7.0, and after nuclease treatment, supernatants were prepared by ultracentrifugation at 105 000 *g* for 1 h and extensive dialysis against the above buffer.

Adsorption to the affigel and elution

A typical medium-scale experiment was as follows. A 2-l volume of crude cell-free Gram-positive bacterium culture supernatant was stirred with 40 ml of affinity adsorbent at 4°C for 15 min at a low speed which just prevented sedimentation of the gel. The gel was then allowed to sediment, transferred quantitatively to a suitable sintered glass filter and washed free from protein with 0.05 *M* phosphate

TABLE III

PURIFICATION OF *B. CEREUS* 569/H/9 EXOPENICILLINASE BY N-ACETYL-D-(−)-PENICILLAMINE SEPHAROSE 4B AFFINITY CHROMATOGRAPHY

Parameter	*Cell-free supernatant*	*Purified enzyme*
Volume (ml)	2000	100
Protein (mg ml^{-1})	2.5	0.0225
Total activity, nitrocefin (U · 10^{-3})	3600	3312
Specific activity		
Nitrocefin (U mg^{-1} · 10^{-3})	0.72	1472
Benzylpenicillin (U mg^{-1} · 10^{-3})	–	1100
Purification	1	2044.4
Recovery (% total activity)	100	92

TABLE IV

PURIFICATION OF EXOPENICILLINASES OF *S. AUREUS*- AND *B. LICHENIFORMIS* 749 C STRAINS BY N-ACETYL-D-(−)-PENICILLAMINE SEPHAROSE 4B AFFINITY CHROMATOGRAPHY

Source and inductor	*Cell-free supernatant*			*Purified enzyme*			*Purification fold*	*Capacity (mg ml^{-1})*
	Protein (μg ml^{-1})	*U ml^{-1} · 10^{-3}*	*Specific activity (U mg^{-1} · 10^{-3})*	*Protein (μg ml^{-1})*	*U ml^{-1} · 10^{-3}*	*Specific activity (U mg^{-1} · 10^{-6})*		
S. aureus PC 1 1711 E 1 μg ml^{-1} MET	610	1.8	2.95	3.4	17.82	5.241	1777	0.4
S. aureus NCTC 9789 1 μg ml^{-1} MET	600	6	10	4.6	58	12.609	1261	0.3
B. licheniformis 749 C No inductor	308	1.2	3.9	2.9	26.85	9.259	2374	0.3

buffer, pH 7.0. The removal of unbound protein was monitored spectrophotometrically at 280 nm, $A^{1\,cm}_{280\,nm}$. The bound enzyme was eluted separately with two 50-ml portions of 1 *M* sodium chloride containing 0.05 *M* phosphate buffer, pH 7.0. The pooled filtrates were desalted by ultrafiltration at 4°C. After sterile filtration and freeze-drying in sterile vials, the enzyme was distributed as about 1000 U per vial. The purification parameters are shown in Tables III and IV. The products are homogeneous according to sodium dodecyl sulphate (SDS)-polyacrylamide gel electrophoresis[13].

RESULTS AND DISCUSSION

The use of N-acetyl-D-(−)-penicillamine–Sepharose 4B as an affinity material by Clarke *et al.*[1] for β-lactamase purification was an excellent improvement because gradual hydrolysis of earlier β-lactam ligand-based affigels[2–7] prevented their use more than once or twice for efficient β-lactamase preparation and purification.

The above authors successfully used their affinity adsorbent for the purification of *B. cereus* 569/H β-lactamase I in two ways. In columns, however, direct chromatography of the crude cell-free culture medium is hampered by the large volumes, therefore they advised preconcentration of the enzyme on Celite. In this manner in relatively large amount of penicillinase was successfully purified.

We suggest treatment of large volumes of cell-free culture media by the batch technique, which makes possible convenient handling of penicillinases of different bacterial origins.

During optimization experiments we found that adsorption of the enzymes onto the affigel was best achieved at 4°C and not more than 15 min of slow and continuous stirring was sufficient for maximum binding of the enzyme. The stirring speed was just enough to prevent spontaneous sedimentation of the affigel. Handling of the gel was easy when, following adsorption of the enzyme, the suspension was allowed to settle.

As adsorption is an equilibrium process, a minimum amount of active principle should remain in the supernatant above the affigel, but repeated batch treatment of two pooled affigel supernatants with a calculated amount of affigel (according to its capacity for the respective penicillinase) proved to be satisfactory. It follows that the maximum binding capacity of the affigel should be assessed for each penicillinase prior to its use. Enzymes of different bacterial sources differ from each other significantly as shown in Tables III and IV, however the affigel can be used generally for penicillinases. The biospecificities of both affigels, that of Clarke *et al.*[1] and ours is shown also by the fact that β-lactamase II, an exocephalosporinase of the *B. cereus* strains used in these studies, is not bound to the affigel, although it is coproduced in about 10% and excreted into the culture medium together with the exopenicillinase β-lactamase I.

When cephalosporinases of Gram-negative bacteria were tried in small-scale experiments (examples listed in Experimental, *Bacterial strains*) we found no adsorption at all. This clearly shows the biospecific binding capability of the N-acetyl-D-(−)-penicillamine–Sepharose 4B affinity material.

We also should like to draw attention to the slow deacetylation of the affigel upon repeated use to an appreciable extent. Deacetylation also takes place during

storage of the affigel at 4°C for a relatively long period (several weeks) if it is not used frequently, but reacetylation four/five times may lead to the recovery of full capacity and good performance. The affigel, however, cannot be used indefinitely probably because of disadvantageous changes in the gel structure.

As mentioned above the stoichiometry of maximum binding capacity theoretically can be considered on a mol ligand per mol enzyme basis. However this is not true in practice. Several factors play a rôle in enzyme protein binding, among which are the following:

(a) Only ligands that are sterically free for access are active; ligands inside the gel beads require diffusion which may or may not be possible during adsorption, *i.e.*, "buried" ligands may not act as binders even if they are linked to the matrix with relative long spacer arms. The enzymes should also avoid the diffusion barrier of ordered water molecules surrounding the matrix backbone. Reduction of the amount of ligand molecules to about half of the original without decreasing the maximum binding capacity shows that most of the coupled ligands in both affigels are sterically handicapped; possibly they are inside the open pore structure of Sepharose 4B (Tables I and II).

(b) Steric hindrance may be caused by gel aging.

(c) As the applicability of the immobilized ligand depends on its specific adsorption, the matrix must be devoid of non-specific absorptive effects because these could obscure the biospecificity and interfere with the action of the bound ligand.

(d) The length of the spacer group between DPA and the matrix. Since shortening of the original spacer arm by omitting epichlorohydrin and phloroglucinol did not reduce the maximum binding capacity of our affigel, we feel that simplification of its preparation is justified.

Finally we should like to mention that both N-acetyl-D-(−)-penicillamine-based affigels show biospecificity for penicillinases, as revealed by their definite inability to bind β-lactamases of cephalosporinase character. This, however, may prompt the suggestion that biospecific cephalosporinase-binding affigels can be constructed with one of the possible cephalosporamine optical isomer derivatives, on a similar theoretical basis.

REFERENCES

1 A. J. Clarke, P. S. F. Mézes and T. Viswanatha, *J. Appl. Biochem.*, 2 (1980) 183.
2 L. J. Crane, G. E. Bettinger and J. O. Lampen, *Biochem. Biophys. Res. Commun.*, 50 (1973) 220.
3 F. Le Goffic, R. Labia and J. Andrillon, *Biochim. Biophys. Acta*, 315 (1973) 439.
4 F. Le Goffic, J. Andrillon-Spiege and R. Letarte, *Biochimie*, 57 (1975) 29.
5 R. G. Coombe and A. M. George, *Anal. Biochem.*, 75 (1976) 652.
6 L A. Enriquez and R. F. D'Amato, *Antimicrob. Agents Chemother.*, 15 (1979) 229.
7 C. Duez, J.-M. Frere, D. Klein, M. Noel, J.-M. Ghuysen, L. Delcambe and L. Dierickx, *Biochem. J.*, 193 (1981) 75.
8 B. L. Toth-Martinez, S. Gál, L. Kiss, F. J. Hernádi and P. Nánási, *Proc. Czechoslovak Congress of Chemotherapy with International Participation, Prague, April 15–19, 1984*, p. 211.
9 L. Kiss, S. Gál, B. L. Toth-Martinez and F. J. Hernádi, *Proc. Chemotherapeutical Conference, Hungarian Pharmacological Society, Hajduszoboşzló, April 24–26*, 1984, p. 10.
10 C. H. O'Callaghan, A. Morris, S. Kirby and A. H. Shingler, *Antimicrob. Agents Chemother.*, 1 (1972) 283.
11 O. H. Lowry, N. J. Rosenbrough, A. L. Farr and R. J. Randall, *J. Biol. Chem.*, 193 (1951) 256.
12 G. L. Ellman, *Arch. Biochem. Biophys.*, 82 (1959) 70.
13 K. Weber and M. Osborn, *Antimicrob. Agents Chemother.*, 5 (1969) 25.

Journal of Chromatography, 448 (1988) 117–126
Elsevier Science Publishers B.V., Amsterdam — Printed in The Netherlands

CHROM. 20 606

TRAPPING EFFICIENCY OF CAPILLARY COLD TRAPS

ANDERS HAGMAN
Department of Analytical Chemistry, Arrhenius Laboratory, University of Stockholm, S-106 91 Stockholm (Sweden)
and
SVEN JACOBSSON*
ACO Läkemedel AB, Research and Development Department, Box 3026, S-171 03 Solna (Sweden)
(First received December 28th, 1987; revised manuscript received April 26th, 1988)

SUMMARY

The ability to retain a series of *n*-alkanes (C_3–C_6 and C_{12}) by cryogenic trapping in different types of simple capillary trap has been studied. The traps were either capillary tube packed with glass beads or open-tubular capillary cold traps. The trapping efficiency was studied as a function of the amount of alkane and the temperature gradient of the trap. The trapping efficiency of open-tubular cold traps is dependent on both these factors, but the packed cold trap retained the alkanes quantitatively.

INTRODUCTION

Cold traps in combination with gas chromatography (GC) are used for two main reasons: enrichment purposes and solute band concentration. Cold traps are included in a great variety of application, such as volatiles in plastics[1], pyrolysis GC[2], atmosphere analysis[3], and in instrumental set-ups, such as multi-dimensional GC[4,5].

The utility of cryogenic trapping has clearly been shown in a review by Brettell and Grob[6]. Despite the widespread use of such devices, a search of the chromatographic literature shows a scarcity of papers that discuss the fundamental processes governing cryogenic trapping, *e.g.* with respect to aerosol formation. Takeoka and Jennings[7] have given a brief discussion of the principles governing cryogenic focusing and Hopkins and Pretorius[8] have given a more elaborated theory of band broadening during cryogenic trapping.

The wealth of applications of different simple cold traps, however, indicates that from a pratical viewpoint cryogenic trapping is of great usefulness. This may well be due to the ease of construction, *i.e.* simply to immerse the trap in a cold medium kept in a Dewar flask, and many of the traps described in the literature are in principle similar to the one shown in Fig. 1. Such cold traps are known to quantitatively retain a variety of organic compounds. However, Graydon and Grob[9] have reported that they have observed significant breakthrough of volatile organics from a simple open cold trap immersed in liquid nitrogen.

0021-9673/88/$03.50

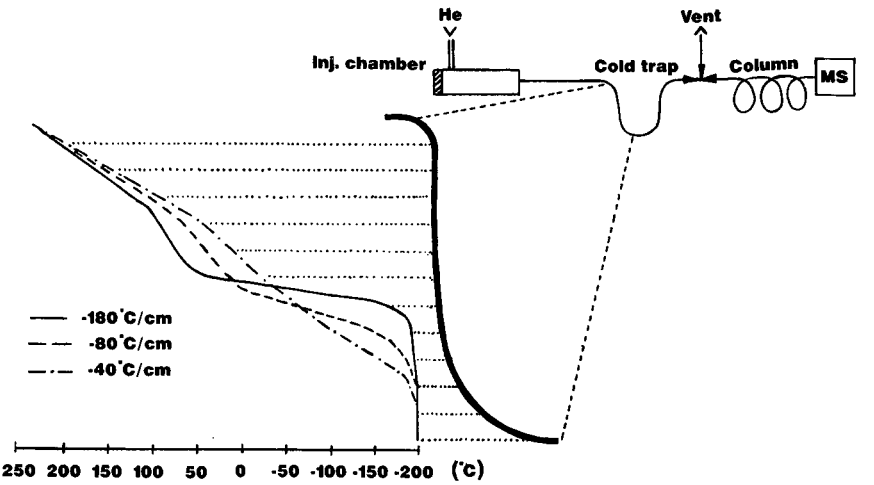

Fig. 1. A schematic diagram of the analytical system, and the profiles of the cold gradients. The distance between two dotted lines indicates 1 cm of the trap.

In our laboratories we have been using simple cold traps for a number of years. For quantitative analysis[10,11] capillary traps packed with glass beads have been the choice in order to enhance the contact between the vapour and the solid surface. However, in order to minimize dead volumes in capillary multi-dimensional GC[4], and to avoid flow-splitting arrangements between the cold trap and the capillary analytical column, the use of open capillary (I.D. less than 320 μm) cold traps has become of interest.

This paper examines the utility of simple cold traps to retain highly volatile organic compounds. The effect of three different negative temperature gradients over the cryogenic trapping zone and the influence of different amounts of compound are studied. Moreover, some basic cold trap design considerations are presented.

EXPERIMENTAL

The analytical system used in this study is described elsewhere[12]. The cold trap was coupled to a gas chromatograph (Packard 428) interfaced to a Jeol D-300 mass spectrometer and Incos 2400 data system.

Three different traps were investigated: one U-shaped glass tube (30 cm × 1.6 mm O.D. × 0.7 mm I.D.) packed with glass beads (40–60 mesh), one uncoated, deactivated fused-silica capillary (30 cm × 0.22 mm I.D.), and one fused-silica capillary (30 cm × 0.22 mm I.D.) coated with OV-101 (film thickness 0.55 μm).

The fused-silica capillary was situated in a U-shaped glass tube (0.8 mm I.D.) similar to the packed cold trap, in order to fix and retain the shape of the cold trap and to faciliate temperature measurements along the fused-silica capillary. The temperature measurements, to determine the temperature gradient of the trap, were carried out with a thin type K thermocouple (0.0125 mm O.D., Omega Engineering, Stamford, CT, U.S.A.) placed between the wall of the fused-silica capillary and the

glass wall. Owing to the thin dimensions of the thermocouple, the packed cold trap could be filled with glass beads even though the thermocouple was placed inside the glass tube prior to packing. Different temperature measuring points were obtained by simply sliding the thermocouple along the inside of the trap. The trap was kept in a Dewar flask (200 ml; I.D. 40 mm) filled with liquid nitrogen. To obtain the different negative temperture gradients the Dewar flask was filled with different levels of liquid nitrogen and was flushed with nitrogen gas at different flow-rates. Cryogenic trapping was studied at the followig negative temperature gradients: −40°C/cm, −80°C/cm, and −180°C/m. The first of these was obtained by lowering the trap 2.0 cm into the liquid nitrogen (*ca.* 55 ml) and flushing the liquid nitrogen surface with 300 ml/min of nitrogen gas. The −80°C/cm gradient was generated by lowering the trap 3.0 cm into the liquid nitrogen and flushing at 150 ml/min, and the −180°C/cm gradient by lowering the trap 4.5 cm into the liquid and without any flush. The temperature gradients were determined by linear regression analysis of the temperature curves in the interval −150 to 50°C (Fig. 1).

The experimental procedure was as follows. Each compound in turn, with 100-μl headspace, was injected at three different concentration intervals and three different cold gradients. Injection was performed with a gas-tight syringe through a septum into the quartz tube of the headspace chamber ($n = 4$–6 at each concentration level and cold gradient). The injected compound was then carried by helium gas to the trap. After a trapping time of 5 min, the Dewar flask was lowered and the trap heating was switched on. The trap was heated to 250°C by applying a high voltage for 2 s to a Kanthal A wire coiled around the glass tube. The voltage was then reduced. The trapped compound was reinjected onto the capillary column (SE-54, 25 m × 0.22 mm I.D.) with a split ratio of 1:10. The breakthrough was monitored by the mass spectrometer. The same amount of the same compound was then injected directly to the gas chromatograph through the heated trap. The compounds studied were *n*-propane, *n*-butane, *n*-pentane, *n*-hexane and *n*-dodecane.

The carrier gas velocity during the trapping and the reinjection was 87 cm/s in the column, and the flow-rate through the trap was 20 ml/min. The flow-rate was kept constant by a flow regulator (Porter VCD-100, Porter Instrument, Hatfield, U.K.). The headspace chamber was kept at 250°C and the oven temperature and the interface between the gas chromatograph and the mass spectrometer was maintained at 150°C. The mass spectrometer was scanned from m/z 35 to 250 at a cycle time of 1 s. The ionization energy was 70 eV.

RESULTS AND DISCUSSION

The cold traps are generally either U-shaped or straight tubes, and, like columns, they can be either open or packed. Some of packing materials that have been used are glass beads[10,11], adsorbents such as Tenax[13–15], Porapak Q[16] and activated carbon[13,17,18]. In the present study the tubes were U-shaped in order to faciliate immersion in a Dewar flask.

The ability of cold traps to retain compounds is dependent, among other factors, on the lowest temperature of the trap. However, since liquid nitrogen is inexpensive, convenient and a commonly used cooling medium, this study has focused on other factors affecting the cryogenic trapping efficiency.

To the best of our knowledge the importance of a negative temperature gradient during trapping was first discussed by Kaiser[17]. He concluded that a too sudden cooling or too low a temperature could cause a micro fog, which could be prevented by a gradient enrichment. In several later publications[2,3,5,7,19,20] the importance of a negative temperature gradient has been stressed. However, few experimental data have been presented to support such conclusions. The importance of the temperature gradient in aerosol formation and growth is, however, apparent in the more fundamental studies on aerosol formation[21].

In this work the influence of three different negative temperature gradients on the trapping efficiency of propane, butane, pentane, hexane and dodecane was experimentally examined. Packed cold traps are known to retain highly volatile compounds, such as ethane, at a temperature of −196°C[22]. Under the experimental conditions given in the experimental part no breakthrough could be observed for propane, butane, pentane, hexane and dodecane in the packed cold trap. The three amounts of compounds studied were 0.17–0.35 μg, 0.86–1.26 μg and 1.90–3.84 μg. The lower limit of detection was *ca.* 1 ng.

The ability of open cold traps to retain the studied compounds has been examined with uncoated and coated fused-silica traps. The results are summarized in Tables I and II. So that the results can be presented in a manageable form, the injected amounts of the compounds have been grouped in three sets. The variance within each set is large, with a average relative standard deviation (R.S.D.) of 29%, and this is reflected in the large R.S.D. of the breakthrough values. However, the correlation was examined by linear and non-linear regression analysis of the non-

TABLE I

TRAPPING EFFICIENCY OF A DEACTIVATED OPEN FUSED-SILICA TUBE

Percent breakthrough for propane, butane, pentane, hexane and dodecane at three different amounts and at three different cold gradients. The cold trap was a deactivated open fused-silica tube (30 cm × 0.22 mm I.D.). The R.S.D. was calculated on the basis of six experiments for each amount injected and each cold gradient. The experimental conditions are given in Experimental.

Compound	*Quantitation ion (m/z)*	*Amount injected (ng)*	*Breakthrough (%)*		
			−40°C/cm	*−80°C/cm*	*−180°C/cm*
Propane	44	290 (32%)	2.5 (22%)	9.8 (29%)	15 (67%)
		960 (23%)	3.2 (16%)	20 (32%)	24 (34%)
		3300 (36%)	10 (30%)	33 (45%)	50 (79%)
Butane	58	266 (26%)	0	3.8 (42%)	13 (62%)
		1040 (28%)	0	6.2 (23%)	20 (32%)
		3160 (20%)	2.0 (55%)	18 (36%)	39 (14%)
Pentane	72	260 (28%)	0	0.8 (32%)	7.0 (60%)
		1060 (25%)	0	4.2 (50%)	13 (25%)
		3550 (15%)	0.7 (29%)	10 (45%)	24 (43%)
Hexane	86	300 (18%)	0	0	1.8 (40%)
		1060 (35%)	0	0	9.2 (65%)
		2960 (30%)	0	1.2 (55%)	19 (62%)
Dodecane	170	210 (40%)	0	0	0
		860 (38%)	0	0	0
		1900 (35%)	0	0	0

TABLE II

TRAPPING EFFICIENCY OF A COATED OPEN-FUSED SILICA TUBE

Percent breakthrough for propane, butane, pentane, hexane and dodecane at three different amounts and at three different cold gradients. The cold trap was a coated (0.55 μm OV-101) open-fused silica tube (30 cm × 0.22 mm I.D.). The R.S.D. was calculated on the basis of four experiments at each amount injected and each cold gradient. The experimental conditions are given in Experimental.

Compound	*Quantitation ion (m/z)*	*Amount injected (ng)*	*Breakthrough (%)*		
			−40°C/cm	*−80°C/cm*	*−180°C/cm*
Propane	44	238 (29%)	2.3 (15%)	8.5 (32%)	21 (36%)
		860 (35%)	8.1 (22%)	25 (43%)	42 (42%)
		3500 (22%)	13 (38%)	45 (56%)	75 (45%)
Butane	58	350 (18%)	0.5 (40%)	6.5 (38%)	8.0 (32%)
		1100 (24%)	1.2 (55%)	12 (25%)	21 (38%)
		3840 (38%)	2.5 (67%)	21 (25%)	38 (40%)
Pentane	72	300 (25%)	0	1.3 (35%)	9 (28%)
		1050 (29%)	0	1.5 (28%)	12 (18%)
		3700 (46%)	1.2 (32%)	4.7 (42%)	19 (25%)
Hexane	86	264 (21%)	0	0	4.5 (29%)
		1260 (32%)	0	0	3.0 (38%)
		2300 (35%)	0	0.7 (36%)	5.0 (42%)
Dodecane	170	170 (18%)	0	0	0
		960 (28%)	0	0	0
		2100 (37%)	0	0	0

clustered data, and the confidence interval of the slope for the curve with the best fit, determined by the correlation coefficient, was tested at the 95% confidence level. For all the compounds examined, except dodecane, the breakthrough is affected by both the temperature gradient and the amount, *i.e.* the concentration (Figs. 2 and 3). Dodecane is probably retained in a region where the effect of the temperature gradient is less pronounced. A comparison of the results obtained reveals that no substantial differences are seen between coated and uncoated traps. This is in accordance with the findings of Graydon and Grob[9] and indicates that, at the low temperature at which the traps are kept, the coatings behave as solids.

As expected, the greater the difference between the cold trap temperature and the boiling point of the compound (or more probably the dew-point, *i.e.* the temperature at which condensation occurs), the more efficient is the trapping.

Breakthrough is considered to occur predominantly by aerosol formation of the first part of the vapour cloud followed by a rapid increase in trapping efficiency[9]. This hypothesis was found to be consistent with our experimental results, although it was not conclusively proved. As an example, the recorded breakthrough of butane is given in Fig. 4. The breakthrough can be seen as a two-phase procedure. The main breakthrough occurs in the early stage of the passage of the vapour cloud into the trap, and a second phase where the condensed compounds are stripped away due to their own vapour pressure. By use of the more selective detection provided by the mass spectrometer, changes in the baseline could be attributed to flow changes or component breakthrough. This attribution is severely restricted by use of, for example, an flame ionization detector.

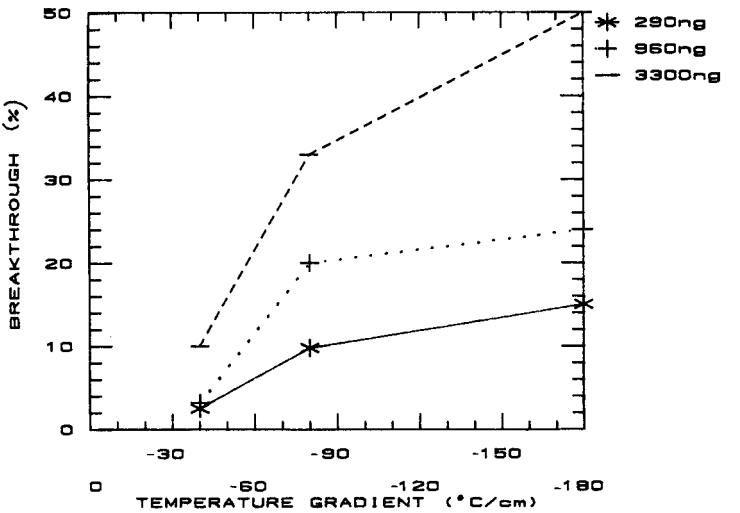

Fig. 2. Trapping efficiency of butane in a deactivated, open fused-silica tube at different temperature gradients and amounts.

To simulate the conditions of multi-dimensional GC, the test compounds were injected into the cold trap as a narrow band so that they occupied a defined volume. Therefore the trapping efficiency could be interpreted as dependent of the concentration. As the vapour cloud passes through the cold trap the band is sharpened because the distribution constant increases at the front of the band. The compounds are trapped in the space defined by the dew-point and the lowest temperature of the cold trap or, by definition, where the condensation is considered to be complete, *i.e.*

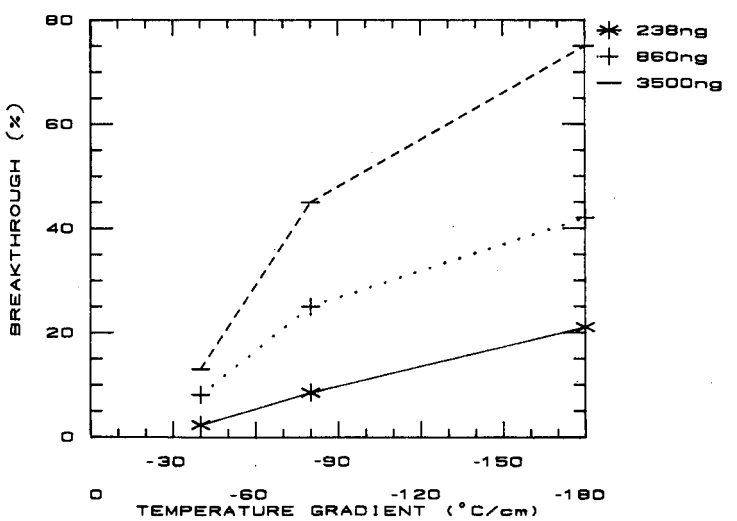

Fig. 3. Trapping efficiency of butane in a coated, open fused-silica tube at different temperature gradients and amounts.

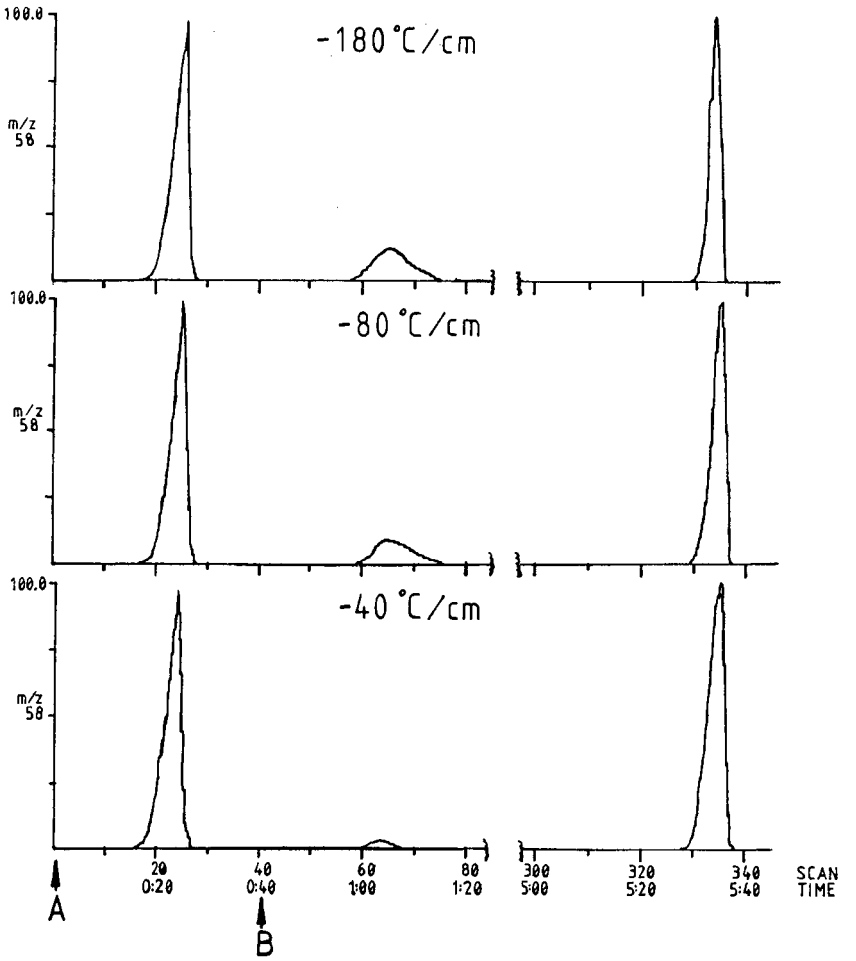

Fig. 4. Mass chromatograms showing the trapping efficiency of butane in a deactivated fused-silica tube at three different temperature gradients; the amount injected was *ca.* 3 μg. (A) Direct injection with heated trap; (B) injection with the cold trap on for 5 min and the liquid nitrogen removed there after.

$T_{complete}$. The time taken by the solute molecules in the vapour phase of the cold trap to diffuse to the cold wall, t_D, could be calculated by the following equation, which is deduced from Einstein's diffusion law[23]:

$$t_D = r_t^2/4D \tag{1}$$

where r_t is the radius of the trap and D is the coefficient of diffusion.

The diffusion equation is valid for a cylinder. The coefficient of diffusion can be calculated for a binary system by the Fuller–Schetter–Giddings equation[24]:

$$D = \frac{1.00 \cdot 10^{-3}\, T^{1.75}(1/M_A + 1/M_B)^{1/2}}{P[(\Sigma_A v_i)^{1/3} + (\Sigma_B v_i)^{1/3}]^2} \tag{2}$$

where D is the binary diffusion coefficient (cm^2/s), T is the absolute temperature, P is the total system pressure (atm.), M_A and M_B are the molecular masses (g/mol) and v is an atomic diffusion volume, a special diffusion parameter to be summed over atoms, groups, and structural features of the diffusing species (helium = 2.88, carbon = 16.5 and hydrogen = 1.98); A = carrier gas (helium) and B = the analyte (*e.g.* propane).

As examples, the coefficient of diffusion for propane is 0.096 cm^2/s at −136°C, and that for butane is 0.11 cm^2/s at −111°C. Hence, with a cold trap radius of 0.11 mm, we can expect diffusion times of $3.2 \cdot 10^{-4}$ s or larger for propane; the corresponding t_D for butane is $> 2.8 \cdot 10^{-4}$ s. If we further assume that, for the bulk of the compound, condensation occurs between the dew-point and $T_{complete}$, then the residence time of the corresponding compound could be calculated. In this context $T_{complete}$ is defined as the temperature where the compound under study exerts a vapour pressure of $1 \cdot 10^{-5}$ mmHg or less. The dew-point defines the temperature at which a given concentration of a compound begins to condense. By use of of the Antoine equation:

$$\ln p = A + B/(C + t) \tag{3}$$

and the iteration procedure of the Newton–Raphson method[25], the dew-point of the studied compounds could be established:

$$t_{n+1} = t_n - S_n/S'_n \tag{4}$$

$$S_n = 1 - P\Sigma y_i e^{-[A_i + B_i/(C_i + t_n)]} \tag{5}$$

$$S'_n = -P\Sigma y_i[B_i/(C_i + t_n)^2]e^{-[A_i + B_i/(C_i + t_n)]} \tag{6}$$

In eqns. 3–6, p is the vapour pressure (mmHg), S_n is the summation for dew-point, S'_n is the derivative of S_n, P is the total system pressure (mmHg), t is the temperature in °C, A, B, and C are constants with the respective values 15.74, −1875, and 248 for propane and 15.72, −2176, and 240 for butane (the constants are calculated for the vapour pressure range 10–100 mmHg), and y_i is the mole fraction of compound i in the vapour phase. In this case, the mole fraction is calculated from an injection time of 1 s into the carrier gas.

For butane (266 ng) these boundary conditions imply that condensation starts at a temperature of −111°C. The calculations of the dew-point are summarized in Table III. The temperature at which butane has a vapour pressure of $1 \cdot 10^{-5}$ mmHg, $T_{complete}$, was estimated to be −170°C. This gives a temperature interval of 59°C, which corresponds to a length of the condensation zone of 0.33 cm at the steepest temperature gradient. With a flow-rate of *ca.* 20 ml/min this corresponds to a residence time (t_{re}) of $3.8 \cdot 10^{-4}$ s.

Thus, the diffusion time to the wall (t_D) is in the critical vicinity of the time available for condenation. The close time-scales of the two events (t_D and t_{re}) suggests that part of the vapour cloud enters a temperature zone in which the vapour becomes suppersaturated before condensation on the wall occurs. The supersaturated vapour would be prone to from droplets, giving rise to aerosols.

TABLE III

DEW-POINT DETERMINATION

Calculation of dew-point for butane by the iteration procedure of the Newton–Raphson method. The gas mole ratio (y) was $3.4 \cdot 10^{-3}$ at 760 mmHg pressure and the starting temperatures for the trials were -100°C and -130°C, respectively.

Trial	*n*	t_n (°C)	S_n/S'_n (°C)
First	t_0	−100	−28
	t_1	−128	+6
	t_2	−122	+5
	t_3	−117	+4
	t_4	−113	+2
	t_5	−111	0
Dew-point		−111°C	
Second	t_0	−130	+6
	t_1	−124	+6
	t_2	−118	+4
	t_3	−114	+2
	t_4	−112	+1
	t_5	−111	0
Dew-point		−111°C	

The numerical interpretation of the concentration dependence is not readily available. Qualitatively, the concentration dependence may be interpreted as a shift of both the dew-point and T_{complete}, or the temperature be at which aerosol formation actually takes place, to higher temperatures than for the corresponding lower concentration. However, the temperature at which the aerosols are actually formed is influenced to a greater extent than the dew-point wiht increasing concentration. Thus, as the concentration increases, a decreasing effective condensatin zone is available, *i.e.* the effective residence time decreases.

In order to prevent aerosol formation, sufficiently long residence times with respect to the diffusion time (t_D) of the compound to be enriched have to be generated in open-tubular capillary cold traps. Ways to achieve this are smooth temperature gradients and low flow-rates, or the use of temperatures that sharpen the solute band without causing a supersaturated vapour to form, and hence an aerosol. In open-tubular capillary cold traps, aerosol formation may also be minimized by using loop-type traps[26], where the flow through the trap passes zones of different temperature gradients. However, this implies an increase of trap volume, and a consequent increase in the band-width. It should be noted that the cooled trap length at the lowest trapping temperature increased with steeper gradients. Hence, the results can not be explained by any decrease of the trap length.

CONCLUSION

This study has demonstrated the dependence of the open cold trap on the temperature gradient and the concentration. For the packed cold trap no such de-

pendence could be shown. Thus, if the trapping performances of different open cold traps are to be compared, one must take into account not only the lowest trapping temperature, the flow-rate, and the trap geometry, but also the temperature gradient and the concentration.

REFERENCES

1 A. Hagman and S. Jacobsson, *J. Chromatogr.*, 395 (1987) 271.
2 C. A. Jacques and S. L. Morgan, *J. Chromatogr. Sci.*, 18 (1980) 679.
3 P. Matuska, M. Koval and W. Seiler, *J. High Resolut. Chromatogr. Chromatogr. Commun.*, 9 (1986) 577.
4 A. Hagman and S. Jacobsson, *J. High Resolut. Chromatogr. Chromatogr. Commun.*, 8 (1985) 332.
5 S. Berg and A. Jonsson, *J. High Resolut. Chromatogr. Chromatogr. Commun.*, 7 (1984) 687.
6 T. A. Brettell and R. L. Grob, *Int. Lab.*, 16 (1986) 30
7 G. Takeoka and W. Jennings, *J. Chromatogr. Sci.*, 22 (1984) 177.
8 B. J. Hopkins and V. Pretorius, *J. Chromatogr.*, 158 (1978) 465.
9 J. W. Graydon and K. Grob, *J. Chromatogr.*, 254 (1983) 265.
10 S. Berg, S. Jacobsson and B. Nilsson, *J. Chromatogr. Sci.*, 18 (1980) 171.
11 Å. Bergman, A. Hagman, S. Jacobsson, B. Jansson and M. Åhlman, *Chemosphere*, 13 (1984) 237.
12 S. Jacobsson, *J. High Resolut. Chromatogr. Chromatogr. Commun.*, 7 (1984) 185.
13 F. Poy and L. Cobelli, *J. Chromatogr. Sci.*, 23 (1985) 114.
14 T. H. Wang, H. Shanfield and A. Zlatkis, *Chromatographia*, 17 (1983) 411.
15 H. T. Badings, C. de Jong and R. P. M. Dooper, *J. High Resolut. Chromatogr. Chromatogr. Commun.*, 8 (1985) 755.
16 M. V. Robillard, S. Siggia and P. C. Uden, *Anal. Chem.*, 51 (1979) 435.
17 R. E. Kaiser, *Anal. Chem.*, 45 (1973) 965.
18 K. Grob and A. Habisch, *J. Chromatogr.*, 321 (1985) 45.
19 D. Kalman, R. Dills, C. Perera and F. DeWalle, *Anal. Chem.*, 52 (1980) 1993.
20 J. A. Rijks, J. Drozd and J. Novák, *J. Chromatogr.*, 186 (1979) 167.
21 A. J. Pesthy, R. C. Flagan and J. H. Seinfeld, *J. Colloid Interface Sci.*, 91 (1983) 525.
22 S. Jacobsson and S. Berg, *J. High Resolut. Chromatogr. Chromatogr. Commun.*, 5 (1982) 236.
23 D. A. McQuarrie, *Statistical Mechanics*, Harper & Row, New York, 1976.
24 E. N. Fuller, P. D. Schetter and J. C. Giddings, *Ind. Eng. Chem.*, 58 (1966) 19.
25 C. J. Liddle, *Brit. Chem. Eng.*, 16 (1971) 193.
26 W. J. Kirsten, P. E. Mattson and H. Alfons, *Anal. Chem.*, 47 (1975) 1974.

Journal of Chromatography, 448 (1988) 127–133
Elsevier Science Publishers B.V., Amsterdam — Printed in The Netherlands

CHROM. 20 590

CHROMATOGRAPHIC AND CYTOGENETIC ANALYSIS OF *IN VIVO* METABOLITES OF FLUORANTHENE

C. POLCARO*, I. NICOLETTI, L. OSSICINI and G. CAPONECCHI
Istituto di Cromatografia CNR, Area della Ricerca di Roma, P.O.B. 10, 00016 Monterotondo Stazione, Rome (Italy)
R. COZZI
Dipartimento di Genetica e Biologia Molecolare, Università "La Sapienza", P. le Aldo Moro 5, 00185 Rome (Italy)
M. FIORE
Centro di Genetica Evoluzionistica CNR, Università "La Sapienza", P. le Aldo Moro 5, 00185 Rome (Italy)
and
F. PALITTI
Dipartimento di Biologia Agraria, Università della Tuscia, Viterbo (Italy)
(Received April 22nd, 1988)

SUMMARY

Fluoranthene metabolites in rat serum were analysed by high-performance liquid chromatography (HPLC) with UV and fluorescence detection and compared with *in vitro* metabolites obtained by incubation with microsomal fraction of rat hepatocytes. In order to resolve very polar fluorescent compounds present in rat serum, a modification of HPLC existing methods for *in vitro* metabolites separation was necessary. Mutagenic 2,3-dihydrodiol was identified in both *in vitro* sample and rat serum: this result is in good accord with cytogenetic analysis on rats bone marrow cells, that shows a slight but significant increase of sister chromatide exchanges.

INTRODUCTION

Fluoranthene (Ft) is a widespread polycyclic aromatic hydrocarbon which shows a high mutagenic activity after metabolic activation in *Salmonella typhimurium*[1] and in human lymphoblasts[2]. It is inactive in rodent bioassays for cancer[3], but has recently been shown to be tumorigenic in a newborn mouse lung adenoma bioassay[4].

In vitro metabolites of Ft activated by the microsomal fraction of Aroclor-treated rat hepatocytes (S9) have been separated by high-performance liquid chromatography (HPLC) and identified by spectroscopic techniques by LaVoie *et al.*[5] and Babson *et al.*[6] as 1-hydroxy-Ft, 3-hydroxy-Ft, 8-hydroxy-Ft and 2,3-dihydroxy-2,3-dihydro-Ft. 7-Hydroxy-Ft[5] and Ft-2,3-quinone[6] have also been found, but Ft-7,8-diol and Ft-1,10b-diol, which are possible oxidation products[7], have not been

0021-9673/88/$03.50

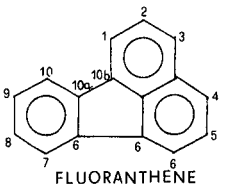

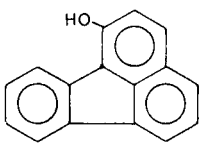

1-HYDROXYFLUORANTHENE

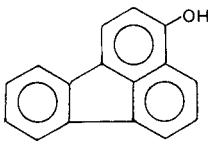

3-HYDROXYFLUORANTHENE

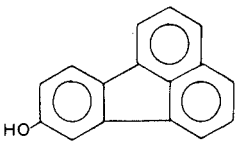

8-HYDROXYFLUORANTHENE

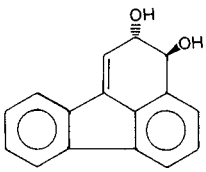

2,3-DIHYDROXY-2,3-DIHYDROFLUORANTHENE

detected[5,6]. Ft-2,3-diol yields the direct-acting mutagen 2,3-dihydroxy-1,10b-epoxy-1,2,3-trihydro-Ft, which is able to react with DNA, forming an N^2-deoxyguanosine adduct[8].

In a previous study[9], it was observed that Ft induces, after metabolic activation with S9 from rats, sister chromatide exchanges (SCE) in Chinese hamster ovary cells grown *in vitro*, whereas no mutagenic activity was observed in bone marrow cells of Ft-treated mice. HPLC analysis of the mice serum showed that Ft metabolism was very slow; in fact, even 24 h after administration Ft was still present as a large peak with a very low formation of polar metabolites, among which isomeric phenols were identified. Therefore, an *in vivo* study of Ft metabolism in rats was performed in order to investigate more exactly the correlation between the *in vivo* and *in vitro* Ft activation in two comparable enzymatic systems.

The aim of this work was the HPLC separation of Ft metabolites in the serum of *in vivo*-treated rats, in order to compare the chromatographic profiles of such *in vivo* samples with those obtained *in vitro* using S9 derived from rats as the metabolic-activating system. *In vivo* chromatographic data were also compared with cytogenetic assays on bone marrow cells of rats.

EXPERIMENTAL

Chromatography

Sample preparation. For *in vitro* metabolic activation, Ft (Merck, Darmstadt, F.R.G.) was dissolved in dimethyl sulphoxide (DMSO) and incubated for 3 h with rat liver homogenate prepared from the livers of young male Sprague-Dawley/CD rats, whose hepatic enzymes were induced with Aroclor (S9). The S9 mixture was prepared according to Natarajan *et al.*[10]. The concentration of Ft was 36 μg/ml.

For the *in vivo* test, male Fisher 344 rats, weighing 200–220 g, were treated

orally with 1 g/kg body weight of Ft dissolved in corn oil, 3, 6 and 24 h after treatment, samples of blood were taken from the aorta of the rats and centrifuged at 150 *g* for 10 min. A 24-h control sample was obtained utilizing a rat that was given only corn oil. About 2 ml of serum were obtained from each rat.

Every experiment was repeated three times.

In vivo and *in vitro* samples were extracted five times with a 5-fold excess volume of ethyl acetate, dried with anhydrous sodium sulphate and evaporated to dryness. The initial volumes were replaced with methanol.

Chemicals were purchased from Carlo Erba (Milan, Italy). The solvents, except DMSO, were of HPLC grade.

Apparatus. A Perkin-Elmer apparatus was used with a Series 4 pumping system, an LC 75 variable-wavelength detector with Autocontrol, a Perkin-Elmer 650-10 S spectrofluorimetric detector and a Rheodyne 7105 valve as injector. A Vydac C_{18} (5 μm) 201 HS 104 prepacked column (25 cm × 4.6 mm I.D.) and a 5-cm precolumn packed with Supelco C_{18} pellicular packing were used. The mobile phase flow-rate was 1 ml/min. The gradient programme is given in Table I.

Cytogenetic assay

In order to perform cytogenetic analysis of SCEs on differently stained chromatids in bone marrow cells, two agar-coated 5-bromodeoxyuridine tablets (50 mg) (Fluka, Buchs, Switzerland) were implanted subcutaneously in rats. Two hours after implantation the rats were treated by gavage with Ft; 22 h later they received an intraperitoneal injection of colchicine (Merck) (3 μg/g body weight) and, after 2 h, their blood was taken from the aorta for analysis by HPLC, as described before (24-h sample). Simultaneously air-dried preparations of bone marrow cells were made according to the technique of Ford and Hamerton[11] and staining was performed according to the method of Perry and Wolff[12]. For each rat 40 well spread metaphases were analysed for SCEs.

RESULTS AND DISCUSSION

To achieve the HPLC separation of *in vivo* rat serum samples, a specific chromatographic system had to be set up. This system represents an improvement over the method of Babson *et al.*[6] for the separation of S9 *in vitro* activated Ft. In fact

TABLE I

GRADIENT PROGRAMME USED IN HPLC

Step	*Acetonitrile (vol.-%)*	*Water (vol.-%)*	*Time (min)*	*Gradient shape*
1	10	90	0	
2	30	70	15	Linear
3	30	70	5	
4	70	30	20	Linear
5	100	0	5	Linear
6	100	0	15	

the elution programme of Babson *et al.*[6] could not resolve the polar metabolites formed in the direct *in vivo* activation, whereas the present gradient profile, starting from a low (10%) proportion of acetonitrile in water and slowly reaching the final 100% concentration of organic modifier shows a good selectivity for these compounds, without altering the resolution of the more retained compounds.

Fig. 1 shows the chromatographic separation of ethyl acetate extracts of *in*

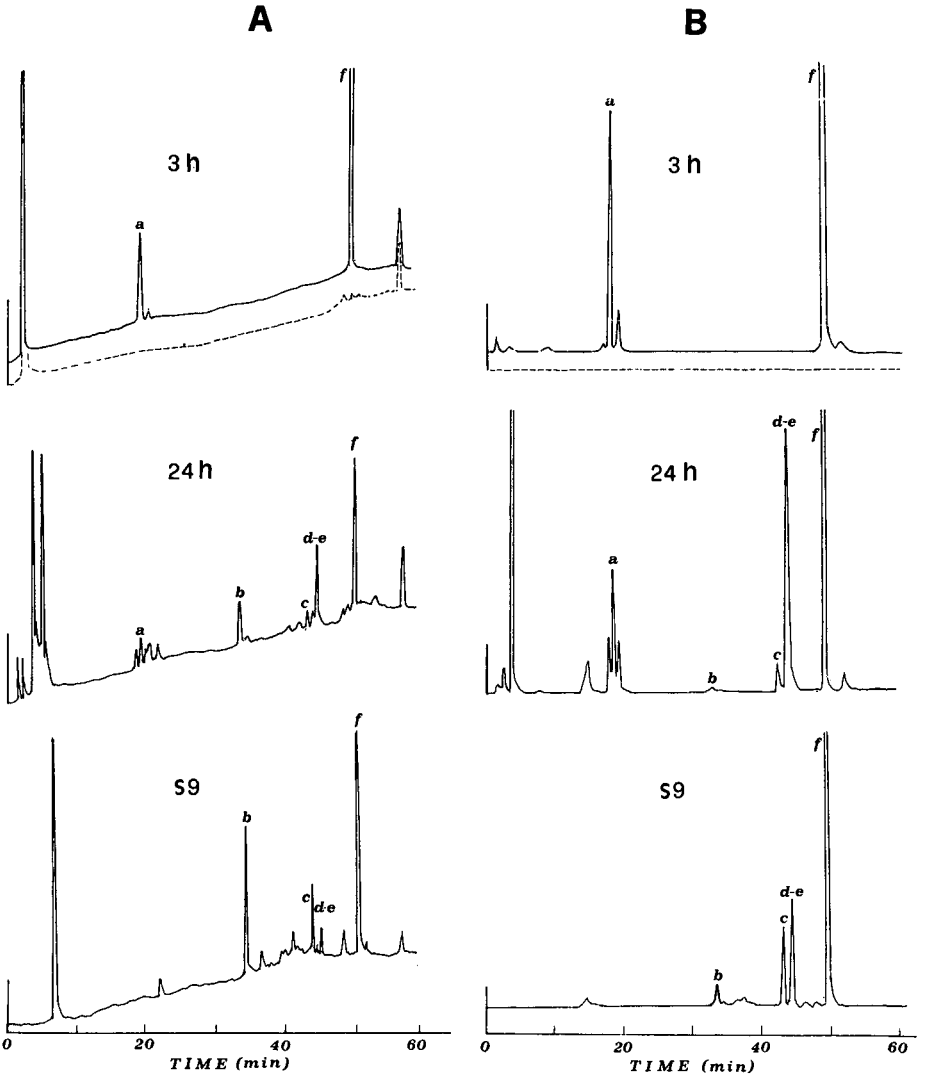

Fig. 1. Chromatographic profiles of *in vitro* S9 activated Ft and *in vivo* rat serum samples taken 3 and 24 h after Ft administration obtained with (A) UV (at 254 nm) and (B) fluorescence (at $\lambda_{ex.}$ 305 nm, $\lambda_{em.}$ 460 nm) detection. The control sample chromatogram is shown by the broken line. Column, Vydac C_{18} (5 μm) (25 cm × 4.6 mm I.D.); mobile phase, acetonitrile–water, gradient as described in Table I; flow-rate, 1 ml/min; temperature, ambient. Peaks: a = unidentified compound; b = 2,3-dihydroxy-2,3-dihydro-Ft; c = 8-hydroxy-Ft; d = 1-hydroxy-Ft; e = 3-hydroxy-Ft; f = Ft.

vitro S9 activated Ft and *in vivo* rat serum. Rat serum samples were taken 3 and 24 h after Ft administration. The chromatogram of the 6-h sample is similar to that of the 3-h sample, apart from an increase in the amount of polar metabolites.

The "*in vivo*" 24-h sample elution pattern is similar to the *in vitro* pattern. In fact, there are peaks with the same retention times of 2,3-diol and phenolic metabolites, which have been isolated and identified in the *in vitro* sample by mass, UV and fluorescence spectrometry (as described elsewhere)[9].

In order to identify these compounds in rat serum, their on-line scanned UV and fluorescence spectra were recorded, stopping the eluent flow during chromatography. The 2,3-diol spectra obtained for the *in vivo* and *in vitro* samples are shown in Fig. 2; in the same way the fluorescence spectrum allowed the identification of 8-hydroxy-Ft (maximum emission wavelength, $\lambda_{em.}$ = 385 nm at excitation wavelength, $\lambda_{ex.}$ = 305 nm).

Unfortunately, 1-hydroxy- and 3-hydroxy-Ft are not resolved with the new gradient program, so the peak corresponding to these substances was analysed as follows. Fluorescence emission spectra of the head and the tail of the peak were scanned at $\lambda_{ex.}$ = 305 nm, giving respectively maxima at $\lambda_{em.}$ = 435 nm (head), characteristics of 1-hydroxy-Ft, and at $\lambda_{em.}$ = 477 nm (tail), characteristic of 3-hydroxy-Ft.

Further, the peaks corresponding to phenolic isomeric metabolites were collected in a single fraction and submitted to mass spectrometric analysis, giving the molecular peak at *m/z* 218, in accordance with the literature and data obtained for the *in vitro* metabolites.

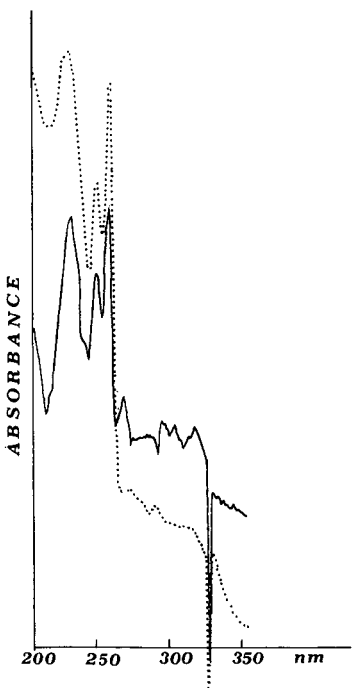

Fig. 2. UV–visibile spectra of 2,3-dihydroxy-2,3-dihydro-Ft in *in vivo* (solid line) and *in vitro* (broken line) samples.

However, the 24-h *in vivo* sample and the S9 *in vitro* activated fluoranthene chromatograms show some differences, particularly the presence of very polar, highly fluorescent compounds in the rat serum sample, whereas no fluorescent peak is present in the initial part of the S9 sample chromatogram. In fact, in the 24-h serum chromatogram it is possible to observe a group of three peaks, including a major compound with a retention time of 19 min 40s, which is indicated in Fig. 1 as peak a, and a group of very polar peaks, eluting near the solvent front, probably due to the decomposition of compound a.

Comparing the 3- and 24-h *in vivo* samples, there is evidence that compound a is formed very early. In three series of *in vivo* samples which were examined, it is almost the only metabolite present at the 3 and 6 h, whereas it is absent from the control sample.

In different serum samples taken 24 h after Ft treatment, compound a and the solvent front eluting peaks both occur, but both are present in varying amounts. The UV and fluorescence spectra of peak a were scanned on-line, giving the following results: fluorescence spectrum, $\lambda_{em.} = 465$ nm at $\lambda_{ex.} = 305$ nm; UV spectrum (0.04 a.u.f.s. range), $\lambda_{max.}$ 214 ($a=0.022$), 238 ($a=0.022$), 282 ($a=0.01$), 290 ($a=0.014$), 350 ($a=0.004$), 365 ($a=0.004$) and $\lambda_{min.}$ 225 ($a=0.016$), 270 ($a=0.008$), 300 ($a=0.0036$).

Up to now, attempts to isolate this compound by HPLC in order to analyse it by fast atom bombardment mass spectrometry have been unsuccessful, because of both the small amount of the sample and the high decomposition rate of the substance under examination.

Isomeric phenolic derivatives of Ft are also present in varying amounts, but 2,3-diol peak is approximately constant. At the same time, cytogenetic analysis showed that fluoranthene induces a slight but significant increase of SCEs in bone marrow cells of 24-h treated rats: $\bar{x}$(SCEs/cell) = 4.5 ± 1.8 in treated rats *versus* $\bar{x}$(SCEs/cell) = 2.6 ± 1.4 in the control.

CONCLUSION

Chromatographic analysis of *in vivo* and *in vitro* metabolites of suspected mutagenic compounds is a necessary approach to the investigation of their effective activation behaviour. With fluoranthene, fluorescence detection was particularly useful for the selective identification of metabolites. The HPLC system showed the presence in the *in vivo* samples of some metabolic products that have not been detected previously in *in vitro* samples. The fact that these compounds are present even a few hours after fluoranthene administration to the rats seems to exclude the possibility that they may be detoxification products of other metabolites. Apart from this, it is possible that the *in vitro* mutagenic 2,3-diol metabolite is formed in rat blood even after a long time. The presence of the 2,3-diol is in accord with the results of a cytogenetic study on bone marrow cells of the same animals, showing a slight increase in SCEs. In a previous study[9] it was shown that fluoranthene was able to induce SCEs in Chinese hamster ovary cells in an *in vitro* cytogenetic test in the presence of S9 mixture from rats. This is consistent with the formation of the active metabolite fluoranthene-2,3-diol. The data from this study show that the direct *in vivo* activation of fluorantene leads to a smaller mutagenic effect than that observed *in vitro*. The

presence of the 2,3-diol in *in vivo* serum samples can explain the small mutagenic effect found *in vivo*.

ACKNOWLEDGEMENTS

The Mass Spectrometry Service of the Area della Ricerca di Roma CNR is acknowledged for measuring the mass spectra. This investigation was supported by Progetti Strategici del CNR "Chimica dei Processi Biologici" e "Mutagenesi".

REFERENCES

1 D. A. Kaden, R. A. Hites and W. C. Thilly, *Cancer Res.*, 39 (1979) 4152.
2 W. G. Thilly, J. G. De Luca, E. E. Furth, H. Hoppe, D. A. Kaden, J. J. Krowlewski, H. L. Liber, T. R. Skopek, S. A. Slapikoff, R. S. Tizard and B. W. Penman, in F. J. de Serres and A. Hollaender (Editors), *Chemical Mutagens. Principles and Methods for Their Detection*, Vol. 6, Plenum Press, New York, 1980, pp. 58 and 79–86.
3 *IARC Monographs on The Evaluation of the Carcinogenic Risk of Chemicals to Humans*, No. 32, IARC, Lyon, 1983, p. 355–369.
4 W. F. Busby, M. E. Goldman, P. M. Newborne and G. N. Wogan, *Carcinogenesis*, 5 (1984) 1311.
5 E. S. LaVoie, S. S. Hecht, V. Bedenko and D. Hoffman, *Carcinogenesis*, 3 (1982) 841.
6 J. R. Babson, S. E. Russo-Rodriguez, R. V. Wattley, P. L. Bergstein, W. G. Rastetter, H. L. Liber, B. M. Andon, W. G. Thilly and G. N. Wogan, *Toxicol. Appl. Pharmacol.*, 85 (1986) 355.
7 W. Rasteller, R. B. Nachbar, S. E. Russo-Rodriguez, R. W. Wattley, W. G. Thilly, B. M. Andon, W. L. Jorgensen and M. Ibrahim, *J, Org. Chem.*, 47 (1982) 4873.
8 J. R. Babson, S. E. Russo-Rodriguez, W. H. Rastetter and G. N. Wogan, *Carcinogenesis*, 7 (1986) 859.
9 F. Palitti, R. Cozzi, M. Fiore, F. Palombo, C. Polcaro, G. Perez and E. Possagno, *Mutat. Res.*, 174 (1986) 125.
10 A. T. Natarajan, A. D. Tates, P. P. W. Buul, M. Mejiers and N. De Vogel, *Mutat. Res.*, 37 (1976) 83.
11 G. T. Ford and J. Hamerton, *Stain Technol.*, 31 (1956) 247.
12 P. Perry and S. Wolff, *Nature (London)*, 251 (1974) 156.

Journal of Chromatography, 448 (1988) 135–143
Elsevier Science Publishers B.V., Amsterdam — Printed in The Netherlands

CHROM. 20 607

NORMAL-PHASE HIGH-PERFORMANCE LIQUID CHROMATOGRAPHY OF TRIACYLGLYCEROLS

S. H. RHODES and A. G. NETTING*
School of Biochemistry, University of New South Wales, P.O. Box 1, Kensington 2033, N.S.W. (Australia)
(First received October 21st, 1987; revised manuscript received April 27th, 1988)

SUMMARY

Triacylglycerols have been separated by normal-phase high-performance liquid chromatography (HPLC) on silica utilising a solvent system consisting of dry acetonitrile–half water saturated hexane (0.7:99.3). This solvent system is UV transparent allowing detection at 200 nm and affords a separation in which retention is primarily dependent on the number of constituent double bonds. There is also a slight separation on chainlength, the longer chainlengths being eluted first. The system is therefore complementary to currently used reversed-phase HPLC systems. Chromatograms for some polyunsaturated fats and oils are given, and the most polyunsaturated triacylglycerols from linseed oil are analysed in more detail. Data are given for the separation and quantitation of the pentafluorobenzyl esters of constituent fatty acids from these triacylglycerols by a similar normal-phase HPLC system.

INTRODUCTION

There have been a considerable number of publications on the high-performance liquid chromatographic (HPLC) separation of triacylglycerols in the reversed-phase mode[1–6], most of which have used mixtures containing acetonitrile and acetone[1,3–6]. In these systems the separation of critical pairs (that is a pair of triacylglycerols in which the carbon number minus twice the number of double bonds is equal) can be difficult and time consuming[3,7] although improvements have certainly been made recently[8,9]. The addition of silver ions to the mobile phase does alter the selectivity[5] but not sufficiently to widely separate critical pairs. Triacylglycerols have also been separated by argentation HPLC[10] and as mercury(II) acetate adducts on silica gel sintered rods[11], but in both cases the peak shape was somewhat unsatisfactory.

Our work on the normal-phase HPLC separation of the pentafluorobenzyl (PFB) esters of fatty acids[12,13] according to the number of double bonds that they contain led us to suspect that this separation could be obtained if the ester functional group was sufficiently masked. More recent experience[14] with the separation of estradiol-17β-fatty acid esters as 3-pentafluorobenzyl ethers by normal-phase HPLC confirmed this view. Since the fatty acyl groups of triacylglycerols should also mask

0021-9673/88/$03.50

the ester functional groups on the glycerol, it seemed likely that a separation according to the number of constituent double bonds might also be possible on normal-phase HPLC.

We wished to utilise the relatively high sensitivity of UV detection at low wavelengths since these normal phase systems[12–14] are susceptible to overloading. This necessitated the investigation of new solvent systems since the dichloromethane used previously[12–14] absorbs below about 235 nm. This paper, then, presents such a normal-phase system in which critical pairs are very widely separated and in which the triacylglycerols are primarily separated according to the number of constituent double bonds.

EXPERIMENTAL

Materials

The following triacylglycerol standards were purchased from Sigma (St. Louis, MO, U.S.A.): tristearoylglycerol, tripalmitoleoylglycerol, trioleoylglycerol, trilinoleoylglycerol, trilinolenoylglycerol and tri-11-eicosenoylglycerol. Some domestically used fats and oils were obtained from local retail outlets: Bartolli olive oil, Lucca, Italy; Eta sunflower oil, polyunsaturated, Vegetable Oils (Vic) P/L, West Footscray, Australia; safflower oil, E.O.I. P/L, Marrickville, Australia; Meadow Lea polyunsaturated margarine (P/S > 2:1), Vegetable Oils P/L, Mascot, Australia, and Glendale raw linseed oil, Glendale Chemical Products P/L, Alexandria, Australia. The pentafluorobenzyl bromide was obtained from Fluka (Buchs, Switzerland).

Flax seeds were purchased from a local produce store and 2.5 g were ground in a mortar in 20 ml hexane and the solution filtered through a sinter. This gave a final concentration of oil of 30 mg/ml.

Instrumentation

HPLC was performed on Waters (Milford, MA, U.S.A.) equipment consisting of an M510 pump and a U6K injector. The column effluent flowed to a Hewlett-Packard (Waldbronn, F.R.G.) diode array detector (1040M) which was interfaced to an HP 300 series computer, a 9133 disc drive, a 7470A plotter and a Thinkjet printer for the manipulation and presentation of data.

The columns were silica spheri-5 (250 × 4.6 mm, 5 μm, Brownlee Labs, Santa Clara, CA, U.S.A.) or Waters silica Semiprep (300 × 7.8 mm, 10 μm). HPLC solvents were Chromar Grade from Mallinckrodt, Aust. P/L (Putney, Australia).

The gas chromatography–mass spectrometry (GC–MS) equipment was as described previously[15], the column being 1.5 m × 2 mm packed with 1.5% OV-1 on Gas Chrom Q (100–120 mesh).

Chromatography

In order to optimise the system for UV detection we investigated solvent modifiers to replace the dichloromethane that had been used previously[12,13]. Tetrahydrofuran (1.6%) in half water saturated hexane gave satisfactory separations but absorbed in the low UV, thus reducing sensitivity. However, 0.7% acetonitrile in half water saturated hexane was UV transparent and give adequate retention of the triacylglycerol mixtures. It was made up by dissolving 7 ml of dry (molecular sieve)

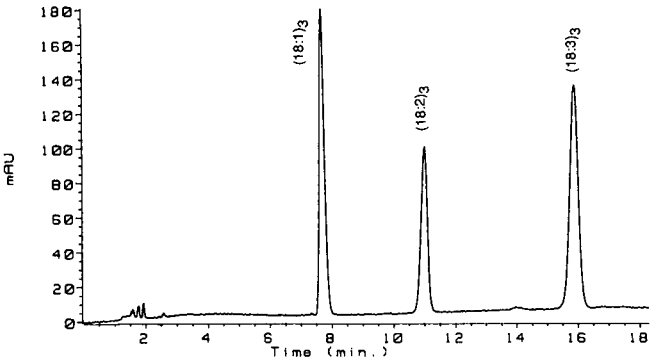

Fig. 1. Triacylglycerol standards (trioleoylglycerol, trilinoleoylglycerol and trilinolenoylglycerol). Normal-phase HPLC on 5-μm silica using dry acetonitrile–half water saturated hexane (0.7:99.3) at 2 ml/min. Detection at 200 nm, bandwidth, 4 nm.

acetonitrile in 496.5 ml of water saturated hexane by vigorous shaking and then making up to 1 l with dry (molecular sieve) hexane. Approximately 1% acetonitrile is the maximum that is soluble under these conditions. The flow-rates were 2 ml/min for the Brownlee column and 4 ml/min for the Waters. The diode array detector was set at 200 nm with a band width of 4 nm for peak detection.

Appropiate fractions were collected from the chromatograph and saponified and derivatised with PFB bromide in a one pot reaction as described previously[13]. They were then either injected directly into the GC–MS system or rechromatographed on the Waters column in 0.18% acetonitrile in half water saturated hexane with detection at 200 nm and 263 nm (bandwidth of 4 nm in both cases) and the resulting peaks checked by GC–MS.

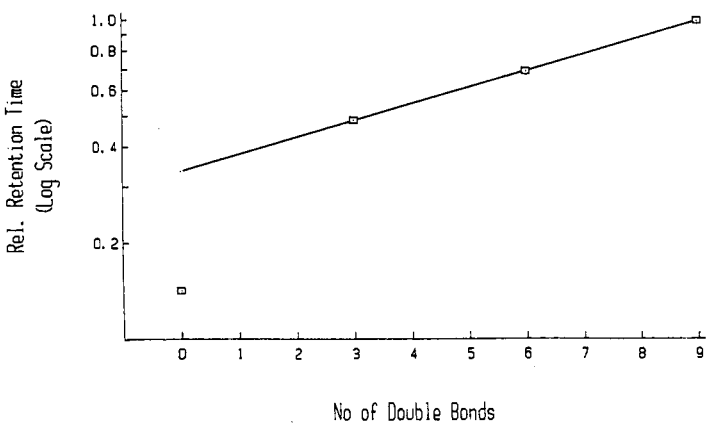

Fig. 2. Log relative retention time *versus* number of constituent double bonds for standards in Fig. 1 plus tristearoylglycerol.

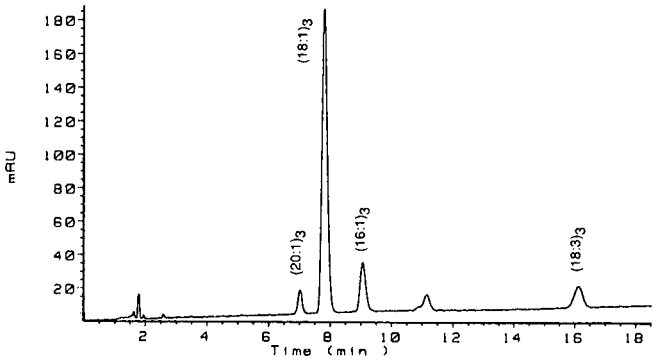

Fig. 3. Triacylglycerol standards (tri-11-eicosenoylglycerol, trioleoylglycerol, tripalmitoleoylglycerol and trilinolenoylglycerol). Conditions as for Fig. 1.

RESULTS AND DISCUSSION

Fig. 1 shows the separation of the three standard triacylglycerols containing C_{18} fatty acids. It can be seen that there is a large separation between the three peaks containing 3, 6 and 9 double bonds respectively. Fig. 2 shows that a linear relationship is obtained when log relative retention time is plotted against the number of double bonds, except that tristearoylglycerol does not lie on the line. This differs from the pentafluorobenzyl esters where, on the log t_R *versus* number of double bonds graph, PFB 18:0 was colinear with PFB 18:1, PFB 18:2 and PFB 18:3 (ref. 12). We suspect that, with triacylycerols, the first double bond in any given chain has a larger effect on t_R than subsequent double bonds in the same chain, each chain interacting independently: but this point requires further investigation. It was also found that, like the system used for the PFB esters[12], this system gave a small separation on chainlength. This is illustrated for tripalmitoleoylglycerol, trioleoylglycerol and tri-11-eicosenoylglycerol in Fig. 3. The separations of some domestically utilised fats and oils are illustrated in Figs. 4–8. It can be seen that the system described here is

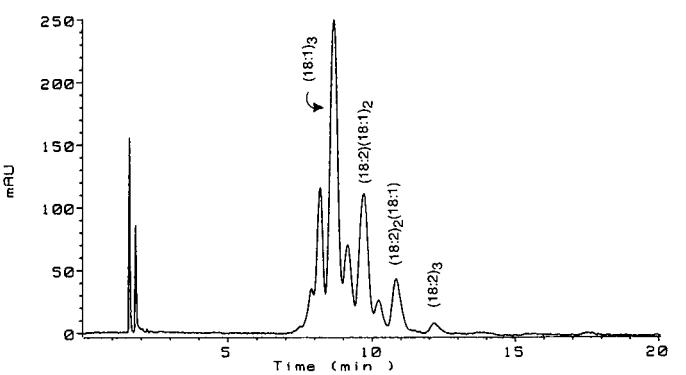

Fig. 4. Olive oil triacylglycerols. Approximately 5 μg total. Conditions as for Fig. 1.

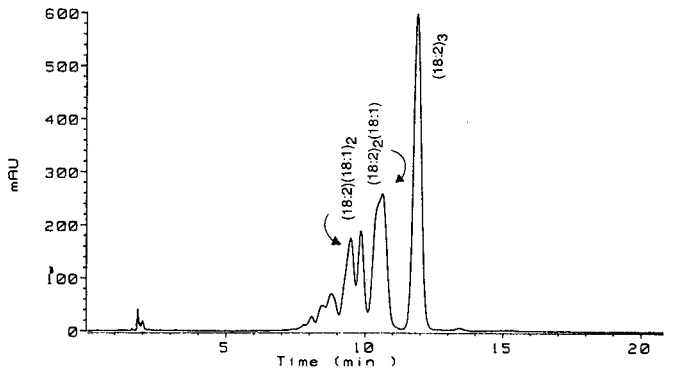

Fig. 5. Sunflower oil triacylglycerols. Conditions as for Fig. 4.

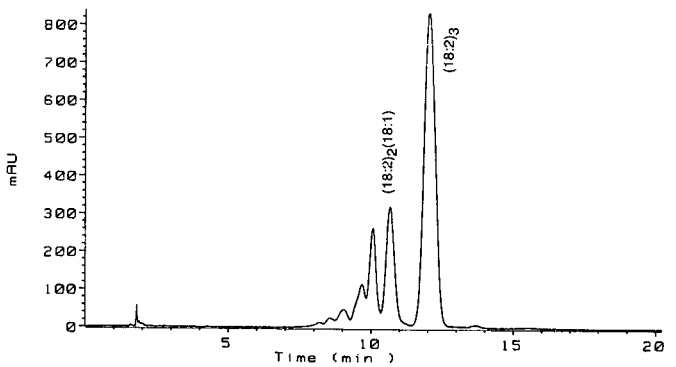

Fig. 6. Safflower oil triacylglycerols. Conditions as for Fig. 4.

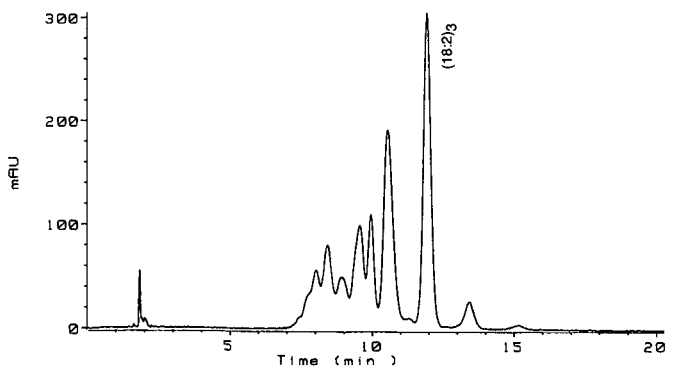

Fig. 7. Polyunsaturated margarine triacylglycerols. Conditions as for Fig. 4.

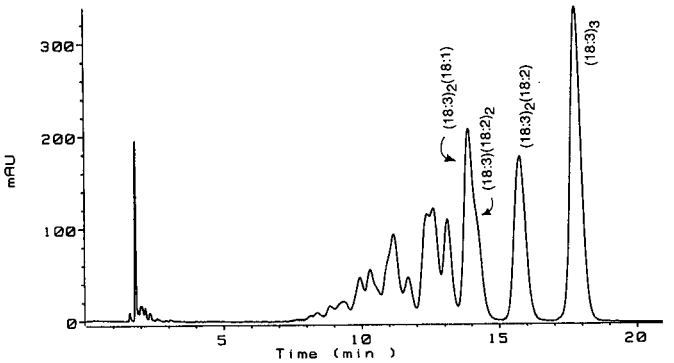

Fig. 8. Linseed oil triacylglycerols. Conditions as for Fig. 4.

particularly suitable for separating out the polyunsaturated triacylglycerols. This is primarily because the number of carbon atoms in the acyl groups of the more unsaturated triacylglycerols are usually restricted to eighteen.

The solvent system described here can take some considerable time to equilibrate with the column and can give retention times that vary slightly with the solvent batch. Thus the standards (Figs. 1 and 3), which were chromatographed on a different day to the fats and oils (Figs. 4–8), gave retention times of some two minutes less for $(18:3)_3$ and some one minute less for $(18:2)_3$. However, when the fats and oils (Figs, 4–8) were coinjected with an internal standard (trilinolenoylglycerol) the relative retention times were reproducible to approximately 3 parts in 1000. Using a log relative retention time *versus* number of double bonds graph, this allowed a preliminary identification of some of the later eluting peaks in the chromatograms. This is the origin of the labels in Figs. 4–8. We examined the later eluting peaks from linseed oil in more detail. After saponification and derivativisation with PFB bromide, subsamples were analysed by GC–MS in the negative ion chemical ionisation (NICI) mode. The $[M - PFB]^-$ ions, which are almost the sole ions in these mass spectra, indicated that the PFB esters from the last peak from linseed oil (Fig. 8) contained 18:3, from the second last peak, 18:2 and 18:3 (in approximately the expected ratios of 1:2), and from the third last, 18:1, 18:2 and 18:3. However, there were various other minor peaks that appeared to correspond to derivativised fatty acids. We therefore used HPLC to re-examine the commercial linseed oil and also the fresh oil extracted from flax seeds. Samples from both these oils were run on the Waters column and the last three peaks collected, saponified and esterified with PFB bromide. Each of the six samples was then reinjected into the HPLC using 0.18% acetonitrile in hexane with detection at 200 nm for maximal sensitivity.

The chromatogram for the fraction containing seven double bonds from the flax seed extract is given in Fig. 9. Examination of the UV spectra of the peaks eluting after 8 min suggested that only those eluting between 9.5 and 14.0 min were PFB esters. Comparison of retention times with standards suggested that these three peaks were PFB 18:1, PFB 18:2 and PFB 18:3 respectively, and that other PFB esters were absent. NICI-MS confirmed the identity of the C_{18} peaks and failed to show the presence of any other PFB fatty acid esters. Similar results were obtained from the

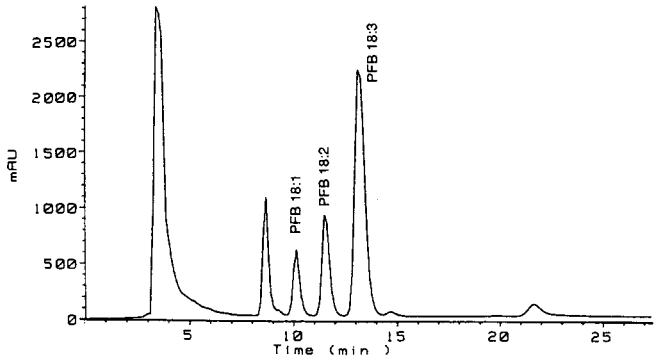

Fig. 9. PFB esters from saponified and esterified 3rd last peak of flax seed extract [corresponds to $(18:3)_2$-(18:1) plus (18:3)-$(18:2)_2$ in Fig. 8]. Total 3rd last peak from the injection of appprox. 3.3 mg flax seed extract onto a 300 × 7.8 mm column (10 μm) was collected, saponified and esterified with PFB bromide and the PFB esters rechromatographed on the same column in dry acetonitrile–half water saturated hexane (0.18:99.82) at 4 ml/min with detection at 200 nm, bandwidth 4 nm.

fraction containing seven double bonds from the commercial linseed oil. The NICI-MS and a detailed spectral analysis of the PFB 18:2 peaks from both the commercial linseed oil and from the flax seed extract respectively, showed that both of these esters were contaminated with a minor component. In the case of the flax seed extract this was apparently insufficient to affect the composition of the esters from this fraction. Integration of the chromatogram corresponding to Fig. 9 at 263 nm gave 22.1% PFB 18:1, 22.4% PFB 18:2 and 55.5% PFB 18:3. The two expected triacylglycerols from this fraction with seven double bonds are $(18:3)_2$-(18:1) and (18:3)-$(18:2)_2$. Table I shows the proportion of fatty acid in each triacylglycerol that this implies. It can be seen that there is excellent agreement between the proportion of PFB 18:3 measured from the chromatogram and that calculated from the triaclglycerols expected. The estimate of 66% $(18:3)_2$-(18:1) and 34% (18:3)-$(18:2)_2$ suggest that the shoulder at the rear of the peak containing seven double bonds (Fig. 8) is due to a slight separation between these two triacylglycerols, (18:3)-$(18:2)_2$ being eluted after $(18:3)_2$-(18:1). A similar calculation from the results for the commercial linseed oil gave 72% $(18:3)_2$-(18:1) and 29% (18:3)-$(18:2)_2$, while Hilditch and Williams[16] gave a figure of approximately 83% $(18:3)_2$-(18:1) for these two triacylglycerols from linseed oil.

The fraction containing eight double bonds from the flax seed extract would, of course, be expected to contain 67% PFB 18:3 and 33% PFB 18:2. Integration of

TABLE I

Triacylglycerol	*Constituent fatty acids (%)*			
	18:3	*18:2*	*18:1*	*Total*
$(18:3)_2$-(18:1)	44.2	–	22.1	66.3
(18:3)-$(18:2)_2$	11.2	22.4	–	33.6
Total	55.4	22.4	22.1	

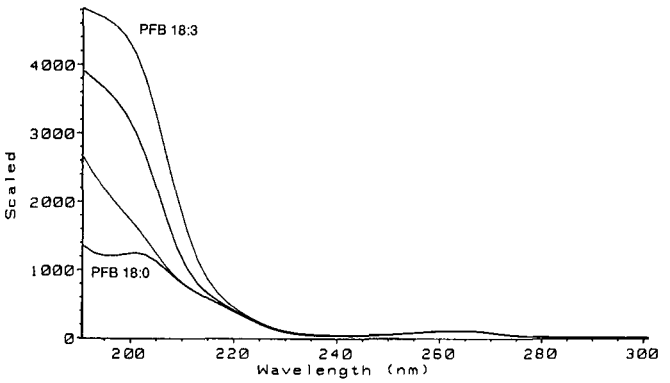

Fig. 10. Ultraviolet spectra of the PFB estes of 18:0, 18:1, 18:2 and 18:3. All spectra normalised to 100 mAU at 263 nm showing effect of double bonds on extinction in far UV.

the chromatogram at 263 nm gave 62% PFB 18:2 and 38% PFB 18:2, indicating that a UV absorbing contaminant was present in PFB 18:2 and this was confirmed by a spectral analysis of this peak. The contaminant, however, did not give a response in NICI. Integration of the chromatogram at 200 nm, followed by correction for the absorbance of the double bonds using the data given below, gives 33.5% PFB 18:2 and 66.5% PFB 18:3. Similar results were obtained for the commercial linseed oil sample.

The fraction containing nine double bonds, from both the flax seed extracts and the commercial linseed oil sample, as well as giving large peaks of PFB 18:3, gave small peaks corresponding in t_R to PFB 18:1 and PFB 18:2. These, however, did not have spectra that corresponded to PFB esters and did not give a response in NICI. The latter of these two peaks presumably corresponded to that interfering with PFB 18:2 in the fraction containing eight double bonds.

Fig. 10 gives the UV spectra, in 0.18% acetonitrile in hexane, of PFB 18:0, PFB 18:1, PFB 18:2 and PFB 18:3 all normalised to 100 mAU at 263 nm. It can be seen that operation in the low UV range markedly increases the sensitivity. Thus at 200 nm the sensitivities are increased approximately 12.2×, 17.4×, 31.8× and 42.8× for PFB 18:0, PFB 18:1, PFB 18:2 and PFB 18:3 respectively. Thus for applications that require high sensitivity this new solvent system offers considerable advantages over that containing dichloromethane described previously[12,13].

In our earlier publication[12] we sought to explain the separation of the fatty acid PFB esters according to the number of double bonds that they contain by reference to Scott's[17] model of the silica surface. That is, under the conditions used[12], the silica surface is covered by a bilayer of water surmounted by a monolayer of dichloromethane. Separation was due to competition between the double bonds in the PFB esters and the dichloromethane molecules for the aqueous surface and the small separation on chainlength was due to the inductive effect reducing the polarity of the carbonyl group. Since the properties of the separations reported here are exactly analagous, we believe that the same physico-chemical principals underlie them and that, therefore, in this system the surface of the silica is covered in a bilayer of water and the separation depends primarily on competition between the double bonds and acetonitrile molecules.

Finally, it seems to us that the separation system described here is ideally suited for the LC–MS of triacylglycerols and would be complementary to the systems reviewed by Kuksis and co-workers[18,19] utilising GC–MS and reversed-phase LC–MS that both separate primarily on chainlength.

ACKNOWLEDGEMENTS

We thank Professor B. V. Milborrow for critical discussions and the provision of laboratory facilities, Mr. R. Lidgard for the mass spectra and the Ramaciotti Foundations of Sydney for the NICI facility and the HP Series 300 computer and accessories.

REFERENCES

1 J. A. Bezard and M. A. Ouedraogo, *J. Chromatogr.*, 196 (1980) 279.
2 B. G. Herslof, *J. High Resolut. Chromatogr. Chromatogr. Commun.*, 4 (1981) 471.
3 B. Petersson, O. Podlaha and B. Toregard, *J. Am. Oil Chem. Soc.*, 58 (1981) 1005.
4 J.-P. Goiffon, C. Reminiac and M. Olle, *Rev. Fr. Corps Gras*, 28 (1981) 167.
5 R. D. Plattner, *J. Am. Oil Chem. Soc.*, 58 (1981) 638.
6 A. H. El-Hamdy and E. G. Perkins, *J. Am. Oil Chem. Soc.*, 58 (1981) 49.
7 A. H. El-Hamdy and E. G. Perkins, *J. Am. Oil Chem. Soc.*, 58 (1981) 867.
8 L. Marai, J. J. Myher and A. Kuksis, *Can. J. Biochem. Cell Biol.*, 61 (1983) 840.
9 F. C. Phillips, W. L. Erdahl, J. D. Nadenicek, L. J. Nutter, J. A. Schmit and O. S. Privett, *Lipids*, 19 (1984) 142.
10 E. C. Smith, A. D. Jones and E. W. Hammond, *J. Chromatogr.*, 188 (1980) 205.
11 B. Petersson, *J. Chromatogr.*, 242 (1982) 313.
12 A. G. Netting and A. M. Duffield, *J. Chromatogr.*, 336 (1984) 115.
13 A. G. Netting, *J. Am. Oil Chem. Soc.*, 63 (1986) 1197.
14 P. E. Martyn, D. Smith and J. B. Adams, *Cell. Mol. Endocrinol.*, in press.
15 A. G. Netting and A. M. Duffield, *Biomed. mass Spectrom.*, 12 (1985) 668.
16 T. P. Hilditch and P. N. Williams, *The Chemical Constitution of Natural Fats*, Chapman and Hall, London, 4th ed., 1964.
17 R. P. W. Scott, *J. Chromatogr. Sci.*, 18 (1980) 297.
18 A. Kuksis, L. Marai and J. J. Myher, *J. Chromatogr.*, 273 (1983) 43.
19 A. Kuksis and J. J. Myher, *J. Chromatogr.*, 379, (1986) 57.

Journal of Chromatography, 448 (1988) 145–156
Elsevier Science Publishers B.V., Amsterdam — Printed in The Netherlands

CHROM. 20 584

CHICK 28 000 M_r VITAMIN D-DEPENDENT CALCIUM-BINDING PROTEIN IN INTESTINE, KIDNEY AND CEREBELLUM

PURIFICATION USING CHROMATOFOCUSING

TOSHIO OKANO*
Department of Hygienic Sciences, Kobe Women's College of Pharmacy, Higashinada-ku, Kobe 658 (Japan)
and
D. ERIC M. LAWSON
AFRC Institute of Animal Physiology and Genetics Research, Babraham, Cambridge CB2 4AT (U.K.)
(First received February 1st, 1988; revised manuscript received March 28th, 1988)

SUMMARY

A purification method has been developed for chick 28 000 M_r vitamin D-dependent calcium-binding protein, involving Blue Sepharose CL-6B column chromatography, heat treatment and chromatofocusing with a microparticulate anion exchanger (Mono P). It allowed the rapid and reproducible purification of milligram amounts of homogeneous calcium-binding protein with good yields from chick intestine, kidney and cerebellum. The calcium-binding proteins thus obtained have the same molecular weight of 28 000, heat stability, calcium binding capability and apparent isoelectric point of 4.0. These physico-chemical properties are in good agreement with those of proteins isolated by a previous procedure, which gave a low and variable yield of calcium-binding protein.

INTRODUCTION

Since a vitamin D-dependent calcium-binding protein (CaBP) was first shown to be present in chick duodenal mucosa[1], its possible function related to vitamin D-dependent calcium absorption has been extensively studied. However, its exact molecular action is still under discussion. Currently available evidence, in particular its high affinity specifically for calcium[2] and the dependence of the synthesis of its mRNA on vitamin D[3,4], suggest that this protein is involved in the molecular mechanism of intestinal calcium absorption. On the other hand, some investigators have suggested that CaBP is not involved directly in the initial calcium uptake process[5] and may act simply as a calcium buffering component[6–8]. This suggestion is supported by the presence of CaBP in tissues without a high calcium transporting capacity such as brain, pancreas, adrenals and retina of both birds[9] and mammals[10]. These problems are compounded by the observation that CaBP is apparently not vitamin D dependent at all these sites, having been identified and assayed merely on the basis of its

0021-9673/88/$03.50

immunological similarity to intestinal CaBP[9–11]. Clearly, more studies are needed at both the physiological and biochemical levels, not only on the chick intestinal CaBP but also on the CaBP-like activity found in the various tissues. Also, most of the physico-chemical properties of CaBP recorded so far have been made on the smaller mammalian CaBP (M_r = 10 000). Consequently, we wished to purify CaBP from several tissues but found that existing procedures[12–15] were not suitable for this purpose because of their poor recoveries and variabilities.

We have developed a new purification method for isolating CaBP using Blue Sepharose CL-6B and chromatofocusing. The proteins that we obtained from chick intestine, kidney and cerebellum with the use of this method showed an apparent homogeneity on sodium dodecyl sulphate polyacrylamide gel electrophoresis (SDS-PAGE) and high-performance liquid chromatography (HPLC) using a micro-particulate anion exchanger (Mono Q) with and without Ca^{2+} in the solvent. The usefulness of the proposed method was also compared with that of the existing method, which is mainly based on the intrinsic charge difference in the molecule of CaBP with and without bound Ca^{2+}.

EXPERIMENTAL

Materials

Crystalline vitamin D_3 was obtained from Sigma (London, U.K.). Blue Sepharose CL-6B and Sephadex G-100 were purchased from Pharmacia (Uppsala, Sweden). Both prepacked columns for HPLC, a Mono P column for chromatofocusing and a Mono Q column for ion-exchange chromatography were also obtained from Pharmacia. The enzyme inhibitors TPCK (N-tosyl-L-phenylalanine chloromethylketone), TLCK (N-tosyl-L-lysine chloromethylketone) and PMSF (phenylmethylsulphonyl fluoride) were supplied by Boehringer (Mannheim, F.R.G.). Rabbit antiserum to chick intestinal CaBP prepared previously by Spencer *et al.*[16] in our laboratory was used in this study. Protein molecular weight markers (Dalton Mark VII-L; Sigma) contained bovine serum albumin (66 000), ovalbumin (45 000), glyceraldehyde-3-phosphate dehydrogenase (36 000), carbonic anhydrase (29 000), trypsinogen (24 000), trypsin inhibitor (20 100) and α-lactalbumin (14 200). All other chemicals were of analytical-reagent grade.

Animals

One-day-old white leghorn chicks were housed in electrically heated tier brooders in an air-conditioned room from which sunlight was excluded. They were fed *ad libitum* on a vitamin D-deficient diet for 3–4 weeks[17] until they were assessed to be in a state of vitamin D deficiency by histological examination of the bones. Chicks recieved orally 12.5 μg of vitamin D in 0.2 ml of ethanol–2-propanol (1:1, v/v) and were killed after 72 h, when the production of CaBP in duodena had reached its maximum.

Preparation of tissue extracts

Duodena were split open lengthwise, rinsed with ice-cold Tris buffer A (13.7 m*M* Tris base, 150 m*M* sodium chloride, 5 m*M* potassium chloride, 1 m*M* 2-mercaptoethanol, pH adjusted to 7.4 with hydrochloric acid) and the mucosa scraped from underlaying serosal layers with a glass slide on ice, and then stored at −20°C before

extraction. Kidney and cerebellum were cut into small pieces with scissors and homogenized in an equal volume of ice-cold Tris buffer with a Polytron homogenizer for 30 s. The homogenates were then centrifuged at 100 000 *g* for 1 h at 4°C. The supernatant solutions were decanted and filtered through a glass filter (80–100 mesh) to eliminate membraneous fat-soluble materials floating on the surface of the supernatant solution and stored at −20°C.

Purification of CaBP

CaBP from chick intestine, kidney and cerebellum was purified by the following two procedures, one of which was a modification of that originally described by Hitchman and Harrison[12] (existing method), and the other our proposed method. All further steps were carried out at 4°C unless stated otherwise and the three tissues were treated in the same manner throughout. Unless indicated otherwise, all recoveries of CaBP were determined by rocket electroimmunoassay (see below).

Existing method. Approximately 20 ml of the supernatant solution were applied to an upward-flow column of Sephadex G-100 (90 × 2.5 cm I.D.) equilibrated with Tris buffer and eluted with the same buffer. The flow-rate was 40 ml/h, 4.5-ml fractions were collected and the CaBP concentration in every other tube was determined. Fractions containing CaBP were pooled and concentrated to a small volume using an Amicon stirred cell using an Amicon UM2 membrane filter under nitrogen pressure (40 kg/cm^2). Proteins recovered from the concentrator were placed in Visking tubing and dialysed against 500 ml of imidazole buffer (20 m*M* imidazole, 20 m*M* sodium chloride, 1 m*M* EDTA, 1 m*M* 2-mercaptoethanol, pH adjusted to 7.0 with hydrochloric acid) for 16 h. The dialysate was then centrifuged at 100 000 *g* in a refrigerated centrifuge for 30 min and the supernatant solution was applied to a DEAE-Sephacel column (30 × 1.5 cm I.D.) equilibrated with imidazole buffer. The column was washed with the same buffer until the eluate was free from protein, as determined by the ultraviolet absorbance (280 nm), and eluted with a 500-ml sodium chloride gradient from 20 to 700 m*M* in imidazole buffer. The flow-rate was 15 ml/h and 4.5-ml fractions were collected. All fractions were assayed for CaBP, which was detected as a single peak on the chromatogram in twelve fractions containing 280 m*M* sodium chloride as measured using a conductivity meter. These fractions were pooled and dialysed against 1000 ml of imidazole buffer containing 20 m*M* sodium chloride and 2 m*M* calcium chloride for 16 h. The dialysate was subsequently applied to another DEAE-Sephacel column (30 × 1.5 cm I.D.) equilibrated with the same buffer as used for dialysis. Development of this column proceeded as described for the preceding column except that 2 m*M* calcium chloride was added in imidazole buffer instead of EDTA. All fractions were assayed for CaBP, which was detected as a clear single peak on the chromatogram.

Proposed method. The supernatant was applied directly to a Blue Sepharose CL-6B column (40 × 1.5 cm I.D.) equilibrated with Tris buffer (13.7 mM Tris base, 20 m*M* sodium chloride, 5 m*M* potassium chloride, 1 m*M* 2-mercaptoethanol, pH adjusted to 7.4 with hydrochloric acid). Column elution was carried out in the downward direction at a flow-rate of 17 ml/h and 4.5-ml fractions were collected. All fractions containing CaBP were pooled, heated at 60°C for 20 min and immediately chilled to 4°C. After centrifugation at 100 000 *g* for 1 h at 4°C, proteins not precipitated from the pooled solution by heat treatment were recovered as the supernatant solution and placed in Visking tubing and dialysed against 500 ml of buffer B (20 m*M* N-methylpiperazine, 1

m*M* 2-mercaptoethanol, pH adjusted to 5.7 with hydrochloric acid) for 6 h with stirring. The dialysate was subsequently applied without concentration to a Mono P column for chromatofocusing.

The system used was a Waters Assoc. ALC/GPC Model 6000 liquid chromatograph equipped with an automated gradient controller, a U6K sample injector and a Model 441 variable-wavelength detector. Milli-Q water (Millipore, Bedford, MA, U.S.A.) with a measured resistance of 18 MΩ or less was used exclusively. The Mono P column was equilibrated with buffer B until the effluent showed the same pH value as this buffer. The sample solution, ranging from 2 to 8 ml in volume and containing up to 20 mg of protein, was applied to the column and washed with buffer B until the eluate was free from proteins, as determined by the ultraviolet absorbance (280 nm). Elution was carried out with Polybuffer 74 (pH 3.7) with a linear pH gradient from 5.7 to 3.7 at a constant flow-rate of 1 ml/min at room temperature. Fractions of 1 ml were collected and assayed for CaBP by rocket electroimmunoassay.

For complete purification, CaBP obtained from the first chromatofocusing was rechromatographed on the same column under the same conditions as those of the first chromatofocusing. The purified CaBP thus obtained was finally applied to a Sephadex G-100 column (90 × 1.5 cm I.D.) and eluted with Tris buffer A containing 2 m*M* calcium chloride to be preserved in the presence of Ca^{2+}, and also to remove unknown component(s) of Polybuffer 74 which show a positive interference in the measurement of protein by the method of Lowry *et al.*[18], although they do not affect the stability of CaBP on prolonged storage at −20°C.

Rocket electroimmunoassay for CaBP

This was carried out by a modification of that originally described by Laurell[19]. Chick intestinal CaBP antiserum was dissolved in 1% agarose (Koch-Light, Colnbrook, U.K.) in pH 8.6, 0.087 *M* barbital buffer at a final concentration of 0.1% at 55°C, and then transferred on to a glass plate to make a 1 × 100 × 200 mm slab of agarose containing antiserum. After standing for 30 min at room temperature to solidify, nineteen sample wells (2 mm) were made and 5 μl of the sample solutions were placed in each well. Electrophoresis at a constant voltage of 40 V per 10 cm was carried out for 6 h at room temperature. The electrode buffer was the same as used for the preparation of the agarose gel. After immunoelectrophoresis, the plate was dried and stained for protein with 0.05% Coomassie Brilliant Blue G. When the heights of the precipitin rockets were plotted against pure CaBP concentrations, a linear calibration graph was obtained over the range of 20–400 ng per 5 μl of sample solution.

SDS-PAGE

Approximately 20 μg of the purified CaBP from intestine, kidney and cerebellum were dissolved in a solution containing dithiothreitol (15 mg/ml), SDS (10 mg/ml) and Tris base (12 mg/ml) and heated at 70°C for 30 min for complete reduction to subunits. The electrophoresis was carried out at 3 mA per gel[20]. Staining of the gel was carried out at 70°C for 1 h in 0.05% Coomassie Brilliant Blue G in acetic acid–2-propanol–water (2:5:13, v/v). Destaining was carried out at 70°C for 15 min in the same solvent without Coomassie Brilliant Blue G and then the gel was left in 10% acetic acid at 30°C until destained. The identification of CaBP in the gel was also performed by the following immunological procedure.

After electrophoresis, the gel was immediately frozen using dry-ice and 1-mm slices of the gel were prepared using a Macrotome GTS (Yeda Research and Development). Each slice was placed on the same agarose gel plate containing antiserum as used in the rocket electroimmunoassay for CaBP and diffusion allowed to proceed in a humid atmosphere at room temperature. After diffusion for 24 h, the plate was dried, stained and destained and the diameter of the precipitin rings were measured.

Ion-exchange chromatography using HPLC

The same HPLC apparatus and equipment as used for chromatofocusing were employed in this experiment. Separation of CaBP was performed on a Mono Q column under the following conditions. Elution of proteins was carried out in a linear gradient of sodium chloride from 50 to 700 m*M* in piperazine buffer (25 m*M* piperazine, pH adjusted to 6.5 with hydrochloric acid) in the presence or absence of 2 m*M* calcium chloride at a constant flow-rate of 1 ml/min with the column pressure varying from 350 to 500 p.s.i.

Other method

Protein was determined by the method of Lowry *et al.*[18] with bovine serum albumin as a standard.

RESULTS

Chick 28 000 M_r CaBP was isolated from intestine, kidney and cerebellar homogenates by the procedure introduced by Hitchman and Harrison[12] in which the proteins in the homogenates were fractionated by a series of chromatographic steps: gel filtration chromatography and DEAE-Sephacel chromatography without and with Ca^{2+} as shown in Fig. 1 (Fig. 1Aa–c for intestine, Fig. 1Ba–c for kidney, Fig. 1Ca–c for cerebellum). After completion of the final chromatographic step, the protein purified from each tissue was subjected to SDS-PAGE to establish its homogeneity. As illustrated in Fig. 2, all proteins had one major and one faint minor band having the respective identical electrophoretic migration rates among tissues (as measured by electrophoresing the proteins in sets of two proteins on a single gel). The protein corresponding to the major band was apparently the native molecule of CaBP on the basis of its molecular weight (28 000), an intrinsic charge difference in the presence and absence of Ca^{2+} and immunoreactivity against CaBP antiserum. On the other hand, the protein corresponding to the minor band was thought to be a degradation, fragment of CaBP as it still had immunoreactivity against CaBP antiserum (as measured by immunodiffusion in 1% agarose gel plate containing anti-CaBP antiserum), but this protein has not been characterized. The overall recoveries of CaBP, as assayed by rocket electroimmunoassay, were from chick intestine 7–35%, kidney 11–32% and cerebellum 12–27%. These values are slightly lower than those reported by Hitchman and Harrison[12] and more variable.

The results of Blue Sepharose CL-6B chromatography used as the first step of our proposed method are shown in Fig. 3. Blue Sepharose CL-6B, having a wide range of binding affinity to a large number of serum proteins and enzymes, showed no interaction with CaBP and, of the total CaBP applied to the column, at least 80% was

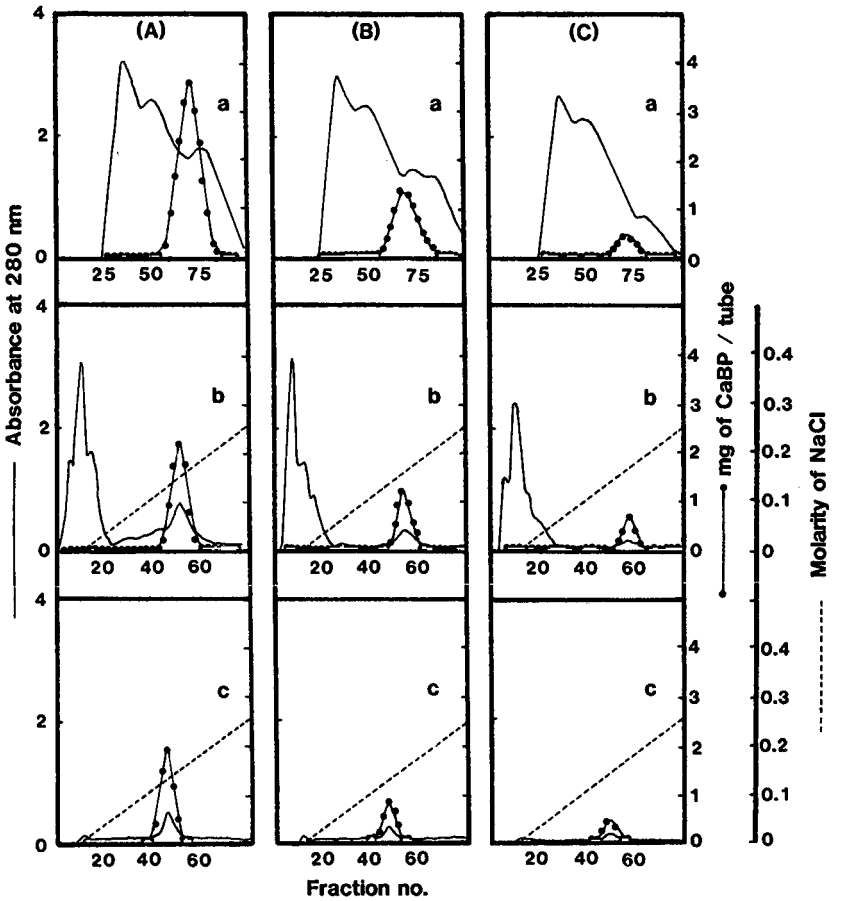

Fig. 1. Chromatograms for the purification of CaBPs from chick (A) intestine, (B) kidney and (C) cerebellum by successive gel filtration and DEAE-Sephacel chromatography in the absence or presence of calcium chloride. (a) Gel filtration on Sephadex G-100; (b) DEAE-Sephacel chromatography in the absence of calcium chloride; (c) DEAE-Sephacel chromatography in the presence of calcium chloride.

recovered. Further, this step provided a useful separation of CaBP from high-molecular-weight lipoproteins, peptides and salt. SDS-PAGE of the CaBP fraction also indicated that large amounts of proteins, including albumins and globulins, were effectively trapped in the column and thereby removed from the original homogenate.

Subsequently, heat treatment of the pooled CaBP solution at 60°C for 20 min was carried out with addition of 1 m*M* dithiothreitol to prevent the polymerization of CaBP. Approximately 30% of non-CaBP proteins in the original solution were denatured and precipitated after heat treatment and centrifugation without significant loss of CaBP. Heat treatment was therefore useful in removing the heat-labile non-CaBP proteins from the solution because CaBP is stable up to 70°C[21]. In addition, CaBP in the heat-treated solution was found to be relatively stable on prolonged storage at 4°C and at −20°C, although we have no evidence that the stability of CaBP attendant on heat treatment is due to the denaturation of protease(s) specific for CaBP.

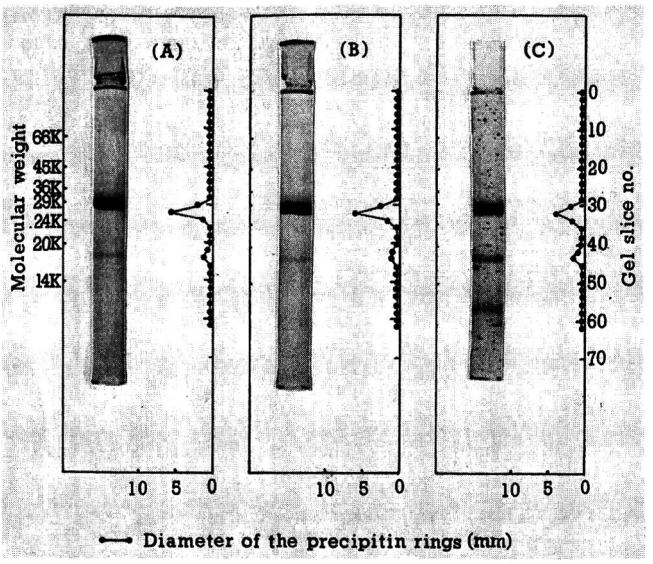

Fig. 2. SDS-PAGE of purified CaBPs isolated from chick (A) intestine, (B) kidney and (C) cerebellum by successive gel filtration and DEAE-Sephacel chromatography in the absence or presence of calcium chloride. Approximate 25 μg of protein were applied to each gel, electrophoresed and identified by staining and immunodiffusion as described under Experimental.

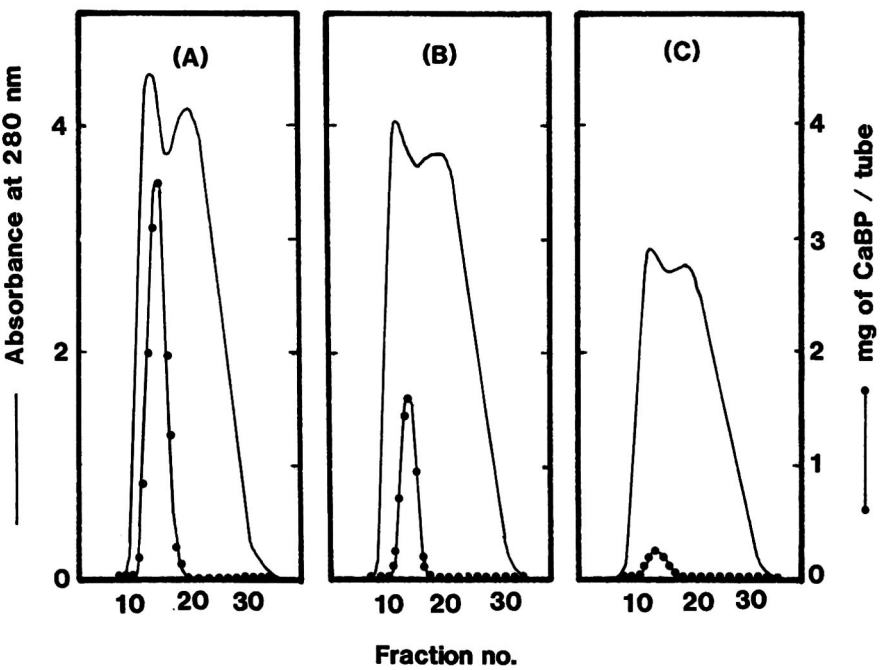

Fig. 3. Chromatography of chick (A) intestine, (B) kidney and (C) cerebellar homogenates on Blue Sepharose CL-6B.

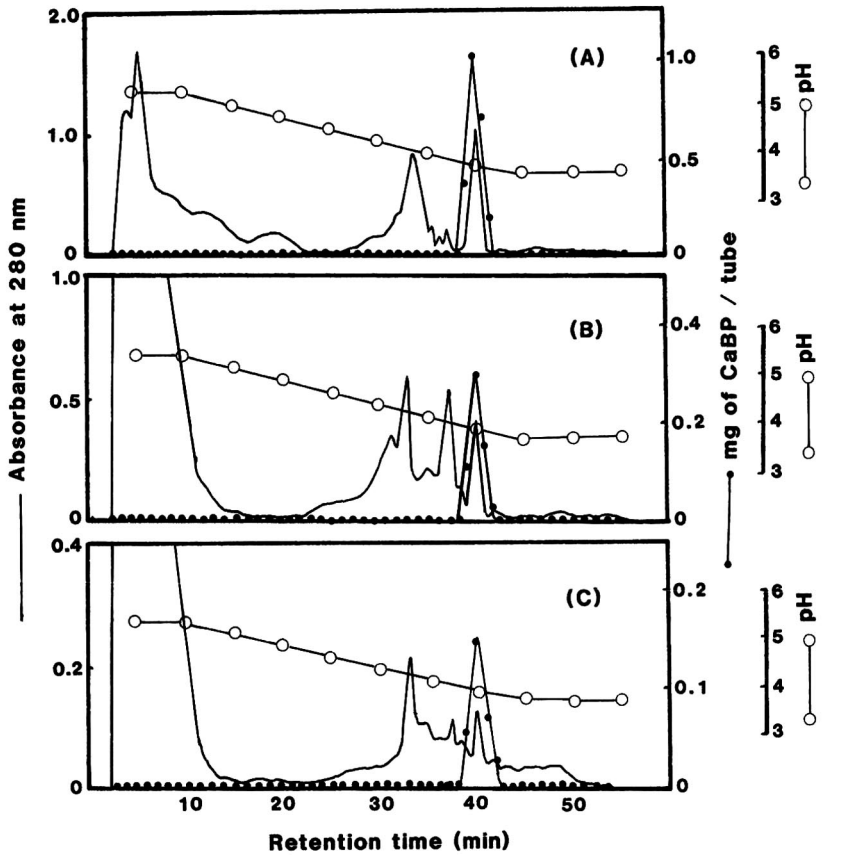

Fig. 4. Purification of chick (A) intestinal, (B) kidney and (C) cerebellar CaBPs by chromatofocusing. The Blue Sepharose CL-6B CaBP eluate was heated at 60°C for 20 min, centrifuged, then dialysed against 20 m*M* N-methylpiperazine (pH 5.7) and 2–8 ml were injected into a Mono P column.

The combination of Blue Sepharose CL-6B and heat treatment is a useful procedure for partially purifying CaBP, as there is a substantial decrease in the amount of protein to be applied to the chromatofocusing column. We also found that heat treatment was more effective than addition of protease inhibitors such as TLCK, TPCK and PMSF, particularly with intestine samples, to improve the stability of CaBP.

The characteristic separation of CaBP from other proteins in the heat-treated solutions from the three tissues by chromatofocusing on a Mono P column is shown in Fig. 4. The peak for CaBP was identified from the retention time (apparent pH value) by comparison with a standard intestinal CaBP and recoveries of CaBP from the column were determined by rocket electroimmunoassay. Chromatofocusing with a linear pH gradient from 5.7 to 3.7 was reproducible and provided a good separation without any detectable cross-contamination from other proteins in a given peak on the chromatogram (Fig. 5). As little as 10 μg of CaBP (as the pure protein) could be

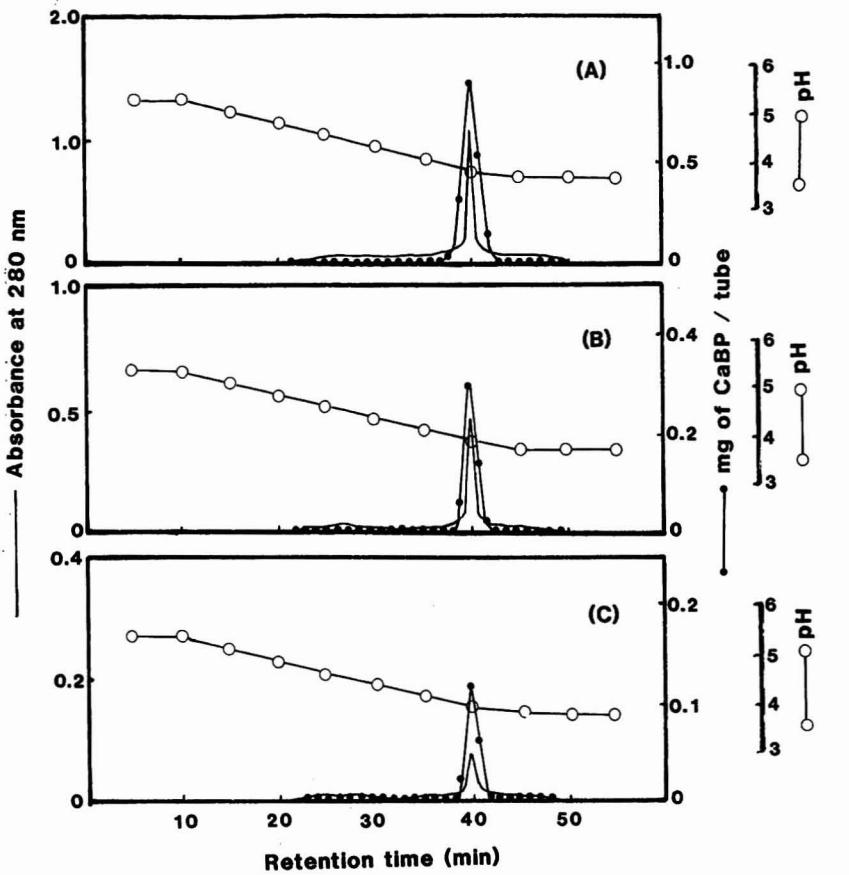

Fig. 5. Rechromatofocusing of chick (A) intestinal, (B) kidney and (C) cerebellar CaBPs obtained from the first chromatofocusing. The first chromatofocusing CaBP fraction was restored to pH 5.7 by passage through a Sephadex G-75 column (50 × 1.5 cm I.D.) equilibrated with 20 m*M* N-methylpiperazine buffer (pH 5.7), then applied to a Mono P column under the same conditions as before.

detected. The protein gave nearly a single band in SDS-PAGE (Fig. 6) and a single peak in anion-exchange chromatography (Mono Q) with and without Ca^{2+} (Fig. 7). Gel filtration chromatography calibrated with seven standard proteins showed that the CaBPs from chick intestine, kidney and cerebellum have the same molecular weight of 28 000. With this overall method, the recoveries of CaBP were from chick intestine 40–55%, from kidney 30–45% and from cerebellar homogenates 46–57%, as shown in Table I.

DISCUSSION

Recent developments in research into vitamin D-dependent CaBP have shown that this protein exists in two forms differing in their molecular weights (28 000 and 10 000)[1,22–24]. Current procedures[12–15] employed for the separation and purification of these proteins involve the use of gel filtration chromatography, ion-exchange

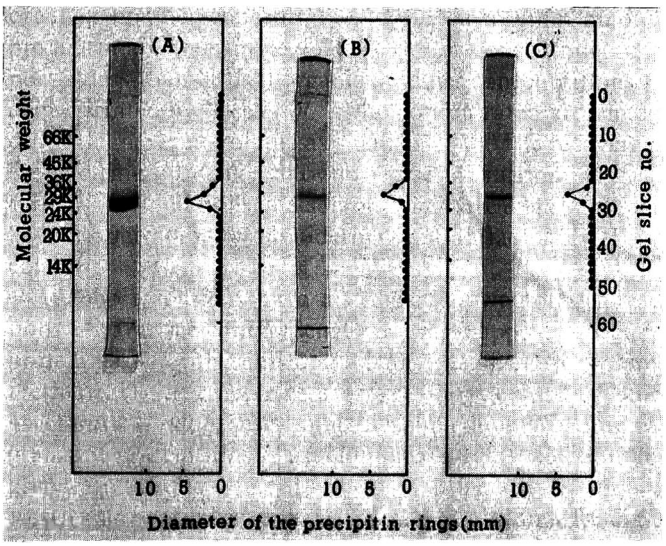

Fig. 6. SDS-PAGE of purified CaBPs isolated from chick (A) intestine, (B) kidney and (C) cerebellum by successive Blue Sepharose CL-6B chromatography, heat treatment and chromatofocusing. Approximately 20 μg of protein were applied to each gel, electrophoresed and identified by staining and immunodiffusion as described under Experimental.

chromatography and preparative discontinuous polyacrylamide gel electrophoresis. Ion-exchange column chromatography, introduced by Hitchman and Harrison[12], which takes advantage of an intrinsic charge difference in the molecule of CaBP with and without bound Ca^{2+}, has been widely accepted for the purification of either 28 000 or 10 000 M_r CaBP. As shown in Fig. 1, the combination of gel filtration chromatography and ion-exchange chromatography with and without Ca^{2+} is useful for purifying CaBP from chick intestine, kidney and cerebellum. However, we have found that this technique required several days for completion and also it had poor reproducibility and low yield. The recovery of the protein varied from 7 to 35% with chick intestine. This method is only effective when large amounts of proteins are available for purification. Therefore, brain and other tissues, having relatively small amounts of CaBP, need another effective purification procedure.

TABLE I

PREPARATION OF CaBPs FROM CHICK INTESTINE, KIDNEY AND CEREBELLUM

Step	*Yield of CaBP (mg)*		
	Intestine	*Kidney*	*Cerebellum*
Original supernatant	12.7	4.7	1.5
Blue Sepharose CL-6B	9.5–12.3	3.4–4.1	1.2–1.3
Heat treatment	7.7–9.2	2.3–2.7	1.1–1.2
1st chromatofocusing	6.4–7.7	1.7–2.1	0.8–1.0
2nd chromatofousing	5.1–7.0	1.4–2.1	0.7–0.9
Recovery (%)	40–55	30–45	46–57

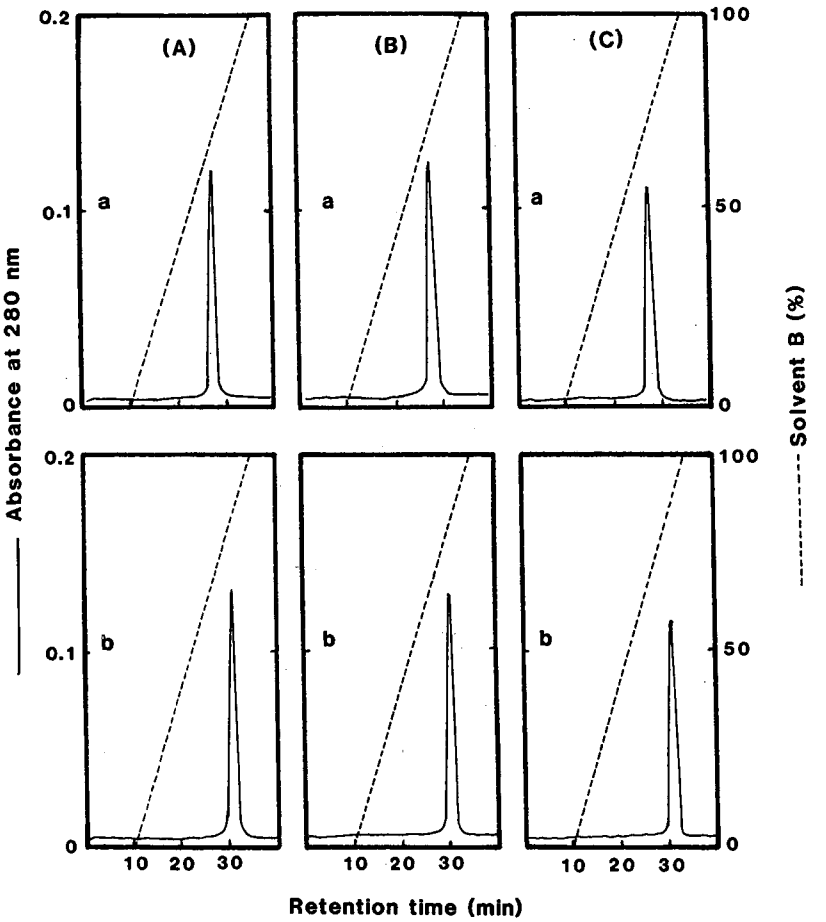

Fig. 7. Ion-exchange HPLC behaviour of (A) intestinal, (B) kidney and (C) cerebellar CaBPs in (a) the presence or (b) the absence of calcium chloride. Elution of proteins was carried out in a linear gradient of sodium chloride from 50 m*M* (solvent A) to 700 m*M* (solvent B) in piperazine buffer (25 m*M* piperazine, pH adjusted to 6.5 with hydrochloric acid) in the presence or absence of 2 m*M* calcium chloride at a constant flow-rate of 1 ml/min.

Our purpose in this study was to establish a simple purification method for CaBP that can be performed with good resolution and reproducibility, and involving minimal manipulation with routine apparatus. We used a combination of three purification: Blue Sepharose CL-6B chromatography, heat treatment and chromatofocusing. As the retention time (apparent pH value) of CaBP on the chromatofocusing trace was highly reproducible, it may be possible in future work to isolate CaBP from relatively crude extracts if care is taken to prevent proteolysis, *e.g.*, by heat treatment.

ACKNOWLEDGEMENTS

We thank Mrs. M. Harding and Mr. P. W. Wilson for the supply of chick CaBP antiserum and their thoughtful discussion and expert advice.

REFERENCES

1 R. H. Wasserman and A. N. Taylor, *Science (Washington, D.C.)*, 152 (1966) 791–793.
2 R. H. Wasserman, R. A. Corradino and A. N. Taylor, *J. Biol. Chem.*, 243 (1968) 3978–3986.
3 R. Spencer, M. Charman, J. S. Emtage and D. E. M. Lawson, *Eur. J. Biochem.*, 71 (1976) 399–409.
4 R. Spencer, M. Charman and D. E. M. Lawson, *Biochem. J.*, 175 (1978) 1089–1094.
5 R. Spencer, M. Charman, P. W. Wilson and D. E. M. Lawson, *Nature (London)*, 263 (1976) 161–163.
6 J. Harmeyer and H. F. Deluca, *Arch. Biochem. Biophys.*, 133 (1969) 247–254.
7 M. Thomasset, C. O. Parkes and P. Cuisiner-Gleizes, *Am. J. Physiol.*, 243 (1982) E483–E488.
8 S. Christakos, E. J. Friedlander, B. R. Frandsen and A. W. Norman, *Endocrinology*, 104 (1979) 1495–1503.
9 A. N. Taylor, *Arch. Biochem. Biophys.*, 161 (1974) 100–108.
10 A. N. Taylor, *Nutrition*, 107 (1977) 480–486.
11 K. G. Baimbridge, J. J. Miller and C. O. Parkes, *Brain Res.*, 239 (1982) 519–525.
12 A. J. W. Hitchman and J. E. Harrison, *Can. J. Biol. Chem.*, 50 (1972) 758–765.
13 E. J. Friedlander and A. W. Norman, in A.W. Norman, K. Schafer, J. W. Coburn, H. F. Deluca, D. Fraser, H. H. Grigoleit and D. Herrath (Editors), *Vitamin D: Biochemical, Chemical and Clinical Aspects Related to Calcium Metabolism*, Walter De Gruyter, New York, 1977, pp. 241–243.
14 C. W. Bishop, N. C. Kendrick and H. F. Deluca, *J. Biol. Chem.*, 258 (1983) 1305–1310.
15 C. S. Fullmer and R. H. Wasserman, *Biochim. Biophys. Acta*, 393 (1975) 134–142.
16 R. Spencer, R. Charman, P. W. Wilson and D. E. M. Lawson, *Biochem. J.*, 170 (1978) 93–101.
17 D. E. M. Lawson and P. W. Wilson, *Biochem. J.*, 144 (1974) 573–583.
18 O. H. Lowry, N. J. Rosebrough, A. L. Farr and R. J. Randall, *J. Biol. Chem.*, 193 (1951) 265–275.
19 C. B. Laurell, *Scand. J. Clin. Lab. Invest.*, 29, Suppl.124 (1972) 1687–1693.
20 K. Weber and M. Osborn, *J. Biol. Chem.*, 244 (1969) 4406–4412.
21 P. B. Bredderman and R. H. Wasserman, *Biochemistry*, 13 (1974) 1687–1693.
22 C. S. Fullmer and R. H. Wasserman, *Biochim. Biophys. Acta*, 317 (1973) 172–186.
23 A. J. W. Hitchman, M. K. Kerr and J. E. Harrison, *Arch. Biochem. Biophys.*, 155 (1973) 221–227.
24 M. E. H. Bruns, E. Fliesher and L. V. Avioli, *J. Biol. Chem.*, 252 (1977) 4145–4150.

Journal of Chromatography, 448 (1988) 157–164
Elsevier Science Publishers B.V., Amsterdam — Printed in The Netherlands

CHROM. 20 620

MICRO HIGH-PERFORMANCE LIQUID CHROMATOGRAPHIC DETERMINATION OF CARDIAC GLYCOSIDES IN β-METHYLDIGOXIN AND DIGOXIN TABLETS

YOUICHI FUJII*, YUKARI IKEDA and MITSURU YAMAZAKI
School of Pharmacy, Hokuriku University, 3 Ho, Kanagawa-machi, Kanazawa 920-11 (Japan)
(Received April 29th, 1988)

SUMMARY

A micro high-performance liquid chromatographic (micro-HPLC) method has been developed for the assay of β-methyldigoxin and digoxin tablets. Quantitation of cardiac glycosides in tablets was carried out by the incorporation of dexamethasone as an internal standard. The procedure consisted of disintegration of tablets, extraction with acetone–ethanol (9:1) and injection for micro-HPLC on an ODS micro column, using acetonitrile–water (28:72) for β-methyldigoxin tablets and methanol–water (1:1) for digoxin tablets; the effluent was monitored by UV detection at 220 nm. The average values of the contents in β-methyldigoxin and digoxin tablets were 99.6 and 100.2% of the labelled amounts, respectively. The proposed method is sufficiently precise and sensitive to examine the content uniformity of tablets.

INTRODUCTION

β-Methyldigoxin and digoxin are pharmaceutically important drugs for the treatment of congestive heart failure and atrial fibrillation. β-Methyldigoxin is produced from digoxin by selective methylation of the hydroxyl group on the C-4 atom of the terminal digitoxose. These cardiac glycosides are used in low doses and there is a narrow margin between the therapeutic and toxic doses. Therefore, it is extremely important to evaluate the exact amounts of cardiac glycosides present in pharmaceutical dosage forms.

Previously published methods of determining digoxin in tablets have utilized colorimetric[1], fluorometric[2], thin-layer chromatographic[3] and gas–liquid chromatographic[4] techniques, but they did not always yield accurate quantitation of intact digoxin in tablets. High-performance liquid chromatography (HPLC) has been shown to be an effective method for the determination of digitalis glycosides in pharmaceutical preparations. Yoshino *et al.*[5] have reported the use of a MicroPak NH_2 column to separate β-methyldigoxin and its related steroids, but satisfactory resolution has not been obtained. The usefulness of a silica gel normal-phase system in the HPLC analysis of digoxin tablets has also been described[6]. The HPLC method employing a reversed-phase column has been widely used for the analysis of digoxin in tablets[7–11].

0021-9673/88/$03.50

On the other hand, Ishii *et al.*[12] have developed micro-HPLC for measuring micro-scale quantities. Previously, we reported the separation and quantitation of digitalis glycosides in *Digitalis purpurea* leaves using micro-HPLC[13,14]. The present paper describes the determination of β-methyldigoxin and digoxin tablets by means of micro-HPLC on a reversed-phase column with UV detection (220 nm) based on the butenolide ring.

EXPERIMENTAL

Instruments

The apparatus was a Familic-100 micro high-performance liquid chromatograph (Japan Spectroscopic, Tokyo, Japan) equipped with an Uvidec-100 UV spectrophotometer monitoring the absorbance at 220 nm. The micro flow-through cell consisted of a quartz tube with a volume of 0.3 μl. The micro column (95 mm × 0.5 mm I.D.) was a PTFE tube packed with SC-01 (Japan Spectroscopic). This was a reversed-phase column containing 5-μm porous silica particles linked covalently with octadecylsilyl (ODS) groups. The separations were performed under ambient conditions.

Materials

β-Methyldigoxin, dimethyldigoxin 1 and 2 were kindly donated by Yamanouchi (Tokyo, Japan). Digoxin was obtained from Aldrich (Milwaukee, WI, U.S.A.) and dexamethasone from Sigma (St. Louis, MO, U.S.A.). The structures of these cardiac steroids are given in Fig. 1. Digoxigenin, digoxigenin monodigitoxoside and bisdigitoxoside were prepared by hydrolysis of digoxin according to the procedure of Haack *et al.*[15]. All of these materials were checked for homogeneity by thin-layer chromatography (TLC), and solvents were purified by redistillation prior to use.

Sample preparation

One β-methyldigoxin 0.1-mg tablet was placed in 20-ml test-tube to which were added 0.3 ml of distilled water. After ultrasonication for 2 min in an ultrasonic cleaning bath, the suspension was extracted with 5 ml of acetone–ethanol (9:1) containing dexamethasone (0.03895 mg) as an internal standard. The mixture was further ultrasonicated for 5 min and centrifuged at 1400 *g* for 5 min. The supernatant was

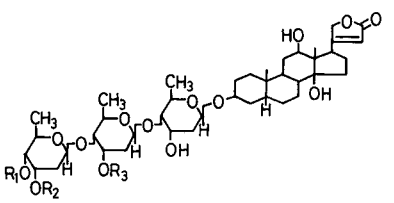

Digoxin : $R_1=R_2=R_3=H$
β-Methyldigoxin : $R_1=CH_3$, $R_2=R_3=H$
Dimethyldigoxin 1 : $R_1=R_3=CH_3$, $R_2=H$
Dimethyldigoxin 2 : $R_1=R_2=CH_3$, $R_3=H$

Fig. 1. Structures of digoxin and its methylated compounds.

transferred to a test-tube and evaporated *in vacuo*. The residue obtained was redissolved in 0.1 ml of methanol and analyzed by micro-HPLC.

The composite assay of β-methyldigoxin tablets was performed by accurately weighing an amount of the powder from ten ground tablets corresponding to 0.1 mg of β-methyldigoxin and following the procedure described above.

For the assay of a digoxin 0.25-mg tablet, one tablet was extracted with 5 ml of acetone–ethanol (9:1) containing dexamethasone (0.11826 mg) and the sample was prepared in the same manner as for the β-methyldigoxin tablet.

Chromatographic procedure

A 0.2-μl volume of each sample was injected into the liquid chromatograph and the flow-rate was adjusted to 8 μl/min. The mobile phase for each separation is listed with each chromatogram. β-Methyldigoxin and digoxin in tablets were determined by the internal standard method. Calibration curves were constructed using the average peak areas from three chromatograms.

Recovery test for β-methyldigoxin

β-Methyldigoxin (0.04235 mg) and an internal standard (0.03895 mg) were added to each β-methyldigoxin tablet, and the mixtures were then extracted with acetone–ethanol (9:1). The sample preparation and chromatographic procedure were carried out in the manner described above.

RESULTS AND DISCUSSION

An initial study was directed towards the chromatographic separation of β-methyldigoxin and related compounds. Fig. 2 depicts the chromatogram obtained

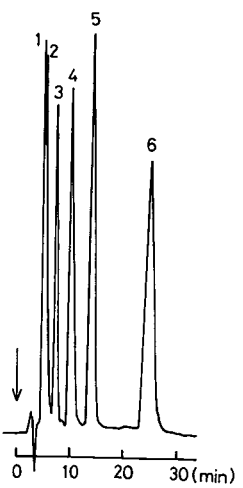

Fig. 2. Separation of a mixture of β-methyldigoxin, digoxin, their decomposition products and an internal standard. Peaks: 1 = digoxigenin; 2 = digoxigenin monodigitoxoside; 3 = digoxigenin bisdigitoxoside; 4 = digoxin; 5 = dexamethasone; 6 = β-methyldigoxin. Conditions: Jasco SC-01 column (95 mm × 0.5 mm I.D.); mobile phase, acetonitrile–water (28:72); flow-rate, 8 μl/min; UV monitor at 220 nm; sample volume, 0.2 μl.

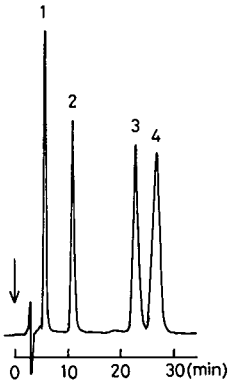

Fig. 3. Separation of a mixture of digoxin and its methylated compounds. Peaks: 1 = digoxin; 2 = β-methyldigoxin; 3 = dimethyldigoxin 1; 4 = dimethyldigoxin 2. Conditions: mobile phase, acetonitrile–water (33:67); other conditions as in Fig. 2.

from the separation of β-methyldigoxin, digoxin and their decomposition products such as digoxigenin, digoxigenin monodigitoxoside and bisdigitoxoside. For the selection of an internal standard, a variety of compounds were investigated and dexamethasone, which can be separated satisfactorily from these substances, was found to be the most suitable. Micro-HPLC was performed on an ODS bonded silica column (SC-01) using acetonitrile–water (28:72) as the mobile phase at a flow-rate of 8 μl/min. A detection wavelength of 220 nm was used, account being taken of the α,β-unsaturated lactone ring attached at C-17 of the steroid nucleus. The separation is sufficiently good and reproducible to permit quantitative work. The PTFE column size employed was much smaller than those in conventional HPLC. Also, the possibility of contamination by digoxin and dimethyldigoxins is present in the manufacture of β-methyldigoxin. Therefore, the chromatographic behaviour of these glycosides was investigated. The separation of digoxin, β-methyldigoxin, dimethyldigoxin 1 and 2 was achieved when acetonitrile–water (33:67) was used as the eluent, as shown in Fig. 3.

On the basis of these data, the determination of β-methyldigoxin in tablets was then undertaken. A β-methyldigoxin tablet was disintegrated by ultrasonication and extracted with acetone–ethanol (9:1) containing an internal standard. Fig. 4 illustrates a typical chromatogram of the extract of a β-methyldigoxin 0.1-mg tablet. The excipients present were ascertained not to interfere with the peaks due to β-methyldigoxin and dexamethasone. No peaks corresponding to the retention time of the internal standard were detected in a chromatogram of the extract in the absence of an internal standard. There was no contamination by dimethyldigoxins in the chromatogram using a mobile phase of acetonitrile–water (33:67). A linear calibration graph was obtained by plotting the peak area ratios of β-methyldigoxin to an internal standard against the amount of β-methyldigoxin (mg): $y = 18.56\,x + 0.02473$, with a correlation coefficient of 0.9996. The range of linearity extends from 0.04 to 0.16 mg. The data for the composite tablet assay are given in Table I. The mean value for the percentage of the label claim was 100.3% with a standard deviation of 0.88%. The accuracy of the assay method was examined by adding an amount of β-meth-

Fig. 4. Chromatogram of the extract of a β-methyldigoxin tablet with an internal standard. Peaks: 1 = dexamethasone; 2 = β-methyldigoxin. Conditions as in Fig. 2.

yldigoxin standard to the tablet sample. Recoveries for the eight samples ranged from 99.5 to 100.1% with a mean of 99.7% and a standard deviation of 0.23%. From the investigation of the tablet recovery *versus* the number of extraction times, the extraction procedure proposed was ascertained to be sufficient for a rapid leaching of β-methyldigoxin from the tablet matrix. These results confirmed the validity of the micro-HPLC procedure and its applicability to the quantitation of β-methyldigoxin tablets.

The determination of digoxin tablets was also undertaken. Fig. 5 shows the chromatogram of digoxin, its degradation products (digoxigenin, its mono- and bis-digitoxosides) and dexamethasone as an internal standard. These compounds were separated into five peaks using methanol–water (1:1) as the eluent. It is interesting that the elution order of digoxin and dexamethasone was reversed when acetonitrile–water was used instead of methanol–water as the mobile phase. The

TABLE I

RESULTS OF THE COMPOSITE ASSAY OF β-METHYLDIGOXIN 0.1-MG TABLETS BY THE MICRO-HPLC METHOD

Sample number	*Weight of tablet powder (mg)*	*Amount found (mg)*	*Amount calculated in terms of one tablet* (mg)*	*Percent of label claim*
1	118.651	0.10050	0.10028	100.28
2	120.424	0.10152	0.09981	99.81
3	114.166	0.09570	0.09924	99.24
4	118.496	0.10001	0.09992	99.92
5	113.402	0.09527	0.09946	99.46
6	120.134	0.10265	0.10116	101.16
7	133.180	0.11354	0.10093	100.93
8	132.008	0.11343	0.10173	101.73
Mean ± S.D.				100.3 ± 0.88

* The average weight of one tablet was 118.393 mg (n = 15).

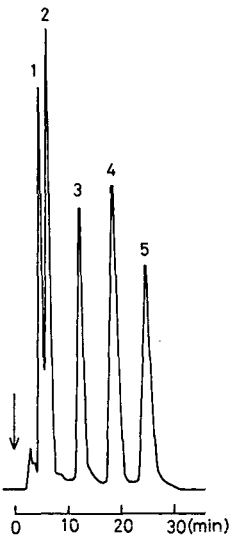

Fig. 5. Separation of a mixture of digoxin, its decomposition products and an internal standard. Peaks: 1 = digoxigenin; 2 = digoxigenin monodigitoxoside; 3 = digoxigenin bisdigitoxoside; 4 = dexamethasone; 5 = digoxin. Conditions: mobile phase, methanol–water (1:1); other conditions as in Fig. 2.

extraction procedure for digoxin tablets was similar to that described for β-methyldigoxin tablets. A representative chromatogram of the extract of a digoxin 0.25-mg tablet after addition of dexamethasone is shown in Fig. 6. The calibration graph of the peak area ratio of digoxin to dexamethasone against the weight of digoxin (mg) was linear over the range 0.1–0.4 mg, and the regression equation was $y = 6.164\,x - 0.02236$ with a correlation coefficient of 0.9997. The micro-HPLC method was satisfactory for the determination of digoxin in tablets.

This assay was applied to the study of single-tablet content uniformity of β-

Fig. 6. Chromatogram of the extract of a digoxin tablet with an internal standard. Peaks: 1 = dexamethasone; 2 = digoxin. Conditions as in Fig. 5.

TABLE II

RESULTS OF SINGLE-TABLET ASSAYS OF β-METHYLDIGOXIN AND DIGOXIN TABLETS BY THE MICRO-HPLC METHOD

Tablet number	*Percent of label claim*		*Tablet number*	*Percent of label claim*	
	*β-Methyldigoxin**	*Digoxin***		*β-Methyldigoxin**	*Digoxin***
1	98.5	100.1	11	100.1	100.5
2	97.9	101.6	12	99.6	100.1
3	99.4	99.5	13	99.7	101.8
4	101.2	100.5	14	101.6	98.5
5	99.6	100.0	15	101.2	99.9
6	97.2	100.8	16	98.8	100.3
7	98.3	99.6	17	97.0	100.0
8	99.3	100.3	18	101.7	101.1
9	99.6	100.4	19	99.2	99.4
10	100.0	99.6	20	101.4	100.2
			Mean ± S.D.	99.6 ± 1.4	100.2 ± 0.76

* 0.1-mg tablet.
** 0.25-mg tablet.

methyldigoxin 0.1-mg tablets and digoxin 0.25-mg tablets. The assay results obtained from 20 determinations of randomly selected tablets are collected in Table II. The data indicate that the contents were within 97.0–101.7% (99.6 ± 1.4%, mean ± S.D.) of the label claim for β-methyldigoxin tablets and within 98.5–101.8% (100.2 ± 0.76%) for digoxin tablets. These values show excellent agreement with the manufacturers nominal content.

In conclusion, the micro-HPLC assay method described has been demonstrated to be accurate, precise and sensitive enough for the determination of β-methyldigoxin and digoxin in individual tablets. The use of dexamethasone as an internal standard enables the quantitative analysis of these cardiac glycosides. Micro-HPLC is a convenient and inexpensive method in comparison with conventional HPLC, because of the simplicity of micro column packing and the use of small amounts of the packing material and eluent. Consequently, this method is suitable for the routine quality assurance of pharmaceutical formulations. It is hoped that it can be adopted for the determination of cardiac steroids in other dosage forms.

REFERENCES

1 J. W. Myrick, *J. Pharm. Sci.*, 58 (1969) 1018.
2 L. F. Cullen, D. L. Packman and G. J. Papariello, *J. Pharm. Sci.*, 59 (1970) 697.
3 S. M. Khafagy and A. N. Girgis, *Planta Med.*, 25 (1974) 350.
4 A. H. Kibbe and O. E. Araujo, *J. Pharm. Sci.*, 62 (1973) 1703.
5 T. Yoshino, M. Shibasaki, Y. Kobayashi and H. Kawata, *Yakuzaigaku*, 36 (1976) 168.
6 A. Sato, Z. Ito, M. Noguchi, K. Oka, T. Ijitsu and S. Hara, *Yakugaku Zasshi*, 104 (1984) 454.
7 T. Sonobe, S. Hasumi, T. Yoshino, Y. Kobayashi, H. Kawata and T. Nagai, *J. Pharm. Sci.*, 69 (1980) 410.
8 B. Desta and K. M. McErlane, *J. Pharm. Sci.*, 71 (1982) 777.

9 M. W. Beasley, P. Skierkowski, R. W. Cleary, A. B. Jones and A. H. Kibbe, *J. Pharm. Sci.*, 72 (1983) 505.
10 H. Tokunaga, T. Kimura and T. Yamaha, *Iyakuhin Kenkyu*, 17 (1986) 94.
11 T. Hagiwara and K. Akiyama, *Bunseki Kagaku*, 36 (1987) 73.
12 D. Ishii, K. Asai, K. Hibi, T. Jonokuchi and M. Nagaya, *J. Chromatogr.*, 144 (1977) 157.
13 Y. Fujii, H. Fujii and M. Yamazaki, *J. Chromatogr.*, 258 (1983) 147.
14 Y. Fujii, Y. Ikeda and M. Yamazaki, *J. High Resolut. Chromatogr. Chromatogr. Commun.*, 10 (1987) 137.
15 E. Haack, F. Kaiser and H. Spingler, *Naturwissenschaften*, 44 (1957) 633.

Journal of Chromatography, 448 (1988) 165–172
Elsevier Science Publishers B.V., Amsterdam — Printed in The Netherlands

CHROM. 20 603

ISOLATION OF RECOMBINANT MYCOBACTERIAL ANTIGENS BY AN AUTOMATIC AND GENERALLY APPLICABLE PURIFICATION METHOD FOR β-GALACTOSIDASE FUSION PROTEINS

BERND SCHOEL and STEFAN H. E. KAUFMANN*

*Max-Planck-Institut für Immunbiologie, 7800 Freiburg (F.R.G.); and *Abteilung für Medizinische Mikrobiologie und Immunologie, Universität Ulm, Oberer Eselsberg, 7900 Ulm (F.R.G.)*

(First received March 11th, 1988; revised manuscript received April 25th, 1988)

SUMMARY

An automated two-dimensional chromatographic method has been developed for the isolation and concentration of recombinant fusion proteins with β-galactosidase. The system consists of an immunoaffinity column with anti-β-galactosidase antibodies as ligand, followed by an anion-exchange column. It was used for the purification and concentration of recombinant fusion proteins from *Mycobacterium tuberculosis* and *M. leprae*. Small amounts of crude lysates of *Escherichia coli* were loaded stepwise onto the immunoaffinity column with intermittent washing, elution and re-equilibration. After several cycles the eluate was passed through the anion-exchanger. Using an immunoaffinity gel of 5-ml volume and the anion-exchanger Mono Q HR 5/5, from 10 ml of crude *E. coli* lysate (containing up to 50 mg of protein) up to 100 μg of recombinant protein in a 2-ml volume could be isolated overnight.

INTRODUCTION

The clonal approach on the genetic level provides defined proteins of the cloned species. An expression library of the pathogens *Mycobacterium tuberculosis* and *M. leprae* has been established in the λgt11 vector system, and several recombinant protein antigens have been identified with monoclonal antibodies[1,2]. Because the host response to these pathogens is mediated by T-cells, an understanding of the antigens recognized by T-lymphocytes is of particular importance[3]. Analysis of recombinant proteins with peripheral blood T lymphocytes, however, requires separation of the antigen of interest, which makes up only a minor part of the lysate from *E. coli* components. Therefore we have developed an automated method for the purification of these recombinant proteins. This procedure is based on the fact that, in the λgt11 system, recombinant proteins are expressed as fusion proteins with β-galactosidase. This common feature of different recombinant fusion proteins makes affinity chromatography directed to β-galactosidase with substrate analogues or antibodies as ligands the method of choice[4]. Because the recombinant fusion proteins failed to

0021-9673/88/$03.50

express β-galactosidase activity, we used purified polyclonal rabbit antibodies directed against β-galactosidase as affinity ligand. With this isolation procedure we were able to purify different recombinant mycobacterial antigens for functional analysis with peripheral blood T-lymphocytes.

METHODS

Culture and lysis of recombinant E. coli clones

E. coli Y1089 containing no λgt11-phage, recombinant *E. coli* clone Y3179 expressing the 18 kDa antigen of *M. leprae*[1], and clones Y3143, Y3144, Y3147, Y3252, Y3272, Y3275 expressing the 65-kilodalton (kDa), 14-kDa. 19-kDa, 19-kDa, 71-kDa, 12-kDa antigens of *M. tuberculosis*[2], respectively, were kindly provided by R. A. Young. *E. coli* clone Y1089G is *E. coli* Y1089 infected with λgt11-phage alone (kindly provided by H. G. Simon), expressing β-galactosidase upon induction. Infection of *E. coli* Y1089 with the λgt11-phage was performed according to Huynh *et al.*[5]. To obtain the large amounts of *E. coli* required for the isolation of recombinant proteins, 500 ml of Luria–Bertani medium[6] were inoculated with a single colony of the recombinant *E. coli* lysogen and incubated on a shaker at 32°C[5]. When the culture had grown to an optical density of 0.5 measured at 600 nm, the temperature was increased to 43°C and incubation was continued for 20 min. Isopropylthiogalactopyranoside (IPTG, Sigma) was added to the cultures, which were further incubated at 37°C for 1 h. In contrast to others[5] we used 1 m*M* IPTG for induction, since with *E. coli* Y1089G we had found that this concentration of IPTG was sufficient for optimal induction of β-galactosidase expression. Cells were rapidly centrifuged for 5 min at 6000 *g* and 25–30°C, pellets were suspended in *ca.* 20 ml of Tris-buffered saline (TBS, 20 m*M* Tris, 150 m*M* sodium chloride pH 7.5) and frozen at −24°C. After thawing, phenylmethylsulphonyl fluoride (2 m*M* final concentration, Sigma) was added, and cells were disrupted by sonification. The sonicate was centrifuged for 20 min at 45 000 *g* to remove cell debris, and supernatants were frozen at −24°C until used.

Preparation of anti-β-galactosidase antibodies

A rabbit was immunized with 1 mg of β-galactosidase (grade VIII from *E. coli*, Sigma) in 0.5 ml of phosphate-buffered saline emulsified in 0.5 ml of complete Freund's adjuvant (Difco). After 4 weeks, the rabbit was boosted in a similar way, and 7–14 days later blood was collected. The immunoglobulin G (IgG) fraction was isolated from the serum with a protein-A Sepharose CL-4B column (Pharmacia), and then passed twice through a column with soluble proteins of *E. coli* Y1089 as ligand (1.2 mg of protein coupled to 1 ml of cyanogen bromide-activated Sepharose 4B (Pharmacia) as matrix) to remove cross-reacting IgG against *E. coli* proteins. Between passages the column was cleared with 0.1 *M* sodium acetate (pH 4.0) and 0.1 *M* diethanolamine (pH 11.0), and re-equilibrated with 50 m*M* Tris (pH 7.5, buffer A). The purified IgG fraction was used for immunoaffinity chromatography and immunostaining of Western blots.

Preparation of the immunoaffinity column

Purified anti-β-galactosidase IgG fraction (1 mg of protein) was coupled to 1 g of dry cyanogen bromide-activated Sepharose 4B (Pharmacia).

Western blots

SDS-polyacrylamide gel electrophoresis (SDS-PAGE) with a discontinuous buffer system[7] was performed in a separation gel with a linear polyacrylamide gradient from 22% to 10%. Crude *E. coli* extracts (15 μg of protein) were loaded on each lane. After electroblotting onto nitrocellulose[8], the sheet was blocked with 2.5% bovine serum albumin (BSA) in TBS. The blot was developed by incubation with 25 ml of anti-β-galactosidase antibodies (6 μg/ml diluted in TBS containing 0.5% BSA and 0.02% sodium azide) for 1 h, followed by three washings with 0.05% Tween 20 in TBS, and incubation with an alkaline phosphatase-labelled antibody against rabbit-IgG (diluted 1:5000 in TBS–0.5% BSA–0.02% sodium azide). After 1 h the nitrocellulose was washed four times with 0.05% Tween 20 in TBS, and finally developed with nitro blue tetrazolium and 5-bromo-4-chloro-3-indolylphosphate, according to the immunoblot kit (Proto Blot immunoblotting system, Promega Biotec).

SDS-PAGE

SDS-PAGE of protein fractions was performed with the PhastSystem (Pharmacia) with 10–15% gradient PhastGels. Gels were stained with the silver stain[9].

Protein assay

Protein concentrations were determined with the Coomassie dye-binding assay, using BSA as standard (BioRad)[10].

Assay of β-galactosidase

β-Galactosidase was assayed with O-nitrophenyl-β-D-galactoside (Sigma) as substrate at 20°C in 0.1 *M* sodium phosphate buffer (pH 7.3) containing 0.1 *M* 2-mercaptoethanol, 1 m*M* magnesium chloride and 2.3 m*M* substrate. The increase of absorbance was recorded at 410 nm.

Two-dimensional chromatography

The immunoaffinity chromatography (IAC) column containing 5 ml of gel and the anion-exchanger Mono Q HR5/5 (Pharmacia) were connected to the fast protein liquid chromatograph (Pharmacia) under two-dimensional chromatographic conditions using the IAC column first (Fig. 1). A superloop containing 10 ml of *E. coli* lysate was used as a sample reservoir.

The affinity chromatographic cycle consisted of the following four steps: (1) re-equilibration of the IAC column with 15 ml of 50 m*M* Tris (pH 7.5, buffer A); (2) loading 1.3 ml of the sample; (3) washing with 20 ml of buffer A and collection of the protein peak; (4) antigen elution with 10 ml of 50 m*M* diethanolamine (pH 11.0). A 9-ml volume of the eluate containing the majority of eluted antigens was collected and directed into a reservoir on a magnetic stirrer with 3/40 volume of 1.5 *M* sodium phosphate buffer (pH 6.5) (for 9 ml of eluate, 0.675 ml of phosphate buffer was required to achieve pH 7.5–8.0). The flow-rate was 1 ml/min, except during the loading step (2) and for the first 4 ml of step (3), when the flow-rate was reduced to 0.34

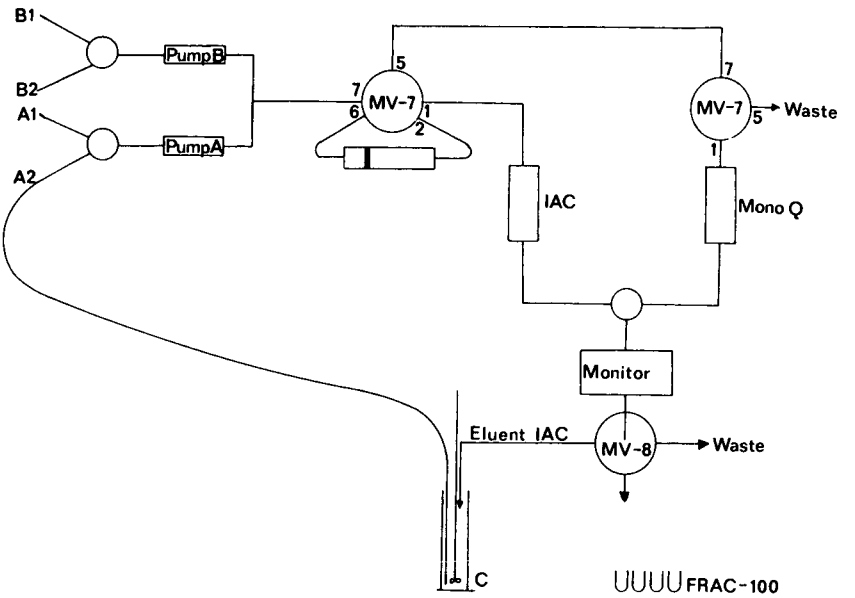

Fig. 1. Flow diagram of two-dimensional automated chromatography on the fast protein liquid chromatograph. MV-7 and MV-8 are motor valves, small circles indicate three-way valves PSV-100. Solution A1, 50 m*M* Tris (pH 7.5); solution B1, 50 m*M* diethanolamine (pH 11.0); solution B2, 50 m*M* Tris–1 *M* sodium chloride (pH 7.5); solution C, 1.5 *M* sodium phosphate (pH 6.5).

ml/min. The superloop and all fractions were stored on ice. After eight cycles the neutralized eluate was pumped onto the anion-exchanger, which had been equilibrated with buffer A. After loading and washing with buffer A the column was developed with a linear salt gradient, and within 30 ml the concentration of sodium chloride was increased to 1 *M* in buffer A. Usually the fusion proteins appeared within 2 ml at *ca.* 0.35 *M* sodium chloride. Recombinant proteins were detected in the collected fractions with a dot blot assay: 2 μl of each fraction were dotted onto a sheet of nitrocellulose, which was developed with anti-β-galactosidase antibodies as first antibody, according to the staining protocol for Western blots.

RESULTS AND DISCUSSION

Recombinant proteins expressed by the λgt11-vector are linked to β-galactosidase, and hence have higher molecular masses than β-galactosidase alone. Fig. 2 shows a Western blot of crude extracts of different *E. coli* clones expressing different proteins of *M. tuberculosis* after immunostaining with purified anti-β-galactosidase IgG. Besides the fusion proteins, in all extracts a uniform band that was recognized by these antibodies was not present in extracts of *E. coli* Y1089. This band is probably a degradation product of the fusion proteins.

In order to set up the isolation procedure for recombinant fusion proteins we used *E. coli* clone Y1089G as a model system. This clone expressed enzymatically active β-galactosidase after induction with IPTG, and hence the chromatographic conditions could be established using an enzymic assay as read-out system. In principle,

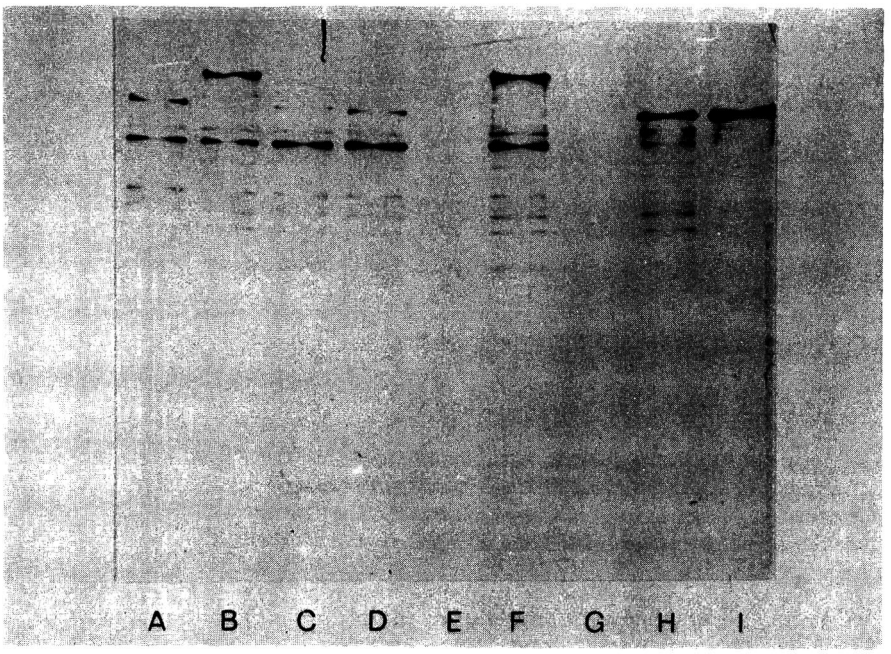

Fig. 2. Western blot of lysates of different *E. coli* clones expressing recombinant proteins of *M. tuberculosis*. Lanes A–F are lysates of clones expressing different mycobacterial proteins: A, Y3275 (12 kDa); B, Y3272 (71 kDa); C, Y3252 (19 kDa); D, Y3147 (19 kDa); E, Y3144 (14 kDa) (no expression); F, Y3143 (65 kDa); G, Y1089 (without λgt11); H, Y1089G (expressing β-galactosidase); I, 2 μg of β-galactosidase (Sigma).

different conditions can be used for the elution of bound antigens from IAC columns. Because we wanted to employ β-galactosidase as an indicator, we determined the stability of β-galactosidase under various elution conditions. The enzyme was destroyed in acidic buffers and chaotropic solvents (pH 7.0) but remained active in alkaline buffers (Table I). Hence in the subsequent experiments 50 m*M* diethanolamine (pH 11.0) was used as elution buffer.

The IAC column was loaded with crude extracts of *E. coli* Y1089G (4 mg/ml protein) and, after washing, was eluted with 50 m*M* diethanolamine (pH 11.0). Yields of up to 85% were achieved within the eluate, and an additional 10% was detected in the washing and re-equilibration fractions. During this step the antigen was diluted ten-fold. A 1-ml volume of immunoaffinity gel was capable of binding 200 μg of β-galactosidase from crude *E. coli* lysates. The purity of the eluted material after IAC is documented in Fig. 3.

Two remaining problems, namely the various binding capacities of different fusion proteins to the IAC column, and dilution during IAC, were solved by automating the chromatographic procedure on the fast protein liquid chromatograph. In a cyclic way, sufficiently small amounts of lysates were loaded onto the IAC column so that all antigen was bound. Afterwards, the IAC column was washed, antigen was eluted and the column was re-equilibrated. The material was eluted into phosphate buffer (pH 6.5) with the high molarity required for neutralization. In this system, the pH reached 7.5–8.0 at the end of all IAC steps. Subsequently the eluted antigen was

TABLE I

STABILITY OF β-GALACTOSIDASE UNDER VARIOUS CONDITIONS USED FOR ELUTION FROM AN IAC COLUMN

*Buffer**	*Remaining enzyme activity (%)***
0.1 *M* Glycine (pH 3.0)	0
0.1 *M* Glycine (pH 4.0)	20
0.1 *M* Diethanolamine (pH 10.0)	97
0.15 *M* Diethanolamine (pH 11.0)	95
0.15 *M* Diethanolamine–1 *M* sodium chloride (pH 11.0)	0
0.15 *M* Diethanolamine–2 *M* sodium chloride (pH 11.0)	27
0.15 *M* Diethanolamine–3 *M* sodium chloride (pH 11.0)	80
3.0 *M* Potassium thiocyanate	0
1.5 *M* Potassium thiocyanate	10
3.0 *M* Guanidine hydrochloride	10
1.5 *M* Guanidine hydrochloride	10

* β-Galactosidase was incubated for 30 min at 0°C.
** Percentage of remaining β-galactosidase activity.

subjected to anion-exchange chromatography on the Mono Q column. On this column β-galactosidase was bound at pH 7.5 and eluted with 100% yield at 0.35 *M* sodium chloride in a linear salt gradient. The complete two-dimensional system had an overall yield of up to 80% β-galactosidase as detected by its enzymic activity, and resulted in a five-fold concentration of the protein compared with the starting material. The process is illustrated schematically in Fig. 1.

Next, we applied this procedure to the purification and concentration of mycobacterial recombinant proteins. Using an IAC column containing 5 ml of affinity gel and the anion-exchanger Mono Q HR 5/5, we were able to isolate overnight (12

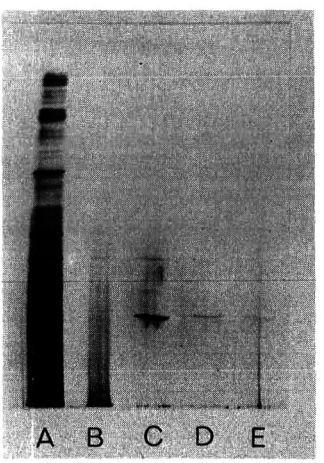

Fig. 3. SDS-PAGE on PhastSystem (Pharmacia) of *E. coli* Y1089G expressing β-galactosidase. Lanes A and B show 100 ng and 1 ng of protein of lysates, respectively; lanes C, D and E show 30 ng, 6 ng and 3 ng of immunoaffinity purified β-galactosidase, respectively.

h) up to 100 μg of recombinant protein within a 2-ml volume from 10 ml of crude *E. coli* lysate containing up to 50 mg of protein. SDS-PAGE of isolated recombinant proteins is documented in Fig. 4.

Although the recombinant proteins usually could be sufficiently purified by our method, in some cases an additional band of lower molecular mass was seen, and in case of clone Y3252 (expressing the 19 kDa protein detected by monoclonal antibody TB-C-13[11] no band was visible on the SDS gel (Fig. 4G) and on the Western blot only a faint band was detectable (Fig. 2C). Accordingly, this protein could not be isolated in sufficiently large amounts. The band of lower molecular mass was recognized by the anti-β-galactosidase antibodies, and probably represented a degradation product. We assume that these problems must be solved by modifying the culture conditions involving higher protein induction and faster lysis in the presence of potent protease inhibitors, rather than by altering the chromatographic procedure.

Recently, an IAC column with a monoclonal antibody as ligand directed against β-galactosidase became commercially available. We did not compare both IAC systems. However, because the recombinant fusion partner can have an influence on the antigenicity of the β-galactosidase molecule, we felt that an antiserum composed of multiple anti-β-galactosidase antibodies might be more appropriate to cover a broad range of fusion proteins.

Tuberculosis and leprosy are chronic infectious diseases that still cause major health problems, and effective vaccines against these pathogens are not available as yet[12]. Until recently the demand for sufficient amounts of pure antigens required for the construction of a novel vaccine could not be adequately met. The cloning of mycobacterial genes has provided a possible way of producing sufficient amounts of antigens of potential interest. Because immunity against tuberculosis and leprosy is mediated by T-lymphocytes, any rational vaccination strategy depends on the iden-

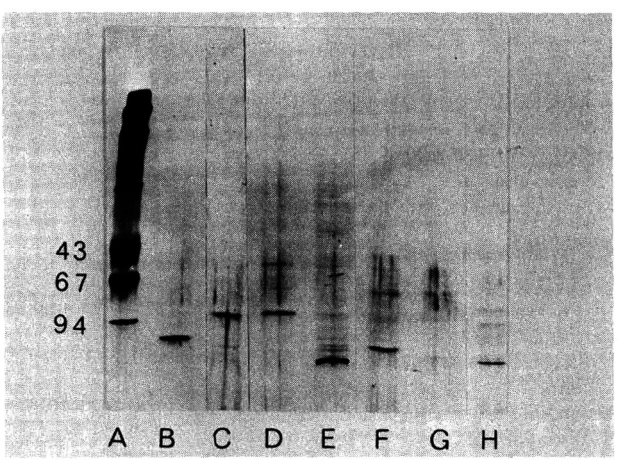

Fig. 4. SDS-PAGE on PhastSystem (Pharmacia) of isolated recombinant mycobacterial antigens. (A) Electrophoresis calibration kit (Pharmacia) indicating phosphorylase b 94 kDa, BSA 67 kDa, ovalbumin 43 kDa; (B) 30 ng of β-galactosidase isolated from *E. coli* Y1089G; (C) 17 ng of 18 kDa protein of *M. leprae*; (D–H) recombinant proteins of *M. tuberculosis*: (D) 11 ng of 19 kDa antigen; (E) 50 ng of 71 kDa antigen; (F) 20 ng of 12 kDa antigen; (G) 5 ng of 19 kDa antigen; (H) 20 ng of 65 kDa antigen.

tification of antigens on the T-cell level[3,12]. While long-term cultured T-cells can be used for testing of whole *E. coli* lysates[13–15], peripheral blood T-lymphocytes fail to respond specifically to these crude antigen preparations owing to contamination by *E. coli* components. Therefore screening of recombinant antigens with peripheral blood lymphocytes depends on prior antigen purification. As will be described elsewhere[16], the purification method introduced here makes it possible to screen recombinant antigens directly with peripheral blood T-lymphocytes.

The method described should not be restricted to recombinant proteins of mycobacterial origin, but could also be applied to other proteins of interest. Furthermore, it should be possible to apply it to fusion proteins expressed in other vector systems using β-galactosidase as fusion partner, *e.g.* the pEX-overexpression vector.

ACKNOWLEDGEMENTS

We thank Dr. R. A. Young for providing the recombinant *E. coli* clones and for helpful discussions. S. H. E. Kaufmann is recipient of the A. Krupp award for young professors. This work was supported by the Immunology of Leprosy component of the UNDP/World Bank/WHO Special Program for Research and Training in Tropical Diseases, by the WHO as part of it Program for Vaccine Development and by the German Leprosy Relief Association. We thank R. Mahmoudi for typing the manuscript.

REFERENCES

1 R. A. Young, B. R. Bloom, C. M. Grosskinsky, J. Ivanyi, D. Thomas and R. W. Davis, *Proc. Natl. Acad. Sci. U.S.A.*, 82 (1985) 2583–2587.
2 R. A. Young, V. Mehra, D. Sweetser, T. Buchanan, J. Clark-Curtiss, R. W. Davis and B. R. Bloom, *Nature (London)*, 316 (1985) 440–452.
3 H. Hahn and S. H. E. Kaufmann, *Rev. Inf. Dis.*, 3 (1981) 1221–1250.
4 A. Ullmann, *Gene*, 29 (1984) 27–31.
5 T. V. Huynh, R. A. Young and R. W. Davis, in D. Glover (Editor), *DNA Cloning Techniques: A Practical Approach*, Vol. 1, IRL Press, Oxford, 1985, pp. 49–78.
6 T. Maniatis, E. F. Fritsch and J. Sambrook, *Molecular Cloning*, Cold Spring Harbor Laboratory, New York, 1982, p. 68.
7 U. K. Laemmli, *Nature (London)*, 227 (1970) 680–685.
8 H. Towbin, T. Staehelin and J. Gordon, *Proc. Natl. Acad. Sci. U.S.A.*, 76 (1979) 4350–4354.
9 C. R. Merril, D. Goldman and M. L. van Keuven, *Methods Enzymol.*, 104 (1984) 441–447.
10 M. M. Bradford, *Anal. Biochem.*, 72 (1976) 248–254.
11 Letter to the Editor, *Infect. Immun.*, 51 (1986) 718–720.
12 S. H. E. Kaufmann, *Microbiol. Sci.*, 4 (1987) 324–328.
13 J. R. Lamb, J. Ivanyi, A. Rees, R. A. Young and D. B. Young, *Leprosy Rev.*, 57 (1987) (Suppl. 2) 131–137.
14 F. Oftung, A. S. Mustafa, R. N. Husson, R. A. Young and T. Godal, *J. Immunol.*, 138 (1987) 927–931.
15 F. Emmrich, J. Thole, J. v. Emden and S. H. E. Kaufmann, *J. Exp. Med.*, 163 (1986) 1024–1029.
16 M. E. Munk, B. Schoel and S. H. E. Kaufmann, *Eur. J. Immunol.*, in press.

Journal of Chromatography, 448 (1988) 173–181
Elsevier Science Publishers B.V., Amsterdam — Printed in The Netherlands

CHROM. 20 629

Note

Fluorimetric determination of aflatoxins in foodstuffs by high-performance liquid chromatography with flow injection analysis

F. LÁZARO, M. D. LUQUE DE CASTRO and M. VALCÁRCEL*
Department of Analytical Chemistry, Faculty of Sciences, University of Córdoba, Córdoba (Spain)
(First received March 29th, 1987; revised manuscript received May 6th, 1988)

Although high-performance liquid chromatography (HPLC) and flow injection analysis (FIA) have significant differences (working pressure, presence of interfaces, cost), they involve a number of common components (liquid reservoirs, pumps, injection valves and continuous detectors) and are complementary in nature. Hence attempts to use HPLC and flow injection analysis in conjuction are justified[1]. A flow injection system has been used as the precolumn reactor of an HPLC unit (Fig. 1A) to determine Zn^{II} through its activation of the catalytic effect of carboxypeptidase A on the decomposition of hippuryl-L-phenylalanine[2], and as a post-column reactor–detector in two different manners: (a) by inserting successive aliquots of the eluate from an HPLC system at high frequency into the same or different flow injection systems[3] (Fig. 1B) and (b) by applying the merging zones approach to merge the eluate from the HPLC system with a large reagent plug (Fig. 1C)[4–6].

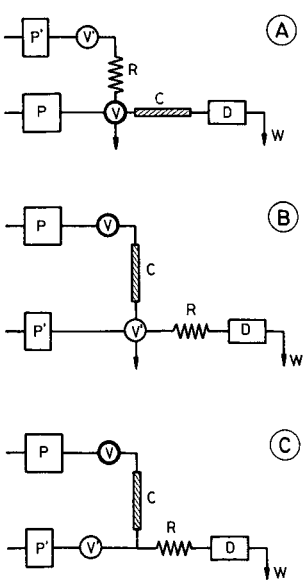

Fig. 1. Types of HPLC–FIA configurations. P, HPLC pump; P', FIA pump; V, HPLC injection valve; V', FIA injection valve; R, reactor; C, analytical column; D, detector; W, waste.

0021-9673/88/$03.50

This paper presents a new approach to the joint use of HPLC and flow injection analysis (Fig. 1C) in which the flow injection sub-system allows the total determination of several related compounds; the individual analysis for each analyte is performed by the HPLC sub-system while the flow injection sub-system acts as a post-column reactor–detector, thereby enhancing the information obtained from the sample. The best field for the joint use of these techniques is the analysis of large numbers of samples of which only a few may be of interest because their toxicity or their role as disease indicators. An example is the analysis of foods for aflatoxins. A study performed on about 300 food samples for these carcinogenic compounds revealed their presence in only 6% of them[7]. Among the different aflatoxins known, the most frequent are B_1, B_2, G_1 and G_2. Fluorimetry is the detection technique most commonly used with these substances because of their native fluorescence (λ_{ex} = 360 nm for all them, λ_{em} = 440 nm for B_1 and B_2 and 470 nm for G_1 and G_2). The maximum allowed content of aflatoxins is of the order of a few micrograms per kilogram[8], hence methods for their determination must be very sensitive. The fluorescence of aflatoxins B_1 and G_1, which is lower than that of B_2 and G_2, can be increased by using strong acids[9] or oxidants such as chloramine T[10] iodine[11] or bromine[12]. Bromine was used as the derivatizing agent in this work. It acts by adding itself to the double bond of the furan ring of aflatoxins B_1 and G_1[13], thereby increasing their fluorescence by a factor of 20 or more.

EXPERIMENTAL

Apparatus

The experimental set-up is shown in Fig. 2. The system was built from a high-pressure dual-piston pump (Model 64; Knauer, Berlin, F.R.G.), a Knauer variable-volume rotary injection valve, a small-bore, low-volume mixing Y-piece (Omnifit 2407), a 200 mm × 4 mm I.D. analytical column filled with Nucleosil 120 Å, 5 μm, C_{18}, and a Perkin-Elmer LS-1 fluorescence detector equipped with a low-volume flow cell (inner volume 4 μl) and connected to a Perkin-Elmer R100 recorder. All connections were made from 0.25 mm I.D. stainless-steel capillary tubing fitted with laboratory-constructed hand-tight Kel-F nut–ferrule combinations. The flow injection sub-system was made up of a four-channel Gilson Minipuls-2 peristaltic pump

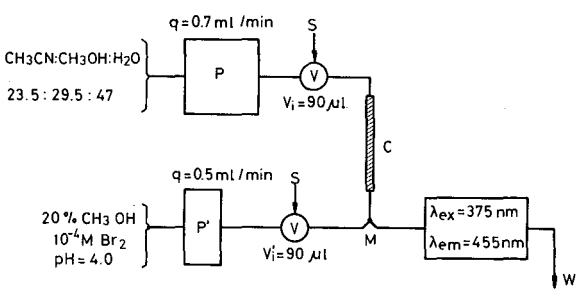

Fig. 2. Integration of HPLC–FIA for the determination of total aflatoxins by FIA and individual aflatoxins by HPLC. P, P', V, V' and C as in Fig. 1; S is the sample and M is the point of mixing of the eluent and derivatizing reagent. V' can be removed and a $1.3 \cdot 10^{-3}$ *M* bromine solution flow-rate of 0.18 ml/min must be used when only the HPLC system is employed.

and a Rheodyne 5041 variable-volume injection valve. All connections were made from 0.3 mm I.D. PTFE tubing. The temperature of the analytical column was kept at 25°C by using a thermostated water-bath.

Reagents

Stock solutions of each of aflatoxins B_1, B_2, G_1 and G_2 (Serva, Heidelberg, F.R.G.) (50 μg/ml in methanol) were prepared by weighing and checked by following the AOAC recommendations[14]. The stock solutions were diluted with methanol–water (1:4) to the desired level prior to analysis. Stock and diluted solutions were kept in the dark at 4°C.

The eluent was prepared by mixing doubly distilled water, HPLC-grade methanol and HPLC-grade acetonitrile (Scharlau, Barcelona, Spain) (47:29.5:23.5) and was microfiltered through a nylon 66 (0.45-μm pore size) filter disk and degassed *in vacuo* in an ultrasonic bath (Sonorex TK 52, Bandelin, Berlin, F.R.G.) prior to use.

Bromine solution (0.2 *M*) was prepared by pouring the contents of a 78.0-g vial of bromine (Merck, Darmstadt, F.R.G.) into 2.5 l of water. After stirring, the solution was filtered and titrated with ammonium iron(II) sulphate (using diethyl-*p*-phenylenediamine as indicator[14]) prior to storage at 4°C in a topaze flask.

All other reagents used in the extraction of aflatoxins (chloroform, benzene, hexane, sodium chloride and ammonium sulphate) were of analytical-reagent grade (Merck).

All glassware in contact with aflatoxins was cleaned with 5% sodium hypochlorite solution. Clean glassware was rinsed with dilute nitric acid (1:4) and doubly distilled water.

Extraction procedures

The procedures used were based on the methods recommended by the AOAC[14], slightly modified for use in flow injection analysis, which usually involves aqueous solutions.

Peanuts. In a 1000-ml separating funnel 100 g of peanuts were extracted with a mixture of 500 ml of methanol–water (55:45, v/v), 200 ml of hexane and 4 g of sodium chloride. After shaking and separating the layers, 25 ml of the methanol–water phase was pipetted into a 100-ml separating funnel and extracted for 1 min with 25 ml of chloroform. The chloroform phase was evaporated to dryness on a steam plate under a stream of nitrogen. The residue was dissolved in 5 ml of methanol and made up to 10 ml with doubly distilled water. The solution was filtered through a nylon 666 (0.45 μm) disc filter and extracted with 10 ml of chloroform. The chloroform phase was again evaporated to dryness and the residue was dissolved in 1 ml of methanol and made up to 5 ml with doubly distilled water.

Maize. In a 1000-ml separating funnel 50 g of maize were mixed with 10 g of diatomaceous earth and extracted with 150 ml of acetone–water (85:15, v/v) for 5 min. The supernatant solution was filtered through a Whatman 2V flutted paper and 50 ml of the filtrate solution were mixed with 20 ml of saturated ammonium sulphate solution, 130 ml of water and 10 g of diatomaceous earth. After agitation, the mixture was filtered and 100 ml of the filtrate solution were extracted with 3 ml of benzene for 30 s. The benzene phase was evaporated to dryness on a steam plate under a stream of nitrogen. The residue was treated as in the extraction of peanuts.

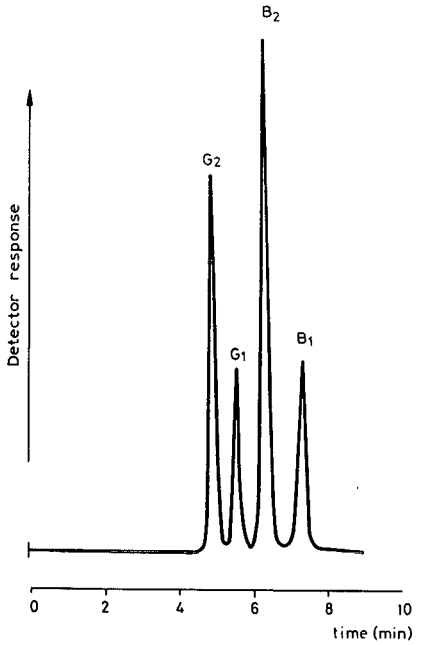

Fig. 3. Chromatogram of a test mixture of standard solutions of aflatoxins G_2, G_1, B_2 and B_1 (10 ng/ml each). Conditions as in Fig. 2.

RESULTS AND DISCUSSION

We recently reported[10] the flow injection determination of total aflatoxins. This work concerned the optimization and implementation of the determination of aflatoxins by the joint use of HPLC and flow injection analysis.

Optimization of the HPLC conditions

A previous study[10] of derivatizing reagents for aflatoxins was performed by the univariate method. The experiment considered the chemical and flow injection variables involved in order to determine the individual influence of each; thus, the modified simplex method (MSM)[15] was used in HPLC to optimize interrelated variables. The response function favours not only the fluorescence intensity of the four peaks, but also less overlapping between peaks and the minimum analysis time. Watson and Carr's response function[16], slightly modified, was used.

The optimum composition of the mobile phase found by the MSM was acetonitrile–methanol–water (23.5:29.5:47), allowing the complete resolution of the four peaks.

The concentration and flow-rate of the bromine solution and the flow-rate of the mobile phase were interrelated; the MSM was also applied and gave optimum values of 0.7 ml/min for the mobile phase (column pressure 120 atm), 0.18 ml/min for the bromine solution (four times lower to avoid excessive dilution of the eluted

TABLE I

FEATURES OF THE HPLC METHOD

Aflatoxin	*Residence time (min)*		*Calibration graph*				
	Mean value	*R.S.D. (%)*	*Intercept, % I_f*	*Slope, % I_f/ (ng/ml)*	*Correlation coefficient*	*Determination range (ng/ml)*	*R.S.D. (%) (n = 11)*
G_2	5.2	1.0	0.02	0.432	0.9998	0.5–200.0	1.7
G_1	5.8	1.1	0.14	0.199	0.9998	0.5–200.0	1.0
B_2	6.5	1.1	0.37	0.560	0.9998	0.5–200.0	1.7
B_1	7.5	0.9	0.13	0.206	0.9999	0.5–200.0	1.8

analytes) and $1.3 \cdot 10^{-3}$ *M* bromine solution (the pH of the aqueous phase was 4.0, *i.e.*, the optimum for this determination).

The methanol content of the bromine solution did not affect the analytical signal up to 20–30%; therefore, the bromine and sample solutions contained 20% of methanol to facilitate the dissolution of aflatoxins and to avoid disturbance of the signal due to changes in the refractive index and dielectric constant.

The maximum analytical signal was obtained by directly connecting the Y connector (point M in Fig. 2) to the detector, the heights of all peaks decreasing with increase in the length of the post-column reactor. This is accounted for by the high rate of the bromine–aflatoxin reaction and the increasing dilution of the sample plug with increasing reactor length.

Features of the calibration graphs

A chromatogram of a test mixture containing four aflatoxins obtained with the HPLC system is shown in Fig. 3. Complete resolution of the peaks was achieved

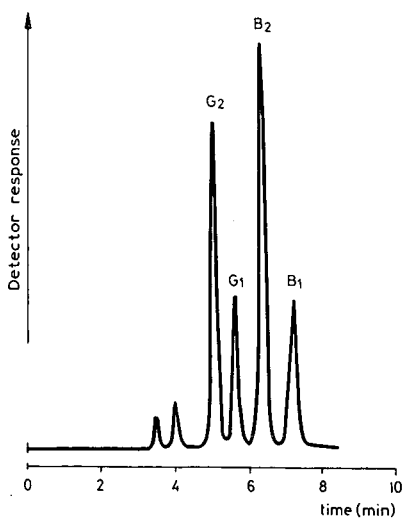

Fig. 4. Chromatogram of an extract of maize spiked with aflatoxins G_2, G_1, B_2 and B_1 (16.4 ng/ml each). Conditions as in Fig. 2.

TABLE II

RECOVERIES OF AFLATOXINS ADDED TO PEANUT AND MAIZE SAMPLES OBTAINED BY THE HPLC METHOD

Sample	*Added (ng)*	*Recovery (%)*			
		G_2	G_1	B_2	B_1
Peanut 1	16.4	104.1	106.9	99.6	100.9
	32.8	101.9	103.2	98.6	100.3
Peanut 2	16.4	106.1	107.2	99.4	99.7
	32.8	106.3	107.5	100.7	99.3
Maize 1	16.4	104.4	104.3	104.7	93.2
	32.8	103.8	101.7	100.2	102.9
Maize 2	16.4	99.2	99.4	101.9	100.5
	32.8	99.7	100.5	98.9	98.4

in 7.5 min. Relevant data for the analytical system are summarized in Table I. The precision was studied with a solution containing 30 ng/ml of each aflatoxin. The within-day repeatabilities for both retention times and peak height showed that the HPLC system was not subject to large fluctuations. The calibration graphs have excellent correlation coefficients (greater than 0.999) and a determination range of 0.5–200.0 ng/ml in all instances.

Application of the HPLC method to maize and peanut samples

A study of the recovery of aflatoxins B_1, B_2, G_1 and G_2 from extracts of maize and peanut (the two matrices in which these toxins occur most frequently) by the proposed method was performed. The concentrations of the analytes in the samples were well above the lower limit of the method (0.5 ng/ml). The analysis was subject to no interferences from other compounds present in the sample (see Fig. 4). The average recovery obtained on addition of 16.4 and 32.8 ng of each aflatoxin to different samples of maize and peanut was 101.7%, with an average deviation of ±2.6% from 100% (see Table II, which shows the reliability of the proposed method).

TABLE III

FEATURES OF THE CALIBRATION GRAPHS FOR THE INTEGRATED HPLC–FIA METHOD

Aflatoxin	*Intercept, % I_f*	*Slope, % I_f/(ng/ml)*	*Correlation coefficient*	*Determination range (ng/ml)*	*R.S.D. (%) (n = 11)*
$G_2+G_1+B_2+B_1$ (FIA)	0.18	0.468	0.9999	1.0–200.0	1.7
G_2 (HPLC)	0.26	0.375	0.9998	1.0–200.0	1.8
G_1 (HPLC)	0.12	0.121	0.9999	1.0–200.0	2.0
B_2 (HPLC)	0.26	0.327	0.9998	1.0–200.0	1.9
B_1 (HPLC)	0.13	0.132	0.9998	1.0–200.0	2.8

TABLE IV

RECOVERIES OBTAINED BY FLOW INJECTION ANALYSIS (INTEGRATED HPLC–FIA) OF TOTAL AFLATOXINS ADDED TO PEANUT AND MAIZE SAMPLES

Sample	*Added (ng)*	*Found (ng)*	*Recovery (%)*
Peanut 1	10.0	10.5	105.0
	20.0	19.2	96.0
Peanut 2	10.0	10.6	106.0
	20.0	18.6	93.0
Maize 1	10.0	9.8	98.0
	20.0	20.8	104.0
Maize 2	10.0	9.5	95.0
	20.0	19.0	95.0

Integrated HPLC–flow injection analysis

The development of this integrated method requires a compromise to be made between the optimum non-coincident values of the variables that affecting the two methods. The emission wavelength chosen was 455 nm [intermediate between the optimum values for flow injection (470 nm) and HPLC (440 nm)]. The most important of the non-coincident variables was the flow-rate of the bromine solution; by using the optimum value for flow injection (1.5 ml/min), the dispersion suffered by the chromatographic peaks was excessive, whereas the optimum flow-rate for HPLC (0.2 ml/min) dramatically reduced the sensitivity of the flow injection method. An intermediate flow-rate (0.5 ml/min) was used with a bromine concentration of $1 \cdot 10^{-4}$ *M*. Under these conditions, the maximum of the flow injection peak was obtained within 18 s and the complete chromatogram was obtained in less than 8 min.

TABLE V

RECOVERIES OBTAINED BY THE HPLC METHOD (INTEGRATED HPLC–FIA) OF AFLATOXINS ADDED TO PEANUT AND MAIZE SAMPLES

Sample	*Added (ng)*	*Recovery (%)*			
		F_2	G_1	B_2	B_1
Peanut 1	16.4	100.4	100.2	100.4	97.7
	32.8	105.8	103.6	106.7	103.5
Peanut 2	16.4	97.0	99.4	98.5	101.6
	32.8	95.3	97.9	96.7	101.6
Maize 1	16.4	101.1	104.6	99.6	104.3
	32.8	102.5	105.6	101.3	105.3
Maize 2	16.4	98.4	100.1	97.3	98.6
	32.8	99.1	98.1	98.1	96.5

Features of the calibration graphs obtained by the integrated method

Table III gives the data for the calibration graphs for HPLC and flow injection analysis. The calibration graphs for the latter method was run with equimolar amounts of the four aflatoxins. The retention times and their relative standard deviations are very similar to those listed in Table I, the correlation coefficients being excellent with a determination range of 1.0–200.0 ng/ml in all instances.

Application of the integrated HPLC–flow injection method to the analysis of peanut and maize samples

The excellent recoveries achieved on addition of different amounts of aflatoxins B_1, B_2, G_1 and G_2 to maize and peanut extracts (100.7% and 99.0% for the HPLC and flow injection methods, respectively) are shown in Tables IV and V, with average deviations of ±2.8% and ±4.5% from 100%. The lower accuracy of the results obtained with the flow injection method could be due to the occurrence in the maize and peanut extracts of interferents with fluorescent properties under the working conditions adopted. These interferents are separated and eluted before the analytes in HPLC (Fig. 4), whereas in flow injection analysis the blank signal due to these compounds is in the range 0.4–2.0% I_f in the maize extracts and 4–8% I_f in the peanut extracts. This necessitates the injection of two successive aliquots of each sample into the flow injection sub-system to determine the real concentrations of the aflatoxins. One aliquot provides a signal due to blank + analytes; in the other, 5 µl of 11 g/l sodium hypochloric solution per ml of sample are added to destroy the aflatoxins present[14], the measurement of this sample providing the blank signal. Studies performed with different extracts with or without aflatoxins revealed different reactivities of the sample matrix, even in samples of the same food. This is the source of the error in the recovery. Nevertheless, the error does not exceed 7%; in addition, hazardous samples can always be analysed by HPLC.

CONCLUSIONS

The proposed integrated method combines the advantages of flow injection analysis, namely rapidity, simplicity and economy, with the separation capability of HPLC. In addition, it avoids the use of HPLC for routine control and results in major time and cost savings. At present our team is engaged in the automation of integrated HPLC–flow injection analysis configurations by using a sampler, a selecting valve and a microcomputer to control the overall process. To simplify and accelerate the extraction process, ultrasound will be applied directly to pulverized solid samples by using a suitable solvent, either off- or on-line[17].

ACKNOWLEDGEMENTS

CICyT is acknowledged for financial support (Grant No. PA86-0146). The authors also express their gratitude to Dr. Merck-Luengo of the Subdirección General de Sanidad Vegetal del Ministerio de Agricultura de España.

REFERENCES

1 M. Valcárcel and M. D. Luque de Castro, *J. Chromatoogr.*, 393 (1987) 3.
2 L. Risinger, L. Ogren and G. Johansson, *Anal. Chim. Acta*, 154 (1983) 251.
3 D. Betteridge, N. G. Courtney, T. J. Sly and D. G. Porter, *Analyst (London)*, 109 (1984) 91.
4 Y. Hirai, N. Yoza and S. Ohashi, *J. Chromatogr.*, 206 (1981) 501.
5 Y. Baba, N. Yoza and S. Ohashi, *J. Chromatogr.*, 318 (1985) 319.
6 Y. Baba, N. Yoza and S. Ohashi, *J. Chromatogr.*, 295 (1984) 153.
7 P. A. Burdaspal and A. Gorostidi, *Alimentaria*, 186 (1985) 21.
8 L. G. M. T. Tuinstra and W. Haasnoot, *J. Chromatogr.*, 282 (1983) 457.
9 E. J. Tarter, J. P. Hanchay and P. M. Scott, *J. Assoc. Off. Anal. Chem.*, 67 (1984) 597.
10 F. Lázaro, M. D. Luque de Castro and M. Valcárcel, *Fresenius Z. Anal. Chem.*, submitted for publication.
11 P. G. Thiel, S. Stockenstroem and P. S. Gathercole, *J. Liq. Chromatogr.*, 9 (1986) 231.
12 W. T. Kok, T. C. H. Van Neer, W. A. Traag and L. G. M. T. Tuinstra, *J. Chromatogr.*, 367 (1986) 231.
13 R. W. Frei, personal communication.
14 *Official Methods of Analysis of the Association of Official Analytical Chemists*, AOAC, Washington, DC, 12th ed., 1975, pp. 462–469.
15 S. N. Deming and L. R. Parker, Jr., *CRC Crit. Rev. Anal. Chem.*, 7(3) (1978) 187.
16 M. W. Watson and P. W. Carr, *Anal. Chem.*, 51 (1979) 1835.
17 P. Linares, F. Lázaro, M. D. Luque de Castro and M. Valcárcel, *Anal. Chim. Acta*, 200 (1987) 51.

Journal of Chromatography, 448 (1988) 182–187
Elsevier Science Publishers B.V., Amsterdam — Printed in The Netherlands

CHROM. 20 612

Note

Isolation of *cis–trans* isomers of canthaxanthin by high-performance liquid chromatography using a calcium hydroxide column and identification of their configurations by ^{1}H NMR spectroscopy

HIDEKI HASHIMOTO and YASUSHI KOYAMA*
Faculty of Science, Kwansei Gakuin University, Uegahara, Nishinomiya 662 (Japan)
and
TOSHIO SHIMAMURA
Nitto Technical Information Centre, Shimo-Hozumi, Ibaraki 567 (Japan)
(Received April 20th, 1988)

The roles of carotenoids in photosynthetic systems are well established[1–4], and the natural selection of certain types of *cis–trans* carotenoids in the specific sites of bacterial photosynthetic organella have been reported[5]. On the other hand, the roles and the configurations of these pigments in animals still remain obscure. Nelis *et al.*[6] found that massive amounts of mono-*cis* isomers of canthaxanthin (4,4′-diketo-β-carotene) were selectively localized in the ovaries, the eggs and the haemolymph of reproductively active females of the brine shrimp *Artemia*, which was the first observation of the *cis*-carotenoid in the animal organella, to the best of our knowledge. In order to reveal the physiological implications of the presence of *cis*-carotenoids in these organella, it is necessary to elucidate both the configurations and the biochemical and biophysical properties of these pigments both *in vitro* and *in vivo*. We have therefore attempted to establish a technique for the isolation and identification of the *cis* isomers of canthaxanthin as the first step in a series of investigations.

cis Isomers of canthaxanthin were first isolated by Gansser and Zechmeister[7] from a stereoisomeric mixture by means of column chromatography using calcium hydroxide as the stationary phase and benzene as the mobile phase. They found three mono-*cis* and three di-*cis* isomers, and tentatively assigned the mono-*cis* isomers to 9-*cis*, 13-*cis* and 15-*cis* on the basis of their electronic and infrared absorption spectra and of co-chromatography with synthetic 15-*cis* isomer. Nelis and co-workers[6,8] used non-aqueous reversed-phase and normal-phase chromatography for the separation of canthaxanthin isomers. They isolated the all-*trans*- and a mixture of *cis*-canthaxanthins by reversed-phase chromatography using a Zorbax ODS column and a ter-

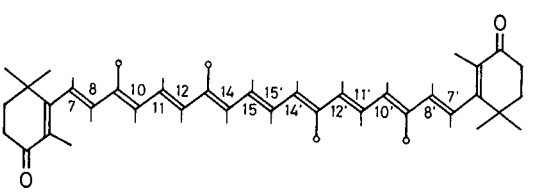

0021-9673/88/$03.50

nary mobile phase consisting of acetonitrile, methanol and dichloromethane. Further, *cis* isomers separated by normal-phase chromatography on ROSIL silica were assigned to 9-*cis*, 13-*cis* and 15-*cis* on the basis of their absorption spectra.

Englert[9] reviewed high-field ^{1}H NMR spectroscopy for the determination of carotenoid configurations and reported a study of *cis* isomers of canthaxanthin, in which the presence of the 9-*cis*, 11-*cis*, 13-*cis*, 15-*cis*, 9,9′-*cis*, 9,11-*cis*, 9,13-*cis*, 9,15-*cis* and 13,13′-*cis* isomers was suggested. Complete publication, however, concerning the isolation and identification of these isomers has not appeared anywhere. In a previous investigation, we established a technique for isolating isomeric β-carotene by high-performance liquid chromatography (HPLC) using a calcium hydroxide column[10,11]. In this investigation, we applied this technique to isomeric canthaxanthin, and succeeded in separating thirteen different *cis–trans* isomers using *n*-hexane–benzene (5:95) as the mobile phase; seven *cis* isomers (9-*cis*, 13-*cis*, 15-*cis*, 9,9′-*cis*, 9,13-*cis*, 9,13′-*cis* and 13,13′-*cis*) were identified by 400 MHz ^{1}H NMR spectroscopy.

EXPERIMENTAL

All-*trans*-canthaxanthin was purchased from Roth (purity 98%) and used without further purification. A mixture of isomeric canthaxanthin was obtained by heating the crystals of the all-*trans* isomer sealed in an ampoule at 215°C for 5 min. The mixture was roughly separated into six fractions by the use of Lo-Bar column chromatography (50 × 3 cm I.D. column packed with calcium hydroxide, Kishida lot E48215T, at 6 kg/cm^2; development with benzene at 3 kg/cm^2). After the development, the calcium hydroxide was pushed out of the column and cut into six fractions. Each fraction was extracted with ethanol and each isomeric component was purified by HPLC.

Columns for HPLC were packed at 300 kg/cm^2 with calcium hydroxide (Nakarai, lot M6E7143, 200–300 mesh) by a method described elsewhere[11]. A 300 × 4 mm I.D. column with *n*-hexane–benzene (5:95) as eluent was used to analyse components having longer retention times (peaks 5, 10 and 11 in Fig. 1a; see below), and

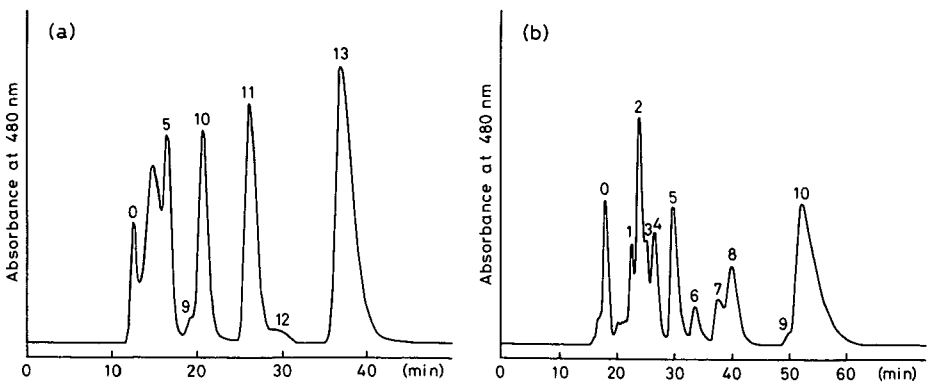

Fig. 1. Elution profiles for a mixture of isomers obtained by melting crystalline all-*trans*-canthaxanthin. Column (4 mm I.D.) packed with calcium hydroxide; eluent, *n*-hexane–benzene (5:95); detection at 480 nm. (a) Column length 300 mm and flow-rate 0.2 ml/min; (b) column length 600 mm and flow-rate 0.3 ml/min. The assignment of the peaks is given in Table II.

TABLE I

CHEMICAL SHIFTS (ISOMERIZATION SHIFTS) OF ISOMERIC CANTHAXANTHIN IN DEUTEROBENZENE (ppm)

	*Peak 13**, *all-trans*	*Peak 11, 9-cis*	*Peak 10, 13-cis*	*Peak 3, 15-cis*	*Peak 4, 9,9'-cis*	*Peak 5, 9,13-cis*	*Peak 2, 9,13'-cis*	*Peak 1, 13,13'-cis*
7H 7'H	6.15	6.18 (+0.03) 6.15 (+0.00)	6.16 (+0.01) 6.15 (+0.00)	6.14 (−0.01)	6.18 (+0.03)	6.18 (+0.03) 6.15 (+0.00)	6.17 (+0.02) 6.16 (+0.01)	6.16 (+0.01)
8H 8'H	6.38	7.13 (+0.75) 6.38 (+0.00)	6.41 (+0.03) 6.39 (+0.01)	6.35 (−0.03)	–	7.11 (+0.73) 6.38 (+0.00)	– 6.41 (+0.03)	6.42 (+0.04)
10H 10'H	6.29	6.22 (−0.07) 6.28 (−0.01)	6.27 (−0.02) 6.29 (+0.00)	6.29 (+0.00)	6.21 (−0.08)	6.23 (−0.06) 6.27 (−0.02)	6.19 (−0.10) 6.28 (−0.01)	6.30 (+0.01)
11H 11'H	6.73	6.93 (+0.20) 6.72 (−0.01)	6.72 (−0.01)	6.74 (+0.01)	6.92 (+0.19)	6.91 (+0.18) 6.72 (−0.01)	6.93 (+0.20) 6.71 (−0.02)	6.72 (−0.01)
12H 12'H	6.50	6.42 (−0.08) 6.50 (+0.00)	7.05 (+0.55) 6.50 (+0.00)	6.51 (+0.01)	6.42 (−0.08)	6.99 (+0.49) 6.52 (+0.02)	6.41 (−0.09) 7.05 (+0.55)	7.06 (+0.56)
14H 14'H	6.36	6.33 (−0.03)	6.16 (−0.20) 6.40 (+0.04)	6.90 (+0.54)	6.29 (−0.07)	6.10 (−0.26) 6.38 (+0.02)	6.35 (−0.01) 6.12 (−0.24)	6.19 (−0.17)
15H 15'H	6.70	6.66 (−0.04)	6.94 (+0.24) 6.63 (−0.07)	6.47 (−0.23)	6.62 (−0.08)	– 6.59 (−0.11)	6.58 (−0.12) 6.94 (+0.24)	6.90 (+0.20)

* Numbering of peaks as in the chromatogram (Fig. 1).

a 600 × 4 mm I.D. column with the same eluent to analyse components having shorter retention times (peaks 1–4 in Fig. 1b). For the collection of the former components, an automatic collecting system (a Jasco Uvidec 100-IV HPLC apparatus combined with a Jasco AS-L350 intelligent sample processor and a Gilson 210 programmable fraction collector) and a semi-preparative column (300 × 7.5 mm I.D.) with benzene as eluent were used. The latter components were collected manually by using a 500 × 7.5 mm I.D. column with *n*-hexane–benzene (1:1) as eluent.

The 400 MHz ^{1}H NMR spectra of the isomers in deuterobenzene (CEA, 99.93%) solution were recorded on a Jeol JNM GX-400 spectrometer (with a digital resolution of 0.24 Hz); the measuring conditions were as described elsewhere[12].

RESULTS AND DISCUSSION

Fig. 1 shows the elution profiles of isomeric canthaxanthin analysed by using (a) the 300 and (b) the 600 × 4 mm I.D. column and an *n*-hexane–benzene (5:95) as eluent with detection at 480 nm. The all-*trans* isomer gave peak 13. The broad peak which is not numbered in Fig. 1a is resolved into seven peaks (peaks 1–4 and 6–8) in Fig. 1b.

Table I lists the chemical shifts and the "isomerization shifts" (in parentheses) for the isomers which gave peaks 13, 11, 10, 3, 4, 5, 2 and 1. The assignment of the ^{1}H signals for the all-*trans* isomer (peak 13) was made from the ^{1}H–^{1}H COSY spectrum. Where the assignments of the ^{1}H signals for the mono-*cis* isomers are given, their configurations were assigned by using the empirical rule of "isomerization shifts" (changes in chemical shifts of the ^{1}H signals relative to those of the all-*trans* isomer); a high-field shift (hfs) is expected for the ^{1}Hs on the convex side of the *cis* bend, whereas a low-field shift (lfs) is expected for the ^{1}Hs in the concave side of the *cis* bend. The assignment of the ^{1}H signals for the isomer which gave peak 11 was made by using a ^{1}H–^{1}H COSY spectrum, and was assigned to the 9-*cis* isomer (the hfs of the 10H and 12H signals and the lfs of the 8H and 11H signals). The assignments of both the ^{1}H signals and the configurations which gave peaks 10 and 3 were obtained by referring to the previously reported ^{1}H NMR spectra of β-carotene isomers[12], and were assigned to the 13-*cis* and 15-*cis* isomers, respectively.

Once the assignments of the ^{1}H signals for the mono-*cis* isomers had been established, the di-*cis* configurations could be easily identified by referring to the chemical shift of each mono-*cis* configuration. Although only three among five mono-*cis* isomers were found at this stage, considering the majority of the 9-*cis* and 13-*cis* isomers, the major di-*cis* isomers supposedly possess these configurations. We could isolate these isomers, which gave peaks 4, 5, 2 and 1; they were assigned to the 9,9′-*cis*, 9,13-*cis*, 9,13′-*cis* and 13,13′-*cis* isomers, respectively. The basis of the configurational assignments is described below.

Peak 4 is assigned to the 9,9′-*cis* isomer. This isomer shows "isomerization shifts" characteristic of the 9-*cis* configuration (the hfs of the 10H and 12H signals and the lfs of the 11H signal), and the number of signals observed shows that the structure of this isomer has a centre of symmetry. The 8H signal is expected to be shifted towards lower field and masked by the signal of ^{1}H in deuterobenzene.

Peak 5 is assigned to the 9,13-*cis* isomer. This isomer gives "isomerization shifts" coprresponding to the 9-*cis* configuration (the hfs of the 10H signal and the

TABLE II

ASSIGNMENT OF THE PEAKS IN THE CHROMATOGRAM

Peak No.	*Configuration*	*Peak No.*	*Configuration*
1	13,13′-*cis*	8	–
2	9,13′-*cis*	9	–
3	15-*cis*	10	13-*cis*
4	9,9′-*cis*	11	9-*cis*
5	9,13-*cis*	12	–
6	–	13	All-trans
7	–		

lfs of the 8H and 11H signals) and the 13-*cis* configuration (the hfs of the 14H and 15′H signals and the lfs of the 12H signal). It gives also chemical shifts characteristic of the all-*trans* configuration (the chemical shifts of the 7′H–14′H signals). The 15H signal was supposedly masked by the 11H signal.

Peak 2 is assigned to the 9,13′-*cis* isomer. The "isomerization shifts" of this isomer are simply an addition of those of the 9-*cis* configuration (the 10H, 11H and 12H signals) and those of the 13′-*cis* configuration (the 12′H, 14′H, 15′H and 15H signals; see the values for the 12H, 14H, 15H and 15′H signals of the 13-*cis* isomer). The chemical shifts characteristic of the all-*trans* configuration are not retained. The 8H signal must be masked by the signal of ^{1}H in deuterobenzene.

Peak 1 is assigned to the 13,13′-*cis* isomer. This isomer shows "isomerization shifts" characteristic of the 13-*cis* configuration (the hfs of the 14H signal and the lfs of the 12H and 15H signals), and the number of signals observed indicates the centre of symmetry in the molecular structure.

Table II summarizes the configurational assignment of the peaks. The presence of seven *cis*-isomers is evidenced by ^{1}H NMR spectroscopy. Englert[9] suggested the presence of additional 11-*cis*, 9,11-*cis* and 9,15-*cis* isomers. The assignment of peaks 6, 7, 8, 9 and 12 is in progress.

ACKNOWLEDGEMENT

This work was supported by the Private School Promotion Foundation in Japan.

REFERENCES

1 P. Mathis and C. C. Shenck, in G. Britton and T. W. Goodwin (Editors), *Carotenoid Chemistry and Biochemistry*, Pergamon Press, Oxford, 1982, p. 339.
2 R. J. Cogdell, *Pure Appl. Chem.*, 57 (1985) 723.
3 D. Siefermann-Harms, *Biochim. Biophys. Acta*, 811 (1985) 325.
4 D. Siefermann-Harms, *Physiol. Plant.*, 69 (1987) 561.
5 Y. Koyama, in N. I. Krinsky, M. M. Mathews-Roth and R. F. Taylor (Editors), *Carotenoids '87*, Plenum Press, New York, in press.
6 H. J. C. F. Nelis, P. Lavens, L. Moens, P. Sorgeloos, J. A. Jonckheere, G. R. Criel and A. P. De Leenheer, *J. Biol. Chem.*, 259 (1984) 6063.
7 Ch. Gansser and L. Zechmeister, *Helv. Chim. Acta*, 40 (1957) 1757.

8 H. J. C. F. Nelis, M. M. Z. Van Steenberge, M. F. Lefevere and A. P. De Leenheer, *J. Chromatogr.*, 353 (1986) 295.
9 G. Englert, in G. Britton and T. W. Goodwin (Editors), *Carotenoid Chemistry and Biochemistry*, Pergamon Press, Oxford, 1982, p. 107.
10 K. Tsukida, K. Saiki, T. Takii and Y. Koyama, *J. Chromatogr.*, 245 (1982) 359.
11 Y. Koyama, M. Hosomi, A. Miyata, H. Hashimoto, S. A. Reames, K. Nagayama, T. Kato-Jippo and T. Shimamura, *J. Chromatogr.*, 439 (1988) 417.
12 Y. Koyama, M. Hosomi, H. Hashimoto and T. Shimamura, *J. Mol. Struct.*, in press.

Journal of Chromatography, 448 (1988) 188
Elsevier Science Publishers B.V., Amsterdam — Printed in The Netherlands

CHROM. 20 672

Book Review

Characterisation of proteins, edited by F. Franks, Humana Press, Clifton, NJ, 1988, 576 pp., price US$ 69.50, US$ 79.50 (export), ISBN 0-89603-109-8.

Once my mother decided to try a new recipe for a cake from a cookbook. The recipe was fine but for the fact that in the publishing process one line got lost, *i.e.* the amount of flour that should go into it. The result was interesting but not the cake it was supposed to be ...

Now in this book there is a chapter on amino acids and small peptides. The chapter is fine only in the publishing process one reference got lost and thus from pages 269 to 283 all the information given as to the references is wrong:

Page 269, 2nd last line: Doury-Berthod *et al.* (49) ... but reference 49 is by Gil-Av *et al.*

Page 270, Figure 11 is supposed to be "from ref. 51"; I looked up this paper and it does not contain this figure.

Page 271, line 18: "in a paper by Hare and Gil-Av (51) ..." but reference 51 is by Nimura *et al.*

On page 272, Table I is supposed to contain data from reference 51; again this paper does not contain the data.

Page 273, "... in which Nimura *et al.* (52) demonstrate...", however reference 52 is by Armstrong and DeMond.

And so it goes on to the end.

If this had been published by the Academy of a comic opera country, I would not object but a book with a main author from Cambridge and a U.S.A publisher?

It is obvious that the editor did not read the chapter or does not know the subject sufficiently well to edit such a book. But then this should have been picked up by the staff of the publisher. After all if the publisher does not check the scientific integrity of a work, what does one need him for at all?

There are still other points of editorial neglect. There are journals such as *Hely. Chim. Acta* and *Anal. Boichem* in the reference list on pages 282 and 283.

On page 246 read "Cassidy" for "Cassidey" on line 17.

The publicity on the book states "Frank's original, highly practical approach to Characterisation of Proteins makes this volume an especially valuable handbook for everyone involved in protein studies". I may agree if this poorly edited version is withdrawn and replaced by a well-edited one.

By the way, the cake is what is called a "Bischofsbrot" in Vienna. We worked out how much flour it needs and are glad to supply the recipe on request.

MICHAEL LEDERER

Journal of Chromatography, 448 (1988) 189
Elsevier Science Publishers B.V., Amsterdam — Printed in The Netherlands

CHROM. 20 728

Book Review

Macromolecular sequencing and synthesis —selected methods and applications, edited by D. H. Schlesinger, Alan R. Liss, New York, 1988, 270 pp., ISBN 0-8451-4246-1.

The book contains 20 papers dealing with purification of peptides and proteins, structure determination of peptides and proteins, oligonucleotide sequencing, computer analysis of DNA and protein sequences, peptides synthesis, oligonucleotide synthesis and examples of combined methodologies.

Most papers are long but not reviews, rather papers dealing with specific topics. We first thought that the volume could be a birthday volume or similar (although there is no mention in the preface) but were informed by the author that "The chapters were contributed by established investigators whom I personally know and have the highest regard for their work in the DNA and protein field and who are internationally recognised as leaders in their particular discipline. These topics were not part of any single meeting and all topics covered have been or are in the process of being published in scientific journals. Finally, the origin of the volume was the outcome of discussions by myself and the Alan R. Liss Publishing Co."

Now this seems thus a highly unusual book. As most copies of an edition are bought by scientific libraries, why should they disburse money for material which they will or have received in the journals they subscribe to?

The book may find interest with research workers in the field as a form of collected reprints. It can not be recommended in any other context under the circumstances.

Journal of Chromatography, 448 (1988) 190
Elsevier Science Publishers B.V., Amsterdam — Printed in The Netherlands

CHROM. 20 649

New Editions of Books

Quantitative analysis by gas chromatography (*Chromatographic Science Series*, Vol. 41), by J. Novák, Marcel Dekker, New York, Basle, 2nd, revised and expanded ed., 1988, 275 pp., price US$ 89.95 (U.S.A. and Canada), US$ 107.50 (rest of world), ISBN 0-8247-7818-9.

Dr. Josef Novák died just one year ago. This second edition of his book, *Quantitative Analysis by Gas Chromatography*, has been published with a preface by his widow and with an added chapter by P. A. Leclerq on "Automatic acquisition and handling of chromatographic data" (52 pages).

Praxis der Hochleistungsflüssigchromatographie, by V. R. Meyer, Verlag Moritz Diesterweg, Frankfurt am Main, Verlag Sauerländer, Aarau, Frankfurt am Main, Salzburg, 5th ed., 1988, 275 pp., price DM 59.80; SFr. 56.50, ISBN 3-425-0552-X (Diesterweg), 3-7941-2792-7 (Sauerländer).

Mrs. Meyer completed the first edition of this handbook in 1978 and the book proved so popular that five editions have been published over ten years. The author insists in her preface to this new edition that she limits herself still to principles only, but it must be mentioned that each edition has been brought up to date with numerous references, some as late as 1987. An English translation of the 5th edition will appear later this summer with Wiley (New York, Chichester; ISBN 0-471-91140-2).

Journal of Chromatography, 448 (1988) 191
Elsevier Science Publishers B.V., Amsterdam — Printed in The Netherlands

CHROM. 20 726

Book Review

Journal of planar chromatography —modern TLC, Editors: Sz. Nyiredy (Editor-in-chief), H. Jork, C. F. Poole and B. De Spiegeleer, First issue: February 1988, Dr. Alfred Hüthig Verlag, Heidelberg.

The editorial of the first number states:

we can state that the number of TLC publications has varied between 600 and 800 in recent years. This means that more than 20% of all publications on separation techniques are in planar chromatography. We are introducing "Journal of Planar Chromatography —Modern TLC" as a forum for rapid communication of recent developments in instrumentation, new applications, and improved methods, to present this information to the reader in a clear, concise format, and to open a new channel of communication between scientists from all countries. The Journal should revive discussion in planar chromatography and encourage scientists to pursue new ideas in this field.

Aside of the fact that it is not clear what "a forum for rapid publication" and "a new channel of communication" are, one would question also the wisdom in fractionating the field of chromatography at a moment when many problems are solved by using several techniques together. This is already illustrated in this issue by the fact that one paper deals with electrophoresis, as well as chromatography.

The quality and usefulness of any journal depends, of course, entirely on its editor. So let us examine what he has to offer in this first issue:

On page 29 there is a paper on the "Differentiation and evaluation of Ginsengs and their preparations by means of HPTLC fingerprint analysis". A good photo of the chromatogram is shown in Fig. 5 (p. 33) which however is not better than that obtained in classical TLC, by Wagner *et al.* (*Plant Drug Analysis*, Springer, 1984, p. 239). Furthermore this work is not quoted and, according to the "Guidelines" published some years ago in *Anal. Chem.*, previous work must be mentioned!?!

On pp. 76 and 77 there is a paper on "Imaging analysis of thin layer chromatograms by secondary ion mass spectrometry: analysis of neostigmine and pyridostigmine bromides". In this paper there is a chromatogram, shown in Fig. 3, mentioning as solvent butanol–acetic acid–water while the text says butanol–methanol–water. So here the editorial slip is showing: either the editor or the publisher is careless. But the chromatogram poses another more important problem too: quarternary ammonium bromides travel usually as ion pairs and thus in a real analysis in presence of other anions often yield multispots. This is not discussed in this paper, which makes its usefulness in real analyses questionable, limiting the information of value to acrobatics with the mass spectrometer.

The editorial team is weak in English speaking members (five out of thirty) so the editor will indeed fight a lone and uphill battle if he wants to edit a serious journal. We wish him luck and success for his venture.

PUBLICATION SCHEDULE FOR 1988

Journal of Chromatography and Journal of Chromatography, Biomedical Applications

MONTH	J	F	M	A	M	J	J	A	S	O	N	D
Journal of Chromatography	435/1 435/2 435/3 436/1	436/2 436/3	437/1 437/2	438/1 438/2	439/1 439/2 440 441/1	441/2 442 443	444 445/1 445/2 446	447/1 447/2 448/1	448/2 448/3 449/1	449/2 450/1 450/2 450/3 452	The publication schedule for further issues will be published later.	
Bibliography Section		460/1		460/2		460/3		460/4		460/5		460/6
Cumulative Indexes, Vols. 401–450												451
Biomedical Applications	424/1	424/2	425/1 425/2	426/1 426/2	427/1	427/2 428/1	428/2 429	430/1	430/2 431/1	431/2	432	433 434

INFORMATION FOR AUTHORS

(Detailed *Instructions to Authors* were published in Vol. 445, pp. 453–456. A free reprint can be obtained by application to the publisher, Elsevier Science Publishers B.V., P.O. Box 330, 1000 AH Amsterdam, The Netherlands.)

Types of Contributions. The following types of papers are published in the *Journal of Chromatography* and the section on *Biomedical Applications:* Regular research papers (Full-length papers), Notes, Review articles and Letters to the Editor. Notes are usually descriptions of short investigations and reflect the same quality of research as Full-length papers, but should preferably not exceed six printed pages. Letters to the Editor can comment on (parts of) previously published articles, or they can report minor technical improvements of previously published procedures; they should preferably not exceed two printed pages. For review articles, see inside front cover under Submission of Papers.

Submission. Every paper must be accompanied by a letter from the senior author, stating that he is submitting the paper for publication in the *Journal of Chromatography.* Please do not send a letter signed by the director of the institute or the professor unless he is one of the authors.

Manuscripts. Manuscripts should be typed in double spacing on consecutively numbered pages of uniform size. The manuscript should be preceded by a sheet of manuscript paper carrying the title of the paper and the name and full postal address of the person to whom the proofs are to be sent. Authors of papers in French or German are requested to supply an English translation of the title of the paper. As a rule, papers should be divided into sections, headed by a caption (*e.g.,* Summary, Introduction, Experimental, Results, Discussion, etc.). All illustrations, photographs, tables, etc., should be on separate sheets.

Introduction. Every paper must have a concise introduction mentioning what has been done before on the topic described, and stating clearly what is new in the paper now submitted.

Summary. Full-length papers and Review articles should have a summary of 50–100 words which clearly and briefly indicates what is new, different and significant. In the case of French or German articles an additional summary in English, headed by an English translation of the title, should also be provided. (Notes and Letters to the Editor are published without a summary.)

Illustrations. The figures should be submitted in a form suitable for reproduction, drawn in Indian ink on drawing or tracing paper. Each illustration should have a legend, all the *legends* being typed (with double spacing) together on a *separate sheet.* If structures are given in the text, the original drawings should be supplied. Coloured illustrations are reproduced at the author's expense, the cost being determined by the number of pages and by the number of colours needed. The written permission of the author and publisher must be obtained for the use of any figure already published. Its source must be indicated in the legend.

References. References should be numbered in the order in which they are cited in the text, and listed in numerical sequence on a separate sheet at the end of the article. Please check a recent issue for the lay-out of the reference list. Abbreviations for the titles of journals should follow the system used by *Chemical Abstracts.* Articles not yet published should be given as "in press" (journal should be specified), "submitted for publication" (journal should be specified), "in preparation" or "personal communication".

Dispatch. Before sending the manuscript to the Editor please check that the envelope contains three copies of the paper complete with references, legends and figures. One of the sets of figures must be the originals suitable for direct reproduction. Please also ensure that permission to publish has been obtained from your institute.

Proofs. One set of proofs will be sent to the author to be carefully checked for printer's errors. Corrections must be restricted to instances in which the proof is at variance with the manuscript. "Extra corrections" will be inserted at the author's expense.

Reprints. Fifty reprints of Full-length papers, Notes and Letters to the Editor will be supplied free of charge. Additional reprints can be ordered by the authors. An order form containing price quotations will be sent to the authors together with the proofs of their article.

Advertisements. Advertisement rates are available from the publisher on request. The Editors of the journal accept no responsibility for the contents of the advertisements.